ZooKeys 1089: 1–23 (2022)
doi: 10.3897/zookeys.1089.78182
https://zookeys.pensoft.net

RESEARCH ARTICLE

A peer-reviewed open-access journal
ZooKeys
Launched to accelerate biodiversity research

The complete mitochondrial genome of the Mexican-endemic cavefish *Ophisternon infernale* (Synbranchiformes, Synbranchidae): insights on patterns of selection and implications for synbranchiform phylogenetics

Adán Fernando Mar-Silva[1,2], Jairo Arroyave[3], Píndaro Díaz-Jaimes[1]

1 *Laboratorio de Genética de Organismos Acuáticos, Instituto de Ciencias del Mar y Limnología, Universidad Nacional Autónoma de México, Circuito Exterior S/N, Ciudad Universitaria, 04510 Coyoacán, Mexico City, Mexico* 2 *Posgrado en Ciencias del Mar y Limnología, Universidad Nacional Autónoma de México, Mexico City, Mexico* 3 *Instituto de Biología, Universidad Nacional Autónoma de México, Circuito Exterior S/N, Ciudad Universitaria, 04510 Coyoacán, Mexico City, Mexico*

Corresponding author: Jairo Arroyave (jarroyave@ib.unam.mx)

Academic editor: C. McMahan | Received 19 November 2021 | Accepted 26 January 2022 | Published 11 March 2022

http://zoobank.org/61C2A787-3276-4580-8944-F212A7F5B651

Citation: Mar-Silva AF, Arroyave J, Díaz-Jaimes P (2022) The complete mitochondrial genome of the Mexican-endemic cavefish *Ophisternon infernale* (Synbranchiformes, Synbranchidae): insights on patterns of selection and implications for synbranchiform phylogenetics. ZooKeys 1089: 1–23. https://doi.org/10.3897/zookeys.1089.78182

Abstract

Ophisternon infernale is one of the 200+ troglobitic fish species worldwide, and one of the two cave-dwelling fishes endemic to the karstic aquifer of the Yucatán Peninsula, Mexico. Because of its elusive nature and the relative inaccessibility of its habitat, there is virtually no genetic information on this enigmatic fish. Herein we report the complete mitochondrial genome of *O. infernale*, which overall exhibits a configuration comparable to that of other synbranchiforms as well as of more distantly related teleosts. The K_A/K_S ratio indicates that most mtDNA PCGs in synbranchiforms have evolved under strong purifying selection, preventing major structural and functional protein changes. The few instances of PCGs under positive selection might be related to adaptation to decreased oxygen availability. Phylogenetic analysis of mtDNA comparative data from synbranchiforms and closely related taxa (including the indostomid *Indostomus paradoxus*) corroborate the notion that indostomids are more closely related to synbranchiforms than to gasterosteoids, but without rendering the former paraphyletic. Our phylogenetic results also suggest that New World species of *Ophisternon* might be more closely related to *Synbranchus* than to the remaining *Ophisternon* species. This novel phylogenetic hypothesis, however, should be further tested in the context of a comprehensive systematic study of the group.

Keywords
Blind swamp eel, karst aquifer, mitogenome, systematics, troglobitic, Yucatan Peninsula

Introduction

Ophisternon infernale (Synbranchiformes, Synbranchidae), commonly known as the blind swamp eel, is a rare and elusive freshwater teleost fish endemic to the cenotes and submerged caves of the Yucatan Peninsula (YP) in southeastern Mexico. Like most troglobites, *O. infernale* exhibits typical regressive troglomorphic traits associated with life in absolute darkness, such as the absence of both pigmentation and eyes. Besides its endemism and troglomorphism, *O. infernale* is exceptional in that it is one of two fish species that permanently inhabit the dark and oligotrophic subterranean waters of the YP karst aquifer; the other being the Mexican blind brotula (*Typhlias pearsei*) (Arroyave 2020). The relative inaccessibility of its habitat–submerged caves or cenotes well inside dry caves–coupled with its highly cryptic lifestyle–often found burrowed under the sediment or hiding inside tangles of submerged roots and crevices–have made the study of the blind swamp eel particularly challenging, and as a result very little is known about this intriguing fish species. Notably, the total number of occurrence records for *O. infernale* is less than 20 localities throughout its potential range of distribution (Arroyave et al. 2019). By virtue of its rarity, endemism, and restricted geographic distribution, in addition to the current threats faced by its habitat and region, *O. infernale* has recently been categorized as Endangered (EN) (Arroyave et al. 2019). Unsurprisingly, genetic data from *O. infernale* are virtually nonexistent, and this has hampered efforts at establishing its exact phylogenetic placement (Perdices et al. 2005). Besides their importance for phylogenetic and biogeographic research, genomic data are fundamental for addressing other evolutionary lines of inquiry, such as the genetic basis of troglomorphism (Protas and Jeffery 2012). Hence the need for generating genomic information of such a unique, endangered, and understudied species such as *O. infernale*. In order to provide genomic resources potentially informative for future evolutionary studies, here we present the first complete mitochondrial genome of the troglomorphic and YP-endemic *O. infernale*. In addition to sequencing, assembling, and annotating its mitogenome, we present detailed descriptive (genome size and organization, protein-coding genes [PCGs], non-coding regions, and RNAs features) and comparative (patterns of selection on PCGs, phylogenetic) analyses. Leveraging novel mitogenomic data to shed light on the systematics of Synbranchiformes is particularly relevant and timely because of ongoing conflicting hypotheses of relationships regarding the limits and composition of this teleost order that involve the phylogenetic placement of the monogeneric family Indostomidae with respect to synbranchiforms and closely related euteleost lineages (Van Der Laan et al. 2014; Nelson et al. 2016; Betancur-R et al. 2017). Furthermore, the phylogenetic position of the blind swamp eel, *O. infernale*, in the context of the diversification of the family Synbranchidae, has yet to be established (Perdices et al. 2005).

Material and methods

Sample collection and raw data generation

All methods were carried out in accordance with relevant guidelines and regulations, and the study was carried out in compliance with the ARRIVE guidelines. Sampling of the *O. infernale* individual used to generate the mitogenome presented here was accomplished with the assistance of a professional cave diver who captured the specimen using a custom-made hand net specifically designed for efficient capture and secure storage while cave diving. The sample was collected under collecting permit SGPA/DGVS/05375/19 issued by the Mexican Ministry of Environment and Natural Resources (Secretaría de Medio Ambiente y Recursos Naturales; SEMARNAT) to JA. The sampling locality is the cenote Kan-Chin (Huhí, Yucatán), located at 20°40'11"N, 89°10'6"W. The voucher specimen was euthanized with MS-222 prior to preservation in accordance with recommended guidelines for the use of fishes in research (Nickum et al. 2004), fixed in a 10% formalin solution, and subsequently transferred to 70% ethanol for long-term storage in the Colección Nacional de Peces (CNPE) of the Instituto de Biología (IB) at the Universidad Nacional Autónoma de México (UNAM), where it has been catalogued and deposited (CNPEIBUNAM 23285). A tissue sample (muscle fragment) was taken prior to specimen fixation, preserved in 95% ethanol, and eventually cryopreserved at -80 °C. High-molecular genomic DNA was extracted using the phenol-chloroform protocol (Sambrook et al. 1989). The DNA was sheared by sonication with a Bioruptor pico of Diagenode and Minichiller. Sonication was performed using six cycles of alternating 30 s ultrasonic bursts and 30 s pauses in a 4 °C water bath. For library preparation we used a DNA sample of 200 ng which was quantified using a Qubit fluorometer (Invitrogen). Library preparation was carried out using the KAPA Biosystem Hyper Kit (Kapa, Biosystem Inc., Wilmington, MA). Fragmented DNA was ligated to custom, TruSeq-style dual-indexing adapters (Glenn et al. 2016). Fragments were size selected in a ~300–500 bp range which was enriched through PCR, purified and normalized. The Illumina NextSeq v2 300 cycle kit was used for sequencing paired-end 150 nucleotide reads at the Georgia Genomics Facility, University of Georgia, Athens, USA.

Mitogenome assembly and annotation

The quality of the raw data was assessed with FastQC (Andrews, 2010). Good-quality sequences that did not contain ambiguous nucleotides and reads with average quality of 30Q were demultiplexed, trimmed and merged using Geneious Prime 2020.0.4 (https://www.geneious.com). Mitogenome assembly was conducted with MITObim v.1.9 (Hahn et al. 2013) using two reference mitogenomes from close relatives of *O. infernale* available in GenBank: *Ophisternon candidum* (MT436449) and *Synbranchus marmoratus* (AP004439). These reference mitogenomes were aligned in order to generate a consensus sequence for use during the annotation procedure.

MitoFish MitoAnnotator (Iwasaki et al. 2013) and MITOS (Bernt et al. 2013) were used to identify and annotate protein-coding genes (PCGs), transfer RNAs (tRNAs), and ribosomal RNAs (rRNAs). The resultant annotated *O. infernale* mitochondrial genome was deposited in the GenBank database under accession number OM388306.

Descriptive analyses

Nucleotide and amino acid composition, codon usage profiles of protein-coding genes (PCGs), Relative Synonymous Codon Usage (RSCU), and characterization the non-coding mtDNA control region (CR) were computed with MEGA X (Kumar et al. 2018). Nucleotide composition skewness was calculated with the formulas AT skew = (A – T)/(A + T) and GC skew = (G – C)/(G + C) (Perna and Kocher 1995). Prediction of tRNAs secondary structure was accomplished with tRNAScan-SE 2.0 (Chan and Lowe 2019) through the webserver http://lowelab.ucsc.edu/tRNAscan-SE/, using Infernal without HMM filter search mode and "vertebrate mitochondrial" as sequence source (Lowe and Chan 2016). Analysis and prediction of CR secondary structure in *O. infernale* was accomplished using the software ClustalW (Thompson et al. 2003) as implemented in MEGA X (Kumar et al. 2018) by comparison (via multiple sequence alignment) with reports of secondary CR structure from two other teleost fishes, namely *Siniperca chuatsi* (EU659698) (Zhao et al. 2006) and *Cyprinion semiplotum* (MN603795) (Sharma et al. 2020).

Comparative analyses

We investigated patterns of selection on PCGs on a mitogenomic scale and phylogenetic relationships among major synbranchiform lineages based on all mitogenomic comparative data for the group available on GenBank. To measure of the strength and mode of natural selection acting on PCGs, we estimated the ratio of non-synonymous (K_A) to synonymous (K_S) substitutions (K_A/K_S, also known as ω or d_N/d_S) using the HyPhy 2.5 package (Kosakovsky Pond et al. 2020) as implemented in MEGA X (Kumar et al. 2018) based on the newly assembled mitochondrial genome (*Ophisternon infernale*, OM388306) and seven additional synbranchiform mitogenomes previously available in GenBank: *Ophisternon candidum* (MT436449), *Synbranchus marmoratus* (AP004439), *Monopterus albus* (NC003192), *Mastacembelus armatus* (NC023977), *Mastacembelus erythrotaenia* (NC035141), *Macrognathus aculeatus* (KT443991), and *Macrognathus pancalus* (NC032080). To compare patterns of selection between synbranchiform families, we conducted two separate K_A/K_S analyses, one for synbranchids and one for mastacembelids. The taxonomic sampling for phylogenetic analyses included representatives of the synbranchiform families Synbranchidae and Mastacembelidae, as well as a representative of Indostomidae, a monogeneric family historically classified in the Gasterosteiformes on the basis of morphological evidence (Van Der Laan et al. 2014; Nelson et al. 2016) but more recently assigned to the Synbranchiformes in accordance to the results of molecular phylogenetic studies (Betancur-R. et al. 2013;

Betancur-R et al. 2017). The lack of published mitochondrial genomes of fishes from the synbranchiform family Chaudhuriidae prevented us from including representatives of this taxon in our analyses. The ingroup consisted of the synbranchids *Ophisternon infernale* (OM388306), *Ophisternon candidum* (MT436449), *Synbranchus marmoratus* (AP004439) and *Monopterus albus* (NC003192), the mastacembelids *Mastacembelus armatus* (NC023977), *Mastacembelus erythrotaenia* (NC035141), *Macrognathus aculeatus* (KT443991) and *Macrognathus pancalus* (NC032080), and the indostomid *Indostomus paradoxus* (NC004401). The outgroup consisted of representatives of close relatives of Synbranchiformes such as the anabantiforms *Channa micropeltes* (NC030542) and *Nandus nandus* (AP006809), and the gasterosteiforms *Gasterosteus aculeatus* (NC041244) and *Pungitius pungitius* (NC011571); the last two included to test the phylogenetic position of *I. paradoxus* with respect to members of the Gasterosteiformes. The phylogeny was rooted at the viviparous brotula *Diplacanthopoma brachysoma* (AP004408). Phylogenetic relationships were inferred based on a concatenated alignment of all 13 PCGs. DNA sequence data from each PCG was independently aligned via multiple sequence alignment using the software MUSCLE (Edgar 2004) under default parameters via the "translation align" tool of the software Geneious Prime 2020.0.4 (https://www.geneious.com). The best-fit substitution model for each PCG was determined according to the corrected Akaike Information Criterion (AICc) with the software jModelTest2 (v. 2.1.10) (Darriba et al. 2012) under the following likelihood settings: number of substitution schemes = "3"; base frequencies = "+F"; rate variation = "+I and + G with nCat = 4"; base tree for likelihood calculations = "ML optimized"; and base tree search = "Best" (effectively evaluating among all 24 "classical" GTR-derived models). Individual alignments (*ATP6*=681 bp, *ATP8*=168 bp, *COX1*=1,539 bp, *COX2*=690 bp, *COX3*=783 bp, *CYTB*=1,137 bp, *NAD1*=975 bp, *NAD2*=1,053 bp, *NAD3*=348 bp, *NAD4*=1,380 bp, *NAD4L*=294 bp, *NAD5*=1,836 bp, and *NAD6*=525 bp) were subsequently concatenated using the software 2matrix (Salinas and Little 2014), yielding a data matrix totaling 11,409 aligned bp. Maximum Likelihood inference of phylogeny was carried out on the concatenated alignment partitioned by gene using the software RAxML-NG (v. 1.0.1) (Kozlov et al. 2019) through the CIPRES Science Gateway (Miller et al. 2010), with nodal support estimated by means of the bootstrap character resampling method (Felsenstein 1985) based on 1000 pseudoreplicates.

Results and discussion

Genome size and organization

The complete mitochondrial genome of *O. infernale* presented herein (GenBank accession number OM388306) is 16,804 bp in total length (Fig. 1; Table 1), a somewhat larger size than previously published synbranchiform mitogenomes, which range from 16,493 bp (in *M. erythrotaenia*) (or from 16,152 bp if considering the putative synbranchiform

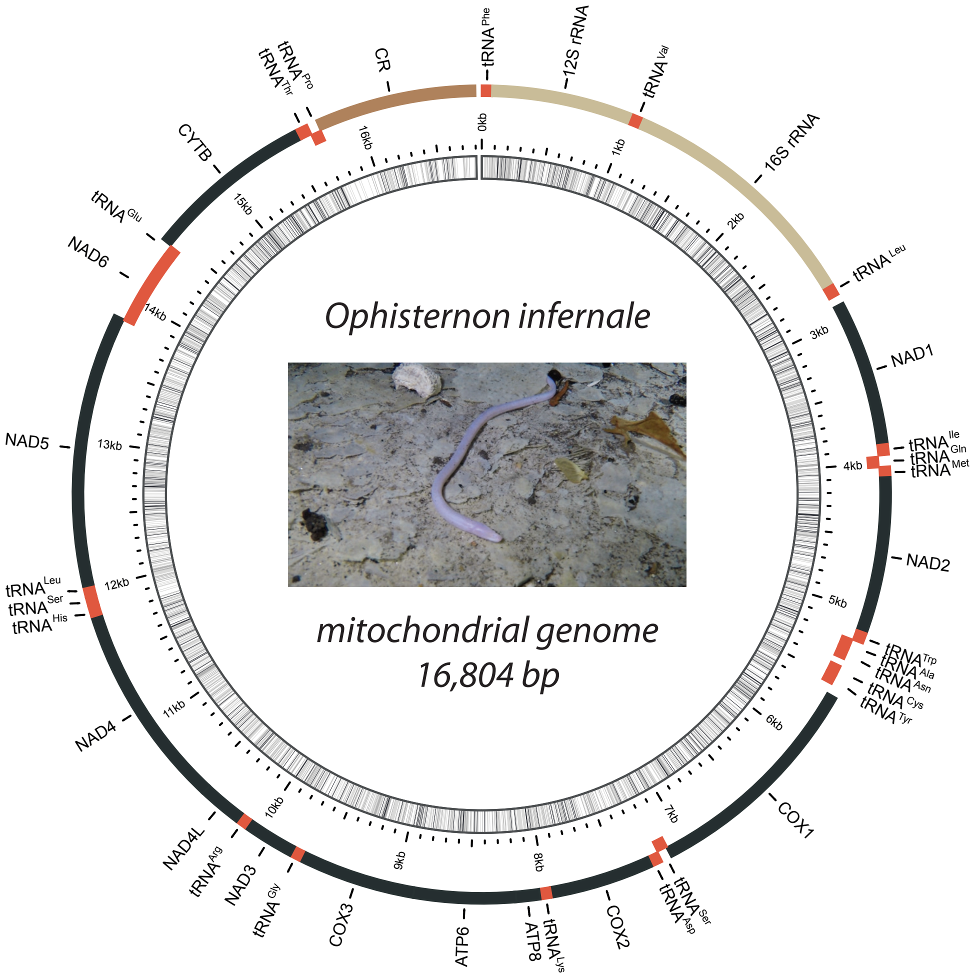

Figure 1. Annotated map of the mitochondrial circular genome of *O. infernale*. The outer ring corresponds to the H- (outermost) and L-strands, and depicts the location of PCGs (in black, except for *ND6* which is encoded in the L-strand and is portrayed in red), the non-coding control region (in dark brown), tRNAs (in red), and rRNAs (in light brown). The inner ring (black sliding window) denotes GC content along the genome. Live specimen photograph taken in the Cenote Kancabchen (Homún, Yucatán), courtesy of cave diver Erick Sosa.

I. paradoxus) to 16,622 bp (in *M. albus*). Although the mitogenome of the synbranchid *S. marmoratus* reported in GenBank (AP004439) is considerably shorter (15,561 bp), this significant difference in length is actually due to it missing the *NAD1* gene (normally ~1,000 bp) as a result of reported technical difficulties during sequencing (Miya et al. 2003). The composition and general arrangement of mitochondrial genes in *O. infernale* is identical to that reported for other synbranchiforms (Li et al. 2016; Han et al. 2018; White et al. 2020) as well as for more distantly related teleosts (Miya et al. 2001, 2003; Satoh et al. 2016), and consists of a total of 37 genes divided into

Table 1. Mitochondrial genes and associated features of *O. infernale*. Intergenic space (IGS) described as intergenic (+) or overlapping nucleotides (–). AA = amino acid.

Locus	Type	One-letter code	Start	End	Length (bp)	Strand	# of AA	Anticodon	Start codon	Stop codon	IGS
$tRNA^{Phe}$	tRNA	F	1	69	69	H		GAA			0
12s rRNA	rRNA		70	1017	948	H					0
$tRNA^{Val}$	tRNA	V	1018	1091	74	H		TAC			0
16s rRNA	rRNA		1092	2766	1092	H					0
tRNA-Leu	tRNA	L	2767	2840	74	H		TAA			63
NAD1	Protein-coding		2904	3872	951	H	316		ATG	TAA	7
$tRNA^{Ile}$	tRNA	I	3880	3949	70	H		GAT			8
$tRNA^{Gln}$	tRNA	Q	3958	4028	71	L		TTG			–1
$tRNA^{Met}$	tRNA	M	4028	4097	70	H		CAT			0
NAD2	Protein-coding		4098	5144	1047	H	337		ATG	AGA	–3
$tRNA^{Trp}$	tRNA	W	5142	5211	70	H		TCA			1
$tRNA^{Ala}$	tRNA	A	5213	5281	69	L		TGC			1
$tRNA^{Asn}$	tRNA	N	5283	5355	73	L		GTT			53
$tRNA^{Cys}$	tRNA	C	5409	5475	67	L		GCA			0
$tRNA^{Tyr}$	tRNA	Y	5476	5542	67	L		GTA			1
COX1	Protein-coding		5544	7082	1539	H	489		GTG	AGA	–4
$tRNA^{Ser}$	tRNA	S	7127	7197	71	L		TGA			2
$tRNA^{Asp}$	tRNA	D	7200	7270	71	H		GTC			2
COX2	Protein-coding		7273	7963	691	H	225		ATG	T	0
$tRNA^{Lys}$	tRNA	K	7964	8036	73	H		TTT			1
ATP8	Protein-coding		8038	8205	168	H	51		ATG	TAA	–8
ATP6	Protein-coding		8196	8878	683	H	223		ATG	TA	0
COX3	Protein-coding		8879	9662	784	H	249		ATG	T	0
$tRNA^{Gly}$	tRNA	G	9663	9731	69	H		TCC			0
NAD3	Protein-coding		9732	10079	348	H	112		ATG	GAC	0
$tRNA^{Arg}$	tRNA	R	10080	10148	69	H		TCG			0
NAD4L	Protein-coding		10149	10445	297	H	97		ATA	TAA	–5
NAD4	Protein-coding		10439	11819	1380	H	445		ATG	T	0
$tRNA^{His}$	tRNA	H	11820	11888	69	H		GTG			0
$tRNA^{Ser}$	tRNA	S	11889	11952	64	H		GCT			–1
$tRNA^{Leu}$	tRNA	L	11952	12024	73	H		TAG			1
NAD5	Protein-coding		12026	13855	1830	H	598		ATG	TA	–2
NAD6	Protein-coding		13852	14373	522	L	172		ATG	T	1
$tRNA^{Glu}$	tRNA	E	14375	14443	69	L		TTC			2
CYTB	Protein-coding		14446	15586	1141	H	369		ATG	T	0
$tRNA^{Thr}$	tRNA	T	15587	15662	76	H		TGT			–1
$tRNA^{Pro}$	tRNA	P	15662	15730	69	L		TGG			0
D-loop	Non-coding		15731	16804	1074	H					0

the following categories: 13 PCGs, 2 rRNAs, 22 tRNAs, and the non-coding control region (CR) (Fig. 1; Table 1). Twenty-eight genes (12 PCGs, 2 rRNAs, 14 tRNAs) plus CR are located on the H-strand, while the remaining nine genes (*NAD6* and 8 tRNAs) are located on the L-strand (Table 1); a configuration that corresponds to those of previously reported synbrachiform mitogenomes (Li et al. 2016; Han et al. 2018; White et al. 2020). The overall base composition of the *O. infernale* mitogenome is T=28.7%, A=31.6%, G=13.2%, and C=26.5%, which is fairly similar to those of other synbrachiform mitogenomes (Table 2). Nucleotide composition, however, is biased toward A+T (60.4%), with *O. infernale* displaying the highest values of this metric among the analyzed synbranchiforms. The mitogenome of *O. infernale* exhibits positive AT (0.046) and negative GC (-0.277) skewness, a general pattern shared with other species of the Synbranchiformes (Table 2).

Table 2. Size and nucleotide composition of the complete synbranchiform mitochondrial genomes (and their concatenated PCGs) analyzed in this study. **NAD1* gene missing from published mitogenome.

Species	GenBank Accession #	Entire genome								Protein-coding genes			
		Length (bp)	A(%)	T(%)	C(%)	G(%)	AT(%)	AT skew	GC skew	Length (bp)	AT(%)	AT skew	GC skew
Ophisternon infernale	OM388306	16804	31.6	28.7	26.5	13.2	60.4	0.046	-0.277	11449	60.1	-0.038	-0.348
Ophisternon candidum	MT436449	16526	31.5	27.5	27.9	13.1	59	0.067	-0.36	11377	59.1	-0.015	-0.374
*Synbranchus marmoratus**	AP004439	15561	30.7	26.8	28.5	14	57.5	0.067	-0.341	10529	57.1	-0.027	-0.355
Monopterus albus	NC003192	16622	28.9	27.2	29.4	14.5	56.1	0.03	-0.34	11430	54.9	-0.052	-0.356
Mastacembelus armatus	NC023977	16487	29.1	25.3	30.9	14.7	54.4	0.069	-0.355	11404	53.1	-0.013	-0.381
Mastacembelus erythrotaenia	NC035141	16493	29	24.5	31.6	14.9	53.4	0.086	-0.357	11417	52.2	-0.003	-0.382
Macrognathus aculeatus	KT443991	16543	30	26.5	28.7	14.8	56.4	0.063	-0.322	11420	55.9	-0.014	-0.345
Macrognathus pancalus	NC032080	16549	29.7	26	29.6	14.7	55.7	0.664	-0.337	11420	54.9	-0.02	-0.363

Protein-coding genes

The 13 PCGs, altogether totaling 11,449 bp, correspond to 68.1% of the *O. infernale* mitogenome. These genes consist of seven regions that code for the subunits of the NADH dehydrogenase (ubiquinone) protein complex (*NAD1-6*, *NADL4*), three that code for the subunits of the enzyme cytochrome c oxidase (*COX1-3*), one that codes for the enzyme cytochrome b (*CYTB*), and two that code for the subunits 6 and 8 of the enzyme ATP synthase F_O (*ATP6*, *ATP8*). Except for *COX1* and *ND4L*, PCGs exhibit an ATG (Met) start codon, which is the standard in eukaryotic systems (Kozak 1983). The start codon exhibited by *COX1* (GTG), however, is fairly common among vertebrates (Nwobodo et al. 2019). Conversely, an initiation-codon change from ATG (Met) to ATA (Ile) such as the one observed in *ND4L* is less common. Notably, of the synbranchiform mitogenomes analyzed, only that of *O. infernale* displays ATA as *ND4L* initiation codon. Most PCGs (10 out of 13) exhibit a TAA stop codon, which is a standard termination codon common in vertebrate mtDNA. However, of these 10 genes only three (*NAD1*, *NAD4L*, *ATP8*) display a complete codon (TAA), while the remaining seven (*ATP6*, *COX2*, *COX3*, *NAD4*, *NAD5*, *NAD6*, *CYTB*) contain an incomplete stop codon (either TA or T). Of the remaining three PCGs, *NAD2* and *COX1* have the stop codon AGA, while *NAD3* has the stop codon GAC (Table

2). PCGs in the mitogenome of *O. infernale* exhibit levels of A+T content (60.1%) comparable to–though slightly higher than–those of other synbranchiforms, which range from 53.1% in *M. armatus* to 59.1% in *O. candidum* (Table 2). In contrast to our findings for the entire mitogenome, AT-skews in PGCs across all synbranchiform mitogenomes analyzed exhibit negative values. Conversely, and in correspondence with our whole-mitogenome results, GC-skews in PGCs also exhibit negative values and highly similar across most analyzed synbranchiforms. A total of 3816 amino acids are encoded by PCGs in the mitogenome of *O. infernale*, with Leu (14.7%), Ser (9.4%), Thr (7.8%), and Pro (7.7%) being the most frequent, while Met (1.1%) being the least common. RSCU values represent the ratio between the observed usage frequency of one codon in a gene sample and the expected usage frequency in the synonymous codon family, given that all codons for the particular amino acid are used equally. The synonymous codons with RSCU values > 1.0 have positive codon usage bias and are defined as abundant codons, whereas those with RSCU values < 1.0 have negative codon usage bias and are defined as less-abundant codons (Gun et al. 2018). Results from RSCU analysis of PCGs in the mitogenome of *O. infernale* indicate that the most frequently used codons are ACC (1.59%), AAA (1.56%), TTA, ATA, and GAA (1.49%), which code for the amino acids Thr, Lys, Leu, Met, and Glu, respectively. On the other hand, codons encoding Prol (CCG, 0.16%), Thr (ACG, 0.2%), Ala (GCG, 0.23%), Ser (TCG, 0.39%), and Leu (CTG, 0.4%; TTA, 0.48%) are the least frequent (Fig. 2; Table 3).

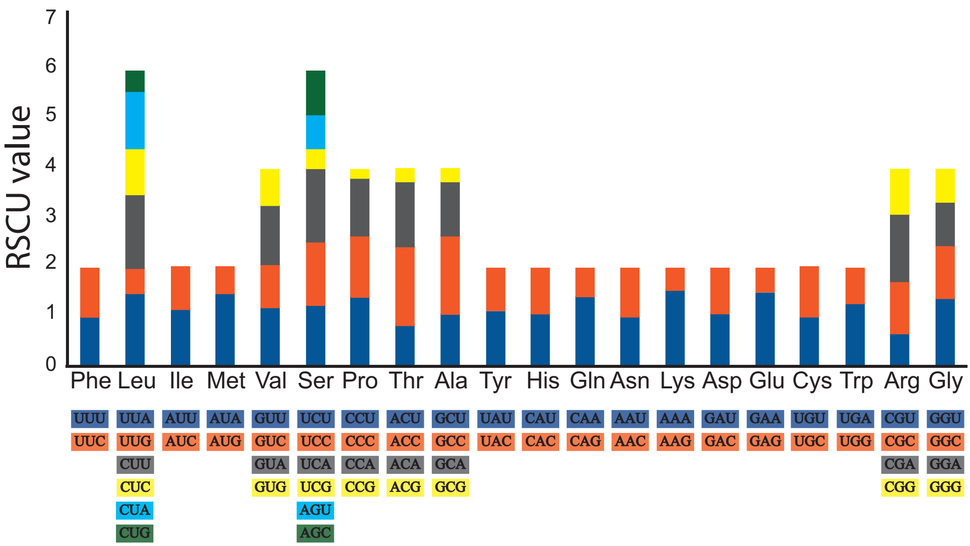

Figure 2. Results from analysis of Relative Synonymous Codon Usage (RSCU) of the mitochondrial genome of *O. infernale*. Codon families are plotted on the x-axis. The label for the 2, 4, or 6 codons that compose each family is shown in the boxes below the x-axis, and the colors correspond to those in the stacked columns. RSCU values are shown on the y-axis.

Table 3. Results from the Relative Synonymous Codon Usage (RSCU) analysis for the PCGs of the mitochondrial genome of *O. infernale*.

Amino acid	Codon	Number	Freq. (%)	RSCU	Amino acid	Codon	Number	Freq. (%)	RSCU
Phe	TTT	110	2.9	1.02	Ala	GCA	48	1.3	1.12
	TTC	105	2.8	0.98		GCG	10	0.3	0.23
Leu	TTA	139	3.6	1.49	Tyr	TAT	119	3.1	1.13
	TTG	45	1.2	0.48		TAC	92	2.4	0.87
	CTT	144	3.8	1.54	His	CAU	59	1.5	1.08
	CTC	85	2.2	0.91		CAC	50	1.3	0.92
	CTA	110	2.9	1.18	Gln	CAA	78	2	1.42
	CTG	37	1	0.4		CAG	32	0.8	0.58
Ile	ATT	134	3.5	1.17	Asn	AAT	101	2.6	1
	ATC	95	2.5	0.83		AAC	102	2.7	1
Met	ATA	119	3.1	1.49	Lys	AAA	78	2	1.56
	ATG	41	1.1	0.51		AAG	22	0.6	0.44
Val	GTT	31	0.8	1.18	Asp	GAT	34	0.9	1.1
	GTC	23	0.6	0.88		GAC	28	0.7	0.9
	GTA	32	0.8	1.22	Glu	GAA	50	1.3	1.49
	GTG	19	0.5	0.72		GAG	17	0.4	0.51
Ser	TCT	73	1.9	1.22	Cys	TGT	30	0.8	0.98
	TCC	80	2.1	1.34		TGC	31	0.8	1.02
	TCA	88	2.3	1.47	Trp	TGA	63	1.7	1.26
	TCG	23	0.6	0.39		TGG	37	1	0.74
	AGT	42	1.1	0.7	Arg	CGT	14	0.4	0.67
	AGC	52	1.4	0.87		CGC	22	0.6	1.06
Pro	CCT	104	2.7	1.42		CGA	28	0.7	1.35
	CCC	91	2.4	1.24		CGG	19	0.5	0.92
	CCA	86	2.3	1.17	Gly	GGT	44	1.2	1.35
	CCG	12	0.3	0.16		GGC	36	0.9	1.11
Thr	ACT	66	1.7	0.87		GGA	30	0.8	0.92
	ACC	120	3.1	1.59		GGG	20	0.5	0.62
	ACA	101	2.6	1.34	Stop	TAA	83	2.2	1.78
	ACG	15	0.4	0.2		TAG	39	1	0.84
Ala	GCT	45	1.2	1.05		AGA	37	1	0.8
	GCC	69	1.8	1.6		AGG	27	0.7	0.58

Transfer and ribosomal RNAs

The mitogenome of *O. infernale* contains the typical 22 tRNAs usually documented for mitogenomes of other teleosts and vertebrates (Lee et al. 1995; Díaz-Jaimes et al. 2016; Satoh et al. 2016; Nwobodo et al. 2019; White et al. 2020). The genomic organization of tRNAs in *O. infernale* is identical to that reported for *O. candidum* (White et al. 2020) and other synbranchids (Li et al. 2016; Han et al. 2018). Altogether, tRNAs total 1547 bp, with individual ones ranging from 64 bp ($tRNA^{Ser}$) to 76 bp ($tRNA^{Thr}$) (Table 1). Fourteen tRNAs are encoded in the H-strand, while the remaining eight in the L-strand (Fig. 1; Table 1). Twenty-one of the 22 tRNAs fold into the canonical cloverleaf secondary structure that consists of four domains (AA stem, D arm, AC arm, and T arm) and a variable loop (Fig. 3). Notably, the $tRNA^{Ser}$ (11889–11952) exhibits an unusual structure in which the D arm is missing. Although any change in tRNA secondary structure could potentially alter its amino acid recognition capability (Nwobodo et al. 2019), it has been

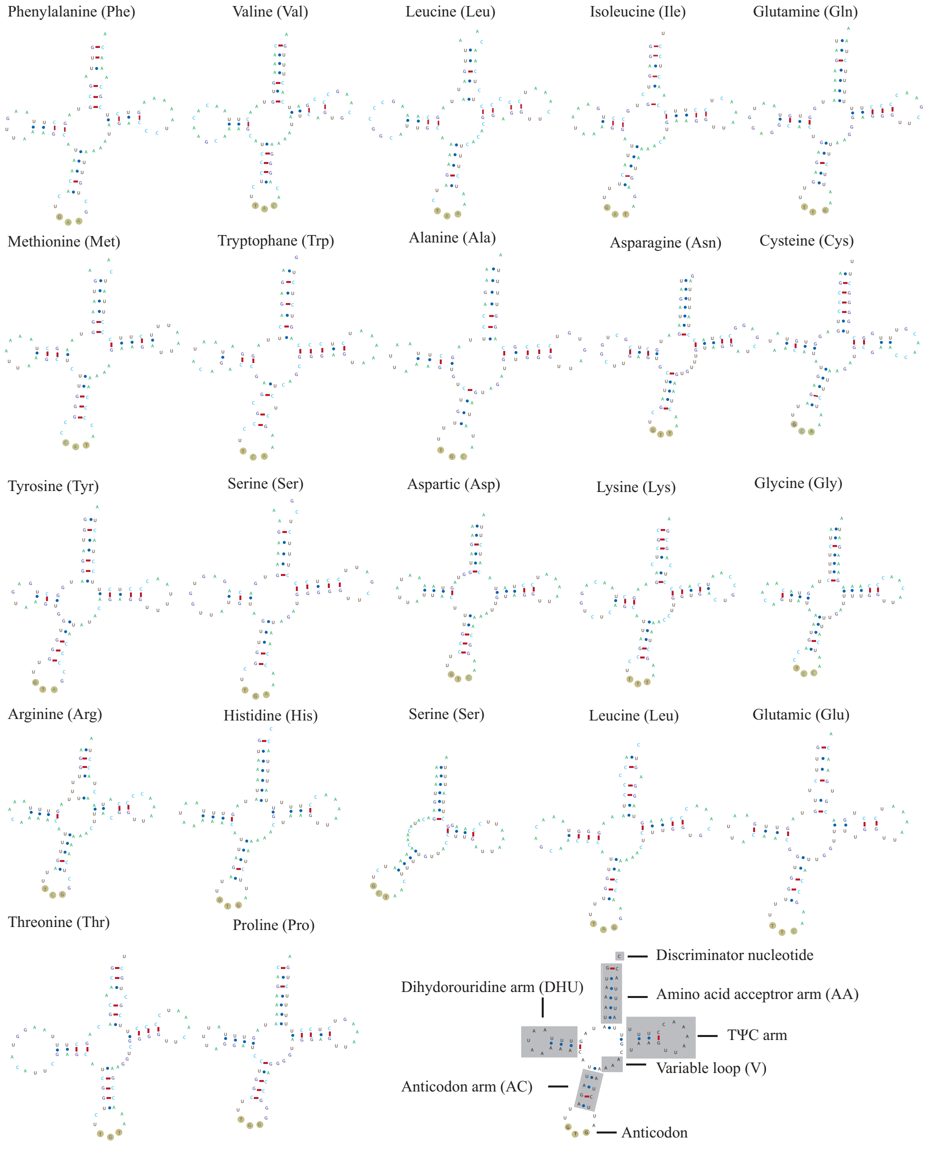

Figure 3. Secondary structure of the 22 tRNA genes of the mitochondrial genome of *O. infernale* predicted by tRNAScan-SE 2.0.

shown that loss of the D arm does not necessarily imply reduced functionality; in fact, almost all tRNAs^{Ser} for AGY/N codons lack the D arm, and truncated tRNAs appear to have been compensated for by several interacting factors (Watanabe et al. 2014). Furthermore, among fishes, loss of the tRNA^{Ser} D arm is not unique to *O. infernale*, for it has been reported in several species, including chondrichthyans such as *Chiloscyllium griseum* (Chen et al. 2013), *Triaenodon obesus* (Chen et al. 2016), and *Cephalloscyllium umbratile* (Zhu et al. 2017), as well as teleosts such as *Oreochromis andersonii* and *O. macrochir* (Bbole et al. 2018). Although most tRNAs present the canonical 7-bp T loop, nonstandard T-loop lengths were observed in $tRNA^{Met}$ (6 bp), $tRNA^{Phe}$ (8 bp), and $tRNA^{Ser}$ (9 bp). Other deviations from the traditional tRNA secondary structure that could affect functionality is the presence of extra loops. The $tRNA^{Arg}$ (10080–10148) in the mitogenome of *O. infernale* exhibits a loop at the base of the AA stem, thus potentially affecting aminoacylation. The nucleotide composition in the tRNAs of the *O. infernale* mitogenome is T=29%, A=31.4%, G=20.2%, and C=19.3%. The genes that code for the mitochondrial *12S* and *16S* rRNA subunits in *O. infernale* are 948 bp and 1092 bp long, respectively, and are located on the H-strand separated by the $tRNA^{Val}$, just like in most teleost fishes (Lee et al. 1995; Satoh et al. 2016).

Non-coding regions

The mtDNA control region of *O. infernale* is 1074 bp long (15731–16804), encoded in the H-strand, and flanked by $tRNA^{Pro}$ and $tRNA^{Phe}$ at the 5' and 3' ends, respectively (Fig. 1; Table 1), which is consistent with our understanding of mitogenome structure and organization in fishes (Lee et al. 1995; Rasmussen and Arnason 1999; Satoh et al. 2016). *Ophisternon infernale* CR nucleotide composition is T=33.1%, A=36.7%, G=10.9%, and C=19.3%, with A+T content (69.8%) larger than that of the entire mitogenome but similar to that of other fishes including synbranchids (Li et al. 2016; Han et al. 2018). Like in other fishes, CR in *O. infernale* is divided into three domains: a central conserved domain flanked and two hypervariable domains (upstream and downstream). Three conserved sequence blocks (CSBs) were detected at the central conserved domain (CSB-F, CSB-E, CSB-D) as well as at the downstream hypervariable region (CSB1, CSB2, CSB3) (Fig. 4). Although additional CBSs have been identified for the central conserved domain (CSB-B, CSB-C) in mammals (Southern et al. 1988), the three identified herein for *O. infernale* are those commonly found in fishes (Broughton and Dowling 1994; Chen et al. 2012). The upstream hypervariable domain in the CR of *O. infernale* has a length of 256 bp and includes two copies of the motif TACAT and three copies of palindromic motif ATGTA. A change in the motif sequence (TGCAT) was observed in *C. semiplotum* and *S. chuatsi* but not in *O. infernale*. Compared to those from the central conserved domain, CSBs in the downstream hypervariable domain displayed larger variation across the three fish species compared. Notably, CSB2 and CSB3 were slightly more conserved than CSB1, a pattern that has been reported for other fishes (Chen et al. 2012).

Patterns of selection on PCGs

Results from K_A/K_S analyses (Fig. 5) indicate that most mtDNA PCGs in synbranchiform fishes have evolved under strong purifying selection (K_A/K_S <<1), preventing major structural and functional protein changes. Exceptions to this general pattern were observed for *COX1* and *NAD6* in synbranchids (Fig. 5a) and for *NAD4* and *NAD6* in

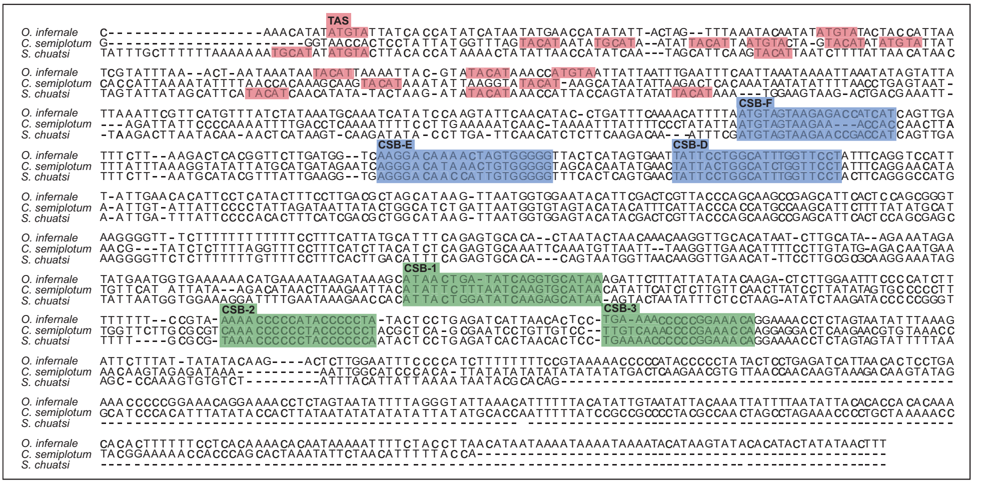

Figure 4. Comparison (multiple sequence alignment) of the mtDNA control region of *O. infernale* with those of fellow teleosts *Siniperca chuatsi* and *Cyprinion semiplotum*. The alignment displays the three canonical domains distinguished by Termination Associated Sequences (TAS) of the upstream hypervariable region (in red), central conserved domain blocks (CSB-F, CSB-E, CSB-D) (in blue), and conserved sequence blocks of the downstream hypervariable region (CSB-1, CSB-2 and CSB-3) (in green).

mastacembelids (Fig. 5b), where significant signals of positive selection were detected. Studies in different groups of animals, including cephalopods (Almeida et al. 2015), rodents (Tomasco and Lessa 2011), and humans (DeHaan et al. 2004), have linked amino acid replacements in *NAD6* to adaptive selection to hypoxic conditions. Because numerous synbranchiform species are known to be fossorial and to inhabit low-oxygen waters, the observed signature of positive selection in *NAD6* might be related to adaptation to decreased oxygen availability. Notably, a recent comparative mitogenomic study of the African tilapias *Oreocrhomis andersonii* and *O. macrochir* similarly uncovered a pattern of positive selection in *NAD6* suggestive of adaptation in response to changing environments (Bbole et al. 2018). In contrast to the pattern observed for *NAD6*, selection in *COX1* and *NAD4* is completely conflicting between synbranchiform families. While in mastacembelids *COX1*–like most mitochondrial genes–has evolved under purifying selection (K_A/K_S <1), the opposite happens in synbranchids. Although speculative at this point, the fact that half of our synbranchid dataset consists of troglomorphic cave-dwelling species (*O. infernale* and *O. candidum*) (vs. none in the mastacembelid dataset) could explain the observed differences in *COX1* selection patterns. Compared to surface waters, subterranean waters such as those of karst environments that harbor populations of *O. infernale* and *O. candidum* (in Mexico and Australia, respectively) contain low dissolved oxygen (Huppop 2000). Because of its role in aerobic metabolism, *COX1* might therefore be a target of directional selection promoting the evolution of more metabolically efficient variants in hypogean lineages (Boggs and Gross 2021). In contrast, the observed conflicting patterns of selection in *NAD4*–another gene involved in cellular respiration–between mastacembelids (positive) and synbranchids (purifying), do not seem to be readily explained by ecological differences related to cave life.

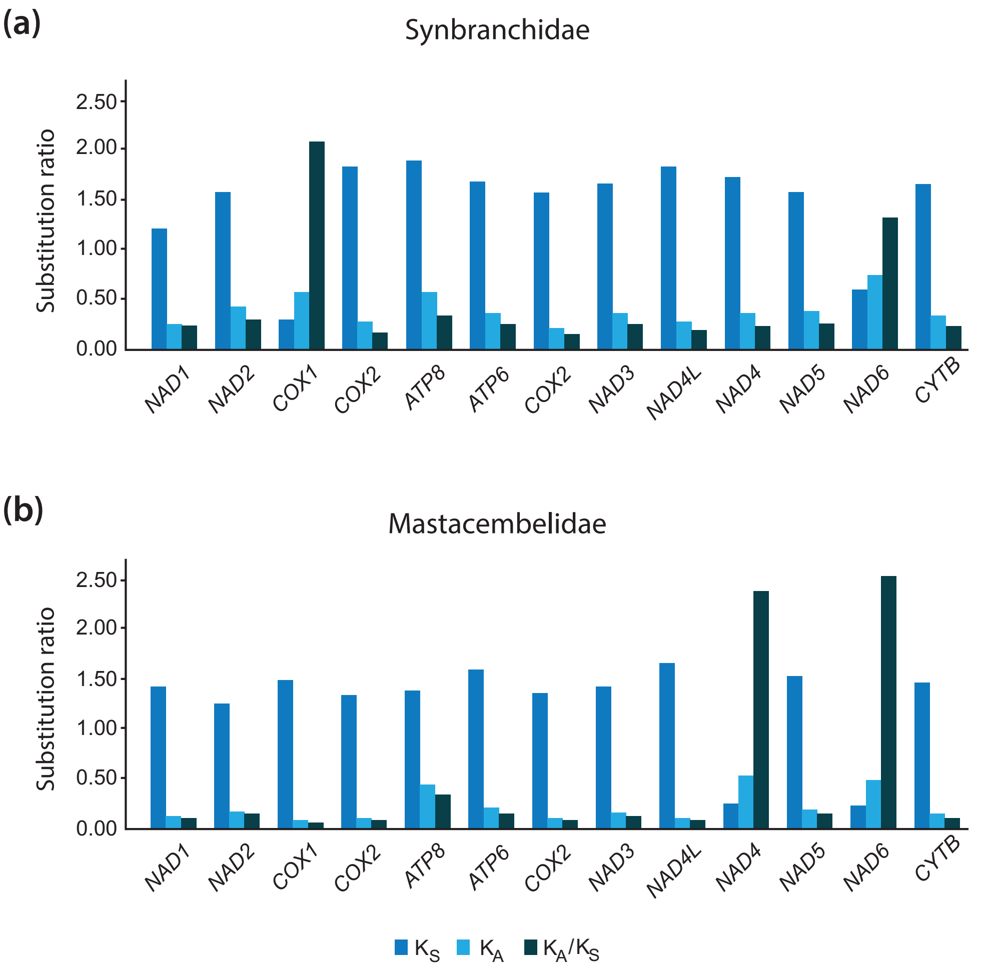

Figure 5. Patterns of selection in mtDNA PCGs of synbranchiform fishes. Results from K_A/K_S ratio analysis on mitochondrial PCGs (x-axis) in synbranchiform fishes of the families Synbranchidae (**a**) and Mastacembelidae (**b**).

Phylogeny and systematics of synbranchiform fishes

Our understanding of phylogenetic relationships in synbranchiform fishes is incipient compared to that of other teleost groups. Despite the fact that for the past two decades molecular systematics has been routinely employed to refine and update the classification of fishes and our knowledge of their evolutionary history (Betancur-R et al. 2017), a comprehensive molecular phylogeny of the Synbranchiformes has yet to be proposed. Apart from a phylogenetic study focused on Central American synbranchids (Perdices et al. 2005), no studies have investigated synbranchiform relationships using comparative DNA sequence data. Surprisingly, recent phylogenetic studies focused on higher-level relationships among major lineages of bony fishes (Betancur-R. et al. 2013; Betancur-R et al. 2017) resulted in the reassignment of armored sticklebacks (family Indostomidae, traditionally placed in the suborder Gasterosteoidei, order Scorpaeniformes) to the order Synbranchiformes. Although the classification of indostomids as gasterosteoids had been previously questioned on the basis of mitogenomic evidence (Miya et al. 2003, 2005; Kawahara et al. 2008), it was not until the phylogenetic classification of Betancur et al. (2013, 2017) that the family Indostomidae was transferred to the order Synbranchiformes. This proposal, however, was not adopted by the most authoritative contemporary standard references of fish systematics (Van Der Laan et al. 2014; Nelson et al. 2016), on the grounds of lack of morphological support and the need for further corroboration. It should be noted that previous molecular phylogenetic studies that cast doubt on the traditional placement of indostomids, whether based on "legacy" markers (Betancur-R. et al. 2013; Betancur-R et al. 2017) or complete mitochondrial genomes (Miya et al. 2003, 2005; Kawahara et al. 2008), relied on a very limited representation of synbranchiform diversity. In contrast, our phylogenetic analysis used mitogenomic data from a comparatively larger taxon sampling that included eight synbranchiform species from five genera (*Ophisternon*, *Synbranchus*, *Monopterus*, *Mastacembelus*, and *Macrognathus*) and two families (Synbranchidae, Mastacembelidae). Notably, our phylogenetic results (Fig. 6) corroborate the notion that indostomids are more closely related to synbranchiforms than to gasterosteoids. Nevertheless, contrary to the findings of studies that have recently challenged the traditional classification of indostomids with respect to synbranchiforms (Kawahara et al. 2008; Betancur-R. et al. 2013; Betancur-R et al. 2017), our inferred phylogenetic placement of *Indostomus* does not render Synbranchiformes paraphyletic. With the caveat that our sampling of synbranchiforms and closely related lineages is only partial, our results imply that indostomids are in fact the sister lineage of the order Synbranchiformes. While this phylogenetic pattern (topology) might be considered sufficient for lumping indostomids with synbranchiforms, examination of relative branch lengths (Fig. 6) suggests that *Indostomus* is indeed a highly divergent lineage. In order to acknowledge their genetic and morphological (Britz and Johnson 2002) distinctiveness, indostomids may in fact warrant an order of their own. Within Synbranchiformes, our results remarkably do not support the monophyly of the synbranchid genus *Ophisternon*, for *O. infernale* is resolved as more closely related to *Synbranchus marmoratus* than to *O. candidum* (Fig. 6). While at first sight this novel finding of a sister-group relationship between *O. infernale* and *S. marmoratus* is certainly unexpected, this hypothesis might not be that far-fetched from a biogeographic perspective, and when considering both the striking external morphological similarity between the two genera and the taxonomic ambiguities surrounding the classificatory history of the group (Rosen and Greenwood 1976). *Synbranchus* is restricted to the New World and comprises three species: *S. marmoratus* (Central and South America), *S. madeirae* (Madeira River basin, Bolivia), and *S. lampreia* (Pará, Brazil). *Ophisternon* as currently delimited exhibits an essentially Gondwanan distribution, with six valid species distributed in Middle America (*O. infernale*, *O. aenigmaticum*), Australia (*O. candidum*, *O. gutturale*), South

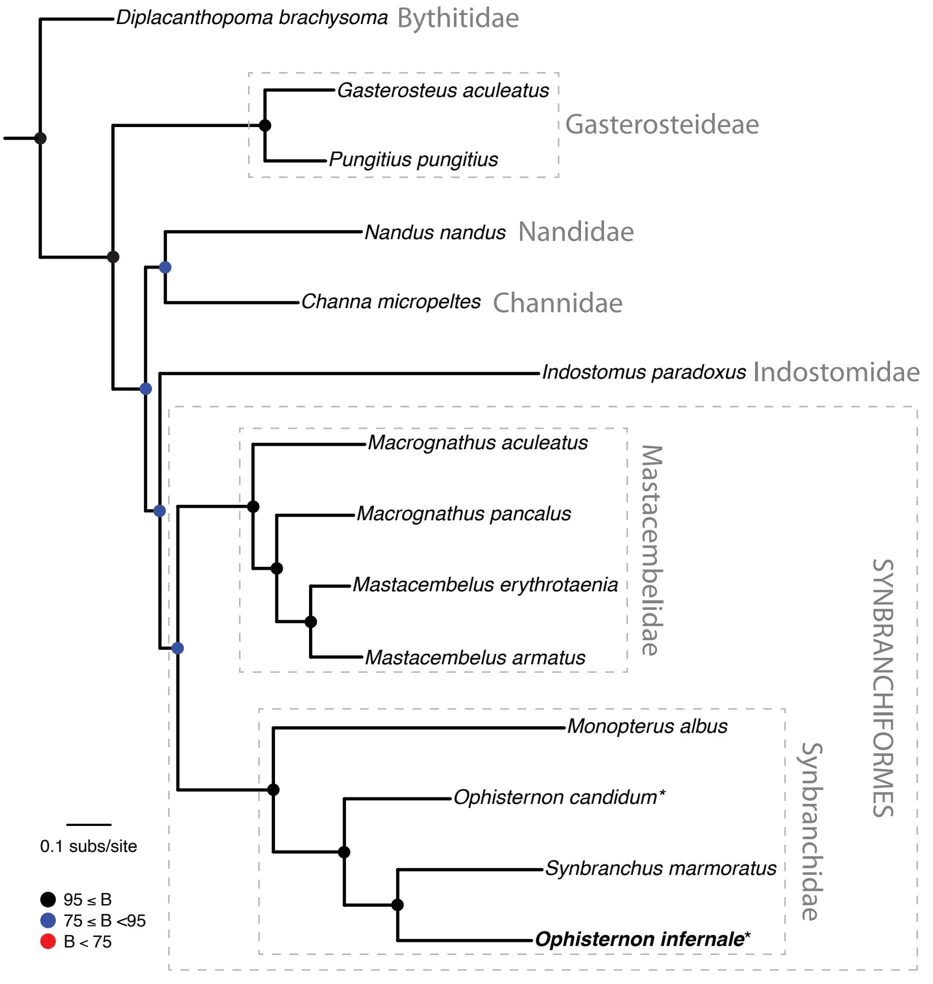

Figure 6. Phylogenetic relationships of major synbranchiform lineages. Molecular phylogeny based on comparative mitochondrial PCGs from relevant available mitogenomes and the newly generated herein for *O. infernale*. Troglobitic cave-dwelling species are marked with an asterisk to distinguish them from surface-dwelling ones. Outgroup taxa not shown. Colored circles on nodes indicate degree of clade support as determined by bootstrap values.

Asia and Western Pacific (*O. bengalense*), and West Africa (*O. afrum*). Assuming that Gondwanan drift vicariance is the main process responsible for the present-day globally disjunct distribution of the genus (Rosen 1975), the split between the Mexican-endemic *O. infernale* and the West Australian-endemic *O. candidum* should be at least as old as the Middle Jurassic separation of Eastern Gondwana (Antarctica, Madagascar, India, and Australia) from Western Gondwana (South America and Africa), dated at ca 165 Ma (McLoughlin 2001). From this it follows that the split between *Ophisternon* and *Synbranchus* should be even older. Notably, the only phylogenetic study that has investigated divergence times via molecular dating in a group of synbranchiforms (Perdices et al. 2005) estimated a comparatively much younger age (< 20 Ma) for the split between *Ophisternon* (*aenigmaticum*) and *Synbranchus* (*marmoratus*). Although marine dispersal and extinction could be invoked in an attempt to reconcile biogeographic patterns with our admittedly limited knowledge of the timescale of synbranchiform diversification, the paraphyly of *Ophisternon* remains problematic. Our phylogenetic results coupled with the abovementioned estimates of synbranchid divergence times (Perdices et al. 2005) lead us to hypothesize that perhaps New World species of *Ophisternon* (*O. infernale* and *O. aenigmaticum*) are in fact more closely related to *Synbranchus* species than to the remaining *Ophisternon* species. As such, New World species of *Ophisternon* would have to be transferred to the genus *Synbranchus*. This phylogenetic scenario is also compatible with a likely very recent origin of the cave-dwelling *O. infernale*. Although there is virtually no information regarding the timing of origin and colonization of the fishes that inhabit the cenotes and submerged caves of the YP karstic aquifer (Arroyave et al. 2021), these aquatic habitats are supposed to be extremely young, effectively established not before 20,000 years ago, at the end of the last glacial maximum in the Northern Hemisphere, when rising sea levels eventually resulted in the flooding of karstic sinkholes and dry caves (Coke IV 2019). Such a recent origin for *O. infernale* is certainly much easier to explain as a result of speciation from a fellow New World lineage, such as *O. aenigmaticum* or *S. marmoratus*. Regardless of the appeal and feasibility of these hypotheses concerning the systematics of New World *Ophisternon* in general and the origins of *O. infernale* in particular, our phylogenetic findings and their interpretation need to be taken with caution because of their absolute reliance on mtDNA only. It is well known that the mitochondrial genome is effectively a single locus (Avise 2012), that individual gene and species trees are not always congruent (Maddison 1997), and that nuclear and mtDNA inheritance patterns are not always congruent either (Funk and Omland 2003). Notwithstanding these limitations, our results emphasize the pressing need for a comprehensive systematic and biogeographic study of synbranchiform fishes, ideally based on genome-wide sequence data.

Conclusions

The first complete annotated mitochondrial genome of *O. infernale*, herein reported, exhibits an organization and arrangement similar to that of other synbranchiform fishes as well as of more distantly related teleosts. Based on our comparative mitogenomic dataset, most mitochondrial PCGs in synbranchiforms appear to have evolved under strong purifying selection, which has prevented major structural and functional protein changes. The few instances of mtDNA PCGs under positive selection might be related to adaptation to decreased oxygen availability and the evolution of more metabolically efficient variants in hypogean synbranchiform lineages. Phylogenetic analysis of mtDNA comparative data from synbranchiforms and closely related taxa (including the indostomid *Indostomus paradoxus*) corroborate the notion that indostomids are more closely related to synbranchiforms than to gasterosteoids, but without rendering the former paraphyletic. Our phylogenetic results also suggest that New World species of *Ophisternon* might be more closely related to *Synbranchus* than to the remaining *Ophisternon* species. This novel phylogenetic hypothesis, however, should be further tested in the context of a comprehensive systematic study of the group.

Acknowledgements

The authors would like to thank the Laboratorio Nacional de Cómputo de Alto Desempeño (LANCAD) and CONACyT for granting computing time on the computer clusters Yotla, Miztli, and Xiuhcoatl, from the Laboratorio de Supercómputo y Visualización en Paralelo (LSVP) of the Universidad Autónoma Metropolitana Unidad Iztapalapa, the Dirección General de Cómputo y Tecnologías de Información y Comunicación of the Universidad Nacional Autónoma de México (DGTIC-UNAM), and the Coordinación General de Servicios de Tecnologías de la Información y las Comunicaciones of the Centro de Investigación y de Estudios Avanzados del Instituto Politécnico Nacional (CGSTIC-CINESTAV), respectively. Special thanks to cave divers Erick Sosa and Kayú Vilchis for their assistance in the field during specimen sampling.

References

Almeida D, Maldonado E, Vasconcelos V, Antunes A (2015) Adaptation of the Mitochondrial Genome in Cephalopods: Enhancing Proton Translocation Channels and the Subunit Interactions. PLoS ONE 10: e0135405. https://doi.org/10.1371/journal.pone.0135405

Andrews S (2010) FastQC: a quality control tool for high throughput sequence data. Babraham Bioinformatics, Babraham Institute, Cambridge, United Kingdom.

Arroyave J (2020) The subterranean fishes of the Yucatan Peninsula. In: Lyons TJ, Máiz-Tomé L, Tognelli M, Daniels A, Meredith C, Bullock R, Harrison I (Eds) The status and distribution of freshwater fishes in Mexico. IUCN and ABQ BioPark, Cambridge, UK and Albuquerque, New Mexico, USA, 42–44. https://portals.iucn.org/library/node/49039.

Arroyave J, Schmitter Soto JJ, Vega-Cendejas M (2019) *Ophisternon infernale*. The IUCN Red List of Threatened Species 2019. https://doi.org/10.2305/IUCN.UK.2019-2.RLTS.T15387A717292.en

Arroyave J, Martinez CM, Martínez-Oriol FH, Sosa E, Alter SE (2021) Regional-scale aquifer hydrogeology as a driver of phylogeographic structure in the Neotropical catfish *Rhamdia guatemalensis* (Siluriformes: Heptapteridae) from cenotes of the Yucatán Peninsula, Mexico. Freshwater Biology 66: 332–348. https://doi.org/10.1111/fwb.13641

Avise JC (2012) Molecular Markers, Natural History and Evolution. Springer Science & Business Media, 522 pp.

Bbole I, Zhao J-L, Tang S-J, Katongo C (2018) Mitochondrial genome annotation and phylogenetic placement of *Oreochromis andersonii* and *O. macrochir* among the cichlids of southern Africa. PLoS ONE 13: e0203095. https://doi.org/10.1371/journal.pone.0203095

Bernt M, Donath A, Jühling F, Externbrink F, Florentz C, Fritzsch G, Pütz J, Middendorf M, Stadler PF (2013) MITOS: Improved de novo metazoan mitochondrial genome annotation. Molecular Phylogenetics and Evolution 69: 313–319. https://doi.org/10.1016/j.ympev.2012.08.023

Betancur-R R, Wiley EO, Arratia G, Acero A, Bailly N, Miya M, Lecointre G, Ortí G (2017) Phylogenetic classification of bony fishes. BMC Evolutionary Biology 17: e162. https://doi.org/10.1186/s12862-017-0958-3

Betancur-R R, Broughton RE, Wiley EO, Carpenter K, López JA, Li C, Holcroft NI, Arcila D, Sanciangco M, Cureton II JC, Zhang F, Buser T, Campbell MA, Ballesteros JA, Roa-Varon A, Willis S, Borden WC, Rowley T, Reneau PC, Hough DJ, Lu G, Grande T, Arratia G, Ortí G (2013) The Tree of Life and a New Classification of Bony Fishes. PLoS Currents 5. https://doi.org/10.1371/currents.tol.53ba26640df0ccaee75bb165c8c26288

Boggs T, Gross J (2021) Reduced Oxygen as an Environmental Pressure in the Evolution of the Blind Mexican Cavefish. Diversity 13: e26. https://doi.org/10.3390/d13010026

Britz R, Johnson GD (2002) "Paradox Lost": Skeletal Ontogeny of Indostomus paradoxus and Its Significance for the Phylogenetic Relationships of Indostomidae (Teleostei, Gasterosteiformes). American Museum Novitates 2002: 1–43. https://doi.org/10.1206/0003-0082(2002)383<0001:PLSOOI>2.0.CO;2

Broughton RE, Dowling TE (1994) Length variation in mitochondrial DNA of the minnow *Cyprinella spiloptera*. Genetics 138: 179–190. https://doi.org/10.1093/genetics/138.1.179

Chan PP, Lowe TM (2019) tRNAscan-SE: Searching for tRNA Genes in Genomic Sequences. In: Kollmar M (Ed.) Gene Prediction: Methods and Protocols. Methods in Molecular Biology. Springer, New York, NY, 1–14. https://doi.org/10.1007/978-1-4939-9173-0_1

Chen C, Li YL, Wang L, Gong GY (2012) Structure of mitochondrial DNA control region of *Argyrosomus amoyensis* and molecular phylogenetic relationship among six species of Sciaenidae. African Journal of Biotechnology 11: 6904–6909. https://doi.org/10.5897/AJB11.3556

Chen X, Sonchaeng P, Yuvanatemiya V, Nuangsaeng B, Ai W (2016) Complete mitochondrial genome of the whitetip reef shark *Triaenodon obesus* (Carcharhiniformes: Carcharhinidae). Mitochondrial DNA Part A 27: 947–948. https://doi.org/10.3109/19401736.2014.926499

Chen X, Ai W, Ye L, Wang X, Lin C, Yang S (2013) The complete mitochondrial genome of the grey bamboo shark (*Chiloscyllium griseum*) (Orectolobiformes: Hemiscylliidae): genomic characterization and phylogenetic application. Acta Oceanologica Sinica 32: 59–65. https://doi.org/10.1007/s13131-013-0298-0

Coke IV JG (2019) Underwater Caves of the Yucatan Peninsula. In: White WB, Culver DC, Pipan T (Eds) Encyclopedia of Caves (Third Edition). Academic Press, 1089–1095. https://doi.org/10.1016/B978-0-12-814124-3.00127-8

Darriba D, Taboada GL, Doallo R, Posada D (2012) jModelTest 2: more models, new heuristics and parallel computing. Nature Methods 9: 772–772. https://doi.org/10.1038/nmeth.2109

DeHaan C, Habibi-Nazhad B, Yan E, Salloum N, Parliament M, Allalunis-Turner J (2004) Mutation in mitochondrial complex I ND6 subunit is associated with defective response to hypoxia in human glioma cells. Molecular Cancer 3: 1–15. https://doi.org/10.1186/1476-4598-3-19

Díaz-Jaimes P, Uribe-Alcocer M, Adams DH, Rangel-Morales JM, Bayona-Vásquez NJ (2016) Complete mitochondrial genome of the porbeagle shark, *Lamna nasus* (Chondrichthyes, Lamnidae). Mitochondrial DNA Part B 1: 730–731. https://doi.org/10.1080/23802359.2016.1233465

Edgar RC (2004) MUSCLE: a multiple sequence alignment method with reduced time and space complexity. BMC bioinformatics 5: e113. https://doi.org/10.1186/1471-2105-5-113

Felsenstein J (1985) Confidence limits on phylogenies: an approach using the bootstrap. Evolution; International Journal of Organic Evolution 39: 783–791. https://doi.org/10.1111/j.1558-5646.1985.tb00420.x

Funk DJ, Omland KE (2003) Species-Level Paraphyly and Polyphyly: Frequency, Causes, and Consequences, with Insights from Animal Mitochondrial DNA. Annual Review of Ecology, Evolution, and Systematics 34: 397–423. https://doi.org/10.1146/annurev.ecolsys.34.011802.132421

Glenn TC, Nilsen RA, Kieran TJ, Finger JW, Pierson TW, Bentley KE, Hoffberg SL, Louha S, León FJG-D, Portilla MA del R, Reed KD, Anderson JL, Meece JK, Aggery SE, Rekaya R, Alabady M, Bélanger M, Winker K, Faircloth BC (2016) Adapterama I: Universal Stubs and Primers for Thousands of Dual-Indexed Illumina Libraries (iTru & iNext). Biorxiv, 1–30. https://doi.org/10.1101/049114

Gun L, Yumiao R, Haixian P, Liang Z (2018) Comprehensive Analysis and Comparison on the Codon Usage Pattern of Whole *Mycobacterium tuberculosis* Coding Genome from Different Area. BioMed Research International 2018: e3574976. https://doi.org/10.1155/2018/3574976

Hahn C, Bachmann L, Chevreux B (2013) Reconstructing mitochondrial genomes directly from genomic next-generation sequencing reads-a baiting and iterative mapping approach. Nucleic Acids Research 41: e129. https://doi.org/10.1093/nar/gkt371

Han C, Li Q, Lin J, Zhang Z, Huang J (2018) Characterization of complete mitochondrial genomes of *Mastacembelus erythrotaenia* and *Mastacembelus armatus* (Synbranchiformes: Mastacembelidae) and phylogenetic studies of Mastacembelidae. Conservation Genetics Resources 10: 295–299. https://doi.org/10.1007/s12686-017-0807-0

Huppop K (2000) How do cave animals cope with food scarcity in caves? In: Ecosystems of the World, vol. 30: subterranean ecosystems. Elsevier, Amsterdam.

Iwasaki W, Fukunaga T, Isagozawa R, Yamada K, Maeda Y, Satoh TP, Sado T, Mabuchi K, Takeshima H, Miya M, Nishida M (2013) MitoFish and MitoAnnotator: A Mitochondrial Genome Database of Fish with an Accurate and Automatic Annotation Pipeline. Molecular Biology and Evolution 30: 2531–2540. https://doi.org/10.1093/molbev/mst141

Kawahara R, Miya M, Mabuchi K, Lavoué S, Inoue JG, Satoh TP, Kawaguchi A, Nishida M (2008) Interrelationships of the 11 gasterosteiform families (sticklebacks, pipefishes, and their relatives): A new perspective based on whole mitogenome sequences from 75 higher teleosts. Molecular Phylogenetics and Evolution 46: 224–236. https://doi.org/10.1016/j.ympev.2007.07.009

Kosakovsky Pond SL, Poon AFY, Velazquez R, Weaver S, Hepler NL, Murrell B, Shank SD, Magalis BR, Bouvier D, Nekrutenko A, Wisotsky S, Spielman SJ, Frost SDW, Muse SV (2020) HyPhy 2.5–A Customizable Platform for Evolutionary Hypothesis Testing Using Phylogenies. Molecular Biology and Evolution 37: 295–299. https://doi.org/10.1093/molbev/msz197

Kozak M (1983) Comparison of initiation of protein synthesis in procaryotes, eucaryotes, and organelles. Microbiological Reviews 47: 1–45. https://doi.org/10.1128/mr.47.1.1-45.1983

Kozlov AM, Darriba D, Flouri T, Morel B, Stamatakis A (2019) RAxML-NG: a fast, scalable and user-friendly tool for maximum likelihood phylogenetic inference. Bioinformatics 35: 4453–4455. https://doi.org/10.1093/bioinformatics/btz305

Kumar S, Stecher G, Li M, Knyaz C, Tamura K (2018) MEGA X: Molecular Evolutionary Genetics Analysis across Computing Platforms. Molecular Biology and Evolution 35: 1547–1549. https://doi.org/10.1093/molbev/msy096

Lee W-J, Conroy J, Howell WH, Kocher TD (1995) Structure and evolution of teleost mitochondrial control regions. Journal of Molecular Evolution 41: 54–66. https://doi.org/10.1007/BF00174041

Li Q, Xu R, Shu H, Chen Q, Huang J (2016) The complete mitochondrial genome of the Zig-zag eel *Mastacembelus armatus* (Teleostei, Mastacembelidae). Mitochondrial DNA Part A 27: 330–331. https://doi.org/10.3109/19401736.2014.892102

Lowe TM, Chan PP (2016) tRNAscan-SE On-line: integrating search and context for analysis of transfer RNA genes. Nucleic Acids Research 44: W54–W57. https://doi.org/10.1093/nar/gkw413

Maddison WP (1997) Gene Trees in Species Trees. Systematic Biology 46: 523–536. https://doi.org/10.1093/sysbio/46.3.523

McLoughlin S (2001) The breakup history of Gondwana and its impact on pre-Cenozoic floristic provincialism. Australian Journal of Botany 49: 271–300. https://doi.org/10.1071/bt00023

Miller MA, Pfeiffer W, Schwartz T (2010) Creating the CIPRES Science Gateway for inference of large phylogenetic trees. In: 2010 Gateway Computing Environments Workshop (GCE), 1–8. https://doi.org/10.1109/GCE.2010.5676129

Miya M, Kawaguchi A, Nishida M (2001) Mitogenomic Exploration of Higher Teleostean Phylogenies: A Case Study for Moderate-Scale Evolutionary Genomics with 38 Newly Determined Complete Mitochondrial DNA Sequences. Molecular Biology and Evolution 18: 1993–2009. https://doi.org/10.1093/oxfordjournals.molbev.a003741

Miya M, Satoh TP, Nishida M (2005) The phylogenetic position of toadfishes (order Batrachoidiformes) in the higher ray-finned fish as inferred from partitioned Bayesian analysis of 102 whole mitochondrial genome sequences. Biological Journal of the Linnean Society 85: 289–306. https://doi.org/10.1111/j.1095-8312.2005.00483.x

Miya M, Takeshima H, Endo H, Ishiguro NB, Inoue JG, Mukai T, Satoh TP, Yamaguchi M, Kawaguchi A, Mabuchi K, Shirai SM, Nishida M (2003) Major patterns of higher teleostean phylogenies: a new perspective based on 100 complete mitochondrial DNA sequences. Molecular Phylogenetics and Evolution 26: 121–138. https://doi.org/10.1016/S1055-7903(02)00332-9

Nelson JS, Grande T, Wilson MVH (2016) Fishes of the world. Fifth edition. John Wiley & Sons, Hoboken, New Jersey, 707 pp. https://doi.org/10.1002/9781119174844

Nickum J, Bart Jr HL, Bowser PR, Greer IE, Hubbs C, Jenkins JA, MacMillan JR, Rachlin JW, Rose JD, Sorensen PW (2004) Guidelines for the use of fishes in research. Fisheries (Bethesda) 29: e26.

Nwobodo AK, Li M, An L, Cui M, Wang C, Wang A, Chen Y, Du S, Feng C, Zhong S, Gao Y, Cao X, Wang L, Obinna EM, Mei X, Song Y, Li Z, Qi D (2019) Comparative Analysis of the Complete Mitochondrial Genomes for Development Application. Frontiers in Genetics 9, 1–12. https://doi.org/10.3389/fgene.2018.00651

Perdices A, Doadrio I, Bermingham E (2005) Evolutionary history of the synbranchid eels (Teleostei: Synbranchidae) in Central America and the Caribbean islands inferred from their molecular phylogeny. Molecular Phylogenetics and Evolution 37: 460–473. https://doi.org/10.1016/j.ympev.2005.01.020

Perna NT, Kocher TD (1995) Patterns of Nueleotide Composition at Fourfold Degenerate Sites of Animal Mitochondrial Genomes. Journal of Molecular Evolution 41: 353–358. https://doi.org/10.1007/BF01215182

Protas M, Jeffery WR (2012) Evolution and development in cave animals: from fish to crustaceans. WIREs Developmental Biology 1: 823–845. https://doi.org/10.1002/wdev.61

Rasmussen A-S, Arnason U (1999) Phylogenetic Studies of Complete Mitochondrial DNA Molecules Place Cartilaginous Fishes Within the Tree of Bony Fishes. Journal of Molecular Evolution 48: 118–123. https://doi.org/10.1007/PL00006439

Rosen DE (1975) A Vicariance Model of Caribbean Biogeography. Systematic Zoology 24: 431–464. https://doi.org/10.2307/2412905

Rosen DE, Greenwood PH (1976) A fourth Neotropical species of synbranchid eel and the phylogeny and systematics of synbranchiform fishes. Bulletin of the American Museum of Natural History 157: 1–70.

Salinas NR, Little DP (2014) 2matrix: A utility for indel coding and phylogenetic matrix concatenation. Applications in Plant Sciences 2(1): e1300083. https://doi.org/10.3732/apps.1300083

Sambrook J, Fritsch EF, Maniatis T (1989) Molecular cloning: a laboratory manual. Molecular cloning: a laboratory manual. https://www.cabdirect.org/cabdirect/abstract/19901616061 [Accessed March 5, 2021]

Satoh TP, Miya M, Mabuchi K, Nishida M (2016) Structure and variation of the mitochondrial genome of fishes. BMC Genomics 17: 1–20. https://doi.org/10.1186/s12864-016-3054-y

Sharma A, Siva C, Ali S, Sahoo PK, Nath R, Laskar MA, Sarma D (2020) The complete mitochondrial genome of the medicinal fish, Cyprinion semiplotum: Insight into its structural features and phylogenetic implications. International Journal of Biological Macromolecules 164: 939–948. https://doi.org/10.1016/j.ijbiomac.2020.07.142

Southern ŠO, Southern PJ, Dizon AE (1988) Molecular characterization of a cloned dolphin mitochondrial genome. Journal of Molecular Evolution 28: 32–42. https://doi.org/10.1007/BF02143495

Thompson JD, Gibson TJ, Higgins DG (2003) Multiple Sequence Alignment Using ClustalW and ClustalX. Current Protocols in Bioinformatics 00: 2.3.1–2.3.22. https://doi.org/10.1002/0471250953.bi0203s00

Tomasco IH, Lessa EP (2011) The evolution of mitochondrial genomes in subterranean caviomorph rodents: Adaptation against a background of purifying selection. Molecular Phylogenetics and Evolution 61: 64–70. https://doi.org/10.1016/j.ympev.2011.06.014

Van Der Laan R, Eschmeyer WN, Fricke R (2014) Family-group names of Recent fishes. Zootaxa 3882: 1–230. https://doi.org/10.11646/zootaxa.3882.1.1

Watanabe Y, Suematsu T, Ohtsuki T (2014) Losing the stem-loop structure from metazoan mitochondrial tRNAs and co-evolution of interacting factors. Frontiers in Genetics 5: 1–8. https://doi.org/10.3389/fgene.2014.00109

White NE, Guzik MT, Austin AD, Moore GI, Humphreys WF, Alexander J, Bunce M (2020) Detection of the rare Australian endemic blind cave eel (Ophisternon candidum) with environmental DNA: implications for threatened species management in subterranean environments. Hydrobiologia 847: 3201–3211. https://doi.org/10.1007/s10750-020-04304-z

Zhao J-L, Wang W-W, Li S-F, Cai W-Q (2006) Structure of the Mitochondrial DNA Control Region of the Sinipercine Fishes and Their Phylogenetic Relationship. Acta Genetica Sinica 33: 793–799. https://doi.org/10.1016/S0379-4172(06)60112-1

Zhu K-C, Liang Y-Y, Wu N, Guo H-Y, Zhang N, Jiang S-G, Zhang D-C (2017) Sequencing and characterization of the complete mitochondrial genome of Japanese Swellshark (*Cephalloscyllium umbratile*). Scientific Reports 7: e15299. https://doi.org/10.1038/s41598-017-15702-0

ZooKeys 1089: 25–36 (2022)
doi: 10.3897/zookeys.1089.79716
https://zookeys.pensoft.net

RESEARCH ARTICLE

A peer-reviewed open-access journal
ZooKeys
Launched to accelerate biodiversity research

New species of *Urodeta* Stainton, 1869 (Lepidoptera, Elachistidae, Elachistinae) from Ghana and Democratic Republic of the Congo, with identification keys to the Afrotropical species of the genus

Virginijus Sruoga[1], Jurate De Prins[2]

1 *Life Sciences Centre of Vilnius University, Saulėtekio str. 7, LT-10257 Vilnius, Lithuania* **2** *Royal Belgian Institute of Natural Sciences, 1000 Brussels, Belgium*

Corresponding author: Virginijus Sruoga (virginijus.sruoga@gmail.com)

Academic editor: Mark Metz | Received 23 December 2021 | Accepted 16 February 2022 | Published 11 March 2022

http://zoobank.org/247A7820-2127-4510-A2BA-5C8D0A03440E

Citation: Sruoga V, De Prins J (2022) New species of *Urodeta* Stainton, 1869 (Lepidoptera, Elachistidae, Elachistinae) from Ghana and Democratic Republic of the Congo, with identification keys to the Afrotropical species of the genus. ZooKeys 1089: 25–36. https://doi.org/10.3897/zookeys.1089.79716

Abstract
Two new species, *Urodeta falcata* **sp. nov.** from Ghana and *U. bisigna* **sp. nov.** from Democratic Republic of the Congo are described. The habitus and genitalia are diagnosed and illustrated in detail. Identification keys to the Afrotropical species of the genus *Urodeta*, based on male and female genitalia, are provided.

Keywords
Microlepidoptera, mining moths, morphology, Sub-Saharan Africa, taxonomy

Introduction

The genus *Urodeta* was established by Stainton (1869) with *U. cisticolella* Stainton, 1869 as the type species. Originally, Stainton (1869) indicated its closeness to *Elachista* Treitschke, but subsequent classifications have associated it with several different families and subfamilies (De Prins and Sruoga 2012).

Moths of the genus *Urodeta* are very small to small with a wingspan of 4–8 mm. The labial palpus is porrect and shorter than the diameter of the head. The forewing pattern is mostly inconspicuous, being unicolourous or with indistinct markings. The most distinctive feature in the male genitalia is the anteriorly directed spines of the gnathos, and females are easily recognized by the apophyses anteriores, which, when present, extend from the middle of segment 8 and spread apart laterad. A more detailed list of the morphological characters diagnosing this genus have been summarized and verified by Kaila (2004, 2011) and Sruoga and De Prins (2011, 2013). The known larvae are leaf-miners in dicotyledonous plants in the families *Cistaceae* (Stainton 1869; Lhomme 1946–1963; Zerkowitz 1946) and *Combretaceae* (Kaila 2011).

Until 2009, *Urodeta* was thought to be monotypic and its distribution restricted to the Mediterranean region. Taxonomic interest in this genus increased following the description of a considerable number of new species from tropical Africa (Mey 2007; Sruoga and De Prins 2009, 2011; De Prins and Sruoga 2012), Australia (Kaila 2011) and Asia (Sruoga and De Prins 2013; Sruoga and Rocienė 2018; Sruoga et al. 2019). The genus *Urodeta* now comprises 26 accepted and validly named species (Kaila 2019) distributed in Europe, Africa, Asia and Australia, but most of the species are known from tropical Africa (Table 1). Kaila (2011) recognized one additional species, but did not name it.

Table 1. *Urodeta* species and their distributions.

Urodeta species	Distribution	Notes	References
hibernella (Staudinger, 1859)	Mediterranean Region	Male and female	Staudinger (1859); Bengtsson (1997); Koster and Sinev (2003)
falcata sp. nov.	Ghana	Male only	Present study
absidata Sruoga & De Prins, 2011	Cameroon	Male and female	Sruoga and De Prins (2011)
aculeata Sruoga & De Prins, 2011	Cameroon	Male only	Sruoga and De Prins (2011)
crenata Sruoga & De Prins, 2011	Cameroon	Male only	Sruoga and De Prins (2011)
cuspidis Sruoga & De Prins, 2011	Cameroon	Male only	Sruoga and De Prins (2011)
faro Sruoga & De Prins, 2011	Cameroon	Female only	Sruoga and De Prins (2011)
tortuosa Sruoga & De Prins, 2011	Cameroon	Female only	Sruoga and De Prins (2011)
acerba Sruoga & De Prins, 2011	Democratic Republic of Congo	Male and female	Sruoga and De Prins (2011)
bisigna sp. nov.	Democratic Republic of Congo	Female only	Present study
bucera Sruoga & De Prins, 2011	Democratic Republic of Congo	Male and female	Sruoga and De Prins (2011)
talea Sruoga & De Prins, 2011	Democratic Republic of Congo	Male and female	Sruoga and De Prins (2011)
falciferella (Sruoga & De Prins, 2009)	Kenya	Female only	Sruoga and De Prins (2009)
gnoma (Sruoga & De Prins, 2009)	Kenya	Male only	Sruoga and De Prins (2009)
spatulata (Sruoga & De Prins, 2009)	Kenya	Male and female	Sruoga and De Prins (2009)
tantilla (Sruoga & De Prins, 2009)	Kenya	Male only	Sruoga and De Prins (2009)
maculata (Mey, 2007)	Namibia	Male and female	Mey (2007)
taeniata (Mey, 2007)	Namibia	Male only	Mey (2007)
acinacella Sruoga & De Prins, 2012	South Africa	Female only	De Prins and Sruoga (2012)
quadrifida Sruoga & De Prins, 2012	South Africa	Female only	De Prins and Sruoga (2012)
trilobata Sruoga & De Prins, 2012	South Africa	Male and female	De Prins and Sruoga (2012)
jurateae Sruoga & Rocienė, 2018	India	Male and female	Sruoga and Rocienė (2018)
pectena Sruoga & Rocienė, 2018	India	Female only	Sruoga and Rocienė (2018)
noreikai Sruoga & De Prins, 2013	Nepal	Male and female	Sruoga and De Prins (2013)
longa Sruoga & Kaila, 2019	Thailand	Female only	Sruoga et al. (2019)
inusta Kaila, 2011	Australia	Male and female	Kaila (2011)
Urodeta sp.	Australia	Described, but not named; male and female	Kaila (2011)

In this study, we describe two new species in the genus *Urodeta* and provide keys to all the known Afrotropical species.

Materials and methods

Adult specimens were examined externally using MBS-10 and Euromex Stereo Blue stereomicroscopes. The forewing length was measured along the costa from wing base to the apex of the terminal fringe scales. For a wingspan, the forewing length was doubled and thorax width added. The width of the head was measured between the inner edges of the antennal bases. Genitalia were prepared following the standard method described by Robinson (1976) and Traugott-Olsen and Nielsen (1977). The genitalia were studied and some morphological structures were photographed in glycerol before permanent slide-mounting in Euparal. The male genital capsule was stained with fuchsin and the abdominal pelt with chlorazol black (Direct Black 38/Azo Black). The genital morphology was examined using a Novex B microscope. Habitus images were taken using a Canon EOS 80D camera fitted with a MP-E 65 mm Canon macro lens, attached to a macro rail (MJKZZ Qool Rail). The photographs of genitalia were made using a Novex B microscope and a E3ISPM12000KPA digital camera. The descriptive terminology of morphological structures follows Kaila (1999, 2011) and Kristensen (2003).

Type specimens are deposited in the Royal Belgian Institute of Natural Sciences, Belgium (**RBINS**).

Taxonomy

Key to the Afrotropical species of *Urodeta* species based on male genitalia

[males of the following species are unknown and not included in the key: *U. bisigna* sp. nov., *U. falciferella*, *U. quadrifida* and *U. tortuosa*]

1	Sacculus entirely separated from remaining valva as an elongate lobe	**2**
–	Sacculus not separated from remaining valva	**3**
2	Valva divided into two separate lobes (sacculus and remaining part of valva); sclerotized phallic tube not dilated basally (Sruoga and De Prins 2011, figs 25–28)	***U. acerba***
–	Valva divided into three distinct lobes (sacculus entirely separated and termen of remaining part of valva deeply emarginated so appear divided into long and narrow lobes); sclerotized phallic tube strongly dilated basally (De Prins and Sruoga 2012, figs 22 and 23)	***U. trilobata***
3	Ventral margin of sacculus partly serrated (Sruoga and De Prins 2011, figs 52–55)	***U. crenata***
–	Ventral margin of sacculus not serrated	**4**

4 Spinose knob of gnathos divided into two separated lobes (Sruoga and De Prins 2011, figs 39–41) .... ***U. bucera***
– Spinose knob of gnathos not divided **5**
5 Inner processes of valvae fused apically and embedded with many small cusp-shaped spines (Sruoga and De Prins 2011, figs 15–20) .... ***U. absidata***
– Valva without inner process embedded with spines **6**
6 Phallus with strongly sclerotized band along ventral margin 7
– Phallus without strongly sclerotized band along ventral margin **11**
7 Valvae are tightly fused together dorso-proximally (Sruoga and De Prins 2011, figs 74–76) .... ***U. talea***
– Valvae not fused together dorso-proximally **8**
8 Indentation of distal margin of juxta wider than width of juxta lobe (Sruoga and De Prins 2011, figs 35 and 36) .... ***U. aculeata***
– Indentation of distal margin of juxta is not wider than juxta lobe or juxta not indented **9**
9 Vesica with a cluster of small internal spines and two large, claw-shaped cornuti (this paper, Figs 4, 6–7, 9, and 10) .... ***U. falcata***
– Vesica with a cluster of small internal spines and more than two large cornuti **10**
10 Vesica with a cluster of small internal spines and four large cornuti (Mey 2007, figs 33 and 34) .... ***U. maculata***
11 Sclerotized phallic tube about 7 times longer than wide; vesica without cornuti (Mey 2007, figs 35 and 36) .... ***U. taeniata***
– Sclerotized phallic tube 3.5–5 times longer than wide; vesica with few large cornuti and many tiny internal spines **12**
12 Vesica with one large cornuti and with group of minute spines (Sruoga and De Prins 2011, figs 58–63) .... ***U. cuspidis***
– Vesica with more than one large cornuti and can be with group of minute spines **13**
13 Sacculus meeting cucullus at sharp angle (about 50–80°); apex of phallus pointed (Sruoga and De Prins 2009, figs 37, 39, and 40) .... ***U. gnoma***
– Sacculus meeting cucullus at blunt angle (about 110–145°); apex of phallus with broad, strongly sclerotized process (Sruoga and De Prins 2009, figs 44–47) .... ***U. spatulata***

Key to the Afrotropical species of *Urodeta* species based on female genitalia

[females of the following species are unknown and not included in the key: *U. aculeata*, *U. crenata*, *U. cuspidis*, *U. falcata* sp. nov., *U. faro*, *U. gnoma*, *U. taeniata*, *U. tantilla*]

1 Corpus bursae with signum **2**
– Corpus bursae without signum **9**
2 Corpus bursae with two signa (this paper, Fig. 14) .... ***U. bisigna***
– Corpus bursae with one signa **3**

3 Both pairs of apophysis (anterioris and posterioris) present **4**
– Apophysis anterioris absent **7**
4 Ductus bursae not coiled **5**
– Ductus bursae coiled (Sruoga and De Prins 2009, figs 41–43)...... ***U. falciferella***
5 Apophysis posterioris long, more than 9 times longer than wide **6**
– Apophysis posterioris very short, about 4.5 times longer than wide (Sruoga and De Prins 2011, figs 42–49) .... ***U. bucera***
6 Ductus bursae with longitudinal folds; signum sickle-shaped (De Prins and Sruoga 2012, figs 6–10) .... ***U. acinacella***
– Ductus bursae without longitudinal folds; signum formed by two weakly connected plates, each with a large spine and few smaller ones (De Prins and Sruoga 2012, figs 14–16) .... ***U. quadrifida***
7 Signum formed by oval sclerotized plate with one large and several small spines (De Prins and Sruoga 2012, figs 24–28) .... ***U. trilobata***
– Signum formed by weakly sclerotized plate with long teeth in row............. **8**
8 Ductus bursae coiled; corpus bursae with minute internal spines, signum formed from 6–7 stout teeth (Sruoga and De Prins 2011, figs 77–82) .... ***U. talea***
– Ductus bursae not coiled; corpus bursae without minute internal spines, signum formed from 4 stout teeth (Mey 2007, figs 30 and 31) ..... ***U. maculata***
9 Corpus bursae divided by narrow prolonged constriction into two parts (Sruoga and De Prins 2011, figs 29–32) .... ***U. acerba***
– Corpus bursae not divided **10**
10 Corpus bursae narrow and long, about 4 times longer than wide (Sruoga and De Prins 2011, figs 21 and 22) .... ***U. absidata***
– Corpus bursae rounded **11**
11 Antrum with strongly sclerotized longitudinal folds (Sruoga and De Prins 2009, figs 48 and 49) .... ***U. spatulata***
– Antrum without strongly sclerotized longitudinal folds **12**
12 Colliculum about 3 times longer than wide; antrum long and weakly sclerotized (Sruoga and De Prins 2011, figs 66–71) .... ***U. faro***
– Colliculum as long as wide; antrum short and strongly sclerotized (Sruoga and De Prins 2011, figs 85–88) .... ***U. tortuosa***

Urodeta falcata **sp. nov.**
http://zoobank.org/50E30AD5-4F6B-47E5-B9F9-3662FD9350CC
Figs 1, 2, 5–14

Material examined. ***Holotype.*** Ghana • ♂; Ashanti Bobiri, 4 km NE Kubease, 6°41'N, 1°20'W; 230 m alt.; 25 May 2011; J. & W. De Prins leg., gen. prep. VS510.

Diagnosis. *Urodeta falcata* is a small, dark-coloured species with indistinct wing markings. In wing pattern and male genitalia, the new species is most similar to *U. aculeata* Sruoga & De Prins, 2011, known from Cameroon, *U. tantilla* Sruoga

Figures 1–4. Collecting localities in Sub-Saharan Africa **1, 2** Bobiri Forest, Ashanti, Ghana **3, 4** Mayumbe Forest, Bas-Congo, Democratic Republic of the Congo.

& De Prins, 2011, known from Kenya and *U. maculata* (Mey, 2007), known from Namibia. However, *U. falcata* can be distinguished most easily by the presence of two claw-shaped cornuti, pointed apex of phallus and long ventral shield of juxta.

Description. Male (Figs 5, 6). Forewing length 2.2 mm; wingspan 5.0 mm (*N* = 1). ***Head*:** frons, vertex and neck tuft pale grey, weakly mottled with dark brown tipped scales; labial palpus vestigial, visible only as very short greyish extension; scape greyish white below, brownish grey above, pecten pale grey; flagellum pale brown, weakly annulated with darker rings basally and slightly serrated apically. ***Thorax*** and tegula strongly mottled with scales basally pale grey and distally brownish grey. Forewing: strongly mottled with scales basally pale grey and distally brownish grey; wing darker beyond middle; fringe brownish grey. Hindwing and its fringe brownish grey.

Female. Unknown.

Male genitalia (Figs 7–14). Uncus short. Spinose knob of gnathos long oval, twice as long as wide, oriented posteriorly (Fig. 12). Valva short and broad; costa concave; ventral margin of sacculus convex, distally meeting emargination of termen at a blunt angle; cucullus short and narrow, tapered apically, inner surface covered with long setae; transtilla short, strongly sclerotized. Ventral shied of juxta about 3 times as long

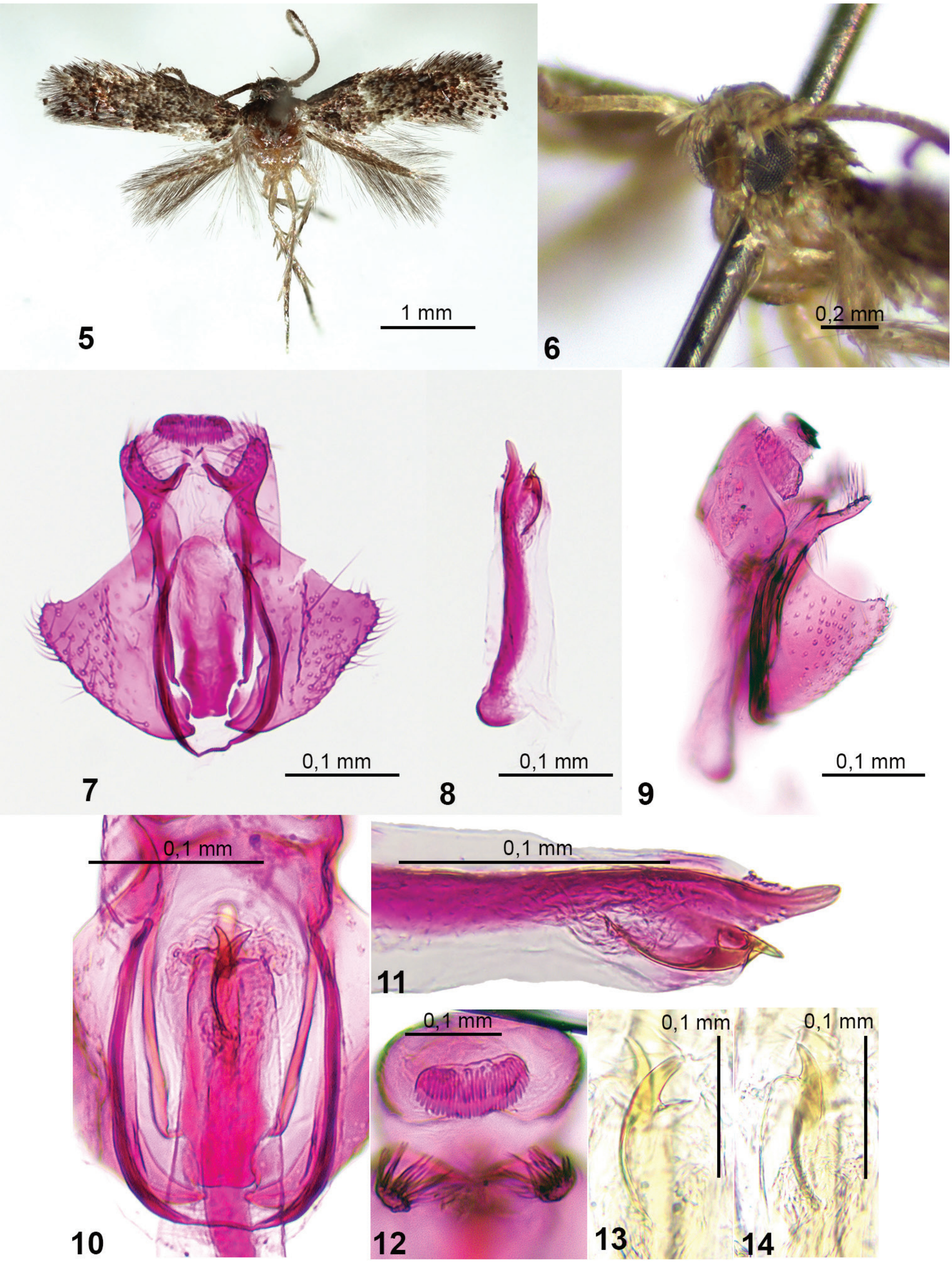

Figures 5–14. *Urodeta falcata* sp. nov., male, holotype **5** habitus **6** head, fronto-lateral view **7** general view of male genitalia (phallus removed) **8** sclerotized phallic tube **9** male genitalia, lateral view **10** central part of genitalia **11** distal part of phallus **12** gnathos and apices of cucullus, distal view **13** ventral cornutus **14** dorsal cornutus (**5, 6, 8–10** in glycerol before permanent mounting in Euparal).

as wide, strongly sclerotized. Vinculum U-shaped, proximal margin weakly concave. Sclerotized phallic tube short, as long as valva, with strongly sclerotized, wide band along ventral margin; distally tapered towards pointed apex; vesica with 2 large curved cornuti and numerous tiny, elongate spines.

Biology. Unknown.

Flight period. Based on the specimen available, adults fly in May.

Distribution. So far, this species is known only from southern Ghana (Figs 1, 2).

Etymology. The species name is derived from the Latin *falcata* (sickle-shaped) in reference to the shape of cornuti in male genitalia.

Remarks. The head of the holotype is somewhat abraded, therefore the description is approximate.

Urodeta bisigna sp. nov.

http://zoobank.org/718EA81F-1BC6-45BA-83DB-0B6F4453571A
Figs 3, 4, 15–18

Material examined. ***Holotype***. Congo Dem. Rep. • ♀; Bas-Congo, Nat. Res. Luki-Mayumbe, 05°27'S, 13°05'E; 320 m alt.; 29 Mar. 2006; J. De Prins leg., gen. prep. VS511.

Diagnosis. *Urodeta bisigna* is a small, lightly-coloured species, with indistinct wing markings. In female genitalia, the new species is comparable to Afrotropical species with vestigial apophyses and a comb-shaped signum consisting of few stout spines, i.e., *U. maculata* (Mey, 2007) known from Namibia, *U. bucera* Sruoga & De Prins, 2011 and *U. talea* Sruoga & De Prins, 2011, known from Democratic Republic of the Congo. However, *U. bisigna* is distinguished most easily by its additional irregularly shaped signum.

Description. Female (Figs 15, 16). Forewing length 2.2 mm; wingspan 5.0 mm ($N = 1$). ***Head*:** frons, vertex and neck tuft creamy white, neck tuft weakly mottled with brown tipped scales; labial palpus vestigial, visible only as very short greyish extension; scape creamy white, mottled with brown tipped scales above, pecten creamy white; flagellum greyish brown, annulated with paler rings basally and slightly serrated apically. ***Thorax*** and tegula creamy white, mottled by brown tipped scales. Forewing: creamy white powdered with brownish creamy tipped scales. Denser grey brown scales forming two irregular patches: one in basal part of wing; other extending obliquely at 2/5 of costa towards tornus of wing. Blackish brown scales forming two small irregular spots: one at 2/5 of costa and other opposite at dorsum; fringe greyish white. Hindwing and its fringe pale brownish grey.

Male. Unknown.

Female genitalia (Figs 17, 18). Papilla analis very short, ventral surface setose. Apophysis posterioris vestigial, visible only as tiny extension basolaterally, apophysis anterioris absent. Ostium bursae situated in membrane between sterna 7 and 8. Antrum and colliculum not distinct. Ductus bursae very long, spirally coiled in proximal

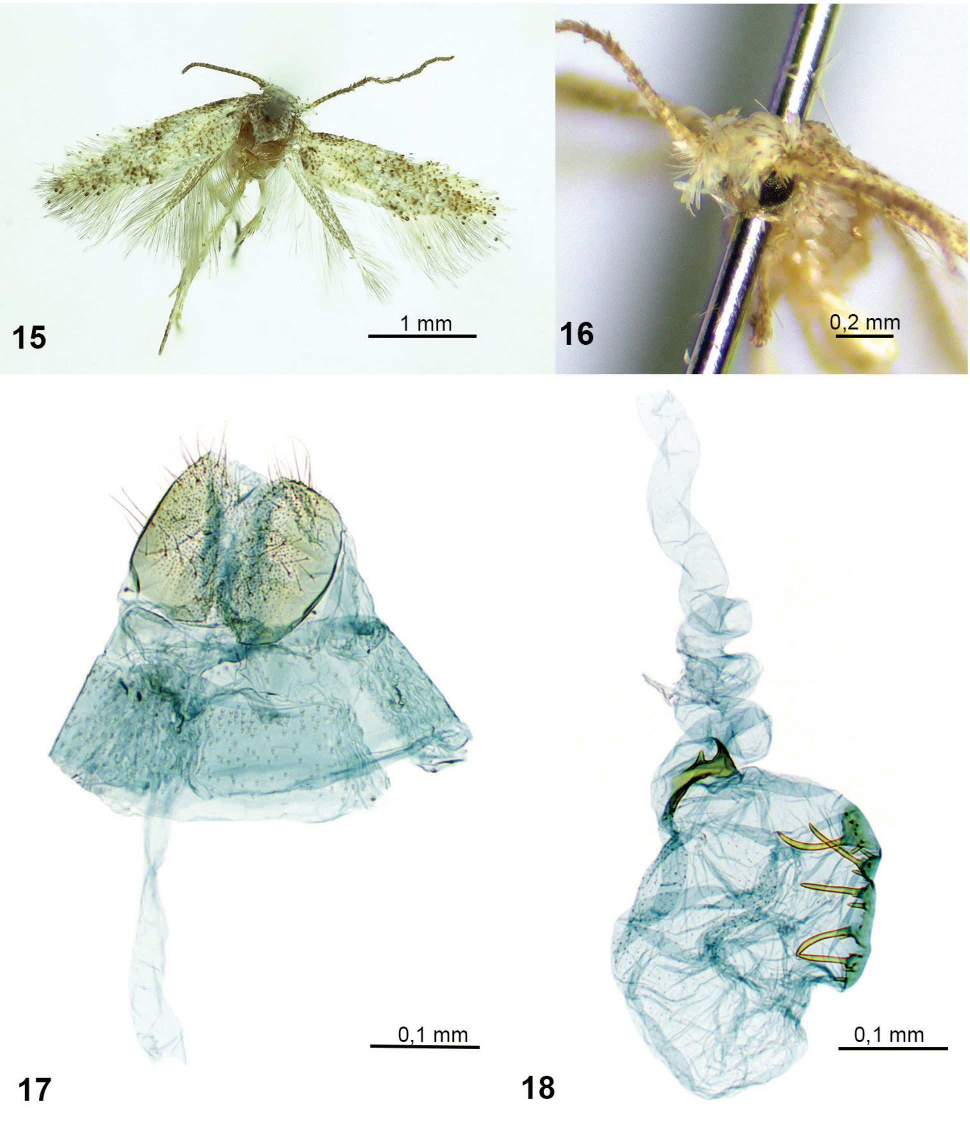

Figures 15–18. *Urodeta bisigna* sp. nov., female, holotype **15** habitus **16** head, fronto-lateral view **17** caudal part of female genitalia **18** ductus and corpus bursae.

1/2. Corpus bursae with minute internal spines and two signa, one comb shaped, consisting of 5 stout teeth, slightly varying in size and few smaller spines; another signum irregularly shaped, with one short spine.

Biology. Unknown.

Flight period. Based on the specimen available, adults fly in March.

Distribution. So far, this species is known only from western Democratic Republic of the Congo (Figs 3, 4).

Etymology. The species name is derived from the Latin prefix *bi* (two), and signum in reference to presence of two signa in female genitalia.

Remarks. The forewing in the holotype is somewhat abraded, therefore the description is approximate.

Discussion

In these times of biodiversity loss (De Prins 2022) in Central Africa and elsewhere we recognize the importance of adding two new species for science. The description of two new species brings the total number of known species of Afrotropical *Urodeta* to 20. They comprise nearly 77% of the world fauna of the genus. The largest species richness of *Urodeta* in tropical Africa is reported from Cameroon (6 spp), Democratic Republic of the Congo (4 spp), and Kenya (4 spp). With the description of *Urodeta falcata* sp. nov., the genus *Urodeta* and the subfamily Elachistinae are recorded from Ghana for the first time.

The recent discoveries of *Urodeta* species from Africa, Asia and Australia (Mey 2007; Sruoga and De Prins 2009, 2011, 2013; Kaila 2011; De Prins and Sruoga 2012; Sruoga and Rocienė 2018; Sruoga et al. 2019) show that species richness and geographical distributions are much greater than were previously assumed. The main reason for our limited understanding of this group of moths in the Afrotropical region is a lack of adequate field work. All Afrotropical species of *Urodeta* are known only from their type localities. Although a trend towards endemism of micromoths is evident (De Prins and De Prins 2011–2021), distributions of smaller, more obscure moths might change with targeted collecting efforts outside of the type localities (De Prins et al. 2009).

Acknowledgements

Virginijus Sruoga received partial support from Institute of Biosciences of Life Sciences Center (Vilnius University, Lithuania). Jurate De Prins thanks Stefan Kerkhof (RBINS, Brussels) for inspiring discussions on the Lepidoptera collection management and Frédérik Hendrickx (RBINS, Brussels) for his logistic support of taxonomic studies based on the RBINS collection. The comments of anonymous reviewers are also appreciated.

References

Bengtsson BÅ (1997) Scythrididae. In: Huemer P, Karsholt O, Lyneborg L (Eds) Microlepidoptera of Europe 2: 1–301.

De Prins J (2022) Editorial. Two urgent topics: Climate change and biodiversity loss. Phegea 50(1): 2–3.

De Prins J, De Prins W (2011–2021) Afromoths, online database of Afrotropical moth species (Lepidoptera). World Wide Web electronic publication (http://www.afromoths.net). [accessed 17 December 2021]

De Prins J, Sruoga V (2012) A review of the taxonomic history and biodiversity of the genus *Urodeta* (Lepidoptera: Elachistidae: Elachistinae), with description of new species. Zootaxa 3488(1): 41–62. https://doi.org/10.11646/zootaxa.3488.1.2

De Prins J, Mozūraitis R, Lopez-Vaamonde C, Rougerie R (2009) Sex attractant, distribution and DNA barcodes for the Afrotropical leaf-mining moth *Phyllonorycter melanosparta* (Lepidoptera: Gracillariidae). Zootaxa 2281(1): 53–67. https://doi.org/10.11646/zootaxa.2281.1.4

Kaila L (1999) Phylogeny and classification of the Elachistidae *s.s.* (Lepidoptera: Gelechioidea). Systematic Entomology 24(2): 139–169. https://doi.org/10.1046/j.1365-3113.1999.00069.x

Kaila L (2004) Phylogeny of the superfamily Gelechioidea (Lepidoptera: Ditrysia): an exemplar approach. Cladistics 20(4): 303–340. https://doi.org/10.1111/j.1096-0031.2004.00027.x

Kaila L (2011) Elachistine moths of Australia (Lepidoptera: Gelechioidea: Elachistidae). Monographs on Australian Lepidoptera. Vol. 11. CSIRO Publishing, Melbourne, x + 443 pp. https://doi.org/10.1071/9780643103481

Kaila L (2019) An annotated catalogue of Elachistinae of the World (Lepidoptera: Gelechioidea: Elachistidae). Zootaxa 4632(1): 1–231. https://doi.org/10.11646/zootaxa.4632.1.1

Koster S, Sinev S (2003) Momphidae, Batrachedridae, Stathmopodidae, Agonoxenidae, Cosmopterigidae, Chrysopeleiidae. In: Huemer P, Karsholt O, Lyneborg L (Eds) Microlepidoptera of Europe 5: 1–387. https://doi.org/10.1163/9789004473850

Kristensen NP (2003) Skeleton and muscles: adults. In: Kristensen NP (Ed.) Lepidoptera, Moths and Butterflies, 2 Morphology, physiology and development. Handbook of Zoology 4(36): 39–131. https://doi.org/10.1515/9783110893724.39 [De Gruyter, Berlin, New York]

Lhomme L (1946–1963) Catalogue des Lépidoptères de France et de Belgique. Tineina. Le Carriol, par Douelle, Lot, 489–1253.

Mey W (2007) Microlepidoptera: Smaller families. In: Mey W (Ed.) The Lepidoptera of the Brandberg Massif in Namibia. Part 2. Esperiana Memoir 4: 9–30.

Robinson GS (1976) The preparation of slides of Lepidoptera genitalia with special reference to the Microlepidoptera. Entomologist's Gazette 27: 127–132.

Sruoga V, De Prins J (2009) The Elachistinae (Lepidoptera: Elachistidae) of Kenya with descriptions of eight new species. Zootaxa 2172(1): 1–31. https://doi.org/10.11646/zootaxa.2172.1.1

Sruoga V, De Prins J (2011) New species of Elachistinae (Lepidoptera: Elachistidae) from Cameroon and the Democratic Republic of the Congo. Zootaxa 3008(1): 1–32. https://doi.org/10.11646/zootaxa.3008.1.1

Sruoga V, De Prins J (2013) A new species of *Urodeta* (Lepidoptera: Elachistidae: Elachistinae) from Nepal, the first record of the genus from Asia, showing an ancient distribution pattern. Zootaxa 3599(1): 94–100. https://doi.org/10.11646/zootaxa.3599.1.9

Sruoga V, Rocienė A (2018) Three new species of Elachistidae (Lepidoptera: Gelechioidea) from India. Zootaxa 4394(4): 575–585. https://doi.org/10.11646/zootaxa.4394.4.8

Sruoga V, Kaila L, Rocienė A (2019) The Elachistinae (Lepidoptera: Gelechioidea, Elachistidae) of Thailand, with description of eight new species. European Journal of Taxonomy 574(574): 1–34. https://doi.org/10.5852/ejt.2019.574

Stainton HT (1869) The Tineina of Southern Europe. John van Voorst, London, viii + 370 pp. https://doi.org/10.5962/bhl.title.26568

Staudinger O (1859) Diagnosen nebst kurzen Beschreibungen neuer andalusischer Lepidopteren. Entomologische Zeitung [Entomologischer Verein zu Stettin]: 211–259.

Traugott-Olsen E, Nielsen ES (1977) The Elachistidae (Lepidoptera) of Fennoscandia and Denmark. Fauna Entomologica Scandinavica 6: 1–299.

Zerkowitz A (1946) The Lepidoptera of Portugal. Journal of the New York Entomological Society 54: 115–165.

ZooKeys 1089: 37–51 (2022)
doi: 10.3897/zookeys.1089.77273
https://zookeys.pensoft.net

RESEARCH ARTICLE

A peer-reviewed open-access journal
ZooKeys
Launched to accelerate biodiversity research

A new species of anthothelid octocoral (Cnidaria, Alcyonacea) discovered on an algal reef of Taiwan

Tzu-Hsuan Tu[1], Chang-Feng Dai[2]

1 *Department of Oceanography, National Sun Yat-sen University, Kaohsiung 804, Taiwan* **2** *Institute of Oceanography, National Taiwan University, Taipei 106, Taiwan*

Corresponding author: Tzu-Hsuan Tu (thtu@mail.nsysu.edu.tw)

Academic editor: Bert W. Hoeksema | Received 29 October 2021 | Accepted 23 February 2022 | Published 16 March 2022

http://zoobank.org/7AC63168-D762-4EB5-8118-FD35110E6EE8

Citation: Tu T-H, Dai C-F (2022) A new species of anthothelid octocoral (Cnidaria, Alcyonacea) discovered on an algal reef of Taiwan. ZooKeys 1089: 37–51. https://doi.org/10.3897/zookeys.1089.77273

Abstract
A molecular phylogenetic analysis of 132 octocoral species reveals a close relationship between specimens collected from the intertidal pools of the Datan Algal Reef, Taoyuan, Taiwan, and *Erythropodium caribaeorum* (Duchassaing & Michelotti, 1860), but the two species have distinct morphological features. On the basis of morphological differences in polyps and sclerites, we identify and describe a new *Erythropodium* species: *E. taoyuanensis* **sp. nov.** The distinct identifying features of *E. taoyuanensis* **sp. nov.** include the upright contractile polyps from thin encrusting membranes and abundant 6-radiate sclerites. Using an integrative approach, we present the findings of morphological comparisons and molecular phylogenetic analyses to demonstrate that *E. taoyuanensis* **sp. nov.** is distinct from other *Erythropodium* species. Our study contributes to the knowledge of octocoral biodiversity in marginal habitats.

Keywords
28S rDNA, Anthothelidae, *cox2*-IGR-*cox1*, molecular phylogeny, *msh1*, northwestern Pacific, Scleraxonia

Introduction

The Datan Algal Reef located in northwestern Taiwan, which occupies the intertidal flat toward the sublittoral along the 27-km long coastline of Taoyuan City, is composed of crustose coralline algae. Both sandy and muddy habitats occur in a mosaic pattern within the algal reef (Kuo et al. 2020). The porous algal reefs host a relatively high benthic diversity and biomass, such as crustaceans, polychaetes, and sipunculans (Lin 2020). Because of the geographic location and availability of hard substratum, the Datan Algal Reef may be a stepping stone to connecting reef-associated species between tropical corals and non-reefal coral communities in the Taiwan Strait (Chen 2017), while the physical environment in the algal reef may be considered a marginal habitat for most corals (Kuo et al. 2020). The sedimentation rates in the Datan Algal Reef are extremely high, ranging between 3,818 and 29,166 mg cm^{-2} day^{-1} (Kuo et al. 2020), which far exceeds the rate (10 mg cm^{-2} day^{-1}) in a healthy shallow water tropical to subtropical coral reef (Rogers 1990). Therefore, the water column in rock pools is turbid and contains a high concentration of sand and particles formed by erosion, wave action, and tidal currents. Although the physical conditions may deter most corals, a stable population of the caryophyllid coral *Polycyathus chaishanensis* Lin et al., 2012 live in the tidal pool off the Datan Algal Reef (Kuo et al. 2020).

Meanwhile, the Datan Algal Reef is currently facing destruction from the development and construction of liquefied natural gas (**LNG**) storage terminals and ports by the Taiwan Chinese Petrol Corporation (**CPC**). Therefore, multiple environmental impact assessment surveys have been conducted. The intertidal surveys led to the discovery of a species of *Erythropodium* Kölliker, 1865 in the tidal pools (Lin 2020).

Erythropodium is a genus of shallow water soft corals forming endosymbiotic association with Symbiodiniaceae belonging to the family Anthothelidae Broch, 1916. Although it is widely distributed from tropical to temperate regions, its populations are not abundant (Bayer 1961). *Erythropodium* has been documented in a relatively small and fragmented geographical range, including the Caribbean Sea, the Southwestern Atlantic, northern Australia, and the Solomon Islands, with only three nominal species recorded worldwide (Duchassaing and Michelotti 1860; Bayer 1961; Utinomi 1971; Carpinelli et al. 2020). Furthermore, *Erythropodium* has not been recorded in the North Pacific Ocean. Its traditional diagnostic morphological features include thick encrusting sheet-like colonies without conspicuous upright lobes or branches, predominant 6-radiate sclerites, and a purplish red coenenchyme surface (Kölliker 1865; Bayer 1961, 1981) separate it from other genera within Anthothelidae. *Erythropodium caribaeorum* (Duchassaing & Michelotti, 1860), the type species of this genus is originally distributed in the Caribbean Sea and has invaded into the Southwestern Atlantic Ocean (Carpinelli et al. 2020). The other two species only reported in their type locality include *E. salomonense* Thomson & Mackinnon, 1910 in the Indian Ocean and *E. hicksoni* (Utinomi, 1971) in the south Pacific Ocean. Here, we describe and illustrate an additional species, *E. taoyuanensis* sp. nov. The freshly collected material was also subjected to molecular phylogenetic analyses, the results of which substantiated the taxonomic findings that led us to assign the new *Erythropodium* species.

Materials and methods

Collection and morphological analysis

Based on an environmental impact assessment report, the Datan Algal Reef, Taoyuan, Taiwan was divided into two subsections, Datan G1 and Datan G2 (Kuo et al. 2020). Collection and observation were conducted in Datan G2, during the spring low tide on June 24, 2021. Specimens were collected by reef walking and stored in seawater. After collection, one of the specimens (NMMB-CR000148) was preserved in absolute ethanol, and the remaining specimens were maintained in seawater with the addition of magnesium chloride overnight and then preserved in 75% ethanol. The holotype and paratypes are deposited at the National Museum of Marine Biology and Aquarium, Pingtung County, Taiwan (**NMMB-CR**). Selected fragments from four specimens were dissolved in sodium hypochlorite to examine sclerites under both light microscope and scanning electron microscope (S-3000N, Hitachi, Japan).

Molecular phylogenetic analysis

Polyps from four colonies (NMMB-CR000148 to NMMB-CR000151) were used to extract DNA. DNeasy PowerSoil Kit (Qiagen, CA, USA) was used for DNA extraction, according to the manufacturer's protocol. The primer pair COII8068XF and COIoctR was used to amplify *cox2*-IGR-*cox1* (France and Hoover 2002; McFadden et al. 2011). Furthermore, we designed a new primer pair (MSH-Antho-F: ARTTCTATGAACTTTGGCATGAGC and MSH-Antho-R: YTAGCATVGGGTTCAGAGGG) from sequences of Anthothelidae including *Erythropodium*, *Anthothela*, and *Iciligorgia* to amplify partial *mtMutS* region. The nuclear *28S rDNA* was amplified according to Halàsz et al. (2015), using the primers 28S-Far and 28S-Rab (McFadden and van Ofwegen 2013). The amplicons were purified and further sequenced using the ABI 3730 DNA Analyser. The sequences of NMMB-CR000148 were deposited in GenBank with accession numbers, OK480042, OK483343, and OK482879 for *cox2*-IGR-*cox1*, *mtMutS*, and *28S rDNA*, respectively and compared with sequences listed in McFadden and van Ofwegen (2012) and partial species in van der Ham et al. (2009) (Suppl. material 1: Table S1).

The obtained sequences were edited using Geneious Prime v. 2021.2.2 (Biomatters, New Zealand) aligned to data from McFadden and van Ofwegen (2012) and partial species in van der Ham et al. (2009) using MUSCLE alignment. Maximum-likelihood (ML) analyses were run using RAxML-NG v. 1.0.3 (Kozlov et al. 2019) with TVM+I+G and GTR+I+G models applied to mitochondrial genes and 28S rDNA, respectively. Bayesian inference (BI) was run using MrBayes v. 3.2.7 (Huelsenbeck and Ronquist 2001) with the same data partitions, while a GTR model was applied separately to each partition because MrBayes does not support the TVM model. Topologies were edited using FigTree v. 1.4.4 (accessible at http://tree.bio.ed.ac.uk/software/figtree/). Because the stoloniferan genus *Cornularia* Lamarck, 1816 is the sister taxon to all other octocorals, the sequences of *C. cornucopiae* (Pallas, 1766) and *C. pabloi* McFadden & van Ofwegen, 2012 were used as outgroups to root the phylogenetic trees (McFadden and van Ofwegen 2012).

Results

Taxonomy

The following key used to identify species of *Erythropodium* is based on the original descriptions of *E. caribaeorum*, *E. hicksoni*, and *E. salomonense* (Duchassaing and Michelotti 1860; Thomson and Mackinnon 1910; Utinomi 1971), Bayer's (1961) description of *E. caribaeorum*, and the direct examation of type specimens of the new described *E. taoyuanensis* sp. nov.

Key to species of *Erythropodium*

1	Coenenchyme thin generally < 1 mm. Polyps contractile, do not fully retract into coenenchyme	***E. taoyuanensis* sp. nov.**
–	Coenenchyme thick generally > 1 mm. Polyps retractile, fully retract into coenenchyme	**2**
2	Sclerites in the form of rod present	***E. caribaeorum***
–	Sclerites in the form of rod absent	3
3	Coenenchymal sclerites are capstan-like triradiates or tetraradiates	***E. hicksoni***
–	Coenenchymal sclerites are double-spheres	***E. salomonense***

Systematics

Class Anthozoa Ehrenberg, 1831
Subclass Octocorallia Haeckel, 1866
Order Alcyonacea Lamouroux, 1812
Family Anthothelidae Broch, 1916
Genus *Erythropodium* Kölliker, 1865

***Erythropodium taoyuanensis*, sp. nov.**
http://zoobank.org/A83374ED-B308-4C8C-9708-531A5A32840C
Figs 1–4

Material examined. ***Holotype.*** Taiwan, Taoyuan, Datan Algal Reef; 25°02'7.849"N, 121°02'56.059"E; –30 cm (below sea level); 24 Jun. 2021; T.-H. Tu and E.-J. Lin leg.; tidal pool, hand collecting; GenBank: OK480042, OK483343, and OK482879; NMMB-CR000148.

Paratype. Taiwan; same data as holotype; NMMB-CR000149.

Other material. Taiwan; same data as holotype; 21 Sep. 2020; NMMB-CR000150.Taiwan; same data as holotype; 21 Sep. 2020; M.-H. Lin and L.-C. Liu leg.; NMMB-CR000151.

Diagnosis. The holotype colony is composed of upright polyps arising separately from a encrusting membrane less than 1 mm thick or a network of ribbon-like stolons. When fully extended, polyps are around 3 mm long, and the tentacles are slender with 10–13 pairs of pinnules on either side of the rachis. Polyps are contractile and cannot fully retract into the basement layer. Sclerites are mostly 6-radiate sclerites, with a few being irregular radiates. When alive, polyps are yellowish pink, and the basement layer is magenta.

Description of the holotype. (Figs 1, 2). ***Colonial morphology.*** The holotype is an encrusting colony and attaching on barnacles and coralline algal substrate. When alive, the colony consisted of densely distributed polyps, up to 20/cm^2, arising from the basement layer, which is completely covered by sand (Fig. 1a). In its preserved state, the holotype measures 57.0 mm × 33.8 mm × 22.8 mm. The thickness of the basal membrane in the alcohol-preserved holotype is less than 1 mm.

Polyps. When fully extended, the polyps may attain approximately 2.5–3.0 mm in length (Fig. 1b). The fully spread tentacles are cylindrical, slender, and up to 2.5 mm × 0.8 mm, with 10–13 pairs of pinnules arranged in a single row on either side of the tentacle rachis (Fig. 1b). The polyps are contractile in both live and preserved state (Fig. 1); when contracted, they are cylindrical and measuring from the attachment at stolons to the tentacle base are around 1.5 mm in width (Fig. 1c, d). The pinnules (0.2–0.9 mm long) gradually taper at the end to a sharp tip. The polyps are associated with symbiotic unicellular algae.

Sclerites. Sclerites are present in all parts of the holotype and evenly distributed in the coenenchyme, polyp body wall, tentacles, and pinnules. Six-radiate sclerites are the commonest type, representing more than 90% of sclerites in anthocodiae and tentacles. They are 0.032–0.068 mm in length and 0.025–0.036 mm in width with simple tubercles (Fig. 2a). The polyp wall contains abundant 6-radiate sclerites, derivatives of radiates which are 0.028–0.132 mm in length and 0.025–0.083 mm in width, with prominent tubercles and table-radiates (Fig. 2b). The average size of sclerites in the polyp wall is greater than that in the polyps. Sclerites in the cortex are similar to those of the polyp wall but larger in size, including 6-radiate sclerites (0.042–0.120 mm in length and 0.034–0.076 mm in width) and irregular radiates (0.046–0.080 mm in length and 0.100–0.130 mm in width) (Fig. 2c). Furthermore, some sclerites in the cortex are fused to form clumps.

Color. In life, colors of tissue, autozooids, and cortical layer are translucent, white to yellowish, and pink to magenta, respectively. Under light microscope, sclerites are translucent, magenta, or reddish.

Variation. Paratype (NMMB-CR000149) and non-type specimens (NMNB-CR000150 and NMNB-CR000151) show variation in the density of polyps ranging 5–20/cm^2. Six-radiate sclerites are the commonest type of sclerites in the examined specimens, while their sizes are varied not only in different parts of a colony but also differ from what was observed in the holotype and across the specimens.

The length and width of 6-radiate sclerites in the examined specimens is 0.020–0.068 mm and 0.020–0.053 mm, respectively, in polyp tissue; 0.024–0.098 mm and 0.018–0.070 mm, respectively, in polyp wall; and 0.022–0.118 mm and 0.026–0.075 mm, respectively, in cortex (Figs 3, 4). All examined specimens possess similar diagnostic features as the holotype from the level of colony to sclerits including upright polyps arising from a encrusting membrane, contraticle polyps, and predominant six-radiate sclerites. The major differences between examined specimens are reflected in the density and size variation of polyps and sclerites, respectively.

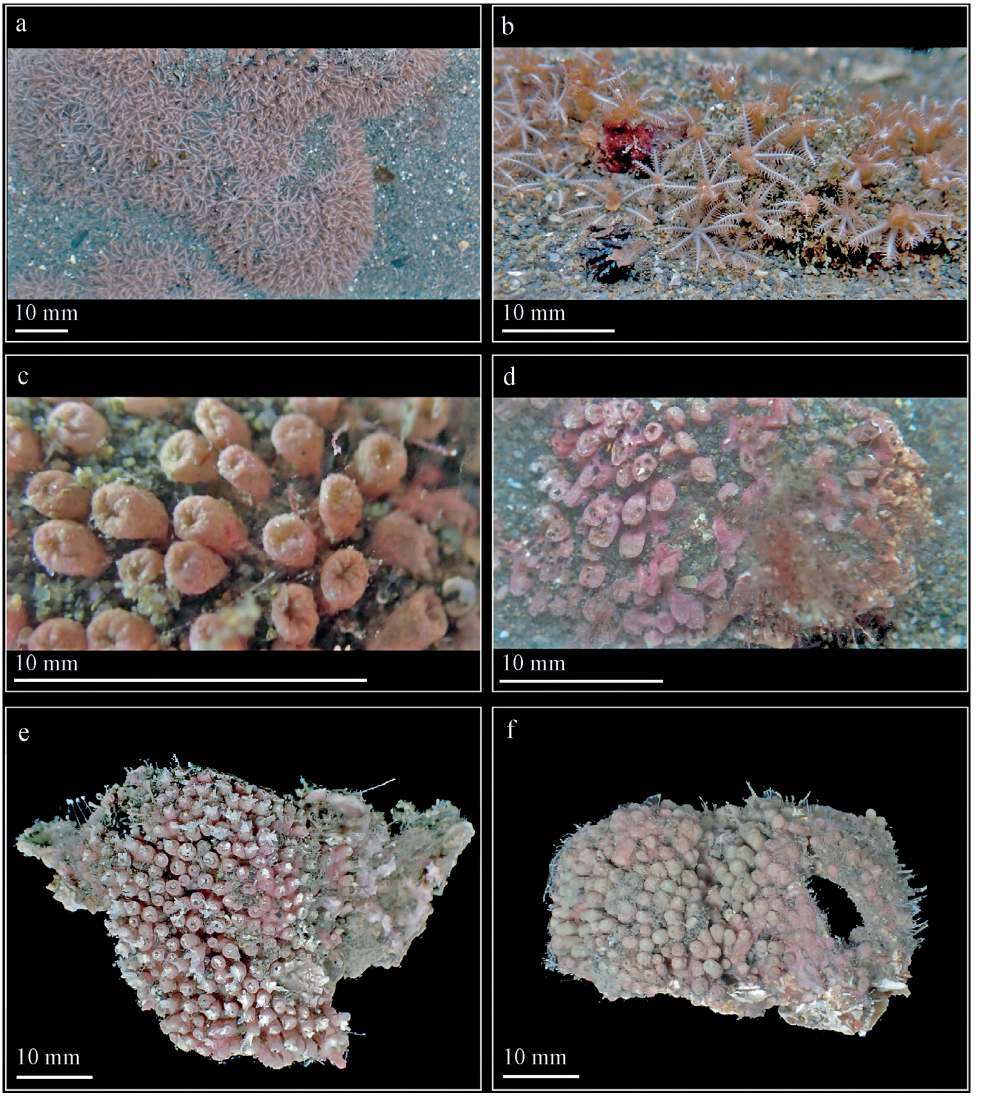

Figure 1. *Erythropodium taoyuanensis* sp. nov. **a** intertidal population *in situ* **b** close-up of **a c, d** contracted polyps *in situ* **e** holotype (NMMB-CR000148) in preserved state **f** paratype (NMMB-CR000149) in preserved state.

Differential diagnosis. When comparing the morphology of *E. taoyuanensis* sp. nov. to the other three *Erythropodium* species, basal membrane, pinnule arrangement, retractile or contractile ability of polyps, and shape and size of sclerites (Table 1) were examined, with the contractibility of polyp and shape of sclerites considered as the most distinct characters.

According to Duchassaing and Michelotti (1860), Bayer (1961), and Carpinelli et al. (2020), the diagnostic features of *E. caribaeorum* include an encrusting and membranous carpet-like colony, retractile polyps, elongated pinnules, thick cortical layer, and predominantly 6-radiate sclerites (Table 1). While the colonies of *E. taoyuanensis* sp. nov. form firm expansions on rocks similar to the colonial form of *E. caribaeorum*, the thinner cortical layer, shorter pinnules, and contractile polyps are distinct features. Furthermore, the types and shapes of radiates are the main features to distinguish these two species. Compared with *E. caribaeorum*, *E. taoyuanensis* sp. nov. possesses irregular radiates with generally enlarged tubercles having tiny protuberances. Compared with the creamy white and 3-mm-thick basal membrane in *E. hicksoni* (Table 1), the basal membrane in *E. taoyuanensis* sp. nov. is pink in the preserved state, similar to the color as in life, and thinner—generally less than 1 mm thick. Although pinnules in both species are arranged in a single pair of rows (one at each side of a tentacle), *E. hicksoni* normally has nine pairs of pinnules per tentacle, whereas *E. taoyuanensis* has 10–13 pairs. In addition, the polyps are retractile in *E. hicksoni* but contractile in *E. taoyuanensis*. Sclerites in *E. hicksoni* include triradiates, tetraradiates, flattened rods, and spindles. However, *E. taoyuanensis* sp. nov. has only 6-radiate sclerites. Finally, *E. salomonense* and *E. taoyuanensis* sp. nov. can be distinguished by the type and shape of the radiates. Additionally, the retractile polyps in *E. salomonense* (Table 1) are distinct from the contractile polyps in *E. taoyuanensis*. The above variations support that *E. taoyuanensis* is distinct from the other nominal *Erythropodium* species.

Etymology. The specific name *taoyuanensis* alludes to the city's name, Taoyuan, where the specimens were collected.

Table 1. Diagnostic traits of nominal *Erytropodium* species.

Species name	Diagnostic traits				
	Colony	Coenenchyme	Polyp	Sclerite	References
Erythropodium caribaeorum	Encrusting, membranous carpet-like colony	Thick cortical layer, ~3 mm	Retractile polyps with elongated pinnules arragned in a single pair of rows	Dominant 6-radiate sclerites and irregular radiate scleirtes	Duchassaing and Michelotti 1860: pl. I. figs 8–11; Bayer 1961: 75; fig. 16e–h; Carpinelli et al. 2020: 177; figs 1, 2
Erythropodium hicksoni	Membranous colony	Thick cortical layer, ~3 mm	Retractile polyps with 9 pairs of pinnules per tentacle	Triradiates, quadriradiates, flattened rods, and spindles	Utinomi 1971: 8–10, fig. 2; pl. 7. fig. 3
Erythropodium salomonense	Encrusting form	Thick cortical layer, 1.5–2 mm	Retractile polyps	Spindles, double spheres, irregular sclerites	Thomson and Mackinnon 1910: 174–175; pl. 12, fig. 8; pl. 13, fig. 9
Erythropodium taoyuanensis	Encrusting, membranous carpet-like colony	Think cortical layer, generally < 1 mm	Contractile polyps with 10–13 pairs of pinnules per tentacle	Dominant 6-radiate sclerites and derivatives of radiates	Present study

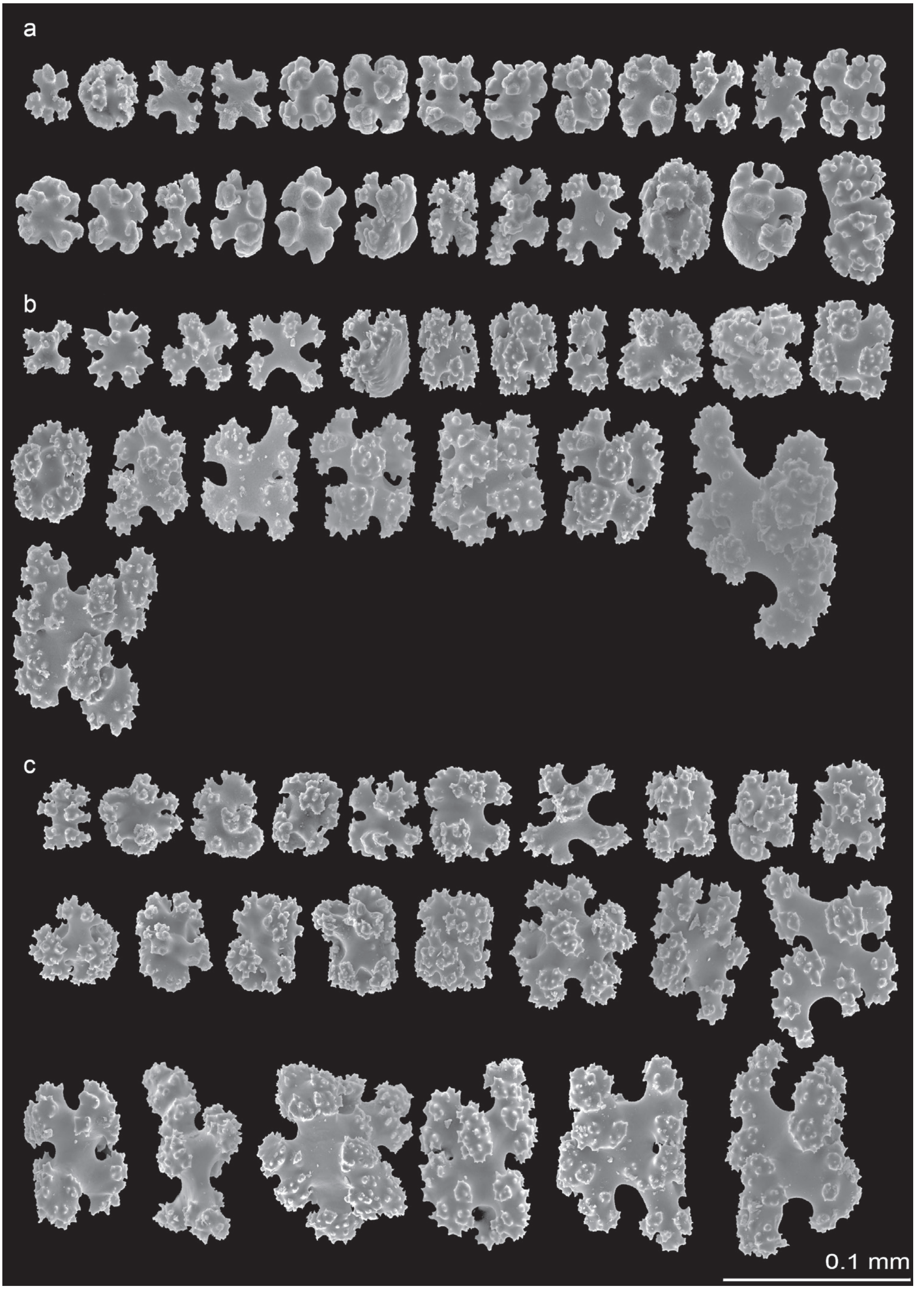

Figure 2. *Erythropodium taoyuanensis*, holotype, NMMB-CR000148 **a** sclerites of the polyp **b** sclerites of the polyp wall **c** sclerites of the cortex.

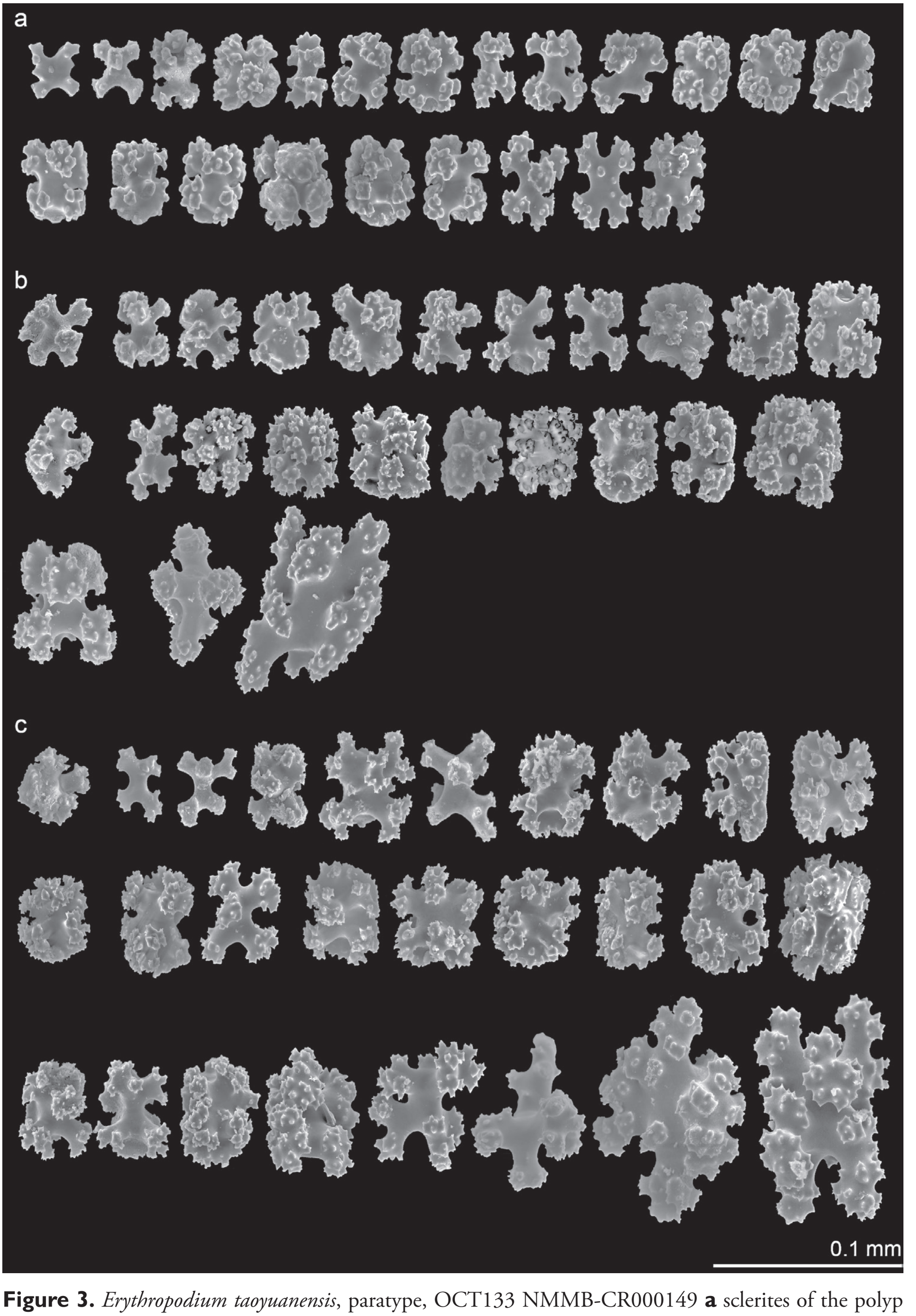

Figure 3. *Erythropodium taoyuanensis*, paratype, OCT133 NMMB-CR000149 **a** sclerites of the polyp **b** sclerites of the polyp wall **c** sclerites of the cortex.

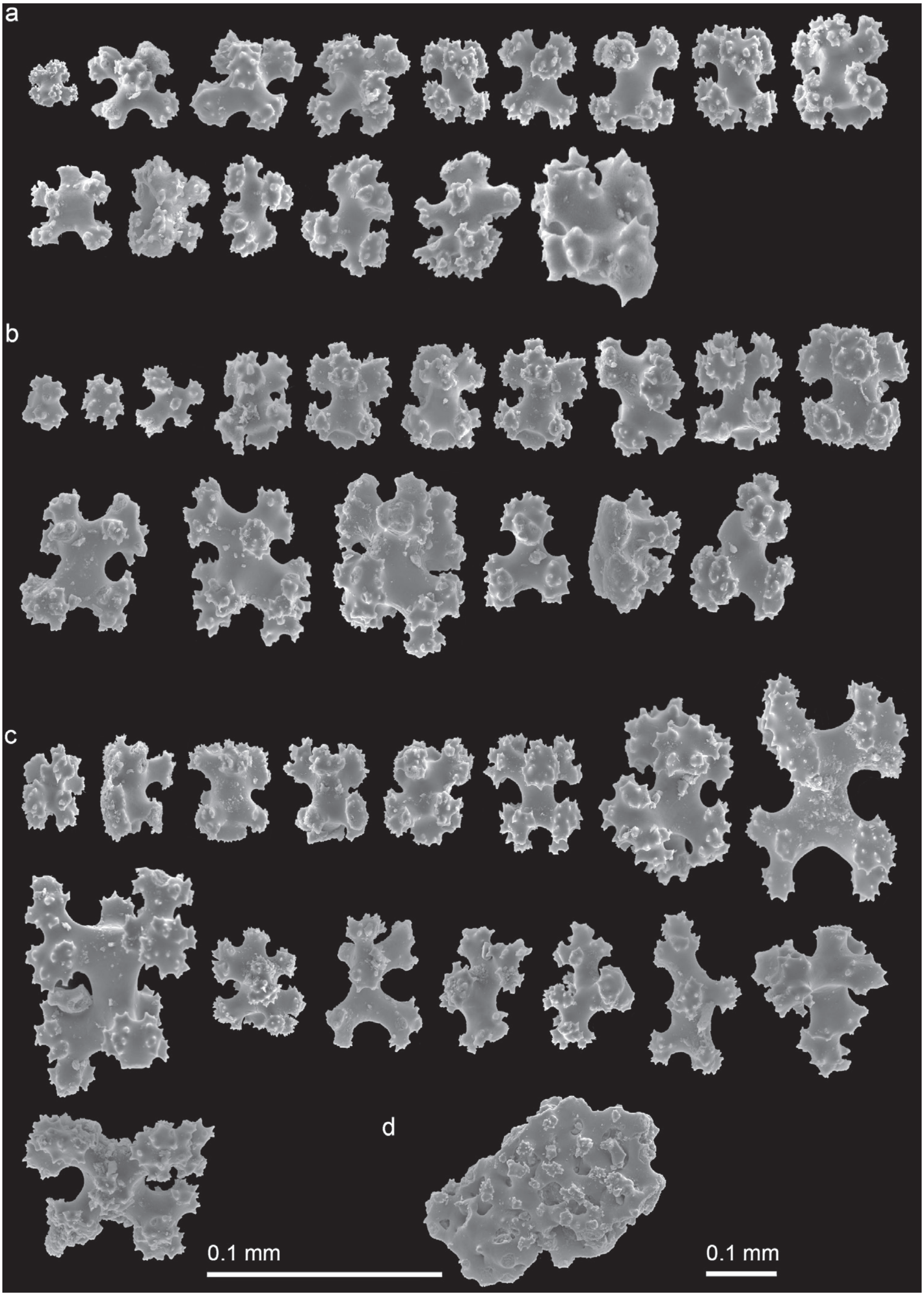

Figure 4. *Erythropodium taoyuanensis*, NMMB-CR000151 **a** sclerites of the polyp **b** sclerites of the polyp wall **c** sclerites of the cortex **d** fused sclerites in the cortex.

Distribution. The Datan G2 in Datan Algal Reef, Taoyuan, Taiwan, is the only location where this species is known; it has a biodiverse coralline algal reef. *Erythropodium taoyuanensis* sp. nov. is one of the dominant sessile organisms encrusting the rocks at this location and is generally restricted to near the low tidal line, and it may be exposed to the air during the spring low tide.

Phylogenetic analyses

Sequencing nuclear *28S rDNA*, and mitochondrial *cox2*-IGR-*cox1* and *msh1* resulted in 784, 777, and 585 bps, respectively, yielding a concatenated alignment of 2542 bps containing 1641 phylogenetically informative sites. All four *E. taoyuanensis* sp. nov. specimens in this collection had identical genotypes at the sequenced regions. The genetic distances (uncorrected *p*) between the specimens from the Datan Algal Reef and *E. caribaeorum* are 6.2% at *msh1*, 3.7% *cox2*-IGR-*cox1*, and 4.5% at 28S. As has been demonstrated previously based on analyses of similar datasets (McFadden and van Ofwegen 2012, 2013), both ML and BI indicated that the concatenated alignment supported the division of octocorals into two major clades: one composed of Holaxonia–Alcyoniina and the other composed of the majority of Calcaxonia, Pennatulacea, *Heliopora*, and Scleraxonia (Fig. 5). In the latter clade, the family Parasphaerascleridae McFadden & van Ofwegen, 2013 of Alcyonacea is strongly supported as the sister taxon to a group consisting of previously recognized Calcaxonia–Pennatulacea and *Anthomastus*–Coralliidae clades, and a small subgroup of a heterogenous mix of scleraxonians plus the stoloniferan genus *Telestula* Madsen, 1944 (Fig. 5). Both phylogenetic analyses placed specimens of *E. taoyuanensis* sp. nov. in the subgroup composed of heterogeneous scleraxonians including the genera *Erythropodium*, *Ideogorgia*, *Homophyton*, and *Diodogorgia* of Anthothelidae and *Briareum* of Briaeidae (Fig. 5) with strong support (ML bootstrap = 100%; BI poster probability = 1.0). Within the subgroup, both ML and BI indicated that *E. taoyuanensis* sp. nov. is a sister taxon to *E. caribaeorum* (GenBank accession number: GQ342480, specimen RMNH.Coel. 40829).

Discussion

Erythropodium taoyuanensis sp. nov. has only been discovered in the tidal pools at Datan G2 of the Datan Algal Reef. The tidal pool is periodically exposed to air and experiences variation in salinity, dissolved oxygen content, and temperature. Therefore, it is not a typical habitat for octocorals, and only a couple of species of *Sinularia* or *Asterospicularia* of Xeniidae have been observed in Taiwanese reefs (Dai 1991; Benayahu et al. 2004). By contrast, the low-water level also brings plentiful sunlight, which helps intertidal plant life grow quickly. In the Datan Algal Reef, the water column has a high sediment rate (Kuo et al. 2020). Therefore, living in tidal pools might help the zooxanthellate *E. taoyuanensis* overcome the turbid water. *Erythropodium taoyuanensis* sp. nov. is the first *Erythropodium* species identified to be distributed in the subtropical Indo-

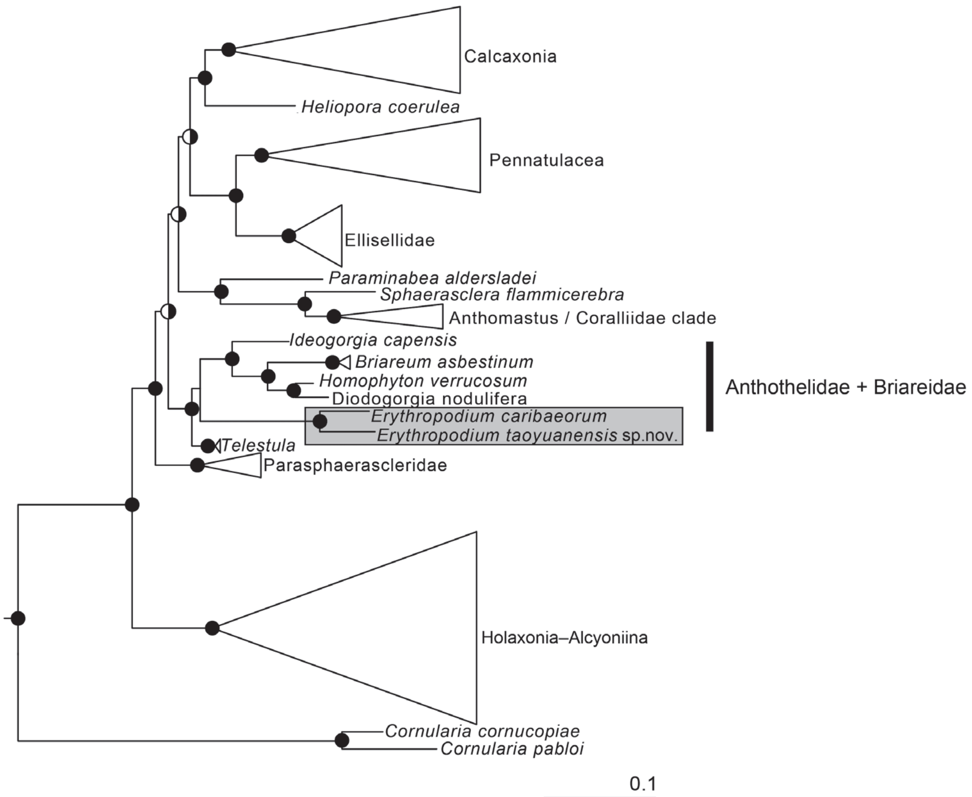

Figure 5. Phylogenetic relationship reconstruction (2543 nt of concatenated *msh1*, *cox2*-IGR-*cox1*, *28S rDNA*) of the Holaxonia–Alcyoniina clade of Octocorallia. Solid circles at nodes indicate strong support from both maximum-likelihood (bootstrap value > 70%) and Bayesian inference (posterior probability > 0.95); split circles indicate strong support from one analysis only (left half solid: supported by maximum-likelihood; right half solid: supported by Bayesian analyses).

Pacific Ocean; other *Erythropodium* species have been reported in the Caribbean Sea, southwestern Atlantic, and temperate waters of the Indo-Pacific (Bayer 1961; Utinomi 1971; Carpinelli et al. 2020). This study is also the first to document an *Erythropodium* species off Taiwan. Meanwhile, the restricted distribution of *E. taoyuanensis* sp. nov. and members of *Erythropodium* in Taiwan further emphasize that their conservation is urgent. Unfortunately, their only known habitat, the Datan Algal Reef, is currently polluted by concrete from the construction of LNG receiving terminals and ports.

Morphologically, the specimens (NMMB-CR000148 to NMM-CR000151) collected from the Datan Algal Reef possessed the diagnostic feature of *Erythropodium*, such as thin, firm colony expansions on rocks and sclerites that are all derivatives of 6-radiate sclerites (Kölliker 1865; Bayer 1961). Therefore, they are considered to be an *Erythropodium* species, while the morphological features of polyps and composition of sclerites subsequently separate the specimens from the nominate species of *Erythropodium*.

As the orginal descriptions of the three norminal *Erythropodium* species were based on the light-microsope observations and lacking definite figures representing diaonstic features, a future thorough redescription of the type specimens will contribute towards further identification of this genus. Molecular evidence has revealed that the genetic distances between the specimens from the Datan Algal Reef and *E. caribaeorum* are greater than general intraspecific variation of most octocorals, thereby further supporting that the specimens are a new *Erythropodium* species. Although *E. salomonense* and *E. hicksoni* were not included in our molecular analyses, the distinct morphological features still support the separation of *E. taoyuanensis* sp. nov. from the two nominal species. In summary, the new species described here is supported by both morphological and molecular evidence.

Acknowledgements

We thank M.-H. Lin, L.-C. Liu, and E.-J. Lin for assistance with collection of samples and fieldwork. P.-H. Chen assisted with DNA sequencing. Financial support was provided by the Taiwanese Ministry of Science and Technology (MOST 109-2116-M-110-001-MY3).

References

Bayer FM (1961) The shallow-water Octocorallia of the West Indian region. Studies on the Fauna of Curaçao and Other Caribbean Islands 12: 1–373.

Bayer FM (1981) Key to the genera of Octocorallia exclusive of Pennatulacea (Coelenterata: Anthozoa), with diagnoses of new taxa. Proceedings of the Biological Society of Washington 94: 902–947.

Benayahu Y, Jeng MS, Perkol-Finkel S, Dai CF (2004) Soft corals (Octocorallia: Alcyonacea) from southern Taiwan: II. Species diversity and distributional patterns. Zoological Studies (Taipei, Taiwan) 43: 548–560.

Carpinelli ÁN, Cordeiro RTS, Neves LM, De Moura RL, Kitahara MV (2020) *Erythropodium caribaeorum* (Duchassaing & Michelotti, 186) (Cnidaria: Alcyonacea), an additional alien coral in the Southwestern Atlantic. Zootaxa 4822(2): 175–190. https://doi.org/10.11646/zootaxa.4822.2.2

Chen CA (2017) The migration of global marine creature—The stepping-stone for the migration pathway in the Taiwan Strait. The Scientific Monthly 573: 692–699. [in Chinese]

Dai CF (1991) Reef environment and coral fauna of southern Taiwan. Atoll Research Bulletin 354: 1–24. https://doi.org/10.5479/si.00775630.354.1

Duchassaing de Fombressin P, Michelotti G (1860) Mémoire sur les coralliaires des Antilles. Imprimerie Royale, Turin, 89 pp. https://doi.org/10.5962/bhl.title.11388

France SC, Hoover LL (2002) DNA sequences of the mitochondrial COI gene have low levels of divergence among deep-sea octocorals (Cnidaria: Anthozoa). Hydrobiologia 471(1/3): 149–155. https://doi.org/10.1023/A:1016517724749

Halàsz A, Reynolds AM, McFadden CS, Toonen RJ, Benayahu Y (2015) Could polyp pulsation be the key to species boundaries in the genus *Ovabunda* (Octocorallia: Alcyonacea: Xeniidae)? Hydrobiologia 759(1): 95–107. https://doi.org/10.1007/s10750-014-2106-z

Huelsenbeck JP, Ronquist F (2001) MrBayes: Bayesian inference of phylogenetic trees. Bioinformatics (Oxford, England) 17(8): 754–755. https://doi.org/10.1093/bioinformatics/17.8.754

Kölliker RA (1865) Die Bindesubstanz der Coelenteraten. In: Icones histologicae; oder, Atlas der vergleichenden Gewebelehre. Verlag von Wilhelm Engelmann, Leipzig, 87–181. https://doi.org/10.5962/bhl.title.11946

Kozlov AM, Darriba D, Flouri T, Morel B, Stamatakis A (2019) RAxML-NG: A fast, scalable and user-friendly tool for maximum likelihood phylogenetic inference. Bioinformatics (Oxford, England) 35(21): 4453–4455. https://doi.org/10.1093/bioinformatics/btz305

Kuo C-Y, Keshavmurthy S, Chung A, Huang Y-Y, Yang S-Y, Chen Y-C, Chen CA (2020) Demographic census confirms a stable population of the critically-endangered caryophyllid coral *Polycyathus chaishanensis* (Scleractinia; Caryophyllidae) in the Datan Algal Reef, Taiwan. Scientific Reports 10(1): 10585. https://doi.org/10.1038/s41598-020-67653-8

Lin S-M (2020) Report of 2020 algal reef ecological survey. Ocean Conservation Administration, Ocean Affairs Council, Taiwan, Kaohsiung, 127 pp. https://www.oca.gov.tw/ch/home.jsp?id=220&parentpath=0,2,219&mcustomize=research_view.jsp&dataserno=202101280022 [in Chinese]

McFadden CS, van Ofwegen LP (2012) Stoloniferous octocorals (Anthozoa, Octocorallia) from South Africa, with descriptions of a new family of Alcyonacea, a new genus of Clavulariidae, and a new species of *Cornularia* (Cornulariidae). Invertebrate Systematics 26(4): 331–356. https://doi.org/10.1071/IS12035

McFadden CS, van Ofwegen LP (2013) A second, cryptic species of the soft coral genus *Incrustatus* (Anthozoa: Octocorallia: Clavulariidae) from Tierra del Fuego, Argentina, revealed by DNA barcoding. Helgoland Marine Research 67(1): 137–147. https://doi.org/10.1007/s10152-012-0310-7

McFadden CS, Benayahu Y, Pante E, Thoma JN, Nevarez PA, France SC (2011) Limitations of mitochondrial gene barcoding in Octocorallia. Molecular Ecology Resources 11(1): 19–31. https://doi.org/10.1111/j.1755-0998.2010.02875.x

Rogers C (1990) Responses of coral reefs and reef organisms to sedimentation. Marine Ecology Progress Series 62: 185–202. https://doi.org/10.3354/meps062185

Thomson JA, Mackinnon DL (1910) Alcyonarians collected on the Percy Sladen Trust Expedition by Mr. J. Stanley. Part II. The Stolonifera, Alcyonacea, Pseudaxonia, and Stelechotokea. Transactions of the Linnean Society of London, Zoology, Series 2, 13: 165–211. https://doi.org/10.1111/j.1096-3642.1910.tb00515.x

Utinomi H (1971) Port Phillip Bay Survey 2. Octocorallia. Memoirs of the National Museum of Victoria 32: 7–17. https://doi.org/10.24199/j.mmv.1971.32.02

van der Ham JL, Brugler MR, France SC (2009) Exploring the utility of an indel-rich, mitochondrial intergenic region as a molecular barcode for bamboo corals (Octocorallia: Isididae). Marine Genomics 2(3–4): 183–192. https://doi.org/10.1016/j.margen.2009.10.002

Supplementary material 1

Table S1

Authors: Tzu-Hsuan Tu, Chang-Feng Dai

Data type: xlsx file

Explanation note: Sequnece used for phyloenetic reconstruction and their respective GenBank Accession numbers, according to McFadden & Ofwegen (2012).

Link: https://doi.org/10.3897/zookeys.1089.77273.suppl1

ZooKeys 1089: 53–72 (2022)
doi: 10.3897/zookeys.1089.78000
https://zookeys.pensoft.net

RESEARCH ARTICLE

A peer-reviewed open-access journal
ZooKeys
Launched to accelerate biodiversity research

A new genus of minute stingless bees from Southeast Asia (Hymenoptera, Apidae)

Michael S. Engel[1,2,3], Lien Thi Phuong Nguyen[4,5], Ngat Thi Tran[4,5], Tuan Anh Truong[6], Andrés F. Herrera Motta[1,2]

1 *Division of Entomology, Natural History Museum, University of Kansas, 1501 Crestline Drive – Suite 140, Lawrence, Kansas 66045, USA* **2** *Department of Ecology & Evolutionary Biology, University of Kansas, Lawrence, Kansas 66045, USA* **3** *Division of Invertebrate Zoölogy, American Museum of Natural History, Central Park West at 79th Street, New York, New York 10024-5192, USA* **4** *Graduate University of Science and Technology, Vietnam Academy of Science & Technology, 18 Hoang Quoc Viet Road, Nghia Do, Cau Giay, Hanoi, Vietnam* **5** *Insect Ecology Department, Institute of Ecology & Biological Resources (IEBR), Vietnam Academy of Science & Technology, 18 Hoang Quoc Viet Road, Nghia Do, Cau Giay, Hanoi, Vietnam* **6** *Bee Research Centre, National Institute of Animal Sciences, 9 Tan Phong, Thuy Phuong, Bac Tu Liem, Hanoi, Vietnam*

Corresponding authors: Michael S. Engel (msengel@ku.edu), Lien Thi Phuong Nguyen (phuonglientit@gmail.com)

Academic editor: T. Dörfel | Received 14 November 2021 | Accepted 10 February 2022 | Published 16 March 2022

http://zoobank.org/9552211D-3DCA-4A14-A2B4-4D207CAE98FB

Citation: Engel MS, Nguyen LTP, Tran NT, Truong TA, Herrera Motta AF (2022) A new genus of minute stingless bees from Southeast Asia (Hymenoptera, Apidae). ZooKeys 1089: 53–72. https://doi.org/10.3897/zookeys.1089.78000

Abstract
A new genus of minute stingless bees (Meliponini: Hypotrigonina) is described from Southeast Asia. *Ebaiotrigona* Engel & Nguyen, **gen. nov.**, is based on the type species *Lisotrigona carpenteri* Engel, recorded from Vietnam, Thailand, Laos, Cambodia, and southern China. The species was previously considered an enigmatic member of *Lisotrigona* Moure, but is removed to a new genus based on its unique male terminalia that differs considerably from that of *Lisotrigona* and instead shares resemblances with *Austroplebeia* Moure, and the presence of yellow maculation (also similar to that of *Austroplebeia*). It is possible that *Ebaiotrigona* is the extant sister group of *Austroplebeia*, but this requires confirmation by future phylogenetic analyses. Based on available biological observations, *Ebaiotrigona carpenteri* could not be confirmed as lachryphagous as is well documented from the tear-drinking species of *Lisotrigona* and *Pariotrigona* Moure.

Abstract in Vietnamese
Một giống mới của ong không ngòi đốt (Meliponini: Hypotrigonina) được mô tả ở Đông Nam Châu Á, *Ebaiotrigona* Engel & Nguyen, **gen. nov.** dựa trên loài chuẩn *Lisotrigona carpenteri* Engel, được ghi nhận ở Việt Nam, Thái Lan, Lào, Cămpuchia và miền nam Trung Quốc. Loài này trước đây được coi là một thành viên bí ẩn của giống *Lisotrigona* Moure, nhưng đã được chuyển sang giống mới dựa trên các đặc

điểm độc nhất của bộ phận sinh dục có sự khác biệt đáng kể so với các loài khác của giống *Lisotrigona* và thay vào đó có những điểm tương đồng với giống *Austroplebeia* Moure, cùng với sự hiện diện của các đốm màu vàng trên cơ thể (cũng tương tự như ở giống *Austroplebeia*). Có thể giống *Ebaiotrigona* có mối quan hệ gần gũi với giống *Austroplebeia*, nhưng điều này cần được chứng minh bằng các phân tích về phát sinh loài trong tương lai. Dựa trên các quan sát về sinh học hiện có, *Ebaiotrigona carpenteri* chưa thể được khẳng định là một trong những loài uống nước mắt (lachyrphagous) như đã được ghi nhận rõ ràng về tập tính của các loài thích uống nước mắt ở hai giống *Lisotrigona* và *Pariotrigona* Moure.

Keywords
Apoidea, *Lisotrigona*, Meliponini, taxonomy, Vietnam

Introduction

Among the considerable diversity of stingless bees (Meliponini), several species stand out for their Lilliputian sizes, typically with body sizes under 4.1 mm. Concomitant with these minute proportions is the further reduction of the wing venation beyond that of most meliponines, lacking closed cells in the hind wing, lacking defined submarginal cells, and the disappearance of 2Rs+M or 3M without a bend apically (Michener 2001). Such diminutive bees occur independently in various lineages of Meliponini and can be found in the genera *Austroplebeia* Moure, *Plebeia* Schwarz, *Proplebeia* Michener, *Scaura* Schwarz, and *Tetragonula* Moure. In addition, ten genera include exclusively tiny species: *Asperplebeia* Engel, *Exebotrigona* Engel & Michener, *Friesella* Moure, *Hypotrigona* Cockerell, *Kelneriapis* Sakagami, *Liotrigona* Moure (sensu Engel et al. 2021), *Liotrigonopsis* Engel, *Lisotrigona* Moure, *Pariotrigona* Moure, and *Trigonisca* Moure (Michener 2001). Michener (2001) discussed the various features of minute Meliponini as well as traits that indicate the relationship, or lack of a close relationship, among the various groups, and considered some genera of this group as synonyms of others (e.g., *Friesella* as a synonym of *Plebeia*, *Tetragonula* as a synonym of *Heterotrigona* Schwarz in a polyphyletic *Trigona* Jurine).

During a revision of *Lisotrigona* (Engel 2000), one species stood out as remarkably distinct from its congeners. *Lisotrigona carpenteri* Engel, based on a type series collected in northern Vietnam, was unique among all other members of the genus for the presence of yellow maculation on the face, pronotal lobe, and sometimes the mesoscutellar apex. At that time, males for any species of the genus were unknown and *L. carpenteri* was interpreted to be an autapomorphic taxon based on these morphological features of the worker caste. Subsequently, males of *L. furva* Engel (Michener 2007a) and *L. cacciae* (Nurse) (under two synonymic names: Viraktamath and Sajan Jose 2017) were discovered, revealing a unique and remarkably distinctive morphology, further emphasizing the distinctiveness of *Lisotrigona* from other minute genera, and particularly its relatives in Asia and Australia, *Pariotrigona* and *Austroplebeia*. Moreover, it was also discovered that *Lisotrigona* and *Pariotrigona* were lachryphagous, collecting tears from the eyes of various vertebrates (Bänziger et al. 2009, 2011; Bänziger and Bänziger 2010; Bänziger 2018). While these significant revelations were brought forward, the biology and males of *L. carpenteri* remained elusive.

Recently, two groups have independently discovered males of *L. carpenteri* and noted the considerable morphological departure in the characters of the terminalia from other *Lisotrigona* (Li et al. 2021; herein). In fact, the terminalia are generally more similar to that of *Austroplebeia* than to any other minute Meliponini, and certainly lack the synapomorphies that otherwise characterize *Lisotrigona* (Michener 2007a). The male terminalia of *L. carpenteri* are so remarkably different from *Lisotrigona* that the species is here considered to belong to a separate genus. Here we provide a description of the genus and the male, and encourage melittologists to seek additional nests, immature stages, and further biological data for this unique species among the Southeast Asian bee fauna.

Materials and methods

Material of *L. carpenteri* was examined from the following collections: Division of Entomology, University of Kansas Natural History Museum, Kansas (**SEMC**); Division of Invertebrate Zoölogy, American Museum of Natural History, New York (**AMNH**); and Insect Ecology Department, Institute of Ecology & Biological Resources (**IEBR**), Hanoi, Vietnam. Morphological terminology follows that of Engel (2001, 2019), Michener (2007b), and Engel et al. (2021). The format for the generic description follows that of Rasmussen et al. (2017), Engel (2019), and Engel et al. (2021). Bees were sampled from sites with a series of nests and swept by net from around the nesting area. Most nests were left undisturbed, although two were exposed but contents were not sampled. Figs 1, 4 were prepared at the University of Kansas, while the remainder were prepared by the Institute of Ecology & Biological Resources.

Systematics

***Ebaiotrigona* Engel & Nguyen, gen. nov.**
http://zoobank.org/99CCDC03-E122-46B9-81F6-D8C11E432DA2

Type species. *Lisotrigona carpenteri* Engel, 2000.

Diagnosis. The new genus resembles both *Lisotrigona* and the smallest individuals of *Austroplebeia*. The presence of yellow maculation on the face and mesosoma of the worker differentiates this caste from those of *Lisotrigona* (Figs 1, 5–7), while in males the clypeus can be brownish to black (refer to Description, vide). In addition, workers of *Lisotrigona* have distinct erect bristles on the antennal scape (lacking in *Ebaiotrigona*) and have minute plumose facial setae covering the entire face, including the upper frons (in *Ebaiotrigona* the upper frons is lacking in plumose setae and instead covered by minute, fine, simple setae). While yellow maculation is shared between workers of *Ebaiotrigona* and *Austroplebeia*, the latter has a more complete wing venation (Fig. 1D for *Ebaiotrigona* venation), with 1Cu, 2Cu, and 3Cu present, at least as nebulous if not tubular veins, and thereby a more completely delimited subdiscoidal (= second cubital) cell. Additionally, *Austroplebeia s.str.* has 6 distal hamuli (versus 5 in *Ebaiotrigona*, *Lisotrigona*, and *Anteplebeina*), and *Anteplebeina* has 1M and 1cu-a confluent (versus 1M distad 1cu-a in *Lisotrigona* and *Austroplebeia s.str.*). Perhaps the most dramatic differences between *Ebaiotrigona* and other minute stingless bees are in the male terminalia. The male terminalia of *Ebaiotrigona* (Fig. 4) lack those distinctive features of *Lisotrigona*, that is, in the latter the gonocoxae are enormously expanded proximally into an incomplete ring, the slender gonostyli with apical setae are articulated at about midlength on the elongate gonocoxae, the genital capsule is schizogonal, and sterna VI and VII are entirely different (cf. Fig. 4 vs figs 4, 5 of Michener 2007a). Instead, in *Ebaiotrigona* the genital capsule is rectigonal, with more transverse gonocoxae in which the gonostyli articulate more distally. Furthermore, the gonostyli are uniquely modified: flattened laterally, with lamellate margins broadened proximally on both ventral and dorsal sides, and tapering apically to an acute point lacking setae. The bulb of the penis valve is enlarged and longer than broad, and abruptly tapers to a thin apical process that is shorter than the basal bulb. In *Lisotrigona*, the bulb is smaller and about as long as the apical process, the former gently tapering into the latter (Michener 2007a).

Description. ♀: Minute, total length ca 3.95–4.15 mm, forewing length ca 2.96–3.10 mm; integument generally smooth and polished, some places with widely scattered minute punctures on head and mesosoma, with distinct pale yellow maculation on face, specifically undersurface of scape, supraclypeal area, and clypeus; pronotal lobe; and sometimes as small triangle on lower parocular area, as thin line on lateral margin of mesoscutum bordering tegula and as apicolateral spots on mesoscutellar apical margin (such yellow maculation absent in *Lisotrigona* and *Pariotrigona*, present but more extensive in *Austroplebeia*). Setae generally pale to white; those of body fine, short, and simple, face with minutely plumose setae except on upper frons with only minute simple setae (in *Lisotrigona* the minutely plumose setae distributed across face, including upper frons), scape with fine minute simple setae but without erect short bristles (erect short bristles present in *Lisotrigona*); mesoscutum with numerous erect, fine, short, simple setae; disc of mesoscutellum with similar setae to those of mesoscutum except twice as long or longer, particularly along posterior margin.

Head as broad as mesosoma, slightly broader than long, with face narrower than compound eye length; vertex gently rounded, not produced or ridged; preoccipital area rounded; scape shorter than antennal-ocellar distance, not reaching median ocellus; ocelli near top of vertex; flagellomere I trapezoidal, longer than flagellomere II; flagellomere II about as long as flagellomere III, each slightly broader than long; middle flagellomeres about as long as or slightly longer than broad; intertorular distance slightly shorter than torulocular distance; upper torular tangent below facial midlength; gena rounded, narrower than compound eye in profile; supraäntennal area with triangular medial elevation bordered laterally by converging furrows forming distinct scapal basins; frontal carina absent, indicated on supraäntennal triangle by weakly demarcated ridge, otherwise a narrowly polished line to median ocellus; malar area nearly linear, subequal to or shorter than 0.5× flagellar diameter (similar to *Lisotrigona* and *Austroplebeia s.str.*; *Pariotrigona* with malar space slightly longer than flagellar diameter; *Anteplebeina* with malar space as long as flagellar diameter); labrum transverse, simple, apical margin rounded; mandible with apical margin slightly oblique, largely edentate except for two small teeth on upper margin of margin (thus, bidentate), teeth well defined, acute, and incised, interdental spaces distinct but not broadly incised; labial palpomeres I and II with a few, scattered, elongate, apically arched to slightly wavy setae, such setae more clustered apically and sparse elsewhere (similar to that of *Lisotrigona*).

Mesoscutum with median sulcus faintly impressed, extending to slightly beyond mesoscutal midlength; notauli scarcely evident, not impressed; mesoscutellum short, acutely rounded in lateral aspect, overhanging metanotum and extreme base of propodeum, shining transverse depression on mesoscuto-mesoscutellar sulcus simple. Propodeum gently sloping; basal area slightly longer than mesoscutellum, shining, finely and faintly tessellate; propodeal spiracle elongate, nearly meeting metapostnotal lateral arms.

Forewing extending beyond apex of metasoma, with 2Rs, 1rs-m, 1m-cu, 3M, 4M, 1Cu, 2Cu, 3Cu, and 2cu-a absent or at most indicated by spectral traces; membrane hyaline, clear, with weak iridescent reflections apically; prestigma short, subequal to anterior width of 1Rs; pterostigma slender, subparallel margins slightly widening distally to point of 1r-rs, then arching to anterior margin along marginal cell base; marginal cell separated from wing apex by more than its maximum width, apex broadly open, opening about 0.75× maximum marginal cell width, 4Rs trace not angled apically (i.e., not appendiculate); 1M distad 1cu-a (thus, minute 2M+Cu present); submarginal slightly acute; 1M weakly arched; 2M not angled apically (i.e., angle between 2M and spectral 3M linear or at most faintly less than 180°); r-rs slightly longer than 3Rs. Hind wing with 5 distal hamuli; no closed cells and veins posterior to R absent except proximal arch of M+Cu.

Metatibia approximately triangular, approximately 2.8–3.0× as long as greatest width; retromargin gently curved with subangulate distal superior angle, retromarginal setae and superior prolateral surface setae simple; prolateral surface shallowly concave apically, with corbicula occupying slightly less than apical half; retrolateral surface with broad keirotrichiate zone and narrow superior subglabrous zone, without defined clivulus except proximally; keirotrichiate zone approximately 4× as broad as superior glabrate zone, keirotrichiate zone extending to apical margin, with keirotrichiate zone narrowing and superior glabrate zone broadening in apical-most portion of metatibia; inferior penicillum and rastellar comb present, each composed of fine soft setae. Metabasitarsus with proventral margin straight, retrodorsal margin generally paralleling proventral margin, apical margin weakly convex to comparatively straight, distal superior angle not projecting; retrolateral surface without basal sericeous area.

Metasoma subtriangular, about as wide as mesosoma, with metasomal terga smooth and shining except apical margins more matte and faintly and minutely imbricate, all terga almost glabrous, except by minute, erect, simple setae apically forming a narrow band on apical margin, such setae progressively longer, more abundant, and more spread on apical-most terga; sterna largely smooth and glabrous, with long to elongate, fine, erect, simple setae apically.

♂: Darker than worker, apparently without facial maculation of worker (Figs 2, 3), instead yellow areas of worker dark brown to black in drone [brown in Vietnamese male, wholly black in Chinese male (Li Yuran, pers. comm. and unpublished images to MSE)] [note that sometimes areas of yellow maculation start off brownish in individuals who are not fully pigmented and so brown areas of the male could eventually become fully yellow as in the worker; however, the fact that the Vietnamese male appears to be fully pigmented elsewhere on the body (Figs 2, 3) and that the Chinese male is wholly black tends to suggest that drones of *Ebaiotrigona* truly lack facial maculation, but this will require confirmation through extensive future sampling of males throughout the range of the species], except pronotal lobe consistently yellow. Scape shorter and broader than that of worker (Fig. 3); flagellomere I trapezoidal, shorter than pedicel or flagellomere II; flagellomere II about as long as flagellomere III, each slightly longer than broad. Metasomal sternum VI medioapically chamfered, bilobed; sternum VII medially broadly convex and slightly depressed, with shallow apicolateral concavities; genital capsule rectigonal (Fig. 4); gonobase somewhat transverse; gonocoxae broader than long, with gonostylus articulating somewhat proximally; gonostylus elongate and bladelike, flattened laterally, and broadened proximally and lamelliform mesally on dorsal and ventral sides, tapering apically to acute point with a single fine apical seta, seta simple (Fig. 4); penis valves elongate, bulb enlarged, longer than broad, well sclerotized, abruptly tapering to thin elongate apical process, process gently arched and acutely rounded apically, process slightly shorter than bulb, blub without elongate proximal apodeme, instead with short, twisted apodeme (Fig. 4).

Etymology. The new generic name is a combination of the Ancient Greek adjective *ēbaiós* (*ἠβαιός*, meaning "small") and the generic name *Trigona* Jurine. The gender of the name is feminine.

Included species. Currently, the genus includes only the type species, *Ebaiotrigona carpenteri* (Engel), new combination.

The following modifications to the key of Rasmussen et al. (2017) and Engel et al. (2018) allow for the incorporation of *Ebaiotrigona*.

1 Forewing length less than 3.2 mm, wing venation greatly reduced and retrodorsal margin of metatibia without plumose setae; hind wing without closed cells, veins closing radial and cubital cells, if visible at all, clear and unpigmented (spectral); forewing with 2Rs and 1rs-m almost always completely absent, thus without indication of submarginal cells; at least distal part of second cubital cell of forewing undefined or defined completely by unpigmented spectral vein traces (i.e., at least 2Cu and 3Cu absent or spectral); vein M of forewing terminating without bend at about position of anterior end of 1m-cu which, however, is absent (i.e., 3M lacking) **2**

– Forewing length typically over 4 mm, wing venation typically not greatly reduced for Meliponini, but if minute and with some wing reduction, then retrodorsal margin of metatibia with plumose setae intermixed with simple setae; hind wing typically with radial and cubital cells closed by at least weakly brownish nebulous veins; forewing with one or two submarginal cells usually weakly indicated by nebulous traces of 2Rs and 1rs-m, first submarginal cell usually recognizable; second cubital cell of forewing completely indicated by at least faint nebulous veins (i.e., 2Cu present); vein M of forewing usually extending at least slightly beyond position of 1m-cu and angular at apex of tubular portion of vein (i.e., 3M present), the stub of which is usually at least faintly visible **3**

2 Malar space shorter than flagellar diameter; inner margins of compound eyes converging below **2a**

– Malar space almost one-fifth as long as compound eye, much longer than flagellar diameter; inner margins of compound eyes nearly parallel .... ***Pariotrigona* Moure**

2a Yellow maculation present in worker on scape, supraclypeal area, clypeus, pronotal lobe and sometimes on lower parocular area, apically on mesoscutellum, and laterally on mesoscutum; scape without erect bristles; minutely plumose facial setae absent on upper frons; gonocoxae unmodified, with gonostyli articulating more distally; gonostyli elongate, bladelike, expanded and lamellate proximally; genital capsule rectigonal; metasomal sternum VI medioapically chamfered, bilobed .... ***Ebaiotrigona*, gen. nov.**

– Yellow maculation lacking, at most with pale yellow brown areas; scape with erect bristles; minutely plumose facial setae extending across upper frons; gonocoxae with enormous, arched, proximal extensions, with gonostyli articulating near midlength; gonostyli slender elongate; genital capsule schizogonal; metasomal sternum VI with a single medioapical process .... ***Lisotrigona* Moure**

***Ebaiotrigona carpenteri* (Engel), comb. nov.**

Figs 1–7

Lisotrigona carpenteri Engel, 2000: 232. Holotype ♀ (visum, AMNH).

Remark. The worker of this species has been described by Engel (2000). We do not repeat that material here but instead provide descriptive details for the hitherto undocumented male.

Descriptive notes. ♂: Body length 3.5 mm; forewing length 2.9 mm; head width 1.29 mm; head length (lower margin of clypeus to anterior margin of median ocellus and to summit of head) 1.04 mm, 1.19 mm, respectively; compound eye length, upper and lower interorbital distances 0.92 mm, 0.53 mm, 0.45 mm, respectively.

Compound strongly converging below, inner orbits only feebly concave above; compound eye length greater than upper interocular distance; antennae arising below lower third of face so that distance from lower clypeal margin to lower margin of antennal torulus is about one-half distance from upper margin of torulus to lower margin of median ocellus; clypeus about twice as broad as long, lower margin scarcely below lower ocular tangent, upper margin separated from antennal torulus by about one-half torular diameter; head surface in vicinity of antennal toruli depressed, not visible in profile; interocellar distance over twice ocellocular distance, almost 3× ocellar diameter; ocelli on submit of vertex, head surface declivitous immediately behind lateral ocelli with no ridge or carina; genal area much narrower than compound eye in profile; malar area linear (mandibular base almost in contact with lower compound eye margin); mandibles comparatively long, conspicuously crossing one another, mandibular apex slender, apical margin oblique with lower apical angle pointed, upper portion of apical margin faintly sinuous and simulating a faint preapical bump (scarcely large enough to denote as a "tooth") (Fig. 3B); antennal scape short, its length less than half

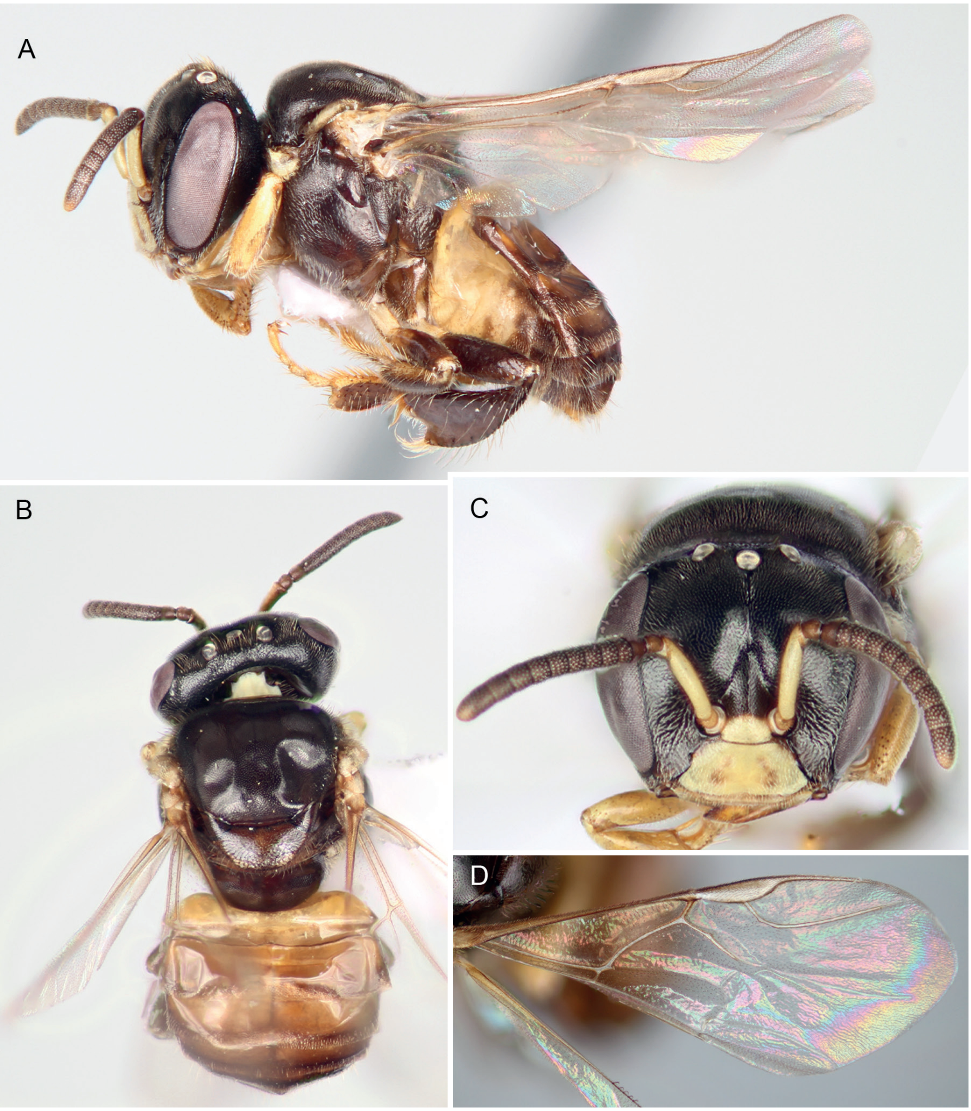

Figure 1. Worker of *Ebaiotrigona carpenteri* (Engel), comb. nov., light morph **A** lateral habitus **B** dorsal habitus **C** facial view **D** forewing.

distance from antennal torulus to median ocellus; flagellum slightly tapering, covered with short, dense setae; flagellomere I shorter than pedicel, nearly 3× as broad as long; flagellomere II about 1.25× as broad as long, flagellomere III about as broad as long, subsequent flagellomeres progressively shorter so that flagellomeres IV–VI are shorter than broad, flagellomeres VII–X progressively longer, longer than broad, flagellomere XI with broadly rounded apex. Male terminalia as in Fig. 4.

Integument of head and mesosoma black except basal one-third of scape (grading into black distal half), mandible, labrum, clypeus, spot between antennae, mesoscutellum, metanotum, propodeum, legs except coxae and femora, and all metasomal segments, brown or suffused with brown ranging to black (darkest in Chinese male: Li Yuran, pers. comm. and image to MSE); pronotal lobe markedly yellow; protibia, meso- and metatibial apices, and tarsi light yellowish brown; tegulae yellowish brown; wings clear, veins light brown; stigma translucent, light brownish.

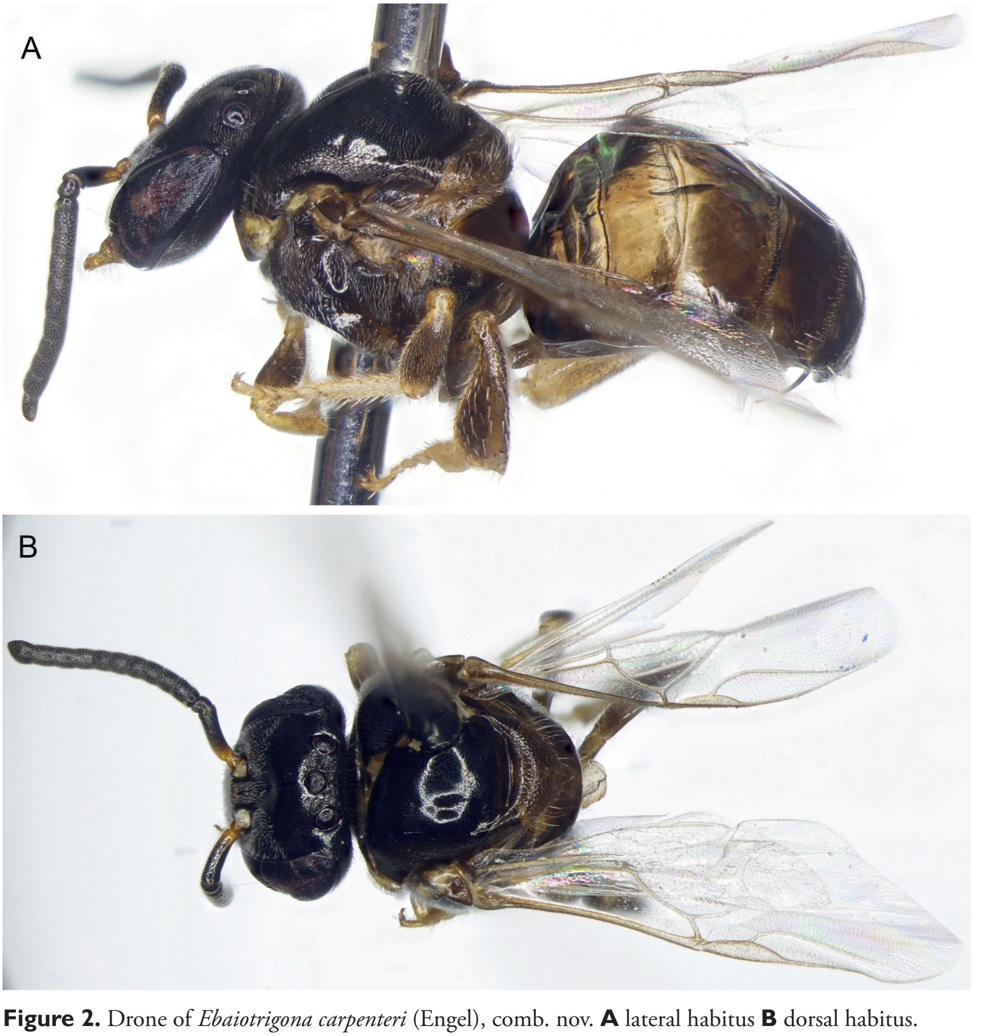

Figure 2. Drone of *Ebaiotrigona carpenteri* (Engel), comb. nov. **A** lateral habitus **B** dorsal habitus.

Integument shining, smooth, head and mesosoma with well separated, fine, small punctures, punctures on lateral part of mesoscutum denser; punctures on mesoscutellum much stronger and denser than those on mesoscutum, separated by 2–3× a puncture width; mesepisternum centrally with coarse punctures separated by 2–3× a puncture width, otherwise integument between punctures smooth; basal area of propodeum shining, minutely tessellate, glabrous; posterior surface smooth, shining. Metasomal terga smooth except minute punctures on narrow posterior margins.

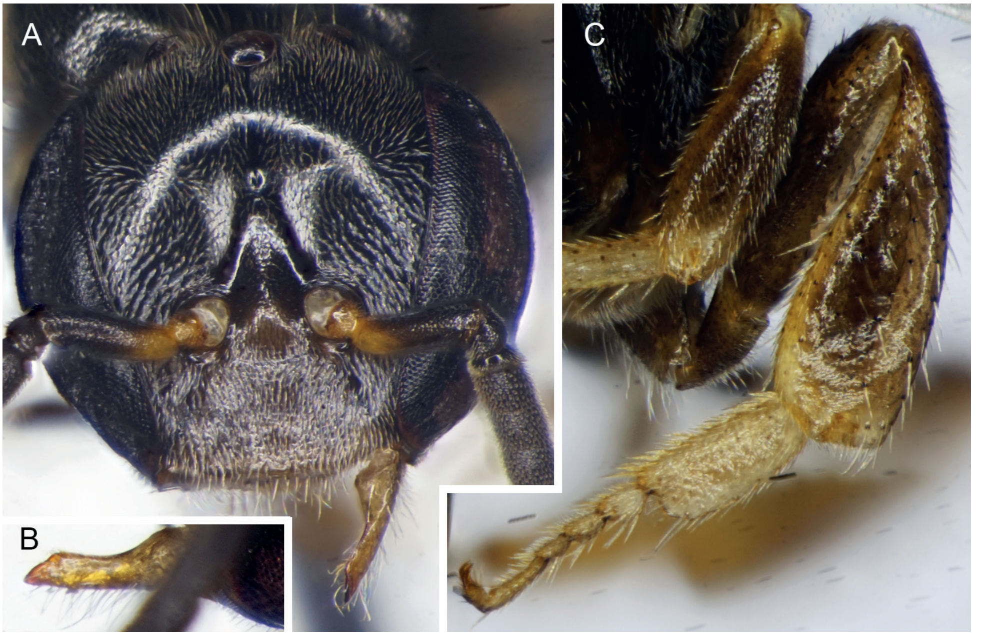

Figure 3. Drone of *Ebaiotrigona carpenteri* (Engel), comb. nov. **A** facial view **B** outer view of mandible **C** metatibia and metatarsus.

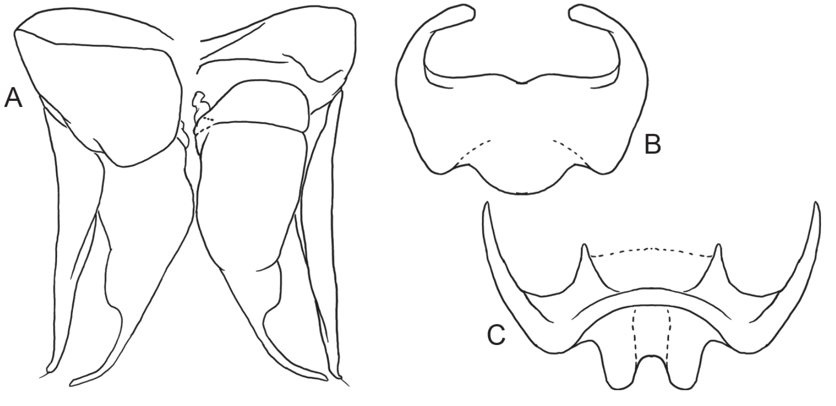

Figure 4. Male terminalia of *Ebaiotrigona carpenteri* (Engel), comb. nov. **A** genital capsule (left = dorsal, right = ventral) **B** metasomal sternum VII **C** sternum VI.

Pubescence mostly exceptionally short, mostly yellowish white, setae of lower half of face white and conspicuously plumose, other setae simple or nearly so. Posterior part of mesoscutellum with zone of upcurved setae, longest on body except for some on apical margin of clypeus and mandible, about 2.5× as long as median ocellar diameter, otherwise long setae (nearly 2× ocellar diameter) sparse on apical margin of clypeus, vertex, coxae, and trochanters, rather numerous on mandibular lower margin. Setae of mesoscutum short, some setae at apicolateral corner longer, about as long as ocellar diameter. Metasomal terga I–IV glabrous except for minute erect setae on posterior margins.

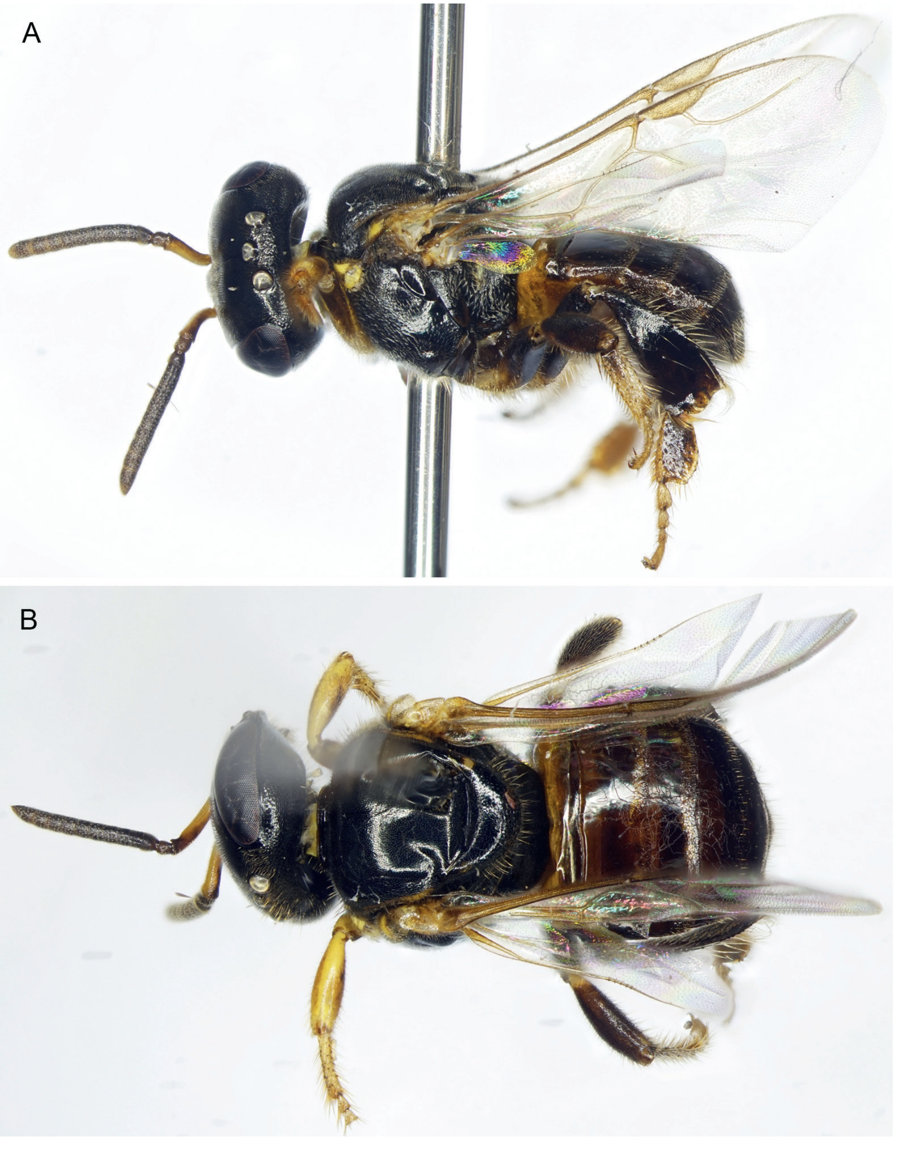

Figure 5. Worker of *Ebaiotrigona carpenteri* (Engel), comb. nov., dark morph **A** lateral habitus **B** dorsal habitus.

Figure 6. Worker of *Ebaiotrigona carpenteri* (Engel), comb. nov., intermediate light morph **A** lateral habitus **B** dorsal habitus.

Variation. Workers exhibit noticeable variation in overall coloration, and can loosely fall into a lighter and dark morph, although there are individuals who seemingly intergrade and so these morphs are not discrete (Figs 1, 5–7). Generally, areas of maculation on the clypeus, ventral surface of scape, mesoscutal lateral borders, axilla, apicolaterally

Figure 7. Worker faces of *Ebaiotrigona carpenteri* (Engel), comb. nov., showing identical patterns in both dark and intermediate light morph **A** dark morph **B** intermediate light morph.

on mesoscutellum, foreleg, and in isolated areas on the mid- and hind legs can vary from pale to vivid yellow, while the males the tarsi are more consistently yellowish brown to yellow and the podites basal to the tarsi are brown to black (darkest in the Chinese male: Li Yuran, pers. comm. and image to MSE). In addition, the width of the marks on the mesoscutum and mesoscutellum can be exceptionally narrow (mesoscutum) or faint (mesoscutellum), such that they can appear superficially absent. Most noticeably, areas of black on the mesosoma and legs can vary to dark brown (e.g., cf. Figs 1, 5, 6). The metasoma can range from being largely black to dark reddish brown, with lighter brown on the first tergum and basal sterna, to the same pattern but from pallid yellow on the basal sterna and first tergum, with ferruginous on the remaining terga, but blending from light proximally to dark apically, and within a given tergum darkening slightly toward each marginal zone. It should be noted that the holotype worker (AMNH) is of the darker morph.

New material examined. Vietnam: 1♂, 67♀♀, Tân Thành [Village], Yên Thịnh [Community], Yên Thủy [District], Hòa Bình [Province] [20°21.35'N, 105°39.47'E], 22 June 2021, coll. Tuấn Anh Trương et al. [1♂, 6♀♀, nest #1; 5♀♀, nest #2; 5♀♀, nest #3; 3♀♀, nest #4; 2♀♀, nest #5; 12♀♀, nest #7; 8♀♀, nest #9; 8♀♀, nest #19; 12♀♀, nest #16; 6♀♀, nest #21] (IEBR); 18♀♀, Yên Hân [Community], Chợ Mới [District], Bắc Kạn [Province], 27 June 2021, coll. Tuấn Anh Trương et al. [11♀♀, nest #11; 1♀♀, nest #18; 6♀♀, nest #13] (IEBR); 53♀♀, Nam Cường [Community], Chợ Đồn [District], Bắc Kạn [Province], coll. Tuấn Anh Trương et al. (6♀♀, nest #9; 16♀♀, nest #11; 21♀♀, nest #21); 21♀♀, Lân Nghè, Hữu Liên Natural Reserve, Hữu Liên [District], Lạng Sơn [Province], 21°33'48.6"N, 106°24'36.4"E, ca 289 m, 11 June 2018, coll. Liên Thị Phương Nguyễn et al. (IEBR).

Dark morph: 23♀♀, Vũ Quang National Park, Vũ Quang [District], Hà Tĩnh [Province], 18°17'44"N, 105°22'29"E, 12 December 2020, coll. Ngát Thị Trần & Cường Quang Nguyễn (IEBR).

Comments. More than 10 nests were observed in a rocky wall in Yên Thủy, Hòa Bình Province, while six or seven were seen in one locality in limestone cliffs in Bắc Kạn Province (Figs 8, 9). The bees appear to prefer nesting in cavities between stones, either natural limestone cliffs or even amid the rocks of human-built walls, much like that of *Pariotrigona* (Bänziger et al. 2011). The bees were quite a nuisance and frequented human skin where they were lapping sweat, and attempted to approach the eyes of the collectors (Truong pers. obs.), although it is unclear if this was to collect tears or merely as a timid form of defense from a perceived threat near the nests. Similar observations on the behavior of the bees were made in southern China (Li et al. in press). It is possible that the bees rely on tears (lachryphagous) in the same manner as *Pariotrigona* and *Lisotrigona*, although no tear collection could be confirmed nor were bees observed visiting the eyes of cattle or other vertebrates. The bees and nests have a strong foul odor, and future work on the chemistry of their nests and stores is needed to determine their composition and the potential derivation of these smells. Future work will more fully explore the nesting biology, nest architecture, and immature stages of *E. carpenteri*.

Discussion

While *E. carpenteri* was always a unique species as the only minute stingless bee in Southeast Asia with yellow maculation, it has not been until the discovery of the male that its real distinction was revealed. The male terminalia are clearly not of the structure so typical for *Lisotrigona*. Specifically, *E. carpenteri* lacks the enormous proximal extensions of the gonocoxae unique to species of *Lisotrigona* (Michener 2007a). While this form is wholly unique among Meliponini, the result of the almost proximally ringlike gonocoxae approximates the schizogonal condition as the proximal fossae of the gono-

Figure 8. Nests and habitat of *Ebaiotrigona carpenteri* (Engel), comb. nov., at Bắc Kạn Province, Vietnam **A** general habitat **B** nest entrance in limestone cliff **C** exposed nest from between limestone slabs.

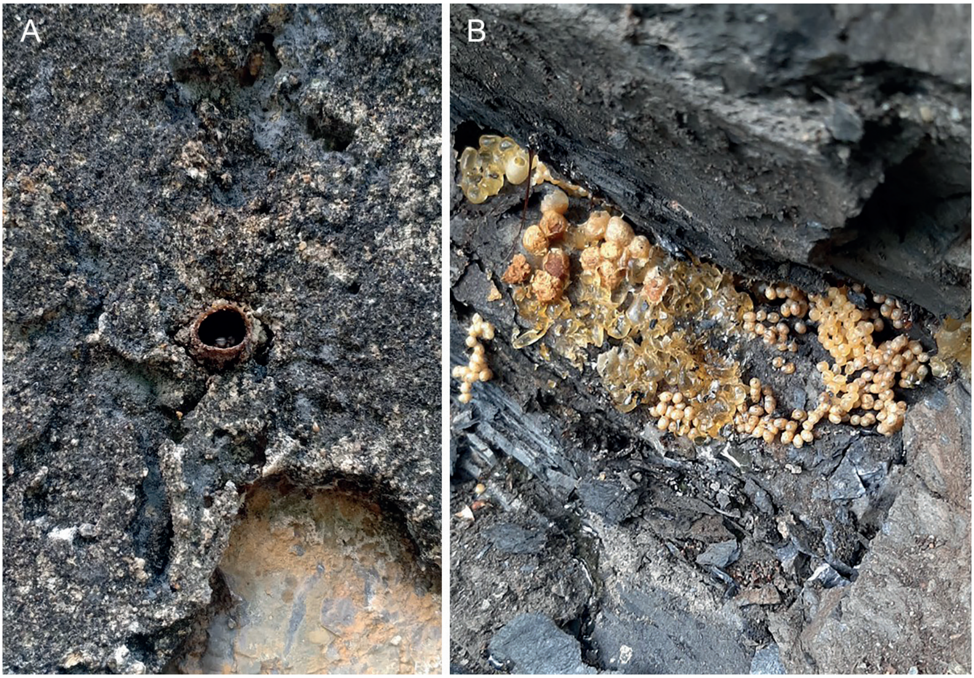

Figure 9. Nests of *Ebaiotrigona carpenteri* (Engel), comb. nov., at Bắc Kạn Province, Vietnam **A** nest entrance **B** exposed nest from between limestone slabs.

coxae open mesally (Michener 1990). Conversely, in *Ebaiotrigona*, *Pariotrigona*, and *Austroplebeia*, the gonocoxae are not so modified, and the opening of the gonocoxae are directed proximally (Michener 2001; Dollin et al. 2010), and thus of the rectigonal configuration with the sole exception of *Pariotrigona*, which is more amphigonal. In addition, in *Lisotrigona* the gonostyli articulate with the gonocoxae about midlength, whereas in the others, including *Ebaiotrigona*, the gonostyli articulate more distally. Unlike all of the other genera, the gonostyli of *Ebaiotrigona* are broadened proximally as lamellae, elongate, and almost bladelike. This form is unique to the genus.

In several respects *Ebaiotrigona* appears more similar to *Austroplebeia*, and this is borne out by the form of the male genitalia. In both genera the basal bulb of the penis valve is quite enlarged and sclerotized, and tapers apically to an elongate, thin, clawlike process. Note that these extensions in *Austroplebeia* and *Ebaiotrigona*, although well sclerotized and often melanized, are easily broken near their base (e.g., from the photograph of Li et al. (2021: fig. 2d), and in additional images of this male sent to MSE these are broken off in the Chinese male reported therein; nonetheless, the Chinese populations should be further explored in the future as to whether or not they represent a species distinct from *E. carpenteri*). In *Pariotrigona* the basal bulb is smaller and somewhat transverse, and is abruptly narrowed to the thin elongate process. In *Lisotrigona*, the penis valves are comparatively short relative to the overall size of the genitalia, with a broad basal bulb and tapering to a comparatively short process that is scarcely longer than the bulb. While the Asian and Australian minute species lack a spatha, *Pariotrigona* is an outlier in that the spatha is present as a large membranous structure. The form of each of these genera is seemingly apomorphic when compared to putative outgroups among related members of the *Hypotrigona* group of genera (Table 1: sensu Engel et al. 2021). *Liotrigona* has another wholly unique form of genitalia. The capsule is elongate and permanently schizogonal, with the gonocoxae much longer than broad and fused ventrally, while the gonostyli articulate apically (Michener 1990). By comparison, the genitalia of *Hypotrigona* are comparatively drab and more generalized with conditions observed broadly across Meliponini. In *Hypotrigona* the capsule is rectigonal, but apomorphically the opening opens dorsally, while the gonocoxae are short and transverse (Michener 1990). The basal bulb of the penis valve is membranous.

Another unique feature of *Ebaiotrigona* is the shape of the sixth metasomal sternum, which is apically bilobed, versus the single medial process of *Lisotrigona*, *Pariotrigona*, and *Austroplebeia*. The seventh sternum also differs from these genera and therefore highlights the distinctiveness of the new genus among Old World Meliponini.

Given the similar male terminalia and the presence of yellow facial maculation, it leads one to wonder if *Ebaiotrigona* could be the extant sister group of *Austroplebeia*, diverging from this genus prior to the Miocene and when the latter still had a presence in mainland Asia (Engel et al. 2021). Naturally, future phylogenetic analyses of morphological and molecular data need to include a broader sampling of Asian species, and certainly including samples of *E. carpenteri*.

Table 1. Asian and Australian species of the *Hypotrigona* group (sensu Engel et al. 2021). Occurrences in brackets are likely but not yet confirmed; data taken from: Ascher et al. (2016), Chinh et al. (2005), Dollin et al. (2015), Engel (2000), Engel et al. (2021), Karunaratne et al. (2017), Le et al. (2021a, 2021b), Lee et al. (2016), Li et al. (in press), Michener (2001, 2007a, 2007b), Nguyen et al. (2021), and Thangjam et al. (in press).

Genus *Austroplebeia* Moure	
Subgenus †*Anteplebeina* Engel	
†*A. fujianica* Engel	China (Fujian) (Miocene)
Subgenus *Austroplebeia* Moure	
A. australis (Friese)	Australia
A. cassiae (Cockerell)	Australia
A. cincta (Mocsáry)	Indonesia (Papua, West Papua), Papua New Guinea
A. essingtoni (Cockerell)	Australia
A. magna Dollin et al.	Australia
Genus *Ebaiotrigona*, **gen. nov.**	
E. carpenteri (Engel), **comb. nov.**	Cambodia, China*, Laos, Thailand, Vietnam
Genus *Lisotrigona* Moure	
L. cacciae (Nurse)	India, Sri Lanka, Thailand, Vietnam**
L. furva Engel	Cambodia, [Laos], Thailand, [Vietnam]***
Genus *Pariotrigona* Moure	
P. pendleburyi (Schwarz)	Brunei, Cambodia, [Indonesia: Kalimantan], Malaysia, Thailand

* Chinese population may be a separate species of *Ebaiotrigona*, something that is in need of future study, particularly given the habitat differences (Li et al. in press).
** Records of *L. cacciae* from Vietnam by Sakagami (1975: as *Hypotrigona scintillans* (Cockerell)) and Le et al. (2021b) remain to be confirmed. Sakagami (1975) refers to "total melanism", which could apply to *L. furva*.
*** Records of *L. furva* from Vietnam by Le et al. (2021a) remain to be confirmed.

The nests and the biology of *E. carpenteri* remain to be explored in greater detail, work that the authors hope to undertake in the forthcoming years. Limited observations on nests were presented by Chinh et al. (2005), who reported nests in tree trunks, rock crevices, and human-made structures. Chinh et al. (2005) reported amorphous brood clusters, like those observed in here (Figs 8, 9). The contents of the honey pots were not explored. Therefore, for the moment one must wonder whether *E. carpenteri* is actually lachryphagous like *Lisotrigona* and *Pariotrigona*, or a typical floral visitor as in *Austroplebeia*. Certainly current observations suggest that while the species laps sweat, like many bees, *E. carpenteri* may not actually imbibe tears (Li et al. in press; herein). A further elaboration of the nests and biology of *E. carpenteri* will be of considerable significance for understanding the distribution and occurrence of lachyrphagy in Asiatic Meliponini. If true, lachryphagy is restricted to *Lisotrigona* and *Pariotrigona*, then it may be that this is a biological synapomorphy for these two genera, with *Ebaiotrigona* more closely allied to *Austroplebeia*. Ideally, once the biology has been more fully elucidated for *E. carpenteri*, an analysis of morphological and molecular data can be undertaken for the *Hypotrigona* group (Table 1) to explore not only phylogenetic relationships but also patterns of biogeographic and biological significance. Fortunately, a large number of nests are available at localities in northern Vietnam for future investigation.

Acknowledgements

We are grateful to Li Yuran for providing a copy of works in press and relevant information on populations of *E. carpenteri* (or a species closely related to it) from southern China, and to three reviewers for their helpful comments on the manuscript. This is a contribution of the Division of Entomology, University of Kansas Natural History Museum and was supported by grants from the Ministry of Science and Technology of Vietnam (NVQG-2021/ĐT.06) and Vietnam Academy of Science and Technology (ĐLTE00.04/22-23).

References

Ascher JS, Heang P, Kheam S, Ly K, Lorn S, Chui S-X, Greef S, Chartier G, Phauk S (2016) A report on the bees (Hymenoptera: Apoidea: Anthophila) of Cambodia. Cambodian Journal of Natural History 2016(1): 23–39.

Bänziger H (2018) Congregations of tear drinking bees at human eyes: foraging strategies for an invaluable resource by *Lisotrigona* in Thailand (Apidae, Meliponini). Natural History Bulletin of the Siam Society 62(2): 161–193.

Bänziger H, Bänziger S (2010) Mammals, birds and reptiles as host of *Lisotrigona* bees, the tear drinkers with the broadest host range (Hymenoptera, Apidae). Mitteilungen der Schweizerischen Entomologischen Gesellschaft [Bulletin de la Société Entomologique Suisse] 83(3–4): 271–282.

Bänziger H, Boongird S, Sukumalanand P, Bänziger S (2009) Bees (Hymenoptera: Apidae) that drink human tears. Journal of the Kansas Entomological Society 82(2): 135–150. https://doi.org/10.2317/JKES0811.17.1

Bänziger H, Pumikong S, Srimuang K-O (2011) The remarkable nest entrance of tear drinking *Pariotrigona klossi* and other stingless bees nesting in limestone cavities (Hymenoptera: Apidae). Journal of the Kansas Entomological Society 84(1): 22–35. https://doi.org/10.2317/JKES100607.1

Chinh TX, Sommeijer MJ, Boot WJ, Michener CD (2005) Nest and colony characteristics of three stingless bee species in Vietnam with the first description of the nest of *Lisotrigona carpenteri* (Hymenoptera: Apidae: Meliponini). Journal of the Kansas Entomological Society 78(4): 363–372. https://doi.org/10.2317/0409.14.1

Dollin AE, Dollin LJ, Rasmussen C (2015) Australian and New Guinean stingless bees of the genus *Austroplebeia* Moure (Hymenoptera: Apidae) – a revision. Zootaxa 4047(1): 1–73.

Engel MS (2000) A review of the Indo-Malayan meliponine genus *Lisotrigona*, with two new species (Hymenoptera: Apidae). Oriental Insects 34: 229–237. https://doi.org/10.1080/00305316.2000.10417261

Engel MS (2001) A monograph of the Baltic amber bees and evolution of the Apoidea (Hymenoptera). Bulletin of the American Museum of Natural History 259: 1–192. https://doi.org/10.1206/0003-0090(2001)259%3C0001:AMOTBA%3E2.0.CO;2

Engel MS (2019) Notes on Papuasian and Malesian stingless bees, with the descriptions of new taxa (Hymenoptera: Apidae). Journal of Melittology 88: 1–25. https://doi.org/10.17161/jom.v0i88.11678

Engel MS, Kahono S, Peggie D (2018) A key to the genera and subgenera of stingless bees in Indonesia (Hymenoptera: Apidae). Treubia 45: 65–84.

Engel MS, Herhold HW, Davis SR, Wang B, Thomas JC (2021) Stingless bees in Miocene amber of southeastern China (Hymenoptera: Apidae). Journal of Melittology 105: 1–83. https://doi.org/10.17161/jom.i105.15734

Karunaratne WAIP, Edirisinghe JP, Engel MS (2017) First record of a tear-drinking stingless bee *Lisotrigona cacciae* (Nurse) (Hymenoptera: Apidae: Meliponini), from the central hills of Sri Lanka. Journal of the National Science Foundation of Sri Lanka 45(1): 79–81. https://doi.org/10.4038/jnsfsr.v45i1.8042

Le TN, Ha HT, Nguyen OTT, Tran GH, Vu QT, Nguyen HTT, Diep PTL, Nguyen LTP, Nguyen HTM (2021a) Cycloartane triterpenoids and biological activities from the propolis of the stingless bee *Lisotrigona furva*. Vietnam Journal of Chemistry 59(4): 426–430.

Le TN, Nguyen TP, Nguyen MT, Trinh HK, Vu OTK, Dinh TN, Tran NT, Nguyen LTP (2021b) Chemical constituents and antimicrobial activity of *Lisotrigona cacciae* propolis collected in Hoa Binh Province. Vietnam Journal of Science, Technology, and Engineering 63(2): 70–73. https://doi.org/10.31276/VJSTE.63(2).70-73

Lee S, Duwal RK, Lee W (2016) Diversity of stingless bees (Hymenoptera, Apidae, Meliponini) from Cambodia and Laos. Journal of Asia-Pacific Entomology 19(4): 947–961. https://doi.org/10.1016/j.aspen.2016.04.018

Li Y-R, Wang Z-W, Yu Z-R, Corlett RT (2021) Species diversity, morphometrics, and nesting biology of Chinese stingless bees (Hymenoptera, Apidae, Meliponini). Apidologie 52(6): 1239–1255. https://doi.org/10.1007/s13592-021-00899-x

Li Y-R, Qu Y-F, Xu H-L, Wang Z-W (2021) A new record of sweat-sucking stingless bee, *Lisotrigona carpenteri* Engel 2000, from a natural savanna in southwest China. Journal of Apicultural Research

Michener CD (1990) Classification of the Apidae (Hymenoptera). University of Kansas Science Bulletin 54(4): 75–163.

Michener CD (2001) Comments on minute Meliponini and the male of the genus *Pariotrigona* (Hymenoptera: Apidae). Journal of the Kansas Entomological Society 74(4): 231–236.

Michener CD (2007a) *Lisotrigona* in Thailand, and the male of the genus (Hymenoptera: Apidae: Meliponini). Journal of the Kansas Entomological Society 80(2): 130–135. https://doi.org/10.2317/0022-8567(2007)80[130:LITATM]2.0.CO;2

Michener CD (2007b) The Bees of the World [2nd edn.]. Johns Hopkins University Press, Baltimore, MD, [xvi+[i]+] 953 pp. [+20 pls.]

Rasmussen C, Thomas JC, Engel MS (2017) A new genus of Eastern Hemisphere stingless bees (Hymenoptera: Apidae), with a key to the supraspecific groups of Indomalayan and Australasian Meliponini. American Museum Novitates 3888: 1–33. https://doi.org/10.1206/3888.1

Sakagami SF (1975) Stingless bees (excl. *Tetragonula*) from the Continental Southeast Asia in the collection of Berince [sic] P. Bishop Museum, Honolulu (Hymenoptera, Apidae). Journal of the Faculty of Science, Hokkaido University, Series VI, Zoology 20(1): 49–76.

Thangjam R, Rao S, Viraktamath S, Sharma LD (In press) First report of drinking tear and sweat by *Lisotrigona* bees (Apidae: Meliponini) from India. Journal of Apicultural Research

Viraktamath S, Sajan Jose K (2017) Two new species of *Lisotrigona* Moure (Hymenoptera: Apidae: Meliponini) from India with notes on nest structure. The Bioscan 12(1): 21–28.

ZooKeys 1089: 73–92 (2022)
doi: 10.3897/zookeys.1089.79999
https://zookeys.pensoft.net

RESEARCH ARTICLE

A peer-reviewed open-access journal
ZooKeys
Launched to accelerate biodiversity research

Parasitic crustaceans (Branchiura and Copepoda) parasitizing the gills of puffer fish species (Tetraodontidae) from the coast of Campeche, Gulf of Mexico

Ana Luisa May-Tec[1], Carlos Baños-Ojeda[1], Edgar F. Mendoza-Franco[1]

1 *Instituto de Ecología, Pesquerías y Oceanografía del Golfo de México (EPOMEX), Avenida Héroe de Nacozari No. 480, CP. 24029, Universidad Autónoma de Campeche, San Francisco de Campeche, Campeche, Mexico*

Corresponding author: Edgar F. Mendoza-Franco (efmendoz@uacam.mx)

Academic editor: Kai H. George | Received 1 January 2022 | Accepted 16 February 2022 | Published 16 March 2022

http://zoobank.org/48EA9BA7-B23F-403E-859A-BACA28ABD63E

Citation: May-Tec AL, Baños-Ojeda C, Mendoza-Franco EF (2022) Parasitic crustaceans (Branchiura and Copepoda) parasitizing the gills of puffer fish species (Tetraodontidae) from the coast of Campeche, Gulf of Mexico. ZooKeys 1089: 73–92. https://doi.org/10.3897/zookeys.1089.79999

Abstract
New information on the marine parasitic crustaceans from the Campeche coast, Gulf of Mexico (GoM), can improve our baseline knowledge of the ecology of both the host and parasite by providing, for example, parameters of infection. Such knowledge is especially important for fish farming, so that appropriate quarantine measures can be established. Our aim was to morphologically identify the parasitic crustaceans infecting puffer fish of commercial importance in the coastal zone of Campeche, Mexico. We provide new information on four known species of parasitic crustaceans from 92 specimens representing five species of tetraodontid fish. The parasitic crustaceans *Argulus* sp. (Branchiura, Argulidae), *Caligus haemulonis* (Caligidae), *Pseudochondracanthus diceraus* (Chondracanthidae), and *Taeniacanthus lagocephali* (Taeniacanthidae) (all Copepoda) were found on *Lagocephalus laevigatus*, *Sphoeroides nephelus*, *S. parvus*, *S. spengleri*, and *S. testudineus*. This study revealed the occurrence of *P. diceraus*, which is of importance in aquaculture, on *Sphoeroides annulatus* in the Mexican Pacific. Additionally, our results and other documentary records provide the first evidence of the interoceanic occurrence of the same parasitic crustacean species in the south-southwest of Gulf of Mexico, the Atlantic Ocean, and the Pacific Ocean. Moreover, our study provides valuable information on the biodiversity of parasitic crustaceans present in the GoM on puffer fish which are of great commercial importance for human consumption, fisheries, and aquaculture.

Keywords
Argulidae, aquaculture, biodiversity, Caligidae, Chondracanthidae, fisheries, interoceanic, Taeniacanthidae

Introduction

Parasitic crustaceans are commonly known to cause serious lesions on farmed fish, causing destruction of gill tissue and favoring secondary infection, diseases, and massive mortality worldwide (Dezfuli et al. 2011; Aneesh et al. 2014; Misganaw and Getu 2016). Consequently, their presence represents a significant threat in aquaculture, with substantial potential economic losses. The probability of these organisms being introduced into farming systems is high, especially when an infected fish is caught from the wild and introduced into marine aquaculture (Bouwmeester et al. 2021).

In Mexico, studies on parasitic crustaceans belonging to Branchiura and Copepoda are scarce considering the high diversity of host species inhabiting the vast aquatic ecosystems (Morales-Serna et al. 2012). Knowledge of parasite diversity is an important step to understand how an ecosystem will respond to environmental stressors (Bennett et al. 2021). In particular, changes in the richness of parasitic species or individual parasites are indicative of environmental impact (Sures et al. 2017; Vidal-Martínez et al. 2019, 2022). The Gulf of Mexico (**GoM**) is characterized by activities such as overfishing and extraction of petroleum, which have a negative effect on biodiversity (Soto et al. 2014; Mendoza-Franco et al. 2018). However, this impact is difficult to estimate because of the limited biodiversity data.

The diversity of fish on the Campeche coast includes species such as puffer fish (Tetraodontiformes, Tetraodontidae) which are considered an economically important resource in southern Mexico and have the potential for aquaculture (Chávez-Sánchez et al. 2008). Notwithstanding this potential, knowledge of their parasitic crustaceans is rudimentary. This information is crucial to implement control tools and to create strategies for their safe management, especially for the commercial species.

Our aim was to identify morphologically the parasitic crustaceans infecting *Lagocephalus laevigatus* (Linnaeus, 1766), *Sphoeroides nephelus* (Goode & Bean, 1882), *S. parvus* (Shipp & Yerger, 1969), *S. spengleri* (Bloch, 1785), and *S. testudineus* (Linnaeus, 1758), all commercially important in the coastal zone of Campeche, Mexico. The geographic distribution of these copepods on puffer fish from the tropics is briefly discussed based on our findings and previous records.

Material and methods

Using gill nets, we collected 92 puffer fish (69 *L. laevigatus*, 17 *S. spengleri*, 2 *S. testudineus*, 2 *S. parvus*, and 2 *S. nephelus*) from Seybaplaya, Campeche, southern Gulf of Mexico (19°42.580'N, 90°44.155'W), between November 2020 and April 2021. Fish were kept on ice for a maximum of 8 h and transported to the Laboratory of Aquatic Parasitology of EPOMEX (Instituto de Ecología, Pesquerías y Oceanografía del Golfo de México), Universidad Autónoma de Campeche (**UAC**). In the laboratory, we removed fish gills, placed them in bowls with 4% formaldehyde solution, and examined them under a Leica EZ4 stereomicroscope. We detached the parasitic crustaceans from gills by using fine needles, counted them, preliminarily identified them, fixed them in 70% alcohol, labeled them, and stored them in vials. We mounted individual specimens on slides and cleared them with glycerin at different concentrations (1:10, 1:5, 1:2). We examined dissected crustacean body parts following Humes and Gooding (1964). We identified crustaceans based on morphometrics using an Olympus microscope DM 2500. We follow the terminology of Ho (1970), Ho and Lin (2004), Lin and Ho (2006), and Møller et al. (2008) for *Caligus*, *Taeniacanthus*, *Pseudochondracanthus*, and *Argulus*, respectively. Measurements are provided in millimeters and expressed as a range. The prevalence, mean abundance, and intensity range are those proposed by Bush et al. (1997). We obtained synonyms for each host and crustacean species from FishBase (Froese and Pauly 2021) and World of Copepods (Walter and Boxshall 2021), respectively. Host body lengths are expressed as total length (**TL**). We deposited voucher specimens in the Colección Nacional de Invertebrados (**CNIN**), Universidad Nacional Autónoma de México, Mexico City, Mexico.

Results

In total, 92 tetraodontid fish specimens were collected. The most abundant fish species was *L. laevigatus*, followed by *S. spengleri*, while *S. testudineus*, *S. parvus*, and *S. nephelus* were the least abundant species. Three parasitic crustacean species were found on *L. laevigatus* and a single species was found on the four *Sphoeroides* spp.

Subclass Branchiura Thorell, 1864
Order Arguloida Yamaguti, 1963
Family Argulidae Leach, 1819
Genus *Argulus* Müller, 1785

***Argulus* sp.**

Current host. Smooth puffer *Lagocephalus laevigatus* (Linnaeus) (Tetraodontidae) (TL: 27.5–47 cm).

Site of infection. Gills.

Infection parameters. Prevalence: 9% (six fish infected of 69 examined); mean abundance: 0.14 ± 1.03; intensity range: 1–3 individuals.

Source of current specimens. Two voucher specimens deposited in the CNIN (171); collected on 30 November 2020.

Remarks. These specimens are identified morphologically as *Argulus* sp., mainly by the shape and armature of cephalothoracic appendages, the presence of a modification of the first maxilla into a cup-like, stalked sucker, and legs (Møller et al. 2008). However, the specimens are larval stages, so their shape and size had not yet sufficiently developed for specific identification (Fig. 1). We report a species of *Argulus* from the coast of Campeche, Mexico, for the first time.

Figure 1. Parasitic crustacean *Argulus* sp. (Branchiura, Argulidae) on *Lagocephalus laevigatus* from the Campeche coast, Gulf of Mexico.

Subclass Copepoda Milne Edwards, 1840
Order Cyclopoida Burmeister, 1834
Family Chondracanthidae Milne Edwards, 1840
Genus *Pseudochondracanthus* Wilson, 1908

***Pseudochondracanthus diceraus* Wilson, 1908**

Previous records. *Sphoeroides maculatus* (Bloch & Schneider, 1801) (type host) from California (Wilson 1908); *S. nephelus* and *L. laevigatus* from Florida (Bere 1936); *S. spengleri* and *S. trichocephalus* (Cope, 1870) (as *S. tricocephalus*) from the coast of North Carolina to Florida, USA (Ho 1970); *S. annulatus* (Jenyns, 1842) (all Tetraodontidae) from the Pacific coast of Mexico (Morales-Serna et al. 2011).

Current hosts. Southern puffer *Sphoeroides nephelus* (TL: 21.6–21.6 cm), least puffer *S. parvus* (TL: 19.5–23 cm), bandtail puffer *S. spengleri* (TL: 13.9–24.0 cm), and checkered puffer *S. testudineus* (TL: 17.2–26.0 cm).

Site of infection. Gills.

Infection parameters. *Sphoeroides nephelus*: prevalence: 100% (two fish infected of two examined); mean abundance: 5 ± 1.4; intensity range: 4–6 copepods. *S. parvus*: 100% (two fish infected of two examined); 2 ± 1.4; 1–3 copepods. *S. spengleri*: 89% (16 fish infected of 18 examined); 5.72 ± 4.89; 1–19 copepods. *S. testudineus*: 100% (two fish infected of two examined); 4 ± 1.4; 3–5 copepods.

Source of current specimens. Ten voucher specimens (5 ♂, 5 ♀) from *S. spengleri* plus voucher and two specimens from *S. nephelus*, *S. parvus*, and *S. testudineus* deposited in the CNIN (172); collected on 27 April 2021.

Description (based on 10 females and 7 males). Adult female body 2.20–3.57 long. Head 0.75–0.87 long and 0.50–0.80 wide. Female genital complex elliptical, and entirely covered with small spines. Length of genital portion 1.34–2.35, and 0.56–1.0 wide. Length of egg strings 2.29–4.21 (Fig. 2A). Male body, 0.25–0.43 long and 0.12–0.20 wide (Fig. 2B). Urosome curved ventrally. Legs absent.

Remarks. *Pseudochondracanthus diceraus* was originally described by Wilson (1908) on the gills of common puffer *S. maculatus* from Massachusetts, USA. This parasitic copepod has also been reported in the same host from Massachusetts to North Carolina, in *S. spengleri* from North Carolina to Florida, in *S. trichocephalus* from the East coast of US, as well as in *L. laevigatus* and *S. nephelus* from the Gulf of Mexico, US coast (Wilson 1908; Bere 1936; Ho 1970). In Mexican Pacific waters, *P. diceraus* infected *S. annulatus* (Morales-Serna et al. 2011). *Pseudochondracanthus diceraus* differs from the other congeneric species in having the trunk region covered with scale-like sclerotization (see Ho 1970: figs 236–251), which we clearly observed in the present specimens. Morphometrical comparison between the newly collected specimens and previous descriptions revealed insignificant differences. *Sphoeroides parvus* and *S. testudineus* are new host records for *P. diceraus*, and Seybaplaya, Campeche, Mexico, is a new geographic record for this copepod species.

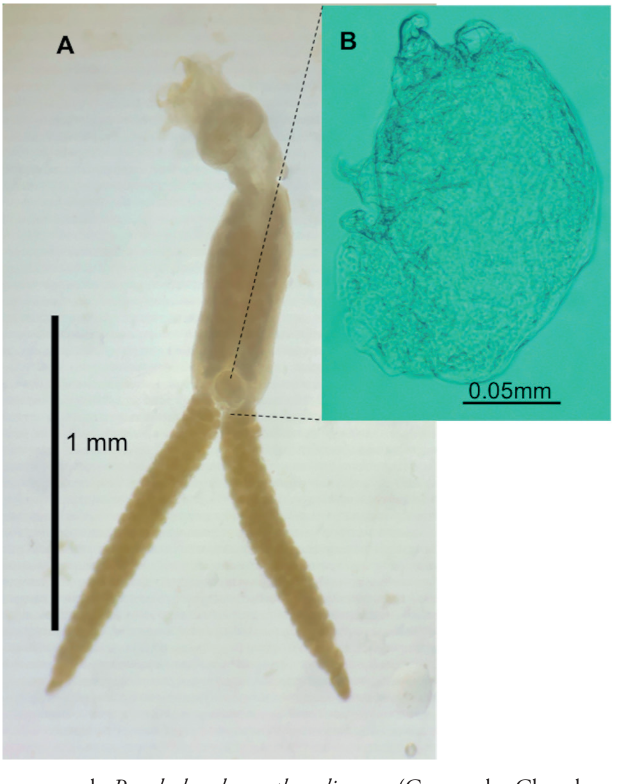

Figure 2. Parasitic copepods *Pseudochondracanthus diceraus* (Copepoda, Chondracanthidae) on puffer fish from the Campeche coast, Gulf of Mexico **A** female **B** male.

Family Taeniacanthidae Wilson, 1911
Genus *Taeniacanthus* Sumpf, 1871

Taeniacanthus lagocephali Pearse, 1952

Irodes lagocephali Pillai, 1963: 124, fig. 7. Syn.
Taeniacanthus sabafugu Yamaguti & Yamasu, 1959: 102, pl. 4, figs 79, 89.

Previous records and localities. *Lagocephalus laevigatus* (type host) from Padre Island (Texas coast), Brazil, Alabama (Texas), Mississippi, and the Argentine Sea (Pearse 1952; Dojiri and Cressey 1987; Cantatore et al. 2012); *L. spadiceus* (Richardson, 1845) from Japan and the Mediterranean coast of Turkey (Yamaguti and Yamasu 1959; Özak et al. 2012); *L. lunaris* (Bloch & Schneider, 1801) from India (Pillai 1963); *L. inermis* (Temminck & Schlegel, 1850) from India (Umadevi and Shyamasundari 1980); *L. gloveri* (Abe & Tabeta, 1983) from Japan (Izawa 1986); *L. wheeleri* (Abe, Tabeta & Kitahama, 1984) from Taiwan (all Tetraodontidae) (Lin and Ho 2006).

Current host. Smooth puffer *Lagocephalus laevigatus* (Linnaeus) (Tetraodontidae) (TL: 20.3–48.5 cm).

Site of infection. Gills.

Infection parameters. Prevalence: 40% (28 fish infected of 69 examined); mean abundance: 1.10 ± 2.90; intensity range: 1–9 copepods.

Source of current specimens. Ten voucher specimens (10 ♀) deposited in the CNIN (173); collected on 30 November 2020.

Description (based on 10 females). Total body length (not including setae of caudal rami) 2.52–3.33; cephalothorax length 0.54–0.76 and width 0.76–1.01 (Fig. 3A). Three thoracic segments as wide as cephalothorax (0.53 × 0.96; 0.53 × 0.90; 0.64 × 0.83). Urosome comprises five segments; genital complex (double-somite) much wider 0.26–0.35 than long 0.13–0.21. Anal somite with four interrupted rows of spinules and one row near the intersection of each caudal ramus. Caudal ramus (0.050 × 0.04) bearing six setae: two long apical, one short subterminal at inner and outer corners, one short dorsal, and one short seta on outer margin near center. Maxillary hook large, slender, slightly curved, located on the anteroventral surface of cephalothorax to junction of first and second segments of first antenna. First maxillae with two pinnate setae. Second maxillae bi-segmented, bearing two terminal spiniform processes on second segment. Maxilliped three-segmented; basal segment unarmed; second segment armed with two basal setae; and terminal segment forming a claw curved with serrations on convex margin of distal portion.

Remarks. Pearse (1952) originally described *T. lagocephali* infecting the gills of *L. laevigatus* from Padre Island, Texas. Yamaguti and Yamasu (1959) reported it as *Taeniacanthus sabafugu* from *L. spadiceus* from Japan, and Pillai (1963) described it as *Irodes lagocephali* from *L. lunaris* and *L. inermis* from India. Subsequently, Ho (1970) recognized all these copepod species from *L. spadiceus*, *L. lunaris*, and *L. inermis* as synonyms of *T. lagocephali*. This parasitic copepod is characterized by having

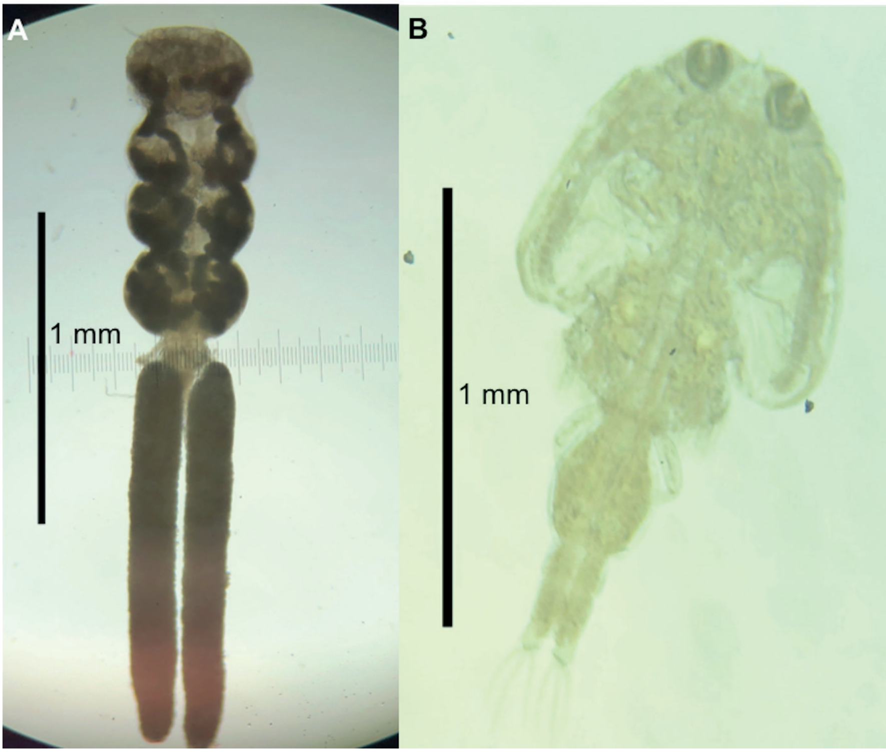

Figure 3. Parasitic copepods on *Lagocephalus laevigatus* from the Campeche coast, Gulf of Mexico. **A** *Taeniacanthus lagocephali* **B** *Caligus haemulonis*

a cephalothorax with three thoracic segments equal in width, a maxilliped with a terminal curving claw, and a digitiform process (Dojiri and Cressey 1987: fig. 33). We also observed these morphological characteristics in our specimens, and they are consistent with the original description and the specimens redescribed by Dojiri and Cressey (1987), Lin and Ho (2006), and Özak et al. (2012). However, some metric differences were observed in the total length between the newly collected specimens from *T. lagocephali* and those reported from *L. spadiceus* by Özak et al. (2012) from the Mediterranean coast of Turkey (2.95 mm vs 1.9 mm). These are probably due to intraspecific variation over large geographic distances or from effects of hosts; that is, host body size is one of five alternative hypotheses which can potentially generate a geographic pattern in parasite body size, while following the Bergmann's rule suggested by Poulin (2021). Studies have demonstrated a positive relationship between the parasite body size and the host body size (Poulin et al. 2003). So, *L. laevigatus* reaches sizes larger than *L. spadiceus* (100 cm vs 37.4 cm), and this can explain the metric differences of *T. lagocephali* found on these hosts. Furthermore, Lin and Ho (2006) reported four setae on the third segment of the antennule, while Dojiri and Cressey (1987) and Özak et al. (2012) reported five on the same segment, the number we observed in our specimens. Additionally, the number of rows of spinules on the ventral surface (three) of the anal segment reported by Lin and Ho (2006) contrast with the four rows of spinules reported by Dojiri and Cressey (1987), Özak et al. (2012), and in our material. Another explanation for these morphological differences could be result of a phenotypic variation in this species, and a phylogenetic study comparing these morphologic differences may contribute to a better understanding of this variation.

Taeniacanthus lagocephali has been reported on *Lagocephalus* spp. from the Oriental region (Japan and Taiwan), the Ethiopian region (West Africa), the Nearctic region (GoM coast of Mississippi, Alabama, and Texas), and the Neotropical region (Brazil) (Pearse 1952; Yamaguti and Yamasu 1959; Pillai 1963; Umadevi and Shyamasundari 1980; Izawa 1986; Dojiri and Cressey 1987; Lin and Ho 2006; Cantatore et al. 2012; Özak et al. 2012). The wide distribution of this parasite could be attributed to its host specificity to the genus *Lagocephalus* and its capacity to exploit this host genus in different geographic ranges. Host specificity is a determinant key in how the parasites can be established into new areas (Poulin et al. 2011). In Mexico, Taeniacanthidae has been represented only by *Taeniacanthodes dojirii* Braswell, Benz & Deets, 2002 in the ray *Narcine entemedor* (Narcinidae) from Bahía de Los Angeles, Santa Rosalía, Gulf of California (Braswell et al. 2002). Our present record is the first occurrence of *T. lagocephali* on *L. laevigatus* from the GoM. Together with the only species previously reported (Braswell et al. 2002), the number of species of Taeniacanthidae in Mexico is now two.

Order Siphonostomatoida Burmeister, 1835
Family Caligidae Burmeister, 1835
Genus *Caligus* Müller, 1785

***Caligus haemulonis* Krøyer, 1863**

Previous records. See Table 1.

Current host. Smooth puffer *Lagocephalus laevigatus* (Linnaeus) (Tetraodontidae) (TL: 20.3–48.5 cm).

Site of infection. Gills.

Infection parameters. Prevalence: 49% (34 fish infected of 69 examined); mean abundance: 3.63 ± 7.45; intensity range: 1–30 copepods.

Source of current specimens. Ten voucher specimens (5 ♀, 5 ♂) deposited in the CNIN (174); collected on19 January 2021.

Description (based on 10 females and 10 males). Adult female body caligiform, 2.70–3.30 long. Cephalothorax 1.50–1.80 long and 1.43–1.63 wide. Female genital complex longer than wide, lacking distinct posterolateral lobes (Fig. 3B). Caudal rami armed with five pinnate setae. Female antenna with distal claw strongly curved. Sternal furca of female with incurved tines. Maxilliped with smooth myxal margin, with a tiny process on inner margin of the claw. Male 2.10–2.50 long. Cephalothorax 1.10–1.30 long and 0.95–1.47 wide. Sternal furca more incurved in males. Male maxilliped with large, acutely pointed process on myxal margin opposing tip of claw. In both sexes, post-antennal process large and strongly curved. Last exopodal segment of leg I with one long seta at inner distal angle, three distal spines, and posterior margin a single naked vestigial seta. Outer margin of second endopodal segment of leg II with setules. Leg IV with robust first exopodal segment bearing marginal setule; second segment with well-developed spines.

Remarks. Currently, the genus *Caligus* comprises more than 270 valid species worldwide (Walter and Boxshall 2021) on a wide variety of marine fish. In Mexican waters 31 species of *Caligus* are known, 21 from the Pacific, seven from GoM, and three from both the Atlantic and Pacific coasts (Morales-Serna et al. 2014). *Caligus haemulonis* has been recorded on the Atlantic coast from Florida to Brazil on a wide variety of fish families and only one species of ray (*Aetobatus narinari*) on the Campeche coast (Rodríguez-Santiago et al. 2016) (Table 1). The morphologic characteristic of our specimens coincide with the original description of *C. haemulonis* (Krøyer 1863; Boxshall and El-Rashidy 2009).

Caligus haemulonis and 13 other parasitic copepods are included in the *Caligus productus* group; they are characterized by loss of two and reduction or loss of the third of the three plumose setae on the distal exopod segment of the first swimming leg (see Boxshall and El-Rashidy 2009: figs 5, 6). In particular, *C. haemulonis* lacks the plumose setae and has a tiny naked vestigial seta on the posterior margin of the distal exopodal segment of leg I, as seen in the present specimens and the description of Cressey (1991), who was the first to observe this character. We found differences in the body length between our specimens and those reported by Suárez-Morales et al. (2010): females 2.70–3.30 mm vs 3.1–3.2 mm from *H. sciurus* and *H. plumierii* (Haemulidae) in Suárez-Morales et al. (2010) from Mexico, 3.56 mm in Cressey (1991), 3.33–3.92 mm on *Orthopristis ruber* and *Haemulon steindachneri* (all Haemulidae) from Brazil in Luque and Takemoto (1996), and 2.96–3.92 mm in Boxshall and El-Rashidy (2009) from Brazil; males measured 2.10–2.50 mm vs 1.75–1.81 mm from haemulids in Suárez-Morales et al. (2010) from Mexico; 1.86–3.26 mm in Cressey (1991) from Florida and Boxshall and El-Rashidy (2009) from Brazil. The variability in the size of parasites can be attributed to their stage of maturity, because the measurements of the collected specimens (females and males) are within the size range reported in previous studies (Cressey 1991; Luque and Takemoto 1996; Boxshall and El-Rashidy 2009; Suárez-Morales et al. 2010). The characteristics of the female sternal furca (i.e., tines slightly thinner) in our specimens and those reported by Suárez-Morales et al. (2010) are identical (see Suárez-Morales et al. 2010: 169, 171, figs 1, 2). *Caligus haemulonis* is an ectoparasite on a wide variety of teleosts (Margolis et al. 1975; Cressey 1991; Chaves and Luque 1999; Boxshall and El- Rashidy 2009; Suárez-Morales et al. 2010) and some elasmobranchs (Kabata 1979; Tang and Newbound 2004; Rodríguez-Santiago et al. 2016). Our material represents a new host record of this parasitic copepod species in the Mexican GoM.

Table 1. Previous records of *Caligus haemulonis* on a wide variety of fish teleost (14 families) and one elasmobranch species having cosmopolitan distribution.

Host	Locality	Reference
Ariidae		
Ariopsis felis (Linnaeus, 1766) (as *Hexanematichthys felis*, *Galeichthys felis* and *Arius felis*)	Atlantic coast of USA	Wilson 1908
Aspistor luniscutis (Valenciennes, 1840) (as *Arius luniscutis*, *Notarius luniscutis*)	Brazil	Luque and Tavares 2007
Bagre marinus (Mitchill, 1815) (as *Felichthys marinus* and *Bagre marina*)	Atlantic coast of USA	Wilson 1908
Carlarius heudelotii (Valenciennes, 1840) (as *Arius heudelotii*)	Africa, Mediterranean	Brian 1924
Genidens barbus (Lacepède, 1803)	Brazil	Luque and Tavares 2007
Carangidae		
Campogramma glaycos (Lacepède, 1801) (as *Lichia vadigo*)	Mediterranean	Brian 1924
Caranx crysos (Mitchill, 1815)	Louisiana	Causey 1953
Caranx rhonchus Geoffroy Saint-Hilaire, 1817 (as *Caranx angolensis*)	Africa South	Capart 1959
Trachurus trachurus (Linnaeus, 1758)	Africa South	Capart 1959
Engraulidae		
Anchoa marinii Hildebrand, 1943	Brazil	Luque and Tavares 2007
Ephippidae		
Chaetodipterus faber (Broussonet, 1782)	Brazil, Florida	Cezar and Luque 1999
Haemulidae		
Anisotremus virginicus (Linnaeus, 1758)	Belize	Cressey 1991
Haemulon carbonarium Poey, 1860	Belize	Cressey 1991
Haemulon macrostomum Günther, 1859	Belize	Cressey 1991
Haemulon plumierii (Lacepède, 1801)	Belize	Cressey 1991
Haemulon sciurus (Shaw, 1803) (type host)	Danish West Indies of Insular Caribbean	Krøyer 1863
Haemulon steindachneri (Jordan & Gilbert, 1882)	Brazil	Luque and Takemoto 1996
Orthopristis ruber (Cuvier, 1830)	Brazil, Florida	Luque and Takemoto 1996
Plectorhinchus mediterraneus (Guichenot, 1850) (as *Diagramma mediterraneum*)	Africa, Mediterranean	Brian 1924
Kyphosidae		
Girella tricuspidata (Quoy & Gaimard, 1824)	Australia	Boxshall and El-Rashidy 2009
Monacanthidae		
Aluterus schoepfii (Walbaum, 1792) (as *Aleuterus schoepfi*)	Florida	Cressey 1991
Myliobatidae		
Aetobatus narinari (Euphrasen, 1790) (as *Stoasodon narinari*)	Tabasco to Campeche coast Gulf of Mexico	Rodríguez-Santiago et al. 2016
Polynemidae		
Polydactylus quadrifilis (Cuvier, 1829)	Africa	Oldewage and Avenant-Oldewage 1993
Pomatomidae		
Pomatomus saltatrix (Linnaeus, 1766) (as *Temnodon saltator*)	Mediterranean	Brian 1924
Rachycentridae		
Rachycentron canadum (Linnaeus, 1766)	USA	Williams and Bunkley-Williams 1996
Sciaenidae		
Argyrosomus regius (Asso, 1801) (as *Sciaena aquila*)	Mediterranean	Brian 1924
Bairdiella chrysoura (Lacepède, 1802)	Florida	Cressey 1991
Menticirrhus americanus (Linnaeus, 1758) (as *Menthicirrhus americanus*)	Brazil, Florida	Chaves and Luque 1999
Micropogonias furnieri (Desmarest, 1823) (as *Micropogon furnieri*)	Brazil	Alves and Luque 2000

Host	Locality	Reference
Paralonchurus brasiliensis (Steindachner, 1875)	Brazil	Ribeiro et al. 2002, Luque et al. 2003
Pogonias cromis (Linnaeus, 1766)	Florida	Bere 1936
Pseudotolithus moorii (Günther, 1865) (as *Corvina camaronensis*)	Africa South	Capart 1959
Sciaena umbra Linnaeus, 1758 (as *Corvina nigra*)	Mediterranean	Brian 1924
Sciaenops ocellatus (Linnaeus, 1766) (as *Sciaenops ocellata*)	Louisiana	Causey 1953
Umbrina sp.	Africa South	Capart 1959
Serranidae		
Centropristis striata (Linnaeus, 1758)	Florida	Wilson 1908
Sparidae		
Archosargus probatocephalus (Walbaum, 1792)	Florida	Cressey 1991
Archosargus rhomboidalis (Linnaeus, 1758)	Brazil	Cordeiro and Luque 2005
Dentex sp.	Africa, Mediterranean	Brian 1924
Dentex gibbosus (Rafinesque, 1810) (as *D. filosus*)	Africa South	Capart 1959
Pagrus sp.	Africa, Mediterranean	Brian 1924
Pagrus pagrus (Linnaeus, 1758)	Brazil	Paraguassú et al. 2002
Triglidae		
Prionotus punctatus (Bloch, 1793)	Brazil	Bicudo et al. 2005
Trigla lyra Linnaeus, 1758	Africa South	Capart 1959

Discussion

This study represents the first records of branchiuran and copepod parasites on tetraodontids of the Campeche coast. Previous records from this area mentioned the presence of 15 species of copepods parasitizing elasmobranchs; some have also been reported for other elasmobranch species worldwide (Rodríguez-Santiago et al. 2016). However, of these species only one copepod (*C. haemulonis*) coincides with those reported in our study. All records we have reported here are new host records or new geographic records. Below, we briefly discuss the distribution of the puffer fish hosts that these crustaceans parasitize.

Members of *Argulus* have a wide range of fish hosts and environments (freshwater and marine) around the world. In the GoM, 10 species have been reported, especially from the north-northwest coast of the USA (Poly 2009). In Mexican waters, six species of *Argulus* are recorded: *Argulus chromidis* Krøyer, 1863 and *Argulus rhamdiae* Wilson, 1936 on *Rhamdia guatemalensis* Günther, 1864 from Yucatán (Wilson 1936), *Argulus flavescens* Wilson, 1916 on *Ariopsis assimilis* Günther, 1864 (as *Arius assimilis*) from Chetumal (Suárez-Morales et al. 1998), *Argulus mexicanus* Pineda, Paramo & del Rio, 1995 on *Atractosteus tropicus* Gill, 1863 from Tabasco (Pineda et al. 1995), *Argulus ambystoma* Poly, 2003 on *Ambystoma dumerilii* Dúges, 1870 from Lake Patzcuaro, Michoacan (Poly 2003), and *Argulus yucatanus* Poly, 2005 on *Mayaheros urophthalmus* Günther, 1862 (as *Cichlasoma urophthalmus*) from Yucatán (Poly 2005). All these records are from freshwater fishes, except for *A. flavescens*, which occurs in freshwater, marine, and brackish-water fishes (Suárez-Morales et al. 1998). These infections have rarely been found to have severe effects on natural fish populations (Taylor et al. 2005). However, their presence is important, especially in fishes with aquaculture potential, such as puffer fish. These ectoparasites cause dermal damages that promotes secondary infections and, in severe cases, high mortality in aquaculture systems where these types of infections are intensified (Patra et al. 2016). Additional adult specimens of *Argulus* sp. are necessary to determine the species.

The morphological characteristics of specimens *Taenicanthus lagocephali* in *L. laevigatus* collected here agree with the original description and redescription of specimens from North and South America (Pearse 1952; Dojiri and Cressey 1987). The geographic proximity of GoM to the Atlantic Ocean and the wide host distribution could explain the morphological similarity of our specimens to Atlantic populations. However, some differences have been found with the description of *T. lagocephali* from the Mediterranean coast and Taiwan. These could probably be attributed to intraspecific variation in the geographic distance of the hosts. We believe that future studies incorporating phylogenetic analyses are necessary to confirm the identity and to accurately assess the distribution of these species, as well as to understand their host specificity.

Cressey (1991) and Suárez-Morales et al. (2010) have suggested that in the Mexican Caribbean, despite its high ichthyological diversity, haemulids are the preferred hosts of *C. haemulonis*, with a prevalence ranging from 6 to 13%. However, we found a higher prevalence in *L. laevigatus* (> 40%), which suggests that *C. haemulonis* does not present a host preference, as proposed. However, to affirm this assumption, a study is necessary that includes the haemulids as the abundant fishes on the Campeche coast (Crespo-Guerrero et al. 2019; Borges-Ramírez et al. 2020). *Caligus haemulonis* has a broad host range; this characteristic is especially important to fish farming because the introduction of infected wild fish could cause its transmission to new hosts. Therefore, the record of *C. haemulonis* in puffer fishes from southern Mexico accounts for the geographic range of this parasitic copepod and its expansion to new hosts in the region. In addition, this information could contribute to implementation of measures to prevent its transmission—that is, quarantine of wild fish—to farmed fish such as puffer fish.

With exception of *L. laevigatus*, all other species of *Sphoeroides* examined were parasitized with *P. diceraus.* This suggests that *Sphoeroides* spp. could be the preferred hosts of this parasite. Future examination of other hosts in the same area is necessary to confirm this assumption. This is the first record of *P. diceraus* parasitizing a puffer fish from the GoM. In previous studies on parasitofauna of puffer fishes from the southern of GoM (Vidal-Martínez and Mendoza-Franco 2008; Pech et al. 2009), this copepod was not reported. Special attention should be paid to the presence of *P. diceraus*, which has caused high mortality in the culture of *S. annulatus* (Fajer-Ávila et al. 2011).

Our findings suggest that the composition of ectoparasites on puffer fishes from the Campeche coast differs from that reported for the Yucatán Peninsula by Vidal-Martínez and Mendoza-Franco (2008) and Pech et al. (2009), despite the wide distribution of host species. These differences in ectoparasite composition might be due to the physicochemical (water quality, nutrients, and water flow rates) and biological characteristics of the regions along the south-southwest coast from Tabasco to Campeche, and along the south-southeast coast in the Yucatán Peninsula. This hypothesis has been partially tested through a comparative study of the parasitofauna of flounder fish from the Yucatán Peninsula (i.e., *Syacium papillosum* and *Syacium gunteri*) (Vidal-Martínez et al. 2019). Vidal-Martínez et al. (2019) found variation in the parasite composition associated with environmental variables, suggesting the existence of two subregions in the Yucatán Peninsula (the Campeche Sound and the Yucatán Shelf). However, a comparative study of the parasitofauna of *Sphoeroides* spp. between the two regions, considering the ecological data, could contribute to a better understanding of the differences.

The occurrence of *P. diceraus* in the Pacific and along the Campeche coast is noteworthy. *Pseudochondracanthus diceraus* was originally described in commercially important fish *Sphoeroides maculatus* from the Atlantic and Pacific coast of the USA (Wilson, 1908); however, *S. maculatus* is a fish native to the North Atlantic. Its presence in the Pacific is remarkable and it is tempting to speculate that its presence there is the result of translocation of parasites associated with the natural distribution of their hosts or a consequence of anthropogenic activities (i.e., host introductions; Goedknegt et al. 2016; Paredes-Trujillo et al. 2020). However, the distribution mechanisms of copepod species are not well understood, and information has mainly focused on taxonomy. Nevertheless, *P. diceraus* has previously been reported on *S. spengleri* and *S. nephelus* from Florida and the US Gulf Coast (Wilson 1908; Bere 1936; Ho 1970). The GoM is part of the geographical range of this puffer fish, so the presence of *P. diceraus* on the Campeche coast can be attributed to the natural distribution of these *Sphoeroides* spp.

On the other hand, the broad geographic distribution of *P. diceraus* could be explained by a hypothesis suggested by Kritsky (2012) who suggested that the geological formation of the Panamanian isthmus approximately 3.2 Ma ago divided ancestral hosts as well as their monogeneans into eastern Pacific and western Atlantic populations.

Therefore, the geographical distribution of both parasitic crustacean and the monogeneans could be attributed to the dispersal capabilities of their hosts (Skern-Mauritzen et al 2014; Paladini et al 2021). Therefore, we suggest that parasitic crustaceans could have undergone a similar distribution and speciation. However, a phylogenetic hypothesis based on molecular and morphological data for these parasitic crustaceans on puffer fish would provide the needed information on their diversification as evidence of a speciation process associated with geological history or the influence of ecological factors; this would provide a more comprehensive understanding of the biogeographical distribution of parasitic crustaceans in the tropics.

Conclusions

We have revealed the occurrence of marine parasitic crustaceans of importance for fish aquaculture on the Campeche coast. We have deduced that the composition of ectoparasites on puffer fishes of the Campeche coast and Yucatán Peninsula differ and this difference is associated with differing environmental characteristics of each area, despite the geographical proximity. Our results represent only a small fraction of diversity of parasitic crustaceans present in the GoM, but they provide valuable new information on the geographical distribution and hosts in the region (i.e., the occurrence of an interoceanic copepod species), which is especially relevant aquaculture. To explore host specificity, the ecological and parasite-host interaction associated with their distribution, studies focusing on morphology and phylogenetics are essential.

Acknowledgements

This research was supported financially by a postdoctoral grant (216405) and a master student fellowship (scholarship number 1077567) from CONACyT, Mexico, to A.L.M.-T. and C.B.-O., respectively. We thank to Francisco Javier Gómez Criollo (EPOMEX) for help with identifying the fish, and Mariela del Carmen Rosado Tun (Aquatic Parasitology, EPOMEX) for assistance during the laboratory work. We would like to express our sincere thanks to the administrative and academic authorities of the Universidad Autónoma de Campeche (UAC-EPOMEX) for facilities. We are very grateful to the anonymous referees for the evaluation of our paper and for the constructive critics.

References

Alves DR, Luque JL (2000) Metazoarios parásitos de *Micropogonias furnieri* (Osteichthyes: Sciaenidae) do litoral do estado do Rio de Janeiro, Brasil. Parasitología al Día 24: 40–45. https://doi.org/10.4067/S0716-07202000000100006

Aneesh PT, Sudha K, Helna AK, Anilkumar G, Trilles JP (2014) Multiple parasitic crustacean infestation on belonid fish *Strongylura strongylura.* ZooKeys 353: 339–353. https://doi.org/10.3897/zookeys.457.6817

Bennett J, Presswell B, Poulin R (2021) Biodiversity of marine helminth parasites in New Zealand: What don't we know? New Zealand Journal of Marine and Freshwater Research, 1–16. https://doi.org/10.1080/00288330.2021.1914689

Bere R (1936) Parasitic copepods from Gulf of Mexico fish. American Midland Naturalist 17(3): 577–625. https://doi.org/10.2307/2419936

Bicudo AJA, Tavares LER, Luque JL (2005) Metazoários parasitos da cabrinha *Prionotus punctatus* (Bloch, 1793) (Osteichthyes: Triglidae) do litoral do estado do Rio de Janeiro, Brasil. Revista Brasileira de Parasitologia Veterinária 14: 27–33. https://doi.org/10.4025/actascibiolsci.v27i2.1320

Borges-Ramírez MM, Mendoza-Franco EF, Escalona-Segura G, Rendón-von Osten J (2020) Plastic density as a key factor in the presence of microplastic in the gastrointestinal tract of commercial fishes from Campeche Bay, Mexico. Environmental Pollution 267: e115659. https://doi.org/10.1016/j.envpol.2020.115659

Bouwmeester MM, Goedknegt MA, Poulin R, Thieltges DW (2021) Collateral diseases: Aquaculture impacts on wildlife infections. Journal of Applied Ecology 58(3): 453–464. https://doi.org/10.1111/1365-2664.13775

Boxshall GA, El-Rashidy HH (2009) A review of the *Caligus productus* species group, with a description of a new species, new synonymies and supplementary descriptions. Zootaxa 2271(1): 1–26. https://doi.org/10.11646/zootaxa.2271.1.1

Braswell JS, Benz GW, Deets GB (2002) *Taeniacanthodes dojirii* n. sp. (Copepoda: Poecilostomatoida: Taeneacanthidae), from Cortez electric rays (*Narcine entemedor*: Torpediniformes: Narcinidae) captured in the Gulf of California, and phylogenetic analysis of and key to species of *Taeniacanthodes.* The Journal of Parasitology 88(1): 28–35. https://doi.org/10.1645/0022-3395(2002)088[0028:TDNSCP]2.0.CO;2

Brian A (1924) Parasitologia mauritanica. Arthropoda (1re partie), Copepoda. Copépodes commensaux et parasites des côtes mauritaniennes. Bulletin du comité d'Études Historiques et Scientifiques de l'Afrique Occidentale Française, 364–427.

Bush AO, Lafferty KD, Lotz JM, Shostak AW (1997) Parasitology Meets Ecology on Its Own Terms: Margolis et al. Revisited. The Journal of Parasitology 83(4): 575–583. https://doi.org/10.2307/3284227

Cantatore DMP, Braicovich PE, Alarcos AJ, Lanfranchi AL, Rossin MA, Vales DG, Timi JT (2012) New records of parasitic copepods (Crustacea, Copepoda) from marine fishes in the Argentinean Sea. Acta Parasitologica 57: 83–89. https://doi.org/10.2478/s11686-012-0003-z

Capart A (1959) Copepodes parasites: resultats scientifiques. Expedition Oceanographique Belge dans les Eaux Côtieres Africaines de I'Atlantique Sud (19481949) 3: 55–126.

Causey D (1953) Parasitic Copepoda from Grand Isle, Louisiana. Occasional Papers of the Marine Laboratory, Louisiana State University 7: 1–18.

Cezar AD, Luque JL (1999) Metazoan parasites of the Atlantic spadefish, *Chaetodipterus faber* (Teleostei: Ephippidae) from the coastal zone of the state of Rio de Janeiro, Brazil. Journal of the Helminthological Society of Washington 66: 14–20.

Chaves ND, Luque JL (1999) Ecology of metazoans parasites of *Menticirrhus americanus* (Osteichthyes: Sciaenidae), coast area from Rio de Janeiro state, Brazil. Revista Brasileira de Parasitologia Veterinária 8: 137–144.

Chávez-Sánchez MC, Álvarez-Lajonchère L, Abdo De La Parra MI, García-Aguilar N (2008) Advances in the culture of the Mexican bullseye puffer fish *Sphoeroides annulatus*, Jenyns (1842). Aquaculture Research 39(7): 718–730. https://doi.org/10.1111/j.1365-2109.2008.01924.x

Cordeiro AS, Luque JL (2005) Aspectos quantitativos dos metazoários parasitos do sargo-de-dente, *Archosargus rhomboidalis* (Linnaeus, 1758) (Osteichthyes: Sparidae), do litoral do estado do Rio de Janeiro, Brasil. Revista Brasileira de Zoociências 7: 7–14.

Crespo-Guerrero JM, Jiménez-Pelcastre A, Nava-Martínez JD (2019) Tensions and territorial conflicts in coastal fishing in the state of Campeche, Mexico (2013–2018). Bulletin of the Association of Spanish Geographers 82: 1–53. https://doi.org/10.21138/bage.2764

Cressey R (1991) Parasitic copepods from the Gulf of Mexico and Caribbean Sea. III. *Caligus.* Smithsonian Contributions to Zoology 497(497): 1–53. https://doi.org/10.5479/si.00810282.497

Dezfuli BS, Giari L, Lui A, Lorenzoni M, Noga EJ (2011) Mast cell responses to *Ergasilus* (Copepoda), a gill ectoparasite of Sea Bream. Fish & Shellfish Immunology 30(4–5): 1087–1094. https://doi.org/10.1016/j.fsi.2011.02.005

Dojiri M, Cressey RF (1987) Revision of the Taeniacanthidae (Copepoda: Poecilostomatoida) parasitic on fishes and sea urchins. Smithsonian Contributions to Zoology 447(447): 1–245. https://doi.org/10.5479/si.00810282.447.i

Fajer-Ávila EJ, Guzmán-Beltrán L, Zárate-Rodríguez WC, del Río-Zaragoza OB, Almazán-Rueda P (2011) Patología causada por adultos de *Pseudochondracanthus diceraus* (Copepoda: Chondracanthidae) parásito del botete diana *Sphoeroides annulatus*. Revista de Biologia Marina y Oceanografía 46: 293–302. https://doi.org/10.4067/S0718-19572011000300001 [Removed Hyperlink Field]

Froese R, Pauly D (2021) FishBase. http://www.fishbase.org [Accessed on 30.06.2021]

Goedknegt MA, Feis ME, Wegner KM, Luttikhuizen PC, Buschbaum C, Camphuysen K, van der Meer J, Thieltges DW (2016) Parasites and marine invasions: Ecological and evolutionary perspectives. Journal of Sea Research 113: 11–27. https://doi.org/10.1016/j.seares.2015.12.003

Ho JS (1970) Revision of the genera of the Chondracanthidae, a copepod family parasitic on marine fishes. Beaufortia 229: 105–218.

Ho JS, Lin CL (2004) Sea Lice of Taiwan (Copepoda: Siphonostomatoida: Caligidae). The Sueichan Press, Keelung, Taiwan, 388 pp.

Humes AG, Gooding RU (1964) A method for studying the external anatomy of copepods. Crustaceana 6(3): 238–240. https://doi.org/10.1163/156854064X00650

Izawa K (1986) On the development of parasitic Copepoda III. *Taeniacanthus lagocephali* Pearse (Cyclopoida: Taeniacanthidae). Publications of the Seto Marine Biological Laboratory 31(1–2): 37–54. https://doi.org/10.5134/176119

Kabata Z (1979) Parasitic Copepoda of British Fishes. The Ray Society, London, 468 pp.

Kritsky DC (2012) Dactylogyrids (Monogenoidea: Polyonchoinea) parasitizing the gills of snappers (Perciformes: Lutjanidae): Revision of *Euryhaliotrema* with new and previously described species from the red sea, Persian Gulf, the Eastern and Indo-West Pacific Ocean, and the Gulf of Mexico. Zoologia 29(3): 227–276. https://doi.org/10.1590/S1984-46702012000300006

Krøyer H (1863) Bidrag til Kundskab om Snyltekrebsene. Naturhistorisk Tidsskrift, Serie III, 2: 75–320, 321–426. [pls 1–9, pls 10–18 (1864)].

Lin CL, Ho JS (2006) Copepods of the genus *Taeniacanthus* Sumpf, 1871 (Poecilostomatoida: Taeniacanthidae) parasitic on marine fishes of Taiwan. Taiwan Shuichanxue Hui Kan 33: 171–191. https://doi.org/10.29822%2fJFST.200606.0008

Luque JL, Takemoto RM (1996) Parasitic copepods on *Orthopristis ruber* and *Haemulon steindachneri* (Osteichthyes: Haemulidae) from the Brazilian littoral, with the description of a new species of *Caligus* (Siphonostomatoida: Caligidae). Revista Brasileira de Biologia 56: 529–546.

Luque JL, Tavares LER (2007) Checklist of Copepoda associated with fishes from Brazil. Zootaxa 1579(1): 1–39. https://doi.org/10.11646/zootaxa.1579.1.1

Luque JL, Alves DR, Ribeiro RS (2003) Community ecology of the metazoan parasites of Banded Croaker, *Paralonchurus brasiliensis* (Osteichthyes: Sciaenidae), from the coastal zone of the state of Rio de Janeiro, Brazil. Acta Scientiarum 25: 273–278. https://doi.org/10.4025/actascibiolsci.v25i2.2009

Margolis L, Kabata Z, Parker RR (1975) Catalogue and synopsis of *Caligus*, a genus of Copepoda (Crustacea) parasitic on fishes. Bulletin - Fisheries Research Board of Canada 192: 1–117.

Mendoza-Franco EF, Rosado-Tun M del CR, Duarte-Anchevida A de JD, del Río-Rodríguez RE (2018) Morphological and molecular (28S rRNA) data of monogeneans (Platyhelminthes) infecting the gill lamellae of marine fishes in the Campeche Bank, southwest Gulf of Mexico. ZooKeys 783: 125–161. https://doi.org/10.3897/zookeys.783.26218

Misganaw K, Getu A (2016) Review on major parasitic crustacean in fish. Fisheries and Aquaculture Journal 7(3): e175. https://doi.org/10.4172/2150-3508.1000175

Møller OS, Olesen J, Avenant-Oldewage A, Thomsen PF, Glenner H (2008) First maxillae suction discs in Branchiura (Crustacea): Development and evolution in light of the first molecular phylogeny of Branchiura, Pentastomida, and other "Maxillopoda". Arthropod Structure & Development 37(4): 333–346. https://doi.org/10.1016/j.asd.2007.12.002

Morales-Serna FN, Rubio-Godoy M, Gómez S (2011) Seasonality of parasitic copepods on bullseye puffer, *Sphoeroides annulatus* (Pisces: Tetraodontidae), from the northwestern coast of Mexico. The Journal of Parasitology 97(4): 565–573. https://doi.org/10.1645/GE-2638.1

Morales-Serna FN, Gómez S, Pérez Ponce de León G (2012) Parasitic copepods reported from Mexico. Zootaxa 3234(1): 43–68. https://doi.org/10.11646/zootaxa.3234.1.2

Morales-Serna FN, Pinacho-Pinacho CD, Gómez S, Pérez-Ponce de León G (2014) Diversity of sea lice (Copepoda: Caligidae) parasitic on marine fishes with commercial and aquaculture importance in Chamela Bay, Pacific coast of Mexico by using morphology and DNA barcoding, with description of a new species of *Caligus.* Parasitology International 63(1): 69–79. https://doi.org/10.1016/j.parint.2013.09.005

Oldewage WH, Avenant-Oldewage A (1993) Checklist of the parasitic Copepoda (Crustacea) of African fishes. Muséé Royal de l'Afrique Centrale Tervuren Belgique. Documentation Zoologique 23: 1–26.

Özak AA, Demirkale I, Yanar A (2012) First record of two species of parasitic copepods on immigrant pufferfishes (Tetraodontiformes: Tetraodontidae) caught in the eastern Mediterranean Sea. Turkish Journal of Fisheries and Aquatic Sciences 12(3): 677–683. https://doi.org/10.4194/1303-2712-v12_3_17

Paladini G, Shinn AP, Taylor NGH, James EB, Haakon H (2021) Geographical distribution of *Gyrodactylus salaris* Malmberg, 1957 (Monogenea, Gyrodactylidae). Parasites & Vectors 14(1): e34. https://doi.org/10.1186/s13071-020-04504-5

Paredes-Trujillo A, Martínez-Aquino A, Rodiles-Hernández R, González-Solís D (2020) Metazoan parasite communities of three endemic cichlid fish species from the upper Grijalva river, Chiapas, Mexico. Helminthologia 57(4): 344–352. https://doi.org/10.2478/helm-2020-0041

Paraguassú AR, Luque JL, Alves DR (2002) Community ecology of metazoan parasites of red porgy *Pagrus pagrus* (Osteichthyes: Sparidae) from the coastal zone of the State of Rio de Janeiro, Brazil. Acta Scientiarum 24(2): 461–467.

Patra A, Mondal A, Banerjee S, Adikesavalu H, Joardar SN, Abraham TJ (2016) Molecular characterization of *Argulus bengalensis* and *Argulus siamensis* (Crustacea: Argulidae) infecting the cultured carps in West Bengal, India using 18S rRNA gene sequences. Molecular Biology Research Communications 5(3): 156–166.

Pearse AS (1952) Parasitic Crustacea from the Texas coast. Publications of the Institute of Marine Science. University of Texas 2: 1–42.

Pech D, Vidal-Martínez VM, Aguirre-Macedo ML, Gold-Bouchot G, Herrera-Silveira J, Zapata-Pérez O, Marcogliese DJ (2009) The checkered puffer (*Sphoeroides testudineus*) and its helminths as bioindicators of chemical pollution in Yucatan coastal lagoons. The Science of the Total Environment 407(7): 2315–2324. https://doi.org/10.1016/j.scitotenv.2008.11.054

Pillai NK (1963) Copepods of the family Taeniacanthidae parasitic on South Indian fishes. Crustaceana 6(2): 110–128. https://doi.org/10.1163/156854063X00507

Pineda R, Páramo S, Río RD (1995) A new species of the genus *Argulus* (Crustacea: Branchiura) parasitic on *Atractosteus tropicus* (Pisces: Lepisosteidae) from Tabasco, Mexico. Systematic Parasitology 30(3): 199–206. https://doi.org/10.1007/BF00010470

Poly WJ (2003) *Argulus ambystoma*, a new species parasitic on the Salamander *Ambystoma dumerilii* from Mexico (Crustacea: Branchiura: Argulidae). The Ohio Journal of Science 103: 52–61.

Poly WJ (2005) *Argulus yucatanus* sp. nov. (Crustacea: Branchiura) parasitic *on Cichlasoma urophthalmus* from Yucatan, Mexico. Gulf and Caribbean Research 17: 1–13. https://doi.org/10.18785/gcr.1701.01

Poly WJ (2009) Branchiura (Crustacea) of the Gulf of Mexico. In: Felder DL, Camp DK (Eds) Gulf of Mexico Origins, Waters, and Biota. Biodiversity. Texas A&M University Press, College Station, 837–840.

Poulin R (2021) Functional biogeography of parasite traits: Hypotheses and evidence. Philosophical Transactions of the Royal Society of London. Series B, Biological Sciences 376(1837): e20200365. https://doi.org/10.1098/rstb.2020.0365

Poulin R, Wise M, Moore J (2003) A comparative analysis of adult body size and its correlates in acanthocephalan parasites. International Journal for Parasitology 33(8): 799–805. https://doi.org/10.1016/S0020-7519(03)00108-5

Poulin R, Krasnov BR, Mouillot D, Thieltges DW (2011) The comparative ecology and biogeography of parasites. Philosophical Transactions of the Royal Society of London. Series B, Biological Sciences 366(1576): 2379–2390. https://doi.org/10.1098/rstb.2011.0048

Ribeiro RS, Luque JL, Alves DR (2002) Aspectos quantitativos dos parasitos da marialuiza, *Paralonchurus brasiliensis* (Ostheichthyes: Sciaenidae) do litoral do estado do Rio de Janeiro, Brasil. Revista Universidade Rural. Série Ciências da Vida 22: 151–154.

Rodríguez-Santiago MA, Morales-Serna FN, Gómez S, Grano-Maldonado M (2016) New records of parasitic copepods (Copepoda: Pandaridae, Eudactylinidae, Caligidae) on five shark species (Pisces: Elasmobranchia) in the Gulf of Mexico. Neotropical Helminthology 9: 177–182. https://doi.org/10.24039/rnh201591786

Skern-Mauritzen R, Torrissen O, Glover KA (2014) Pacific and Atlantic *Lepeophtheirus salmonis* (Krøyer, 1838) are allopatric subspecies: *Lepeophtheirus salmonis salmonis* and *L. salmonis oncorhynchi* subspecies novo. BioMedCentral Genetics 15(1): e32. https://doi.org/10.1186/1471-2156-15-32

Soto LA, Botello AV, Licea-Durán S, Lizárraga-Partida ML, Yáñez-Arancibia A (2014) Environmental legacy of the Ixtoc-I oil spill in the Campeche sound, southwestern Gulf of Mexico. Frontiers in Marine Science 57: 1–9. https://doi.org/10.3389/fmars.2014.00057

Suárez-Morales E, Kim IH, Castellanos I (1998) A new geographic and host record for *Argulus flavescens* Wilson, 1916 (Crustacea, Arguloida), from southeastern Mexico. Bulletin of Marine Science 62: 293–296.

Suárez-Morales E, Reyes-Lizama C, González-Solís D (2010) Parasitic copepods from reef grunts (Teleostei, Haemulidae) with description of a new species of *Lernanthropus* (Siphonostomatoida, Lernanthropidae) from the Mexican Caribbean. Acta Parasitologica 55(2): 167–176. https://doi.org/10.2478/s11686-010-0025-3

Sures B, Nachev M, Selbach C, Marcogliese DJ (2017) Parasite responses to pollution: What we know and where we go in 'Environmental Parasitology'. Parasites & Vectors 10(1): e65. https://doi.org/10.1186/s13071-017-2001-3

Tang D, Newbound DR (2004) A new species of copepod (Siphonostomatoida: Caligidae) parasitic on the tiger shark *Galeocerdo cuvier* (Péron & Lesueur) from Western Australian waters. Systematic Parasitology 58(1): 69–80. https://doi.org/10.1023/B:SYPA.0000023853.90011.17

Taylor NGH, Sommerville C, Wootten R (2005) A review of *Argulus* sp. occurring in UK freshwaters. UK Environment Agency, Bristol, 30 pp.

Umadevi DV, Shyamasundari K (1980) Studies on the copepod parasites of fishes of the Waltair coast: Family Taeniacanthidae. Crustaceana 39(2): 197–208. https://doi.org/10.1163/156854080X00085

Vidal-Martínez VM, Mendoza-Franco EF (2008) *Heterobothrium lamothei* n. sp. (Monogenea: Diclidophoridae) from the gills of *Sphoeroides testudineus* (Pisces: Tetraodontidae) from the coast of Yucatán, Mexico. Revista Mexicana de Biodiversidad 79: 89–93. https://doi.org/10.22201/ib.20078706e.2008.001.515

Vidal-Martínez VM, Velázquez-Abunader I, Centeno-Chalé OA, May-Tec AL, Soler-Jiménez LC, Pech D, Mariño-Tapia I, Enríquez C, Zapata-Pérez O, Herrera-Silveira J, Hernández-Mena DI, Herzka SZ, Ordoñez-López U, Aguirre-Macedo LM (2019) Metazoan parasite infracommunities of the dusky flounder (*Syacium papillosum*) as bioindicators of environmental conditions in the continental shelf of the Yucatan Peninsula, Mexico. Parasites & Vectors 12(1): e279. https://doi.org/10.1186/s13071-019-3524-6

Vidal-Martínez VM, Ocaña FA, Soler-Jiménez LC, García-Teh JG, Aguirre-Macedo ML, May-Tec AL, Árcega-Cabrera F, Herrera-Silveira J (2022) Functional groups of metazoan parasites of the dusky flounder (*Syacium papillosum*) as bioindicators of environmental health of the Yucatan Shelf. Bulletin of Environmental Contamination and Toxicology 108: 24–29. https://doi.org/10.1007/s00128-021-03177-9

Walter TC, Boxshall G (2021) World of Copepods database. http://www.marinespecies.org/copepoda [Accessed on 30.06.2021]

Williams Jr EH, Bunkley-Williams L (1996) Parasites of offshore big game fishes of Puerto Rico and the Western Atlantic. Department of Natural and Environmental Resources, San Juan, the University of Puerto Rico, Mayaguez.

Wilson CB (1908) North American parasitic copepods: A list of those found upon these fishes of the Pacific coast, with descriptions of new genera and species. Proceedings of the United States National Museum 35(1652): 431–481. https://doi.org/10.5479/si.00963801.35-1652.431

Wilson CB (1936) Copepods from the cenotes and caves of the Yucatan Peninsula, with notes on cladocerans. Carnegie Institution of Washington. Publication 457: 77–88.

Yamaguti S, Yamasu T (1959) Parasitic copepods from fishes of Japan with description of 26 new species and remarks on two known species. Biological Journal of Okayama University 5: 89–165.

ZooKeys 1089: 93–108 (2022)
doi: 10.3897/zookeys.1089.73418
https://zookeys.pensoft.net

RESEARCH ARTICLE

A peer-reviewed open-access journal
ZooKeys
Launched to accelerate biodiversity research

First and second instar larvae and adults of a new *Homidia* species (Collembola, Entomobryidae) recorded from Xizang Autonomous Region with three new records

Ling-bin Xiang[1], Shu-sheng Zhang[2], Lei-lei Liu[2], Zhi-xiang Pan[1]

1 *School of Life Sciences, Taizhou University, Taizhou, Zhejiang 318000, China* **2** *Wuyanling National Nature Reserve, Wenzhou, Zhejiang 325500, China*

Corresponding author: Zhi-xiang Pan (pzx1118@hotmail.com)

Academic editor: Louis Deharveng | Received 24 August 2021 | Accepted 21 February 2022 | Published 16 March 2022

http://zoobank.org/6E2DE612-CD05-482D-B47D-9A1C13722B2E

Citation: Xiang L-b, Zhang S-s, Liu L-l, Pan Z-x (2022) First and second instar larvae and adults of a new *Homidia* species (Collembola, Entomobryidae) recorded from Xizang Autonomous Region with three new records. ZooKeys 1089: 93–108. https://doi.org/10.3897/zookeys.1089.73418

Abstract
Three new recorded species of genus *Homidia* were collected from Xizang Autonomous Region, China, in the present paper. Among them, a new species, *Homidia breviseta* Pan, **sp. nov.**, is included in the present paper. This new species can be identified by having a single uninterrupted dark band on central thoracic segment III; 14 macrochaetae on abdominal segment I and seven on the posterior central abdominal segment IV (half segment); and very short bothriotricha on abdominal segments II–IV. It can be easily discriminated from similar species of *Homidia* by its colour pattern, chaetotaxy of the labium, and abdominal segments I and IV. The chaetotaxy of the first and second instar larvae of this new species and a key to four species of genus *Homidia* from Xizang are also provided.

Keywords
Entomobryini, key, larvae, taxonomy, Xizang

Introduction

The genus *Homidia* Börner, 1906 is collembolan taxon widely distributed in southeast China and is generally found in every habitat, such as in leaf litter of forest, farmland, vegetable field, residential area and so on. This genus was established as a subgenus of

Entomobrya (Rondani, 1861) by Börner (1906) and later raised to the generic level by Denis (1929). The significant character for the identification is that the dens bears spines and abdominal segment IV has an anterior series of macrochaetae transversely arranged as "eyebrows" in adults. Also, individuals with transverse bands, spots, or without pigment on the dorsal body are distinctive. *Homidia* species are good at jumping and large enough to be seen in wild by the naked eye. To date, 74 species of this genus have been reported worldwide (Bellinger et al. 1996–2021), and 42 are recorded from China (Ma and Pan 2017; Zhuo et al. 2018; Pan and Yang 2019; Pan and Ma 2021). However, among them only one species, *Homidia tibetensis* Chen & Zhong, 1998, was reported from Xizang.

Lhasa is the administrative centre of Xizang Autonomous Region, and with an altitude around 3600 m, it is one of the highest altitude cities in the world. Annual sunshine averages 3000 h and rainfall 200–510 mm. The climatic conditions results in unique biodiversity, including among Collembola. In order to gather more information about the diversity of Collembola from this region, we spent several days collecting around Lhasa in August 2019. Among the collected material, we found two new records and one new species of the genus *Homidia*. The chaetotaxy of the adult as well as the first and second instar larvae of the new species is described in detail. A comparison of the new species with the most similar species of the genus *Homidia* is provided. A checklist of all *Homidia* species found from Xizang is included as well as a key to separate them.

Materials and methods

Collembolan individuals were sieved from leaf litter in the field, collected with an aspirator, and stored in 99% ethanol at –20 C in the laboratory. Specimens were photographed using a Nikon DS-Fi1 camera mounted onto a Nikon SMZ1000 stereomicroscope, then cleared in lactic acid, mounted in Hoyer's medium under a coverslip, and examined with a Nikon 80i phase-contrast microscope. Lengths of morphological structures were measured from specimens in ethanol by NIS-Elements 3.1 software. Photographs, illustrations, and labels were enhanced by Photoshop CS5 (Abode Systems).

Dorsal chaetotaxy is provided for only one side of the body. The nomenclature of cephalic chaetotaxy, labial palp, labial chaetae, and dorsal thoracic and abdominal chaetotaxy follows the systems of Rueda and Jordana (2020), Fjellberg (1998), Gisin (1967), and Szeptycki (1979), respectively.

Specimens and all types are deposited in the School of Life Sciences, Taizhou University (**TZU**).

Abbreviations

Abd. abdominal segment;
Ant. antennal segment;

Gr.	group;
mac	macrochaeta/e;
mic	microchaeta/e;
ms	specialized microchaeta/e;
sens	specialized ordinary chaeta(e);
S-chaeta/e	specialized chaeta/e, including ms and sens;
Th.	thoracic segment;
VT	ventral tube;
l.p.	lateral process;
asl	above sea level.

Taxonomic account

Fourteen samples (4687–4700) were collected in total from Lhasa from 1-VIII-2019 to 8-VIII-2019. The collection included two new records and one new species of the genus *Homidia: Homidia sichuanensis* Jia et al., 2010, *Homidia sinensis* Denis, 1929, *Homidia breviseta* Pan, sp. nov. (Figs 1, 2, 4–8). A fourth species, *Homidia tibetensis* Chen & Zhong, 1998 (Fig. 3), which had been recorded from Xizang in a previous study (Chen and Zhong 1998), was absent from the present sampling.

The sampling information of three *Homidia* species recorded here are listed in Table 1. *Homidia sichuanensis* was described by Jia et al. (2010) from Sichuan Province, China, and is identified by its colour pattern and the presence of mac p4 and A6–A10 on Th. III and Abd. IV, respectively. It is widely distributed in western China, from Sichuan Province to Guangxi Zhuang Autonomous Region (recorded in our collection S09022603). *Homidia sinensis* was reported by Denis (1929) from Foochow, Fujiang Provnice, China, and is distinct from other species of *Homidia* by its colour pattern, chaetotaxy of the labium and Abd. I, III, and IV. It has a wide distribution, and we found it in most regions of China. *Homidia tibetensis* was described by Chen and Zhong (1998) from Xizang and is only know from there, but the detailed collecting information is not provided in the original description. This species, which is well-characterized morphologically by its colour pattern and chaetotaxy, is not included in our collections.

Key to the *Homidia* species from Xizang

1	Dorsal body with distinct transverse dark bands	**2**
–	Dorsal body without transverse dark band	***H. tibetensis***
2	Lateral head without longitudinal dark band	**3**
–	Lateral head with longitudinal dark bands	***H. sichuanensis***
3	Mac m3ei present on Abd. II and a3 absent on Abd. III	***H. breviseta* Pan, sp. nov.**
–	Mac m3ei absent on Abd. II and a3 present on Abd. III	***H. sinensis***

Table 1. Sampling information of *Homidia* species from Xizang Autonomous Region of China in the present study. All specimens were collected from Chengguan District of Lhasa City, in Xizang.

Sample no.	Location	Coordinates	asl (m)	Habitat	Collector	Species
4688	Lalu National Wetland Park	29°28'5.71"N, 91°4'55.15"E	3603±5	Leaf litter of white poplar forest	Z-X. Pan, C-C. Si	*H. sichuanensis*
4692	Gesan Flower Park	29°39'59.57"N, 91°7'18.38"E	3634±5	Leaf litter of family Rosaceae	Z-X. Pan, C-C. Si, J-F, Jia	*H. breviseta* sp. nov.
4696	Nanshan Park	29°38'15.69"N, 91°6'50.16"E	3633±5	Leaf litter of *Populus simonii*	Z-X. Pan, C-C. Si	*H. sichuanensis*
4698	Nongke Road, Germplasm Center of Xizang	29°38'27.28"N, 91°1'55.58"E	3584±5	Leaf litter of family Asteraceae	Z-X. Pan, J-F, Jia	*H. sinensis*

Homidia breviseta **Pan, sp. nov.**

http://zoobank.org/F1734E97-767C-44B8-B096-218E146502B5
Figures 1–51

Type material. ***Holotype.*** 1♀ on slide, **China**, Xizang autonomous region, Lhasa city, Chengguan District, Gesan flower park, 29°39'59.5764"N, 91°7'18.3828"E, 3634±5 m asl, sample number 4692, collected by Z-X Pan, C-C Si, and F-H Jia, 3-VIII-2019. ***Paratypes.*** 7♀adults, 1 first and 1 second instar larva on slides and 5 adults in ethanol, same data as holotype.

Descriptions of adults. ***Size.*** Body length up to 1.62 mm. ***Colour pattern.*** Ground colour yellow-white in ethanol. Eye patches dark blue. Antennae gradually darker from Ant. I to Ant. IV. A dark narrow transverse band between basal antennae. Lateral Th. II–III with longitudinal bands, and dorsal Th. III with central transverse uninterrupted dark band. Coxa with dark pigment. Dorsal Abd. II and Abd. IV with central irregular dark bands. Dorsal Abd. III and Abd. V from anterior to posterior margin with dark transverse bands, and Abd. III with two lateral unpigmented areas. Dorsal Abd. IV with two middle and posterior transverse bands, the central one interrupted by a middle line (Figs 4, 5). Ventral side of body and VT pale white, without pigment (Fig. 6). Subadults with the same colour pattern as adults, but paler (Fig. 7).

Head. Eyes 8+8, G and H smaller than others and always difficult to observe under light microscope; three chaetae (p, r, and t) within eye patches, with p largest (Fig. 10). Antenna 1.56–2.16 times as long as cephalic diagonal; antennal segments ratio as I:II:III:IV = 1:1.11–1.72: 1.15–1.76:1.97–2.73. Ant. I base with seven (rarely as three) dorsal smooth mic and four ventral (Fig. 11). Ant. II base with five smooth mic (Fig. 12). Ant. III organ with two rod-like and three short guard S-chaetae (Fig. 13). Apical bulb on Ant. IV bilobed (Fig. 14). Prelabral and labral chaetae as 4/5, 5, 4, all smooth; without labral papillae. Clypeus with 16 (6/7/3) chaetae in three lines (Fig. 15). Cephalic chaetotaxy on dorsal side shown in Fig. 10, An series with four (An1–3, An3a), A series with four (A0, A1, A3, A5), M series with four (M1–4), S series with eight (S0–5, S4i, S5i), P series with 18 (Ps2, Ps5, Pi1, Pa1–5, Pm1–3, Pm5, Pp1–3, Pp5, Pp1e, Pp3e) mac. Chaetae on labium basis as $MReL_1L_2$, chaeta e smooth; postlabial chaetae not expanded, with $G_{1–4}$, $H_{1–4}$, X_2, X_3, X all ciliate, X_4 unclear; five

Figures 1–3. Colour pattern of *Homidia* species recorded from Xizang **1** *Homidia sichuanensis* **2** *Homidia sinensis* **3** *Homidia tibetensis* (following Chen and Zhong 1998). Scale bars: 1000 µm

proximal chaetae (Fig. 16). Five papillae A–E on labial palp with 0, 5, 0, 4, 3 guard chaetae, respectively; l.p. normal, with tip beyond apex of papilla E (Fig. 17). Maxillary outer lobe with single apical chaeta, one subapical chaeta, and three sublobal hairs on sublobal plate; subapical chaeta subequal in length to apical one (Fig. 18). Mandible with 4/5 apical teeth and basal strong molar plate (Fig. 19)

Thorax. Complete body sens from Th. II to Abd. IV as 2, 2/1, 2, 2, 28 (26 elongate and two of normal length), 3, ms as 1, 0/1, 0, 1, 0, 0. Th. II with seven medio-medial (m1, m1i, m2, m2i and m2i2 and other two additional mes; arrow shown in Fig. 20), three medio-sublateral (m4, m4i and m4i2) mac and three S-chaetae (ms antero-external to sens); posterior with 39–43 mac; p6 as mic. Th. III with 42–47 mac and two sens; p5, p6 and m6 as mac, p4 as mic (Fig. 20). Coxal macrochaetal formula as 3 (two pseudopores)/4+1, 3 (three pseudopores)/ 4+2 (one pseudopore) mac (Fig. 21). Trochanteral organ with 31–40 smooth chaetae, six or seven in ventral line, and five or six in posterior line (Fig. 22). Inner side of tibiotarsus with slightly ciliated chaetae. Tenent hairs clavate, slightly shorter than inner edge of unguis in length. Unguis with four inner and two lateral teeth. Unguiculus lanceolate with outer edge smooth (Fig. 23).

Abdomen. Abd. IV 5–8 times longer than Abd. III along the dorsal axis. Abd. I with 14 mac (a1–3, a5, a1a, a1i, a2i, m2–5, m2i, m4i, m4p) and two S-chaetae (ms antero-external to sens). Abd. II with seven central (a2, a3, m3, m3e, m3ea and m3ep, m3ei) and one lateral (m5) mac. Abd. III with two central (a2 and m3) and two lateral (am6, pm6, p6 and m7) mac, two sens and one ms (Fig. 24). Abd. IV with 26 elongated and two normal length sens, and 6–9 mac arranged in anterior transversal line; postero-central area with seven mac (A4–6, B4–6, Ae6; one individual

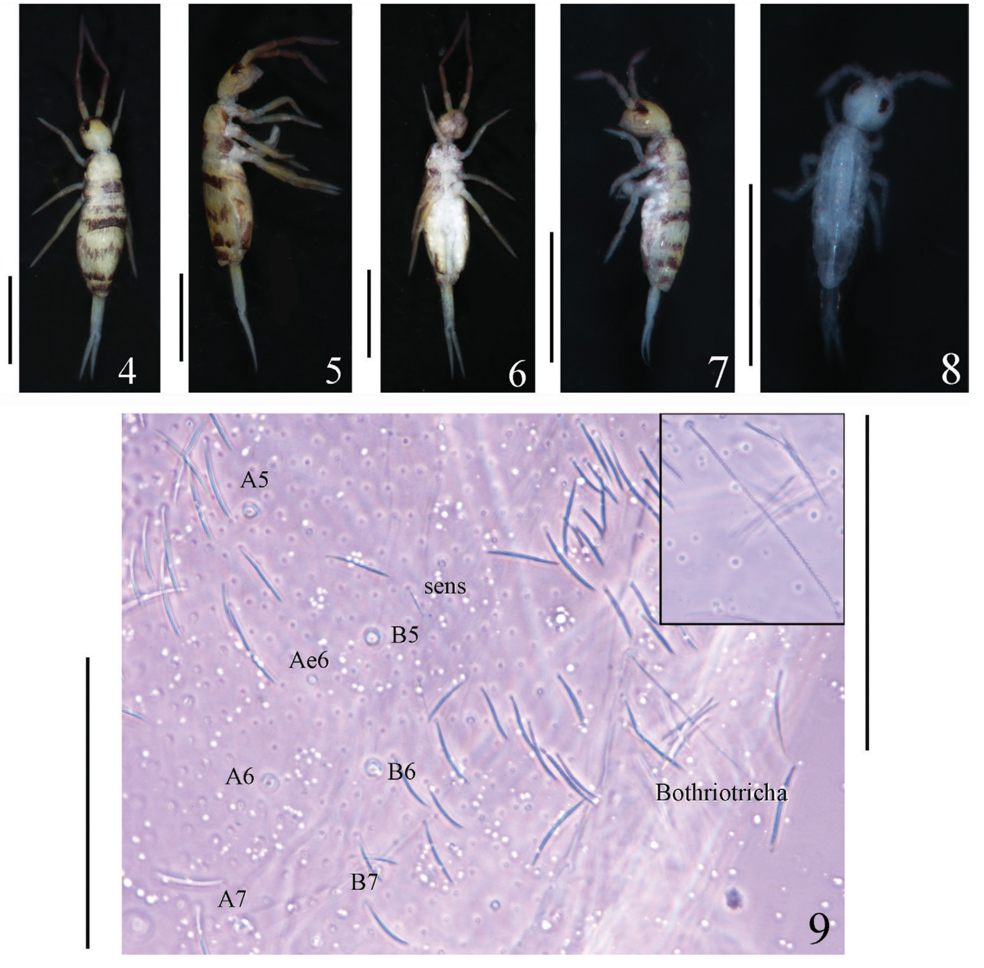

Figures 4–9. *Homidia breviseta* Pan, sp. nov. **4–9** habitus **4** dorsal view of adults **5** lateral view of adults **6** ventral view of adults **7** dorsal view of subadults **8** dorsal view of the first instar larvae **9** dorsal view of Abd. IV, showing mac sockets and short bothriotricha. Scale bars: 1000 μm (**4–6**); 500 μm (**7–8**); 50 μm (**9**; left bar corresponds to large figure, right one to inset).

examined with Ae4 and Ae7), bothriotricha short and no more than two times as long as normal ciliate chaetae (Figs 9, 25). Abd. V with three sens, the middle one posterior to m3, the lateral one between chaetae a5 and m5; a1 as mic; a3, m3, m5, a5, m5, and a6 as mac (Fig. 25). Anterior face of VT with many ciliate chaetae, 3+3 of them as mac, the line connecting proximal (Pr) and external-distal (Ed) mac obliquely to median furrow (Fig. 26); lateral flap with 5–7 smooth and 10–17 ciliate chaetae on each side (Fig. 27); apical posterior face as five (2+1+2) smooth chaetae (two specimens examined here with four smooth chaetae) (Fig. 28). Manubrial plate with three pseudopores and eight or nine ciliate chaetae (Fig. 29). Dens with 23–33 inner spines, distal smooth part slightly shorter than mucro (only basal part shown in Fig. 30). Mucro bidentate with subapical tooth larger than apical one; basal spine

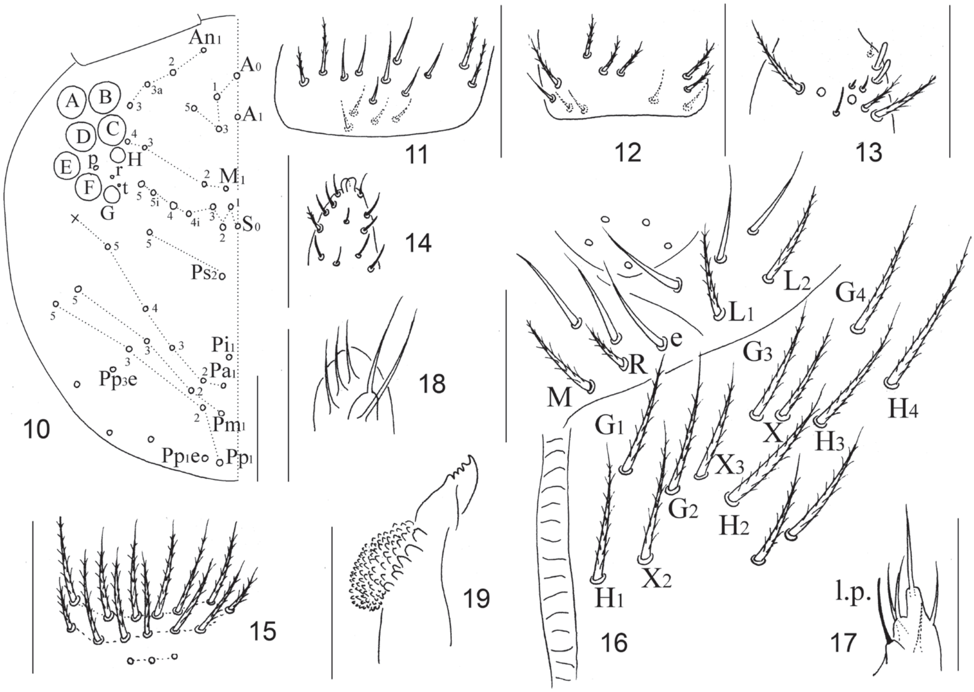

Figures 10–19. Adults of *Homidia breviseta* Pan sp. nov. **10** cephalic chaetotaxy on dorsal side **11** base of Ant. I **12** base of Ant. II **13** Ant. III organ **14** distal part of Ant. IV **15** clypeal chaetotaxy **16** labium **17** labial papilla E **18** maxillary outer lobe **19** right mandible. Scale bars: 50 µm

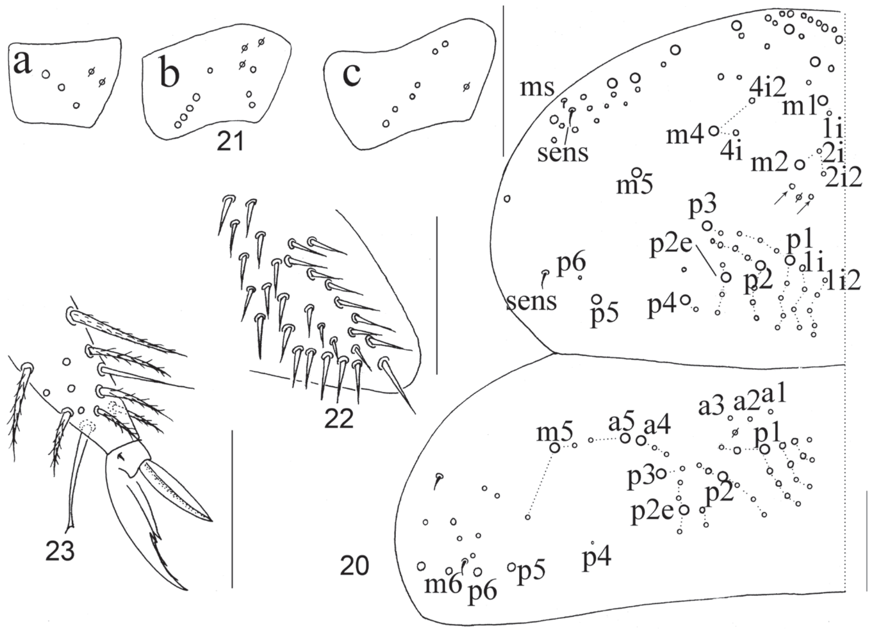

Figures 20–23. Adults of *Homidia breviseta* Pan, sp. nov. **20** chaetotaxy of Th. II–III **21** coxae (**a** fore leg **b** mid leg **c** hind leg) **22** trochanteral organ **23** distal part of tibiotarsus and claw of hind leg. Scale bars: 50 µm.

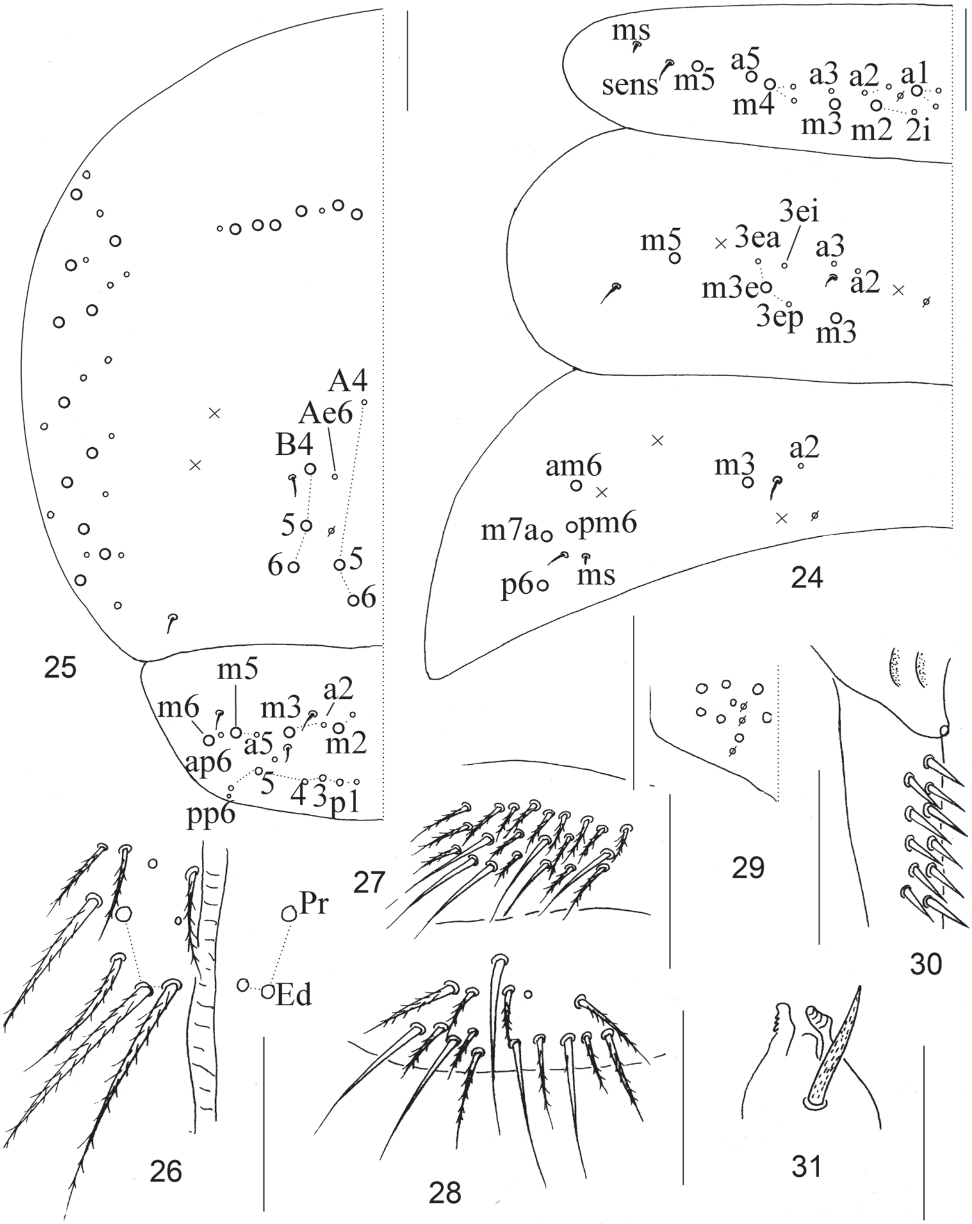

Figures 24–31. adults of *Homidia breviseta* Pan, sp. nov. **24** chaetotaxy of Abd. I–III **25** chaetotaxy of Abd. IV–V **26** anterior face of VT **27** lateral flap of VT **28** posterior face of VT **29** manubrial plaque **30** basal part of dens **31** tenaculum. Scale bars: 50 µm.

short, with tip reaching subapical tooth. Tenaculum with 4+4 teeth and single large, multi-laterally, basally ciliate chaeta (Fig. 31).

Description of the first instar larva. ***Size.*** Body length up to 0.59 mm. ***Colour pattern.*** Ground colour whitish, only eye patches dark blue, others all without pigment (Fig. 8).

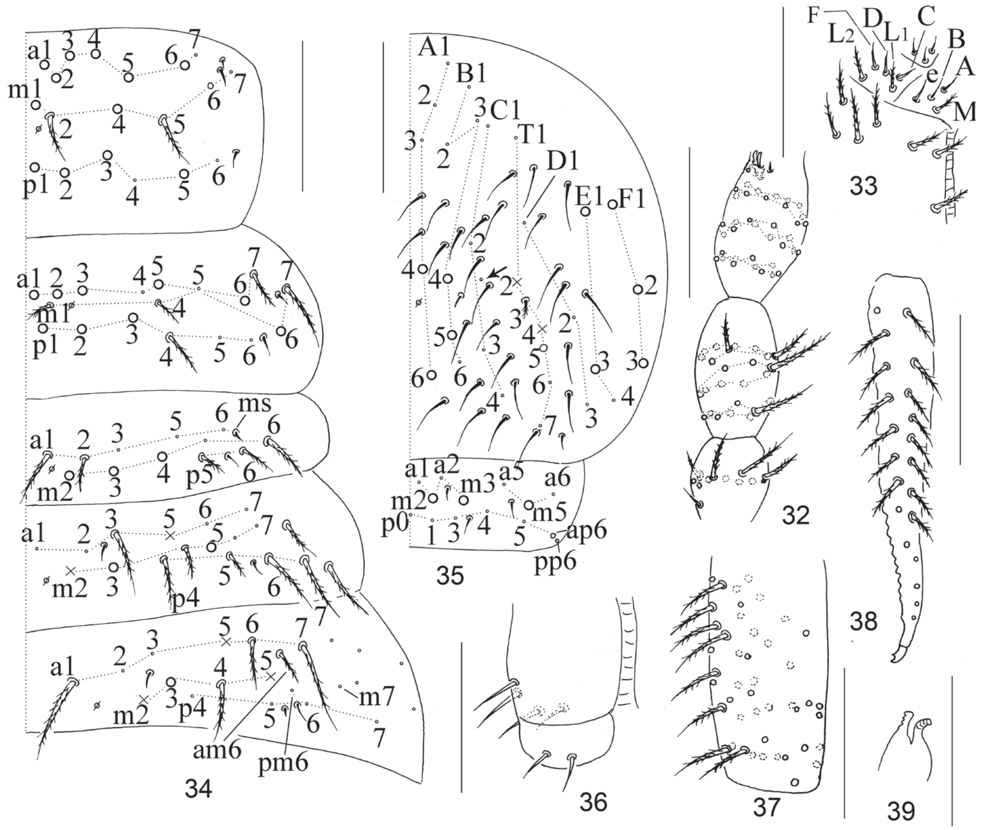

Figures 32–39. The first instar larva of *Homidia breviseta* Pan, sp. nov. **32** chaetotaxy of Ant. I–III **33** labium **34** chaetotaxy of Th. II–Abd. III **35** chaetotaxy of Abd. IV–V **36** ventral tube **37** manubrium **38** dens **39** tenaculum. Scale bars: 50 μm.

Body. Complete tergal sens from Th. II to Abd. V as 2, 2/1, 2, 2, 28, 3, ms as 1, 0/1, 0, 1, 0, 0. Cephalic chaetotaxy on dorsal side with three (An1–3), six (A0–5), four (M1–4), six (S0–5) mac of An, A, M, S series, respectively; eyes 8+8, eye patches with three chaetae (p, r, and t; p largest). Labium with three proximal chaetae, four chaetae (M, e, A and B) in basomedial field and five chaetae (C, D, F, L_1 and L_2) in basolateral field, chaetae M, L_1 and L_2 ciliate, and others smooth; posterior area of labium with two ciliate mac along median furrow (Fig. 33). Th. II with seven anterior (a1–7), six median (m1–2, m4–7), and six posterior (p1–6) primary chaetae arranged in three rows; chaetae a7, m2, m5, m7, and p4, p6 as mic, others as mac, and with three S-chaetae (ms antero-external to sens). Th. III with seven anterior (a1–7), five median (m1, m4–7), and six posterior (p1–6) primary chaetae arranged in three rows and two S-chaetae; chaetae a4, a7, m1, m4, m5, m7, and p4–6 as mic, others as mac. Abd. I with five anterior (a1–3, a5–6), five median (m2–6), and two posterior (p5–6) primary chaetae arranged in three rows and two S-chaetae (ms antero-external to sens); chaetae m2–m4 as mac, others as mic. Abd. II with six anterior (a1–3, a5–7), six median (m2–7), and four posterior (p4–7) primary chaetae arranged in three rows, an additional chaeta external to p7 and

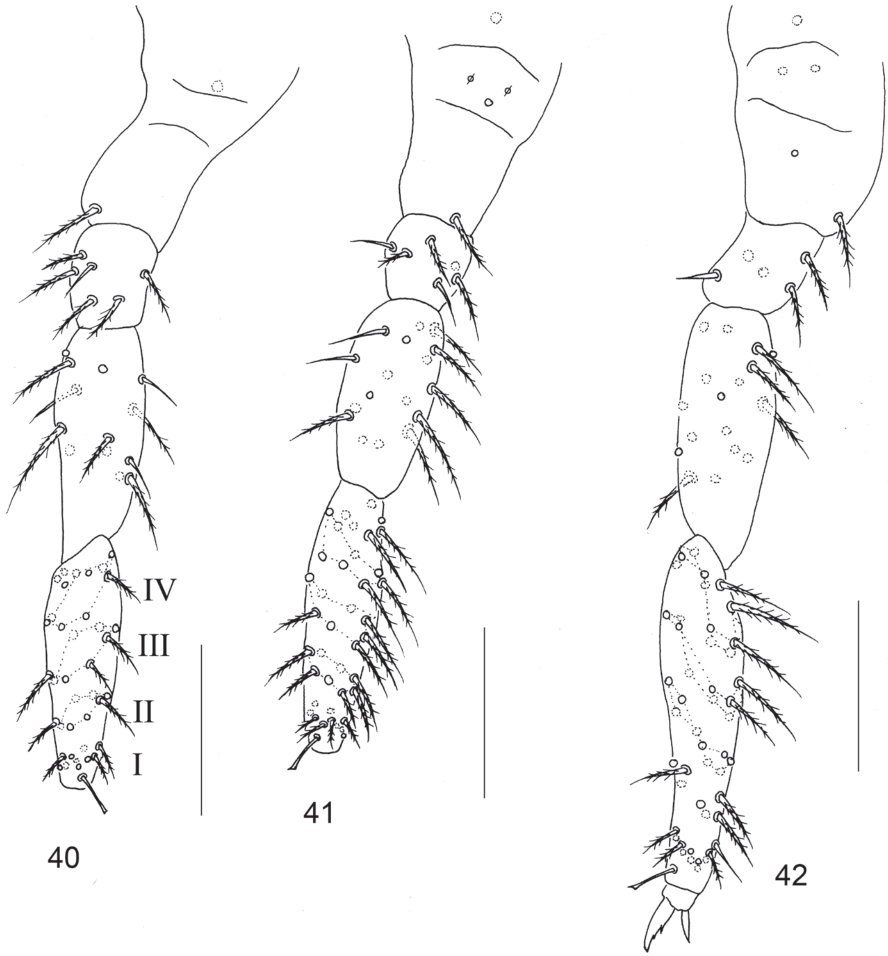

Figures 40–42. Left legs of the first instar larva of *Homidia breviseta* Pan, sp. nov. **40** fore leg **41** mid leg **42** hind leg. Scale bars: 50 µm.

two S-chaetae; chaetae m3 and m5 as mac, a5 and m2 as bothriotricha, others as mic. Abd. III with six anterior (a1–3, a5–7), seven median (m2–5, am6, pm6, m7), and four posterior (p4–7) primary chaetae arranged in three rows, five additional chaetae in lateral region, and three S-chaetae (one ms and two sens); chaeta m3 as mac, m2, a5, and m5 as bothriotricha, others as mic (Fig. 34). Abd. IV with five (A1–4, A6), six (B1–6), four (C1–4), seven (T1–7), three (D1–3), three (E1–3), and three (F1–3) primary ciliate chaetae arranged in seven longitudinal lines, one side with an additional ciliate chaeta between C2 and C3 (shown by arrow in Fig. 35), and 26 elongated and two normal sens; T2 and T4 as bothriotricha. Abd. V with 13 primary chaetae (m2, m3 and m5 as mac; others as mic) and three sens, the median sens posterior to m3 (Fig. 35).

Appendages. Ant. I with 11 ciliate chaetae arranged in one whole and one basal smooth chaeta. Ant. II with 25 ciliate chaetae, arranged in three wholes (from basis to apex as 8/8/9), basis without smooth spiny chaetae. Ant. III with 37 ciliate chaetae

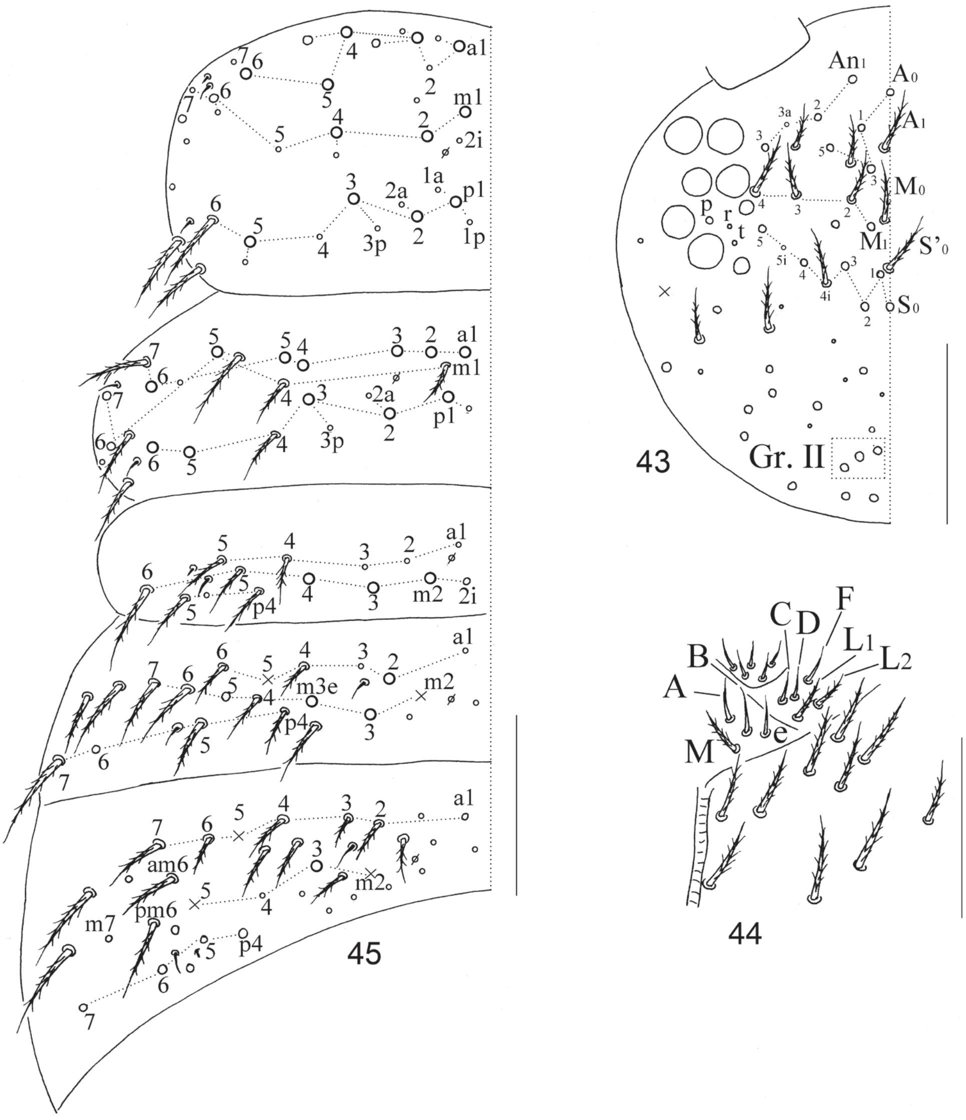

Figures 43–45. The second instar larva of *Homidia breviseta* Pan, sp. nov. **43** cephalic chaetotaxy **44** labium **45** chaetotaxy of Th. II–Abd. III. Scale bars: 50 μm.

arranged in four wholes (11/12/13/2) and five S-chaetae (Ant. III organ) (Fig. 32). Primary chaetae on Ant. IV unclear. Ventral tube with two smooth chaetae on the posterior face and on each lateral flap, anterior face without chaetae (Fig. 36). Manubrium with 46 ciliate chaetae (Fig. 37); dens with numerous ciliate chaetae, without inner dental spines; chaetae bs2, bs1, pi unclear; mucro with subapical tooth larger than apical one, basal spine absent (Fig. 38). Tenaculum with 4+4 teeth and without basal chaetae (Fig. 39). Four segments of fore, mid and hind leg with numerous chaetae, subcoxae with 1, 2, 3 ciliate chaetae, coxae with 1, 1, 2 ciliate chaetae, pseudopore(s) unclear; trochanters with six (one smooth), six (two smooth), five (one smooth and

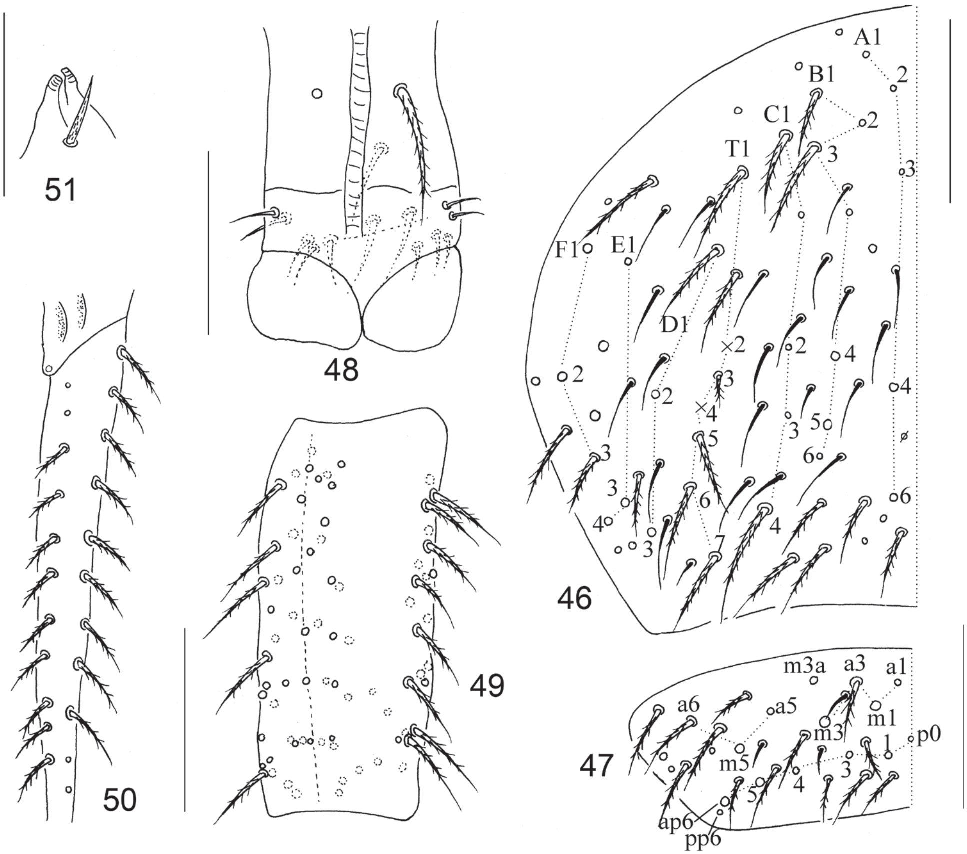

Figures 46–51. The second instar larva of *Homidia breviseta* Pan, sp. nov. **46** chaetotaxy of Abd. IV **47** chaetotaxy of Abd. V **48** ventral tube **49** manubrium **50** dens **51** tenaculum. Scale bars: 50 μm.

one spine like) chaetae; femurs with 17 (three smooth), 17 (smooth chaetae unclear), 17 (two smooth) chaetae; tibiotarsus with 39 (10/8/8/8/4 ciliate and one tenent hair), 41 (10/8/8/8/6 ciliate and one tenent hair), 48 (10/7/9/9/9/2, one tenent hair and one inner smooth chaetae) ciliate chaetae (Figs 40–42).

Description of the second instar larva. ***Colour pattern.*** Ground colour whitish; eye patches dark blue. The colour pattern of the second instar larva is similar to adult, but slighter.

The chaetotaxy of the second instar larva is more complex than first instar, and several primary chaetae with secondary chaetae present in the second instar (Figs 43–54). The detailed comparison between these two instars are tabulated in Table 3.

Ecology. All stages were found in leaf litter of the Family Rosaceae.

Etymology. The specific epithet refers to the very short chaeta bothriotricha on dorsal Abd. II–IV (*brevi* and *seta*).

Remarks. This new species is mostly similar to *Homidia similis* Szeptycki, 1973 in having Th. III, Abd. III, and the middle and posterior of Abd. IV and Abd. V with transverse bands; in the chaetotaxy of the labium, head, Th. III, and Abd. II–III; and

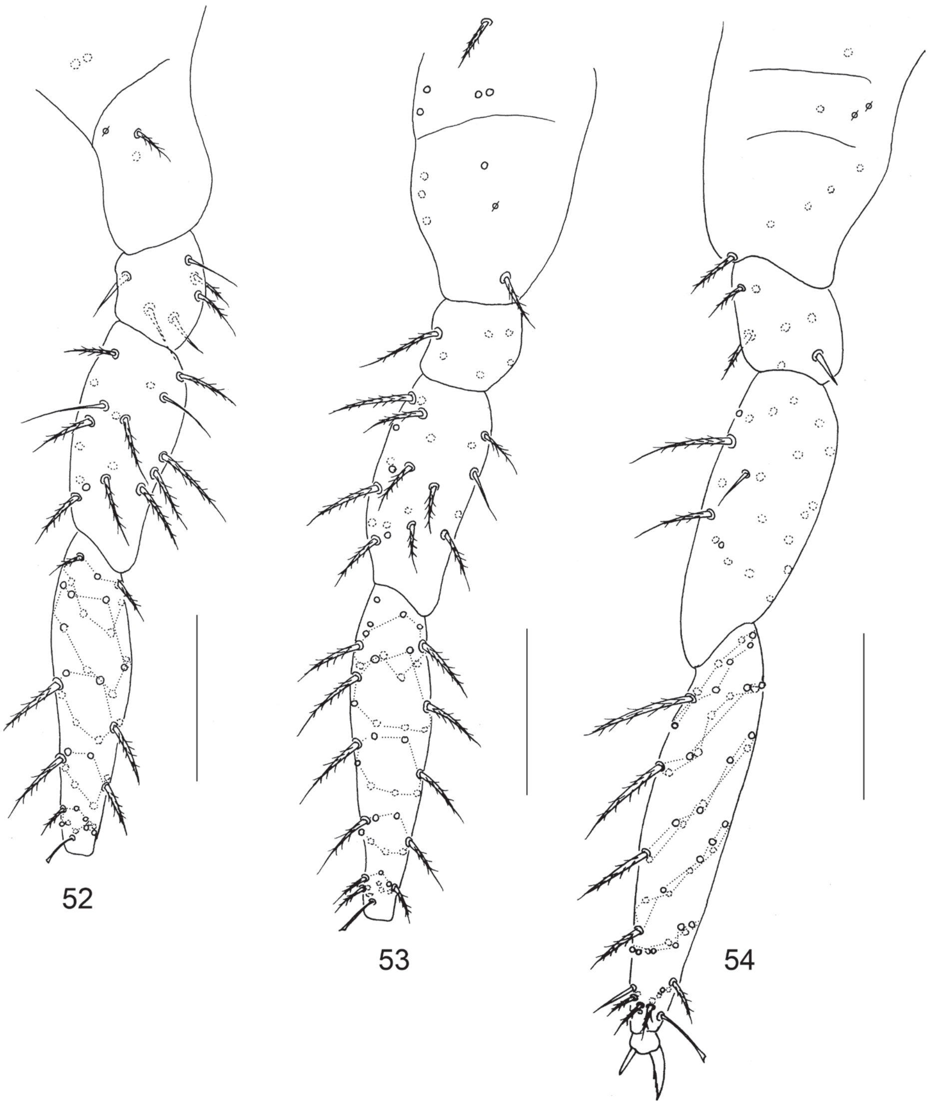

Figures 52–54. Legs of the second instar larva of *Homidia breviseta* Pan, sp. nov. **52** fore leg **53** mid leg **54** hind leg. Scale bars: 50 μm.

smooth chaetae on posterior face (five) and lateral flap (six) of VT. However, the new species can be differentiated from *H. similis* by the uninterrupted band on Th. III (interrupted by a central line in latter), a broad band from the anterior to posterior margin of Abd. III (anterior margin not pigmented in the latter), 14 mac on Abd. I (nine in the latter), and seven posterior central mac on Abd. IV (eight in the latter). Also, the new species is similar to *H. bilineata* Lee & Park, 1984 and *Homidia huashanensis* Jia et al., 2005 in having mac on the dorsal head, Th. II–III, and Abd. II and chaetal formula on labium; however, they can be discriminated by colour pattern, chaetotaxy on Abd. I and posterior central Abd. IV. A detailed comparison of these four similar species is given in Table 2.

Table 2. Comparison between the new species and other similar species of *Homidia*.

Characters	*H. breviseta* sp. nov.	*H. similis*	*H. bilineata*	*H. huashanensis*
Pigment on central Th III	as one complete band	separated to two parts by middle line[*†]	without	not as band
Pigment on Abd. III reaching anterior margin	yes	no[*†]	no	no
Labial papilla	0	4 smooth[*†]	4 smooth[†]	0
Additional mac present posterior to m2 on central Th. II	2	0	not mentioned	0
Mac on coxa of hind leg	4+2	4+3*	4+1	4+2
Mac on Abd. I	14	9*	not mentioned	11-12 (mostly 12)
Mac between A and B series on posterior region of Abd. IV	1 (Ae6)	2 (Ae6 and Ae7)[†]	0	2 (Ae5 and Ae6) or 3 (Ae5–7)
Line connecting Pr to Ed on anterior face of VT to median furrow	oblique	parallel*	parallel	oblique
Distribution	Xizang Autonomous Region	Fujian and Zhejiang Province[‡]; Korea[*†]	Korea	Shaanxi Province

*Refers to the description by Szeptycki (1973), †Refers to the description by Jordana (2012), ‡Refers to the description by Chen et al. (2011).

Table 3. Detailed comparison of chaetotaxy between the first and second instar larvae of *Homidia breviseta* sp. nov.

	Characters		First instar	Second instar
Th. II	a/m/p series		7/6/6	11/9/11
Th. III	a/m/p series		7/5/6	8/6/9
Abd. I	a/m/p series		5/5/2	5/6/3
Abd. II	a/m/p series		6/6/4	6/9 (m3e present) /5
Abd. III	a/m/p series		6/6/4	8/?/4
Abd. IV	ciliate chaetae		30	53
Abd. V	ciliate chaetae		13	27 (m3a present)
Fore leg	subcoxa		1	2
	coxa		1	2
	trochanters		6 (4c[*]+2s[†])	6 (4c+2s)
	femurs		17 (14c+3s)	18
	tibiotarsus[3]	whole I	10	10
		whole II	8	8
		whole III	8	8
		whole IV	8	8
		additional	4	7
Mid leg	subcoxa		2	5
	coxa		1	5
	trochanters		6 (4c+2s)	7
	femurs		17	21 (19c+2s)
	tibiotarsus[3]	whole I	10	10
		whole II	8	8
		whole III	8	8
		whole IV	8	8
		additional	6	3
Hind leg	subcoxa		3	2
	coxa		2	5
	trochanters		5 (1 spine)	6 (1 spine)
	femurs		17 (15c+2s)	22 (21c+1s)

Characters			First instar	Second instar
Hind leg	tibiotarsus[3]	whole I	10	10
		whole II	7	9
		whole III	9	9
		whole IV	9	9
		whole V	9+2	9
Labium	proximal chaetae		3s	5s
Ventral tube	anterior face		0	1c+1c
	lateral flap		2s+2s	5s+5s
	posterior face		2s	3s
Tenaculum	basal chaeta		0	1
Manubrium	chaetae		46c	77c
Mucro	basal spine		absent	present

*Ciliate, †Smooth, ‡Chaetae on tibiotarsus, not including tenent hair and smooth apical chaeta.

This species is the second species of genus *Homidia* described from Xizang, and it can be easily distinguished from the first new species recorded from this region (*H. tibetensis* Chen & Zhong, 1998) by the colour pattern (dorsal central pigments on Th. III and Abd. III in the new species, absent in *H. tibetensis*), chaetotaxy on the labial triangle (M2 absent in the new species, but present in *H. tibetensis*), Abd. I (14 mac in the new species, and 11 in *H. tibetensis*), and posterior part of Abd. IV (seven in new species and only two in *H. tibetensis*).

Acknowledgements

This study was supported by Zhejiang Provincial Natural Science Foundation of China (LTY20C030001), National Natural Science Foundation of China (36101880), and the College Students' Innovation and Entrepreneurship Training Program Project (202010350039). We also give thanks to Prof. Feng-hai Jia (Jiangxi University of Chinese Medicine) for his company in the field to collect specimens.

References

Bellinger P, Christiansen KA, Janssens F (1996–2021) Checklist of the Collembola of the World. http://www.collembola.org [Accessed on: 2021-8-10]

Börner C (1906) Das system der Collembolen nebst Beschreibung neuer Collembolen des Hamburger Naturhistorischen Museums. Mitteilungen aus dem Naturhistorischen Museum in Hamburg 23: 147–188.

Chen JX, Zhong WY (1998) A new species of the genus *Homidia* (Collembola: Entomobryidae) from Xizang Autonomous region, China. Entomologia Sinica 5(1): 50–54. https://doi.org/10.1111/j.1744-7917.1998.tb00297.x

Chen FY, Chen XL, Shi SD (2011) A new record of genus *Homidia* (Collembola: Entomobryidae) in China. Journal of Hebei Agricultural Sciences 15(3): 77–79, 91.

Denis JR (1929) Notes sur les collemboles récoltés dans ses voyages par le Prof. F. Silvestri (II), seconde note sur les Collembola d'Extrême-Orient. Bollettino del Laboratorio di Zoologia Generale e Agraria della R. Scuola Superiore d'Agricoltura in Portici 22: 305–320.

Fjellberg A (1998) The labial palp in Collembola. Zoologischer Anzeiger 237: 309–330.

Gisin H (1967) Espèces nouvelles at lignées évolutives de *Pseudosinella* endogés. Memórias e Estudos do Museu Zoológico da Universidade de Coimbra 301: 5–25.

Jia SB, Chen JX, Christiansen K (2005) A new entomobryid species of *Homidia* from Shaanxi, China (Collembola: Entomobryidae). Journal of the Kansas Entomological Society 78(4): 315–321. https://doi.org/10.2317/040413.1

Jia SB, Zhang YP, Zhao Y, Jordana R (2010) A new species of *Homidia* from China, and description of the dorsal chaetotaxy of all Chinese *Homidia* species (Collembola: Entomobryidae). Zootaxa 2683(1): 23–34. https://doi.org/10.11646/zootaxa.2683.1.2

Jordana R (2012) Synopses on Palaearctic Collembola: Capbryinae & Entomobryini. Soil Organisms 84(1): 1–390.

Lee BH, Park KH (1984) Some Entomobryidae including six new species and one new record of cave form (Collembola) from Korea. Tongmul Hakhoe Chi 27(3): 177–188.

Ma YT, Pan ZX (2017) Two news species of *Homidia* (Collembola: Entomobryidae) from Southwestern China. Zootaxa 4290(3): 519–530. https://doi.org/10.11646/zootaxa.4290.3.6

Pan ZX, Ma YT (2021) Two new species of *Homidia* (Collembola: Entomobryidae) from Eastern China. Zootaxa 4995(1): 179–194. https://doi.org/10.11646/zootaxa.4995.1.11

Pan ZX, Yang WQ (2019) Reports of two peculiar pigmented new species of genus *Homidia* (Collembola: Entomobyridae) from Southern China, with description of subadults chaetotaxy. Zootaxa 4671(3): 369–380. https://doi.org/10.11646/zootaxa.4671.3.3

Rondani C (1861) *Entomobrya* pro *Degeeria* Nic. In: Rondani C (Ed.) Dipterologiae Italicae Prodromi 4: e40.

Rueda J, Jordana R (2020) Checklist of Collembola (Hexapoda: Entognatha) from "malladas" of the Devesa and Racó de l'Olla (Albufera Natural Park, Valencia, Spain) with a description of a sp. nov. Limnetica 39(1): 93–111. https://doi.org/10.23818/limn.39.07

Szeptycki A (1973) North Korean Collembola. I. The genus *Homidia* Börner, 1906 (Entomobryidae). Acta Zoologica Cracoviensia 31(2): 23–39.

Szeptycki A (1979) Morpho-systematic studies on Collembola. IV. Chaetotaxy of the Entomobryidae and its phylogenetical significance. Polska Akademia Nauk, Kraków, 219 pp.

Zhuo PL, Si CC, Shi SD, Pan ZX (2018) Description of a new species and the first instar larave of *Homidia* (Collembola: Entomobyridae) from Taizhou, Zhejiang Province. Entomotaxonomia 40(2): 148–157. https://doi.org/10.11680/entomotax.2018017

ZooKeys 1089: 109–124 (2022)
doi: 10.3897/zookeys.1089.77203
https://zookeys.pensoft.net

RESEARCH ARTICLE

A peer-reviewed open-access journal
ZooKeys
Launched to accelerate biodiversity research

A new species of *Homatula* (Teleostei, Cobitoidea, Nemacheilidae) from the Pearl River drainage, Yunnan, China

Rui Min[1], Yahui Zhao[2], Jingsong Shi[3], Junxing Yang[4,5]

1 *Kunming Natural History Museum of Zoology, Kunming Institute of Zoology, Chinese Academy of Sciences, Kunming, Yunnan 650223, China* **2** *Key Laboratory of Zoological Systematics and Evolution, Institute of Zoology, Chinese Academy of Sciences, Beijing 100101, China* **3** *Key Laboratory of Vertebrate Evolution and Human Origins of Chinese Academy of Sciences, Institute of Vertebrate Paleontology and Paleoanthropology, Chinese Academy of Sciences, Beijing 100044, China* **4** *State Key Laboratory of Genetic Resources and Evolution, Kunming Institute of Zoology, The Innovative Academy of Seed Design, Chinese Academy of Sciences, Kunming, Yunnan 650223, China* **5** *Yunnan Key Laboratory of Plateau Fish Breeding, Kunming Institute of Zoology, Chinese Academy of Sciences, Kunming, Yunnan 650223, China*

Corresponding author: Junxing Yang (yangjx@mail.kiz.ac.cn)

Academic editor: M. E. Bichuette | Received 28 October 2021 | Accepted 30 January 2022 | Published 17 March 2022

http://zoobank.org/539FC236-2F87-4F67-AFA7-A079C5027522

Citation: Min R, Zhao Y, Shi J, Yang J (2022) A new species of *Homatula* (Teleostei, Cobitoidea, Nemacheilidae) from the Pearl River drainage, Yunnan, China. ZooKeys 1089: 109–124. https://doi.org/10.3897/zookeys.1089.77203

Abstract

Based on morphological and molecular analysis of *Homatula* species distributed in the Nanpanjiang River in Yunnan, China, we described a new species, *Homatula robusta* **sp. nov.** It differs from its congeners by a combination of the following characters: naked and robust body with well-developed crests (caudal peduncle depth as a percentage of its length: 70.5–78.5%); lateral line complete; median notch on lower jaw; median gap on lower lip; three pairs of short barbels, with maxillary barbels extending posteriorly to anterior edge of eyes; branched dorsal-fin rays 8½; and vertebrae 37–39. It can further be distinguished from *H. nanpanjiangensis* by several differences of the caudal skeleton such as the number of hypural elements, the presence of epurale and the shape of neural and haemal spines. Phylogenetic analysis of the mitochondrial cytochrome c oxidase subunit I (COI) gene indicated that the new species represents an independent lineage. It is separated from other *Homatula* species by a minimum of 5.3% Kimura-2-parameter distance in the COI gene. Furthermore, we confirmed that *Homatula wenshanensis* should be a member of *Homatula* based on both skeleton and molecular evidence.

Keywords

Molecular phylogeny, morphology, Nanpanjiang River, osteology, taxonomy

Introduction

Homatula, a group of benthic nemacheilids distributed in the eastern slope of the Qinghai-Tibetan Plateau, was established by Nichols in 1925 based on *Nemachilus potanini* Günther, 1896 from the Minjiang River (a tributary of the Yangtze River, Sichuan, China) (Kottelat 1990; Bănărescu and Nalbant 1995; Min et al. 2012). Species of *Homatula* are characterized by the crests along the dorsal and ventral margins of the caudal peduncle supported by rudimentary procurrent caudal-fin rays, the presence of a degenerated non-ossified secondary gas-bladder chamber, and a medium to large-sized body with a maximum standard length of 190 mm (Zhu 1989; Kottelat 1990; Bănărescu and Nalbant 1995; Endruweit et al. 2018).

Currently, 21 valid species are recognized, mostly distributed in China, and only one species is recently reported from Vietnam (Nguyen et al. 2021; Zhou et al. 2021). In China, six species are in the Palaearctic drainages of the Yangtze and Yellow River, four in the Lancangjiang River (upper reaches of the Mekong River), three in the Nujiang River (Salween River), four in the Red River, and three in the Nanpanjiang River (upper reaches of the Pearl River), respectively. None of them is distributed across these large river systems.

Three *Homatula* species have been reported from the Nanpanjiang River, i.e., *H. oligolepis* (Cao & Zhu, 1989), *H. longidorsalis* (Yang, Chen & Kottelat, 1994) and *H. nanpanjiangensis* (Min, Chen & Yang, 2010). In 2009, a medium-sized loach was collected from Luoping County, Yunnan Province, China, which belongs to the Nanpanjiang River drainage. By comparing it to other *Homatula* species, especially the species distributed in the Nanpanjiang River, we describe it as a new species here.

Materials and methods

All specimens were collected in 2009 from Yunnan Province, China and they were fixed either in 95% ethanol or 10% formalin and transferred to 75% ethanol for preservation. For DNA analysis, tissue samples from the left pelvic fin were excised from one or more specimens and placed in 95% ethanol. General methods for measurements and counts were done following Kottelat (1990), pore counts followed Armbruster (2012). Measurements were made with digital calipers to the nearest 0.1 mm from the left side. X-ray images were used to count vertebrae and simple fin rays. Lateral line pores and rays of paired fins were counted under a binocular microscope. The Weberian apparatus was counted as four vertebrae. Caudal vertebrae encompassed all centra bearing a haemal spine, including the urostyle, which was counted as one vertebra. Eye diameter was measured horizontally. Body depth was measured at the dorsal-fin origin. Lateral head length was measured from snout tip to the posterior margin of the operculum, excluding the opercular membrane. Examined specimens were deposited in the collection of the Kunming Natural History Museum of Zoology, Kunming Institute of Zoology (KIZ), Chinese Academy of Sciences.

In order to compare skeletal morphology, we applied Computed Microtomographic (μCT) scans of the holotype of *H. robusta* (KIZ 2009000125), a paratype of *H. nanpanjiangensis* (KIZ 1994000029) and a specimen of *H. wenshanensis* (KIZ 2014005686). Specimens were scanned using a GE Phoenix v|tome|x m dual tube 300/180 kV system in the Key Laboratory of Vertebrate Evolution and Human Origins, Institute of Vertebrate Paleontology and Paleoanthropology (IVPP), Chinese Academy of Sciences. The specimen was scanned with an energy beam of 80 kV and a flux of 80*μA using a 360° rotation and then reconstructed into a 4096*4096 matrix of 1536 slices. The final CT reconstructed skeleton images were exported with a minimum resolution of 6.099 μm. The skeleton images were exported from the virtual 3D model which was reconstructed using Volume Graphics Studio 3.0. Osteological terminology generally follows that of Prokofiev (2009) and Conway (2011) with modifications.

DNA was extracted from fin tissues using standard phenol-chloroform extraction (Sambrook et al. 1989). Mitochondrial cytochrome c oxidase subunit 1 (COI) was amplified by polymerase chain reaction (PCR). The PCR protocols were conducted in 50-μl reactions as follows: initial denaturation step at 95 °C for 5 min, 35 cycles at 94 °C for 30 s, 56 °C for 45 s, and 72 °C for 1 min, and final extension at 72 °C for 10 min. The primers used for COI were LCOIa (CCT ACC TgT ggC AAT CAC RCg C), HCOI (gTg AAT Agg ggg AAT CAg Tg) (Liu et al. 2012). Fragments were sequenced by the Shanghai DNA Biotechnologies Company (China). DNA sequences were aligned using default settings in MAFFT v7 (http://mafft.cbrc.jp/alignment/server/) (Katoh and Standley 2013), and, if necessary, adjusted by eye. MEGA7 (Kumar et al. 2016) was used to calculate the Kimura's 2-parameter genetic distance (K2P). The phylogeny was analyzed using MrBayes 3.2 (Ronquist et al. 2012) with the generalized time reversible model (nst = 6) and the gamma-distributed rate variation and proportion of invariable positions (GTR+ I) for the COI datasets. We ran four simultaneous Monte Carlo Markov chains for 2 000 000 generations, with sampling every 1000 generations, and the first 25% of samples were discarded as burn-in.

Comparative materials

Homatula longidorsalis (Yang, Chen & Kottelat, 1994) (*N* = 24): Holotype: China; Yunnan, Yiliang, Jiuxiang; KIZ 1987003989, 82.0 mm SL. Paratypes: China; Yunnan, Yiliang, Jiuxiang; KIZ 1987003990, 3991–3993, 5090, 5091, 5736–5752, 46.0–89.5 mm SL.

Homatula nanpanjiangensis (Min, Chen & Yang, 2010) (*N* = 20): Holotype: China; Yunnan, Qujing, Luoping; KIZ 1994000023, 86.8 mm SL. Paratypes: China: Yunnan: Qujing: Luoping; KIZ 1994000018–22, 024–037, 72.4–89.7 mm SL.

Homatula oligolepis (Cao & Zhu, 1989) (*N* = 2): China; Yunnan, Zhanyi; KIZ 1985000829, KIZ 652099, 138.2–170.7 mm SL.

Homatula potanini (Günther, 1896) (*N* = 5): China; Sichuan, Meishan; KIZ 2010000266; China; Sichuan, Luoshan; KIZ 2010000279–82, 70.6–80.1 mm SL.

Homatula variegata (Dabry de Thiersant, 1874) (*N* = 9): China; Sichuan, Panzhihua; KIZ 2009002724–2727, 77.4–95.2 mm SL; China; Yunnan, Zhaotong, Yanjin; KIZ 2004008050, 52–53, 57, 61, 76.3–101.6 mm SL.

Homatula laxiclathra Gu & Zhang, 2012 (*N* = 2): China; Shanxi: Ankang: Ningshan: Weihe River: KIZ 2012002359–60, 100.5–120.5 mm SL.

Homatula guanheensis Zhou, Ma, Wang, Tang, Meng & Nie, 2021 (*N* = 6): China: Shanxi, Ankang, Ningshan, Yangtze River; KIZ 2005014508–13, 104.5–135 mm SL.

Homatula wuliangensis Min, Yang & Chen, 2012 (*N* = 34): Holotype: China; Yunnan, Jingdong; KIZ 2008008158, 181.9 mm SL. Paratypes: China; Yunnan, Jingdong; KIZ 2008008156–157, 159–172, 175–176, 179, 184, 197, 199–201, 203, 205, 207, 211, 214–215, 316–318, 64.6–191.1 mm SL.

Homatula disparizona Min, Yang & Chen, 2013 (*N* = 21): Holotype: China; Yunnan, Wenshan, Xichou; KIZ 2012000623. Paratypes: China; Yunnan, Wenshan, Xichou; KIZ 2012000622, 624–634. China; Yunnan, Wenshan, Xichou; KIZ 2014005623–30, 62.8–92.4 mm SL.

Homatula acuticephala (Zhou & He, 1993) (*N* = 26): China; Yunnan, Dali, Haixihai; KIZ 2008005990–6015, 33.7–51.5 mm SL.

Homatula anguillioides (Zhu & Wang, 1985) (*N* = 12): China; Yunnan, Dali, Eryuan, KIZ 2008006532–6543, 68.8–143.3 mm SL.

Homatula pycnolepis Hu & Zhang, 2010 (*N* = 6): China; Yunnan, Dali, Yangbi; KIZ 1998004817, 19, 22, 25, KIZ 2009005288, KIZ 2009005388, 120.1–177.1 mm SL.

Homatula change Endruweit, 2015 (*N* = 12): Holotype: China; Yunnan, Puer, Jiangcheng; KIZ 2012004205, 107.6 mm SL. Paratypes: China; Yunnan, Puer, Jiangcheng; KIZ 2012004208, 4209, 4211, 4215–18, 4221–24, 37.9–76.5 mm SL.

Homatula coccinocola Endruweit, Min & Yang, 2018 (*N* = 5): Holotype: China, Yunnan, Honghe; KIZ 2011002847, 99.6 mm SL. Paratypes: China, Yunnan, Honghe; KIZ 2012001866–1869, 51.1–79.0 mm SL.

Homatula cryptoclathrata Li, Che & Zhou, 2019 (*N* = 2): China; Yunnan, Lincang; KIZ 2005012637, 39, 91.3–100 mm SL.

Homatula wenshanensis Li, Yang, Li & Liu, 2017 (*N* = 3): China; Yunnan, Wenshan; KIZ 2014005685–87, 60.2–110.9 mm SL.

We obtained information on *H. wujiangensis* Ding & Deng, 1990 from Ding and Deng (1990), on *H. anteridorsalis* Li, Che & Zhou, 2019 and *H. nigra* Li, Che & Zhou, 2019 from Li, Che and Zhou (2019), and *H. dotui* Nguyen, Wu, Cao & Zhang, 2021 from Nguyen et al. (2021).

GenBank Accession numbers are listed in Table 1.

Table 1. Voucher and Genbank numbers for study samples; sequences downloaded from GenBank are without voucher numbers.

Taxon	Voucher number	GenBank number
Triplophysa brevicauda	KIZ 050422024	MZ677092
Triplophysa scleroptera	KIZ 20100076	MZ677093
Triplophysa obscura	–	MG238209
Claea dabryi	KIZ 2009003600	MZ677094
Schistura fasciolata	KIZ 2012003668	MZ677096
Schistura macrocephalus	KIZ 2010003135	MZ677098
Schistura latifasciata	KIZ CXY2008062	MZ677099
Schistura callichroma	KIZ 200401055	MZ677095
Schistura caudofurca	KIZ 20150307022	MZ677097
Homatula wujiangensis	–	IHB0301075
Homatula potanini	KIZ 2010000235	MZ677100
Homatula potanini	KIZ 2010000281	MZ677101
Homatula guanheensis	KIZ 2005014512	MZ677105
Homatula guanheensis	KIZ 2005014513	MZ677104
Homatula longidorsalis	KIZ 2008005909	MZ677121
Homatula longidorsalis	KIZ 2008005910	MZ677118
Homatula variegata	KIZ 2009002770	MZ677110
Homatula variegata	KIZ 2009002724	MZ677115
Homutula robusta	KIZ 2009000146	MZ677106
Homatula robusta	KIZ 2009000144	MZ677107
Homatula coccinocola	KIZ 2012001867	MF953210
Homatula coccinocola	KIZ 2012001868	MF953211
Homatula change	KIZ 2015005116	MZ677109
Homatula change	KIZ 2015005117	MZ677108
Homatula cryptoclathrata	KIZ 2005012639	MZ677116
Homatula cryptoclathrata	KIZ 2005012637	MZ677117
Homatula pycnolepis	KIZ 2009003860	MZ677111
Homatula pycnolepis	KIZ 20050423002	MZ677114
Homatula anguillioides	KIZ 2008006539	MZ677124
Homatula acuticephala	KIZ 2008005994	MZ677122
Homatula anguillioides	KIZ 2008006536	MZ677125
Homatula acuticephala	KIZ 2008005990	MZ677123
Homatula wuliangensis	KIZ 2008008160	MF953221
Homatula wuliangensis	KIZ 2008008159	MF953220
Homatula wenshanensis	KIZ 2014005686	MZ677102
Homatula wenshanensis	KIZ 2014005687	MZ677103
Homatula disparizona	KIZ 2012000626	MF953194
Homatula disparizona	KIZ 2012000622	MF953190
Botia dario		KT781503

Results

Taxonomy

***Homatula robusta* sp. nov.**
http://zoobank.org/A27C86D0-FD58-448C-9A85-6129B1A18F66
Figs 1–5, Tables 2, 3

Material. ***Holotype.*** KIZ 2009000125, 83.12 mm SL; collected by Wansheng Jiang and Weiying Wang on 14 March 2009 at Changdi village, Luoping County, Qu-

Figure 1. Lateral **A** dorsal **B** and ventral views **C** of *H. robusta* sp. nov., holotype, KIZ 2009000125, 83.12 mm SL.

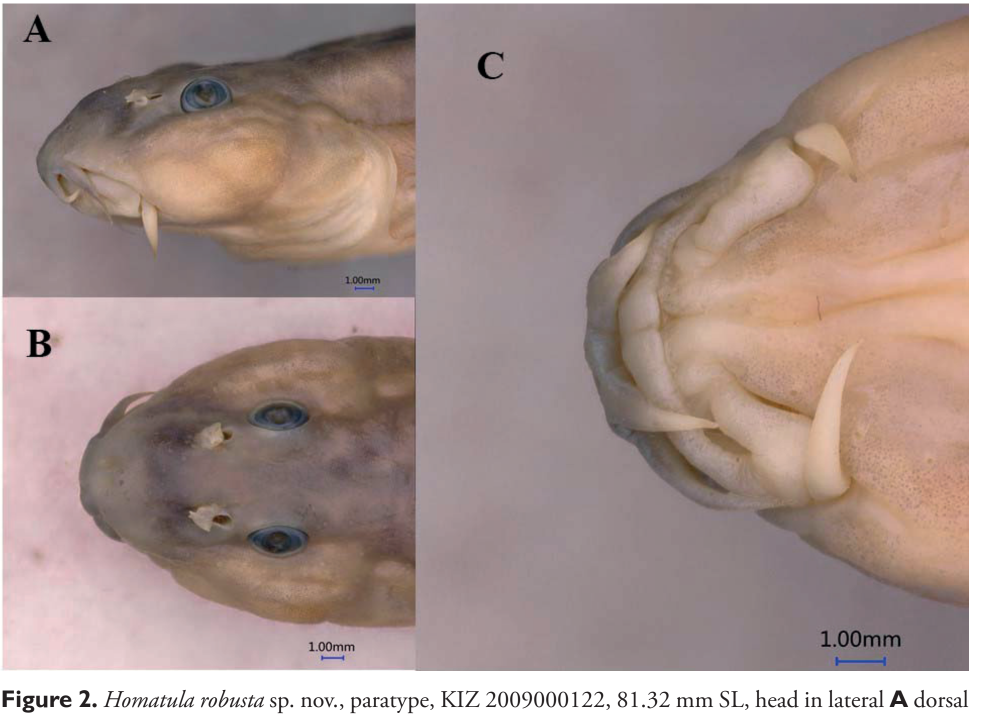

Figure 2. *Homatula robusta* sp. nov., paratype, KIZ 2009000122, 81.32 mm SL, head in lateral **A** dorsal **B** and ventral **C** views.

Figure 3. Lateral view of *H. robusta* sp. nov. KIZ 2009000122 paratype **A** *H. longidorsalis* KIZ 1987003989 **B** *H. nanpanjiangensis* KIZ 1994000023 **C** *H. potanini* KIZ 2010000266 **D**.

jing City, Yunnan Province, China; Nanpanjiang River, upper Pearl River (25°02'N, 104°30'E; ca 1210 m). ***Paratypes.*** KIZ 2009000122, 144, 146, 3 ex. 61.16–81.32 mm SL, same data as for holotype.

Diagnosis. The new species can be distinguished from all other species of *Homatula* by having the following combination of characters: naked and robust body with well-developed crests (caudal peduncle depth as a percentage of its length: 70.5–78.5%), lateral line complete, median notch on lower jaw, median gap on lower lip, three pairs of short barbels, with maxillary barbels extending posteriorly to the anterior edge of eyes, branched dorsal-fin rays 8½, emarginated caudal fin, and vertebrae 37–39.

Table 2. Measurements of four type specimens of *Homatula robusta* sp. nov.

Measurements (mm)	***H. robusta***			
	2009000125	2009000122	2009000144	2009000146
SL	83.12	81.32	73.70	61.16
Head length	18.76	18.28	16.58	13.28
Predorsal length	38.78	37.34	35.16	29.06
Preventral length	41.80	40.94	37.06	29.98
Preanal length	60.42	60.46	54.52	45.60
Preanus length	55.92	56.00	50.16	41.96
Body depth	14.40	13.82	11.72	10.28
Caudal peduncle length (CPL)	16.56	14.78	13.32	9.96
Caudal peduncle depth (CPD)	11.68	11.60	10.20	7.04
Body width	9.36	9.38	8.66	7.06
Dorsal-fin length	11.28	11.48	10.24	7.12
Anal-fin length	12.32	11.94	11.58	9.14
Pelvic-fin length	12.12	12.28	11.22	8.72
Pectoral-fin length	14.82	14.76	13.50	11.12
Head depth at neck	11.84	11.72	10.70	8.56
Snout length	8.64	8.48	7.48	6.10
Head width at eye	13.12	13.34	12.40	9.46
Max head width	14.08	13.90	12.88	10.78
Interorbital width	4.30	4.44	4.24	3.74
eye diameter	2.62	2.34	2.28	2.10

Description. Anterior body cylindrical, posterior body laterally compressed; robust, depth 5.8–6.3 times in length. Caudal peduncle stout, depth 1.27–1.42 times in its length. Crests on dorsal and ventral midlines present and supported by rudimentary procurrent caudal-fin rays; dorsal crest starting immediately posterior of dorsal-fin base, ventral crest starting immediately posterior of anal-fin base.

Snout blunt in lateral view, cheeks inflated. Eyes elliptical horizontally, dorsolaterally positioned. Mouth inferior, slightly arched. Anterior nostril in flap, next to posterior nostril. Lips moderately thick, upper lip smooth, slightly notched medially, lower lip with shallow furrows and median gap. Processus dentiformis on upper jaw present with circular arc edge; lower jaw spoon-like with a median notch. Three pairs of barbels, maxillary barbel reaching anterior margin of eye, outer rostral barbel reaching inner corner of mouth and inner rostral barbel not.

Dorsal-fin rays iv, 8½, distal margin slightly convex. Pectoral-fin rays 11, reaching about halfway from insertion of pectoral fin to insertion of pelvic fin. Pelvic-fin rays 6–8, reaching close to anus, inserted opposite of the first branched dorsal-fin ray. Anus located 1.53–2.17 times eye diameter in front of anal-fin origin. Anal-fin rays iii, 5½. Caudal-fin rays 9+8, distal margin of caudal fin emarginated with upper and lower lobes almost equal in length. Moderate axillary pelvic lobe with free tip.

Body scaleless, or sparse scales scattered along lateral line after posterior end of anal-fiin base, embedded beneath skin. Lateral line completed with 85–89 pores. Supraorbital pores 7, postorbital pores 3, sub- and preorbital pores 12, preoperculo-mandibular pores 10, supratemporal pores 3.

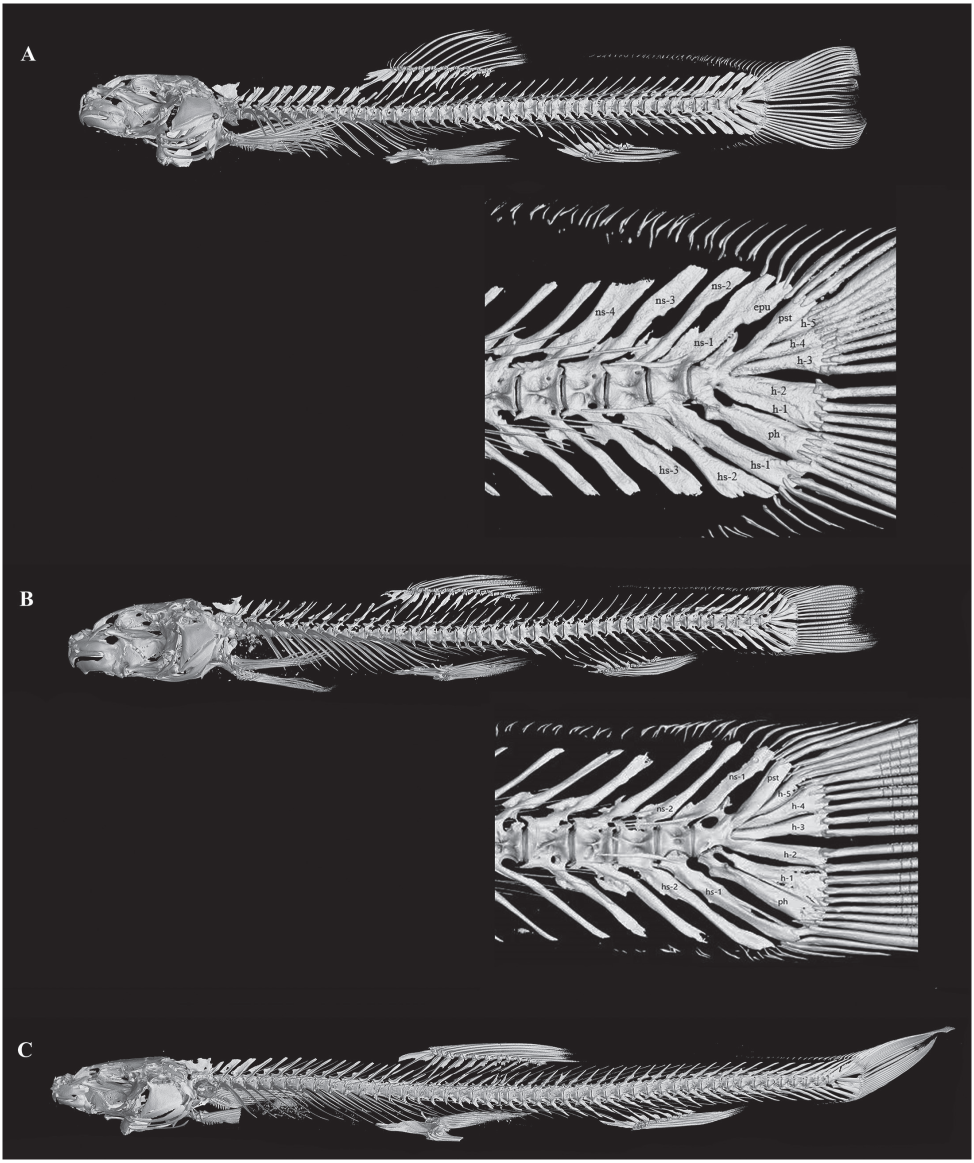

Figure 4. Lateral CT scans of: **A** *H. robusta* sp. nov., KIZ 2009000125, lateral view and structure of caudal skeletons **B** *H. nanpanjiangensis*, KIZ 1994000029, lateral view and structure of caudal skeletons **C** *H. wenshanensis*, KIZ 2014005686, lateral view. Abbreviations: ph—partypurale, ns—neural spine, hs—haemal spine, h—hypural, epu—epurale, pst—pleurostyle.

Vertebrae (three specimens), 4+37–39; four hypural elements with h-1 & h-2 fused, epurale present, last four neural spines (ns-1 to ns-4) and last three haemal spines (hs-1 to hs-3) on the caudal vertebrae are significantly enlarged. U-shaped stomach; intestine almost straight, with small bend next to stomach posterior. Longest recorded length is 83.1 mm SL, 95.7 mm total length (KIZ 2009000125, holotype).

Table 3. Morphometrics of *Homatula robusta* sp. nov. and *Homatula nanpanjiangensis*. SD, standard deviation.

Measurements	*H. robusta*					*H. nanpanjiangensis*				
	N	Min	Max	Mean	SD	N	Min	Max	Mean	SD
SL (mm)	4	61.1	83.12	74.83	8.65	19	63.82	88.74	78.37	7.56
As percent of SL										
Head length	4	13.28	18.76	16.73	2.15	19	15.46	20.36	18.63	1.53
Predorsal length	4	45.92	47.71	46.95	0.72	19	45.62	50.47	47.98	1.37
Preventral length	4	49.02	50.34	49.98	0.56	19	49.58	54.03	51.14	1.14
Preanal length	4	72.69	74.56	73.89	0.73	19	71.25	76.94	74.37	1.47
Preanus length	4	67.28	68.86	68.20	0.61	19	66.55	70.46	69.03	1.01
Body depth	4	15.9	17.32	16.76	0.53	19	12.64	15.30	13.77	0.73
Caudal peduncle length (CPL)	4	16.29	19.92	18.11	1.29	19	16.49	20.92	18.64	1.06
Caudal peduncle depth (CPD)	4	11.51	14.26	13.42	1.11	19	9.45	12.06	10.83	0.66
Body width	4	11.26	11.75	11.52	0.17	19	9.24	13.65	10.73	1.10
Dorsal-fin length	4	11.64	14.12	13.31	0.98	7	12.00	15.83	14.21	1.19
Anal-fin length	4	14.68	15.71	15.04	0.40	6	14.47	16.99	15.56	0.82
Pelvic-fin length	4	14.26	15.22	14.79	0.39	6	13.47	15.67	14.40	0.68
Pectoral-fin length	4	17.83	18.32	18.12	0.18	6	15.35	19.30	17.49	1.16
As percent of head length										
Head depth at neck	4	63.11	64.54	64.06	0.57	19	49.88	61.19	55.01	3.79
Snout length	4	45.11	46.39	45.87	0.47	19	40.92	47.69	44.16	2.28
Head width at eye	4	69.94	74.79	72.23	1.83	19	49.63	72.79	59.56	6.77
Max head width	4	75.05	81.17	77.49	2.33	19	63.22	77.27	69.29	3.72
Interorbital width	4	22.92	28.16	25.24	1.93	19	22.21	26.67	24.29	1.17
Eye diameter	4	12.8	15.81	14.08	1.09	19	13.79	17.94	15.95	1.05
CPD/CPL (%)	4	70.53	78.48	74.07	3.53	19	49.50	65.66	58.22	4.22

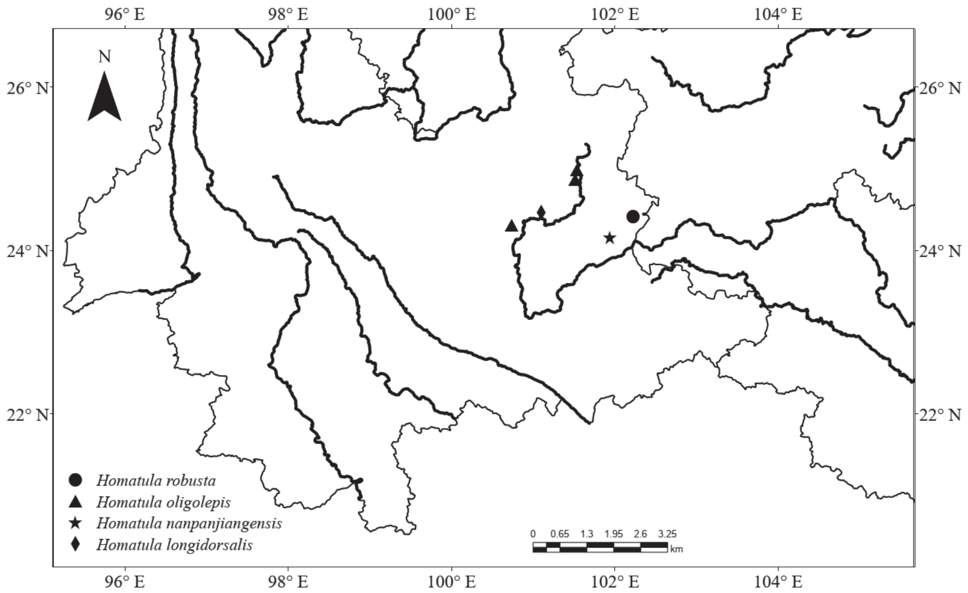

Figure 5. Distribution of *Homatula* from the Nanpanjiang River.

Coloration of preserved specimens. Body light brown with vertical brown bars in formalin-fixed specimens. Bars on predorsal body usually blurred and indistinct, or countable and separated by extraordinary narrow interspaces just in KIZ 2009000122. Bars and interspaces getting wider towards caudal-fin base and approximately equal width on posterior body. Usually, bars regularly shaped and jointed on dorsal midline from opposite sides, or two bars met on upper body and last bar diffused or formed by two combined bars (KIZ 2009000122). Dark black bar on caudal-fin base, reaching dorsal and ventral extremities. All fin rays pale brown and covered by melanophores, series of stripes halfway up each dorsal-fin ray. Color in alcohol-fixed specimens is paler than those in formalin-fixed specimens.

Sexual dimorphism. No sexual dimorphism was observed.

Etymology. Robusta is a Latin word meaning 'strong', in reference to the stout body and caudal peduncle. The Chinese common name is suggested as 粗壮荷马条鳅.

Distribution. Only known from the type locality, Changdi village, Luoping County, Qujing City, Yunnan Province, China (Fig. 5).

Phylogenetic characterization and relationships

The COI molecular dataset included 39 terminal taxa representing 25 species, 15 of which belonged to *Homatula* (Table 1). The COI gene was 1116 bp in length with 313 informative sites, 68 singleton sites, and 717 constant sites. The Bayesian inference (BI) phylogenetic analysis recovered the monophyly of *H. robusta*, *H. wenshanensis* and most species of *Homatula* (Fig. 6). The K2P distance between *H. robusta* and its closest species on the tree, *H. longidorsalis*, is 5.3%. *Homatula wenshanensis* was the sister group of *H. disparizona*. *Homatula potanini* and *H. wujiangensis* (Ding & Deng, 1990) were clustered together, with a K2P distance of 1.5%, and *H. acuticephala* and *H. anguillioides* were clustered together, with a K2P distance of 0.2%.

Discussion

Homatula robusta sp. nov. can be distinguished from its congeners except *H. disparizona*, *H. nanpanjiangensis*, *H. wujiangensis*, *H. oligolepis*, *H. dotui* and *H. wenshanensis* by body scaleless, or sparse scales scattered along the lateral line after anal-fin base (vs. anterior body scaleless or with rudimentary scales in *H. berezowskii*, *H. guanheensis*, *H. laxiclathra*, *H. longidorsalis*, *H. potanini*, and *H. variegata*; whole body scaled besides the head in *H. acuticephala*, *H. anguillioides*, *H. anteridorsalis*, *H. change*, *H. coccinocola*, *H. cryptoclathrata*, *H. nigra*, *H. pycnolepis*, *H. wuliangensis*). The new species can be distinguished from *H. dotui* and *H. wujiangensis* by the complete lateral line (vs. incomplete), presence of brown bars on the body (vs. absence in *H. dotui*), 37–39 vertebrae (vs. 31 in *H. dotui*), normally developed eye, 12.8–15.8% of HL (vs. rudimentary, 4–6% in *H. dotui*), caudal-fin rays 9+8 (vs.

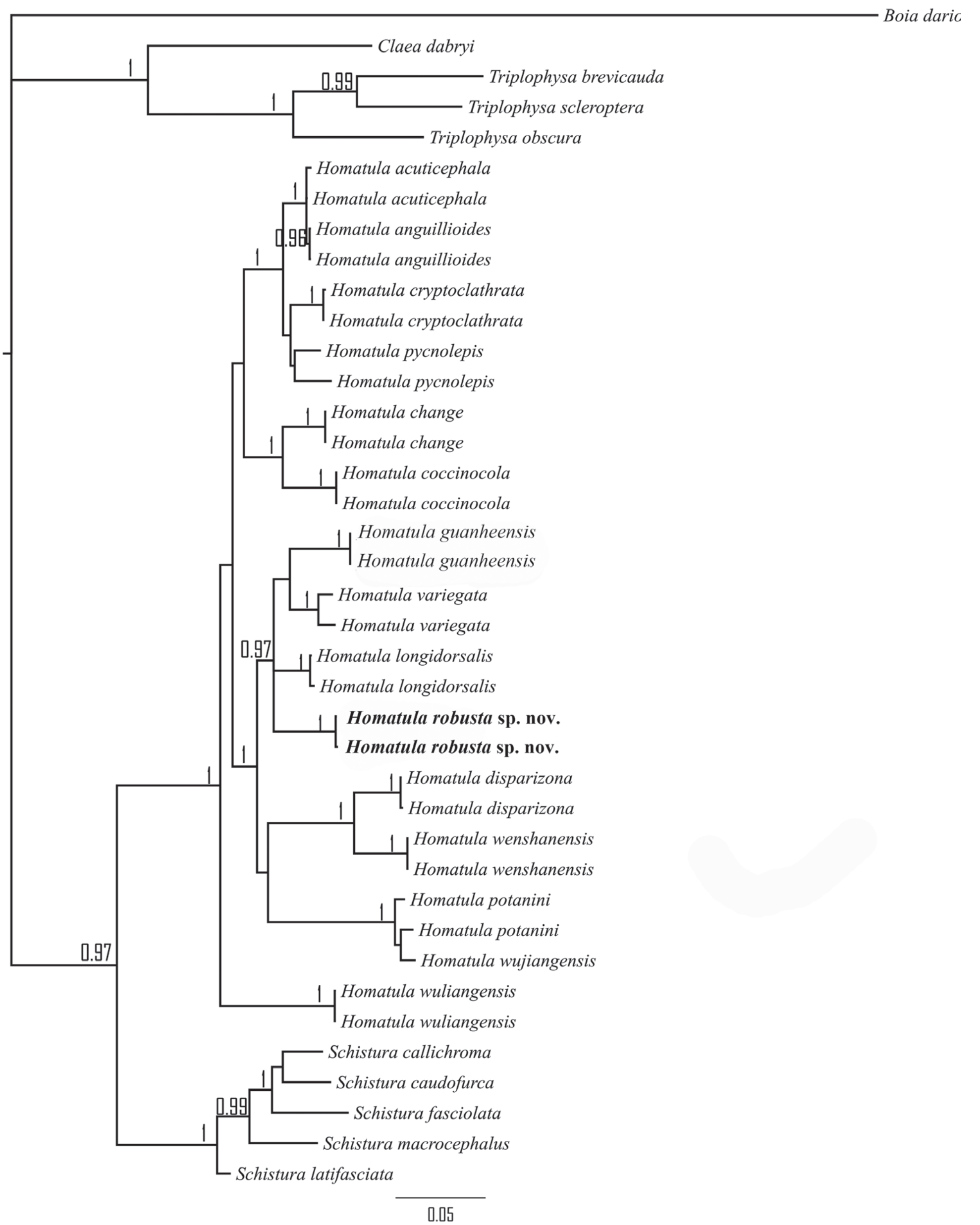

Figure 6. COI MrBayes phylogenetic reconstruction of *Homatula*. BI posterior probabilities of more than 0.95 are plotted on the branches.

8+7 in *H. dotui*), dorsal crest reaching forward beyond the origin of anal-fin base (vs. not reaching the posterior point of anal-fin base in *H. wujiangensis*) and from *H. oligolepis* by the regular bars on the side of the body (vs. vermiform markings on the head and body), 8 ½ branched dorsal-fin rays (vs. 9 ½), vertebrae 37–39 (vs. 39–41). It can be distinguished from *H. disparizona* and *H. wenshanensis* by the stronger body with BD 15.9–17.3% of SL (vs. 12.1–15.4% in *H. disparizona*, 12.1–14.8% in *H. wenshanensis*), vertebrae 37–39 (vs. 39–40 in *H. disparizona*, 47–48 in *H. wenshanensis*), stout caudal peduncle with CPD 70.5–78.5% of Caudal peduncle length (CPL) (vs. 47–62% in *H. disparizona*, 27.3–35% in *H. wenshanensis*), and the median notch on the lower jaw present (vs. absent), caudal fin slightly emarginated (vs. forked in *H. wenshanensis*). *Homatula robusta* can be distinguished from its most similar species, *H. nanpanjiangensis*, on external morphology by the stouter caudal peduncle with CPD 70.5–78.5% of CPL (vs. 49.5–65.7%), deeper body depth (BD) 15.9–17.3% of SL (vs. 12.6–15.3%), shorter barbel with maxillary barbel reaching the anterior margin of the eye (vs. between middle and posterior margin of eye) (Table 3, Fig. 3C), and differed from *H. nanpanjiangensis* on the structures of the caudal skeleton by having four hypural elements with h-1 and h-2 fused (vs. five, h-1 and h-2 separated), epurale present (vs. absent), last four neural spines and last three haemal spines of the caudal centra significantly enlarged (vs. slightly enlarged) (Fig. 4).

Homatula wenshanensis was questioned as member of the genus *Homatula* by Nguyen et al. (2021), because of its indistinct adipose crests along the dorsal and ventral midlines of caudal peduncle, a forked caudal fin and 4+47–48 vertebrae that are not shared by species of *Homatula*. The results of our skeleton scan showed that *H. wenshanensis* has the typical generic character of *Homatula* – crests on caudal peduncle supported by rudimentary procurrent rays (Fig. 4C) – and our COI-based phylogeny showed that *H. wenshanensis* formed an independent lineage sister to *H. disparizona*. Therefore, *H. wenshanensis* is confirmed as a species of the genus *Homatula*.

Homatula is previously believed to be restricted to China. Recently, *H. dotui*, a cave-dwelling species, was reported from central Vietnam (Nguyen et al. 2021). *Homatula dotui* is between *Schistura* and *Homatula* as an independent lineage in the phylogenetic tree built by the cytb gene (Nguyen et al. 2021), which indicates that this cavefish species could belong to an undescribed genus. As stated by Nguyen et al. (2021: 8), a further study should be addressed to confirm the placement of *H. dotui*.

Three species of *Homatula* have been previously reported from the Nanpanjiang River: *H. oligolepis* and *H. longidorsalis* are distributed in the upper Nanpanjiang River; *H. nanpanjiangensis* is distributed in the middle Nanpanjiang River. They possess an elongate body of medium to large size, scaleless (*H. oligolepis* and *H. nanpanjiangensis*) or at least scaleless on the predorsal body (*H. longidorsalis*), 9 ½ branched dorsal-fin rays (*H. oligolepis* and *H. longidorsalis*) or 8 ½ (a few 9 ½ in *H. nanpanjiangensis*), regular vertical bars on each side of body, and bars in front of dorsal-fin base conspicuously thinner than those behind (*H. longidorsalis* and *H. nanpanjiangensis*) or vermiform markings on body and dorsal head (*H. oligolepis*). Here, *H. robusta* sp. nov. is reported from the middle Nanpanjiang River with a stout body. For better identification, a key to species distributed in the Nanpanjiang River is provided.

Key to species of *Homatula* in the Nanpanjiang River

1	Body scaleless or with rudimentary scales present at caudal peduncle	**2**
–	Scales clearly present, covering posterior of body at least, anterior nostril in short tube, 9 ½ branched dorsal-fin rays	***H. longidorsalis***
2	Medium-sized body with regular bars on body, interspaces thinner than bars on predorsal body, SL up to 88.7 mm	**3**
–	Large-sized body with vermiform markings on body and head, SL up to 170.7 mm	***H. oligolepis***
3	Well-developed crests with CPD 70.5–78.5% of CPL, maxillary barbel reaching anterior margin of eye, no more than 13 bars, four hypural elements, epural present, last four neural spines and last three haemal spines on caudal vertebrae significantly enlarged	***H. robusta* sp. nov.**
–	Medium crests with CPD 49.5%–65.7% of CPL, maxillary barbel reaching between middle and posterior margin of eye, ~16 bars on average, five hypural elements, epurale absent, neural and haemal spines on caudal vertebrae slightly enlarged	***H. nanpanjiangensis***

Acknowledgements

We greatly appreciate Dr WS Jiang (Jishou University) and Dr WY Wang for collecting the specimens. For critical comments and helpful suggestions on a draft version of this article I would like to thank three revewers. This project was supported by Biological Resources Programme, Chinese Academy of Sciences (KFJ-BRP-017-16), the National Natural Science Foundation of China (31401956), Strategic Priority Research Program of the Chinese Academy of Sciences (XDA24030505) and Sino BON-Inland Water Fish Diversity Observation Network.

References

Armbruster JW (2012) Standardized Measurements, Landmarks, and Meristics for the Cypriniformes. Zootaxa 3586(1): 8–16. https://doi.org/10.11646/zootaxa.3586.1.3

Bănărescu PM, Nalbant TT (1995) A generical classification of Nemacheilinae with description of two new genera (Teleostei: Cypriniformes: Cobitidae). Travaux du Museum d'Histoire Naturelle 35: 429–495.

Conway KW (2011) Osteology of the South Asian Genus Psilorhynchus McClelland, 1839 (Teleostei: Ostariophysi: Psilorhynchidae), with investigation of its phylogenetic relationships within the order Cypriniformes. Zoological Journal of the Linnean Society 163(1): 50–154. https://doi.org/10.1111/j.1096-3642.2011.00698.x

Ding R, Deng Q (1990) The Noemacheilinae fishes from Sichuan, with description of a new species I. *Paracobitis*, *Nemacheilus* and *Oreias* (Cypriniformes: Cobitidae). Zoological Research 11: 285–290. [In Chinese]

Endruweit M, Min R, Yang J (2018) A new species of *Homatula* from the Red River drainage in Yunnan based on morphological and genetic data (Teleostei: Nemacheilidae). Zootaxa 4375(4): 555–566. https://doi.org/10.11646/zootaxa.4375.4.5

Gu J-H, Zhang E (2012) *Homatula laxiclathra* (Teleostei: Balitoridae), a new species of nemacheiline loach from the Yellow River drainage in Shaanxi Province, northern northern China. Environmental Biology of Fishes 94: 591–599. https://doi.org/10.1007/s10641-011-9965-1

Hu YT, Zhang E, Hu YT, Zhang E (2010) *Homatula pycnolepis*, a new species of nemacheiline loach from the upper Mekong drainage, South China (Teleostei: Balitoridae). Ichthyological Exploration of Freshwaters 21: 67–68. https://doi.org/10.2478/s11687-010-0010-2

Katoh K, Standley DS (2013) MAFFT multiple sequence alignment software version 7: improvements in performance and usability. Molecular biology and evolution 30(4): 772–780. https://doi.org/10.1093/molbev/mst010

Kottelat M (1990) Indochinese Nemacheilines: A Revision of Nemacheiline Loaches (Pisces, Cypriniformes) of Thailand, Burma, Laos, Cambodia and Southern Vietnam. München, 262 pp.

Kumar S, Stecher G, Tamura K (2016) MEGA7: Molecular Evolutionary Genetics Analysis Version 7.0 for Bigger Datasets. Molecular Biology and Evolution 33(7): 1870–1874. https://doi.org/10.1093/molbev/msw054

Li X, Che X-J, Zhou W (2019) Loaches of *Homatula* (Teleostei: Nemacheilidae) from the upper Salween River in Yunnan, China with description of three new species. Zootaxa 4711(2): 330–348. https://doi.org/10.11646/zootaxa.4711.2.6

Liu S, Mayden RL, Zhang J, Yu D, Tang Q, Deng X, Liu H (2012) Phylogenetic relationships of the Cobitoidea (Teleostei: Cypriniformes) inferred from mitochondrial and nuclear genes with analyses of gene evolution. Gene 508: 60–72. https://doi.org/10.1016/j.gene.2012.07.040

Min R, Chen X, Yang J (2010) *Paracobitis nanpanjiangensis*, a new loach (Balitoridae: Nemacheilinae) from Yunnan, China. Environmental Biology of Fishes 87: 199–204. https://doi.org/10.1007/s10641-010-9587-z

Min R, Chen X, Yang J, Winterbottom R, Mayden R (2012) Phylogenetic Relationships of the Genus *Homatula* (Cypriniformes: Nemacheilidae), with Special Reference to the Biogeographic History around the Yunnan-Guizhou Plateau. Zootaxa 3586(1): 78–94. https://doi.org/10.11646/zootaxa.3586.1.9

Min R, Yang J-X, Chen X-Y (2013) *Homatula disparizona*, a new species of loach from the Red River drainage in China (Teleostei: Nemacheilidae). Ichthyological Exploration of Freshwaters 23: 289–384.

Nguyen DT, Wu H, Cao L, Zhang E (2021) *Homatula dotui*, a new cave loach from Central Vietnam (Teleostei: Nemacheilidae). Ichthyological Exploration of Freshwaters 1142: 1–11. http://doi.org/10.23788/IEF-1142

Prokofiev AM 2009 Problems of the Classification and Phylogeny of Nemacheiline Loaches of the Group Lacking the Preethmoid I (Cypriniformes: Balitoridae: Nemacheilinae). Journal of Ichthyology 49(10): 874–898. https://doi.org/10.1134/S0032945209100051

Ronquist F, Teslenko M, van der Mark P, Ayres DL, Darling A, Höhna S, Larget B, Liu L, Suchard MA, Huelsenbeck JP (2012) MrBayes 3.2: Efficient Bayesian Phylogenetic Inference and Model Choice Across a Large Model Space. Systematic Biology 61(3): 539–542. https://doi.org/10.1093/sysbio/sys029

Sambrook J, Fritsch EF, Maniatis T (1989) Molecular cloning: a laboratory manual. Cold Spring Harbor Laboratory Press, 626 pp.

Yang H, Li C, Liu T, Li W (2017) A Report on a New Species of *Homatula* from Yunnan (Cyprinifromes: Noemacheilidae). Journal of Yunnan Agricultural University 32: 1140–1144. [In Chinese]

Zhou C, Ma W, Wang X, Tang Y, Meng X, Nie G (2021) *Homatula guanheensis* sp. nov. (Teleostei: Nemacheilidae), a new species of loach from Henan Province, China. Biodiversity Data Journal 9: e65130. https://doi.org/10.3897/BDJ.9.e65130

Zhou W, He J (1993) *Paracobitis* distributed in Erhai area, Yunnan, China (Pisces: Cobitidae). Zoological Research 14: 5–9. [In Chinese]

Zhu SQ (1989) The loaches of the subfamily Nemacheilinae in China. Jiangsu Science and Technology Publishing House, Nanjing, 150 pp. [In Chinese]

ZooKeys 1089: 125–167 (2022)
doi: 10.3897/zookeys.1089.72645
https://zookeys.pensoft.net

RESEARCH ARTICLE

A peer-reviewed open-access journal
ZooKeys
Launched to accelerate biodiversity research

Habralictus and *Lasioglossum* of Saint Lucia and Saint Vincent and the Grenadines, Lesser Antilles (Hymenoptera, Apoidea, Halictidae)

Jason Gibbs[1], Amber Bass[1,2], Katherine Morgan[1]

1 *Department of Entomology, University of Manitoba, 12 Dafoe Road, Winnipeg, Manitoba, Canada* **2** *Current address: Agriculture and Agri-Food Canada, Canadian National Collection of Insects, 960 Carling Avenue, Ottawa, Ontario, Canada*

Corresponding author: Jason Gibbs (jason.gibbs@umanitoba.ca)

Academic editor: T. Dörfel | Received 6 August 2021 | Accepted 2 February 2022 | Published 18 March 2022

http://zoobank.org/2EC2586C-B2F7-415D-B5DB-03AE8D1056A6

Citation: Gibbs J, Bass A, Morgan K (2022) *Habralictus* and *Lasioglossum* of Saint Lucia and Saint Vincent and the Grenadines, Lesser Antilles (Hymenoptera, Apoidea, Halictidae). ZooKeys 1089: 125–167. https://doi.org/10.3897/zookeys.1089.72645

Abstract

The new species and the first halictid bees documented from Saint Lucia *Habralictus reinae*, *Lasioglossum* (*Dialictus*) *luciae*, and *L.* (*Habralictellus*) *delphiae* are described. A fourth species, *L.* (*D.*) *dominicense*, is tentatively recorded from the island. The species are illustrated and compared to similar ones from the Lesser Antilles. *Lasioglossum* and *Habralictus* from neighbouring Saint Vincent and the Grenadines are reviewed and a key to *Lasioglossum* provided, including the description of another new species, *L.* (*Dialictus*) *gemmeum. Trigona nigrocyanea* Ashmead and *Dufourea subcyanea* Ashmead are synonymised under *Lasioglossum cyaneum* (Ashmead). Notes on the obscure *Lasioglossum* (*Dialictus*) *minutum* (Fabricius) are provided. A new name, *Lasioglossum* (*Homalictus*) *minuens*, is provided for a secondary homonym *Homalictus minutus* Pauly. The potential for additional species richness in Saint Lucia and the Lesser Antilles is briefly discussed.

Keywords

Anthophila, Caribbean, Halictinae, new species, sweat bees, taxonomy

Introduction

The bees of the Caribbean Islands have received sporadic attention from melittologists. Despite the idyllic landscape of these islands, the lack of species richness may have dissuaded many researchers from visiting. However, specimens accumulated in museum collections have allowed for some recent studies on the regional bee fauna. Bees on the major islands in the Greater Antilles, Cuba, Hispaniola, and Puerto Rico, have been documented relatively well (Baker 1906; Alayo 1973, 1976; Eickwort 1988; Genaro 2001a, b, 2006, 2007, 2008, 2016; Engel 2006a; Genaro and Franz 2008; Engel and Prado 2014; Gibbs 2018). However, recent discoveries of new species (Genaro 2016, 2021; Gibbs 2018) suggest that more diversity may be present throughout the Caribbean Islands.

The numerous small islands that make up the Lesser Antilles are generally less well-known for bees. Recent studies in the French West Indies, Guadeloupe and Martinique, have documented bees in the Apidae and Megachilidae (Meurgey 2014, 2016; Meurgey and Dumbardon-Martial 2015). The species list for the Halictidae remains at zero, although halictid bees do occur on these islands (Gibbs 2016; Meurgey 2016). Dominica, which lies immediately between Guadeloupe and Martinique, has recently had its halictid fauna revised with 11 species in five genera documented (Gibbs 2016). Saint-Vincent and the Grenadines has 16 halictid species known (Ashmead 1900; Cockerell 1910; Moure 2007; Ascher and Pickering 2021). It seems reasonable to conclude that islands to the south of Dominica, i.e., Martinique and St. Lucia, should have a comparable fauna of halictid bees.

Saint Lucia is an island of similar size (617 km^2) to Dominica (750 km^2), which lies between Martinique and Saint Vincent and the Grenadines (SVG). Saint Lucia currently has a rather depauperate faunal list of six bee species (Moure et al. 2007a; Raw 2007; Ascher and Pickering 2021), including the apids *Apis mellifera* L. 1758, *Centris decolorata* Lepeletier 1841, *Centris versicolor* (Fabricius 1775), and *Mesoplia azurea* (Lepeletier and Audinet-Serville 1825) and the megachilids *Megachile derelictula* Cockerell 1937 and *M. lanata* (Fabricius 1775). *Apis mellifera* and both *Megachile* are non-native. The first known halictid bees from the island are documented herein. In comparing these new species to bees from neighbouring islands (Ashmead 1900; Smith-Pardo 2009; Gibbs 2012, 2016), we also clarify the taxonomy of some *Lasioglossum* from SVG. Ashmead (1900) first documented and described the bee fauna from SVG. There has since been little additional taxonomic work on *Lasioglossum* on the island (but see Moure 2007). We describe a new species from SVG, propose two synonymies, and remove one additional name from the fauna.

Materials and methods

Many specimens from various collections have been examined for taxonomic studies of Caribbean Halictidae, particularly *Lasioglossum* but also *Habralictus* (Gibbs 2012, 2016, 2018). Saint Lucia material was found at the American Museum of Natural History (**AMNH**), Florida State collection of Arthropods (**FSCA**), Montana Entomology Collection, Montana State University (**MTEC**), and the National Museum of Natural History, Smithsonian Institution (**USNM**). These species are described to formally document the family Halictidae from the island. Material from Saint Vincent and the Grenadines was examined from FSCA, USNM, Natural History Museum (**NHMUK**), University of Kansas Biodiversity Institute and Natural History Museum (**SEMC**), Packer Collection York University, and J.B. Wallis / R.E. Roughley Museum of Entomology (**WRME**). The Packer Collection specimens were returned without full data recorded, but a subset was deposited at WRME.

Species descriptions follow the format of recent papers on Caribbean *Lasioglossum* (Gibbs 2016, 2018), with some modifications based on Gardner and Gibbs (2020). Terminology for structures follows Michener (2007) with modifications based on Engel (2001a) for wing venation and Gibbs (2010a) for the propodeum. Surface sculpturing follows that of Harris (1979). The term 'granular' is used for the surface sculpturing of *Habralictus* following (Michener 1979; Smith-Pardo 2009; Gibbs 2012), although at high magnifications (150×) it seems this granular effect is due to the surface being microreticulate dorsally, i.e., composed of a close network of raised lines, whereas on the pleura the granular sculpturing is more imbricate.

Measurements for head length, head width, clypeal length, lower interocular distance (**LOD**), and upper interocular distance (**UOD**) follow Michener (2007). All measurements were taken using an ocular micrometer in an Olympus SZX16 microscope at 50–63× magnification or 115× for antennae. Body length was measured by adding the length from the base of antenna to the apex of the propodeum with the length of the metasoma. Face length was measured from the clypeal apex to the lower margin of the median ocellus. Antennal measurements were taken on the shortest side of flagellomere two. Intertegular distance (**ITD**) was the smallest distance between the tegulae in dorsal view. Mesoscutal length was the medial length taken in the same orientation as the ITD. Mesoscutellar, metanotal, and propodeal lengths were measured such that the propodeal posterior surface was parallel to the line of sight. Wing length was measured from the proximal end of the basal vein (**M**) to the apex of the marginal cell. Puncture density is measured in terms of relative spacing given as the length of interspaces (IS) between punctures relative to the puncture diameter (**PD**). Setal length is given in terms of mid ocellus diameters (**MOD**). Metasomal terga and sterna are abbreviated with **T** and **S**, respectively, followed by the appropriate number counting from the proximal segment. Similarly, flagellomeres are abbreviated with **F** followed by the appropriate number.

Systematics

Genus *Habralictus* Moure, 1941

Habralictus Moure 1941: 59. Type species: *Habralictus flavopictus* Moure 1941, by original designation

Zikaniella Moure 1941: 57. Type species: *Zikaniella crassiceps* Moure 1941, by original designation

***Habralictus reinae* sp. nov.**
http://zoobank.org/F1285ABB-2BB0-49FC-A551-7CDD6ECA0D33
Figs 1, 2, 3A

Holotype. Saint Lucia • Micoud District • Quilesse Forest Reserve, Laporte, 13.8404, -60.9741, 272 m, 5–7.V.2009, leg. I.A. Foley and R.C. Winton, UV light trap (♂ MTEC, to be deposited in the USNM).

Paratypes. Saint Lucia • Castries District • Barre de l'Isle, 13.93682, -60.95936, 340 m, 25–28.VI.2009, leg. E.A. Ivie, UV light trap (1 ♀ MTEC) • Barre de l'Isle, 13.93682, -60.95936, 340 m, 8–14.VII.2009, leg. C.A. Maier and M. Gimmel, UV light trap (1 ♂ MTEC) • Barre de l'Isle, 13.9342, -60.9586, 340 m, 22–29.V.2009, leg. R.C. Winton, Malaise trap (1 ♀ WRME) • Barre de l'Isle, 13.9342, -60.9586, 340 m, 27.VI–3.VII.2009, leg. C.A. Maier and M. Gimmel, UV light trap (1 ♂ MTEC) • **Micoud District •** Quilesse Forest Reserve, Laporte, 13.8404, -60.9741, 272 m, 5–7.V.2009, leg. I.A. Foley and R.C. Winton, UV light trap (3 ♂ MTEC, 2 ♂ WRME).

Diagnosis. Males of *H. reinae* can be distinguished from other *Habralictus* in the Lesser Antilles by the combination of head narrow (length/width ratio = 1.0–1.07) (length/width ratio = 0.84–0.85 in *H. antillarus*), clypeus with distal maculation 1/3–1/2 longitudinal length (< 1/5 length in *H. antillarus*), supraclypeal and lower paraocular areas polished due to lack of microsculpture (distinctly imbricate in *H. gonzalezi*), mesoscutal punctation indistinct (fine but distinct in *H. claviventris* and *H. insularis*); mesepisternum polished with only weak microsculpture, sparse punctures distinct (dull, indistinctly punctate in *H. gonzalezi*).

Females of *H. reinae* can be recognised by the combination of head wide (length/width ratio = 9.0) (length/width ratio = 0.92–0.97 in *H. gonzalezi*), clypeal punctures not distinct (distinctly punctate in *H. insularis*), clypeal maculation ½ length of clypeus (1/3 in *H. antillarus*) and T3 sparsely punctate (Fig. 3A) as in T4 (more densely punctate in *H. gonzalezi*; Fig. 3B). The female of *H. claviventris* is unknown.

Description. Female (*n* = 2). Length 4.3–4.5 mm; head length 1.1 mm; head width 1.2 mm; intertegular distance 0.86–0.89 mm; wing length 1.6–1.8 mm.

Colouration. Head and mesosoma bright metallic blue-green with golden and bronze reflections. Clypeal apex pale brownish yellow, base bronze. Labrum reddish brown. Mandible yellow with black base and red apex. Scape yellow ventrally, brown dorsally. Flagellum dark brown, F2-F11 orange-brown ventrally. Pronotal lobe brown. Tegula yellowish brown. Wing membrane faintly dusky, veins brown to dark brown. Legs with varying brown and yellow, brown primarily on coxa, femur and meso- and metatibiae, yellow on trochanters, profemur apex, protibia and protarsi, dorsal or anterior surface of mesotibia, and posterior surface of metatibia and variably on posterior surface of metafemur, Metasoma brown and yellow-orange, yellow-orange on base of terga and on sterna, apical terga brown.

Pubescence. Body with sparse pilosity, dull white to faintly yellowish, dark setae on meso- and metatibia, and scattered on T4–T6. Tomentum on pronotal dorsolateral angles and lobe. Mesoscutal pilosity sparse erect. Wing setae dark. T1 without appressed fan. Terga with sparse setae, absent on apical impressed areas.

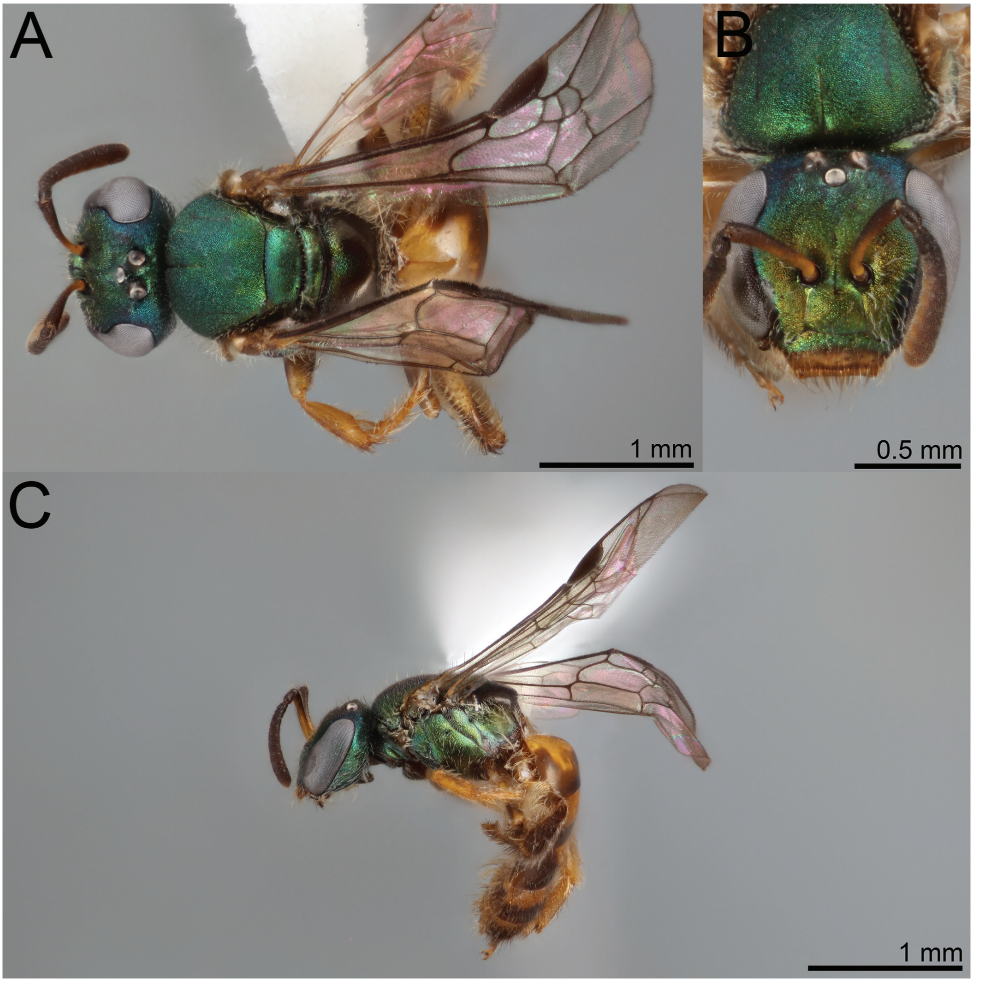

Figure 1. *Habralictus reinae* sp. nov., paratype female **A** dorsal habitus **B** head, frontal view **C** lateral habitus.

Surface sculpture. Clypeal punctures indistinct, sparse (IS = 2–4 PD), denser along apical margin (IS = 1–2 PD), interspaces granular. Face granular with indistinct punctation. Gena imbricate. Tegula punctures obscure. Mesoscutum and mesoscutellum granular with indistinct punctation. Metapostnotum granular, microreticulate basally becoming imbricate toward margin. Mesopleuron granular (imbricate). Propodeal lateral face imbricate, sparsely punctate; posterior face imbricate, sparsely punctate. Metasomal terga finely coriarious. sparse setose punctures (IS = 3–6 PD) along premarginal line of T2-T4 and disc of T3-T5, apical impressed areas impunctate.

Structure. Face length/width ratio 0.78 (± 0.01 SD). UOD/LOD ratio 1.06 (± 0.11 SD). Clypeus projecting ~75% below suborbital tangent; apicolateral denticles rounded knobs. Supraclypeal area length/width ratio 0.97 (± 0.11 SD). Hypostomal carinae parallel. Pronotal angle obtuse. Mesoscutum length/width

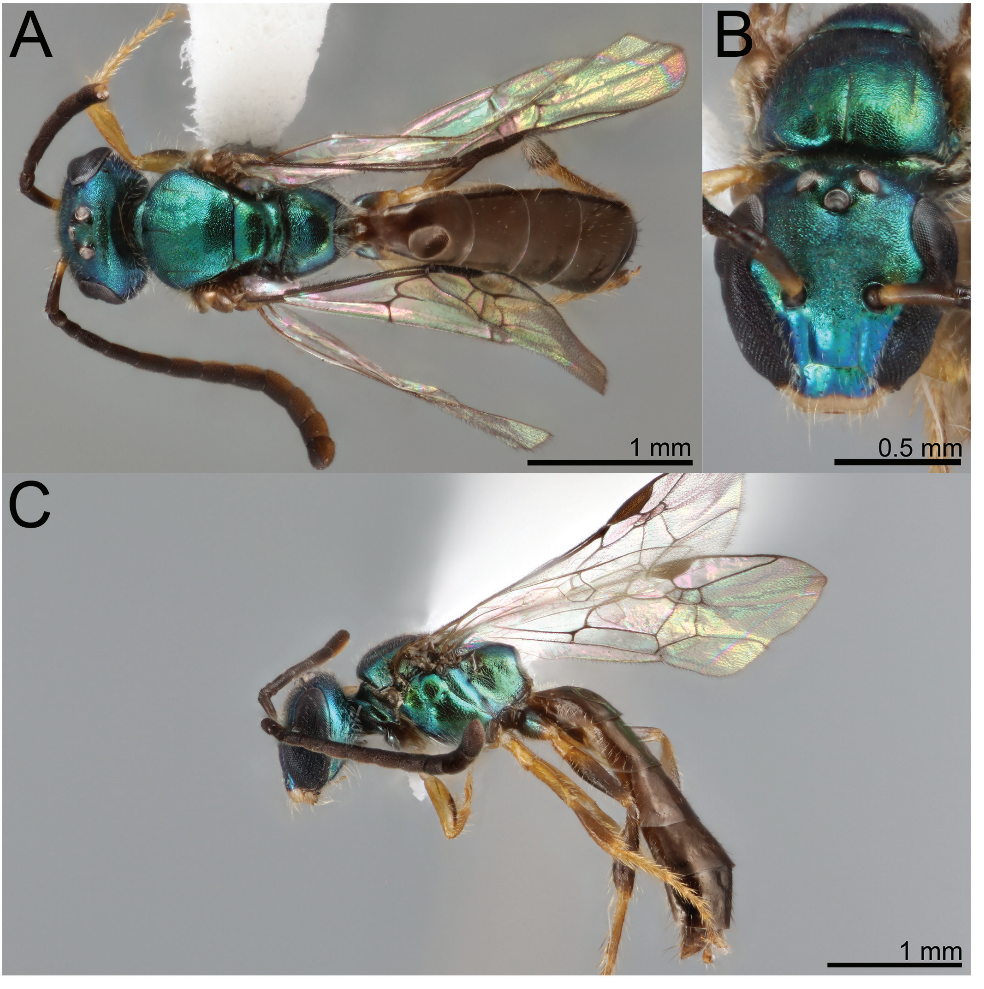

Figure 2. *Habralictus reinae* sp. nov., paratype male **A** dorsal habitus **B** head, frontal view **C** lateral habitus.

ratio 0.91 (± 0.06 SD); mesoscutum/mesoscutellum length ratio 2.93(± 0.33 SD); mesoscutellum/metanotum length ratio 1.73 (± 0.13 SD); metanotum/metapostnotum length ratio 0.5 (± 0.03 SD). Lateral propodeal carinae reaching dorsolateral slope; oblique carina absent. Tegula shape ovoid. Forewing with 3 submarginal cells. Distal hamuli arranged 2-1-2. Inner metatibial spur pectinate, with 3 branches not including apex of rachis, proximal branch much longer than width of rachis. Metasoma ovoid, dorsoventrally flattened, apical impressed area medially ~ 1/2 longitudinal length of basal area.

Male (*n* = 3). Length 4.0–4.3 mm; head length 0.98–1.06 mm; head width 0.94–1.05 mm; intertegular distance 0.65–0.71 mm. Similar to female with usual sex associated modifications.

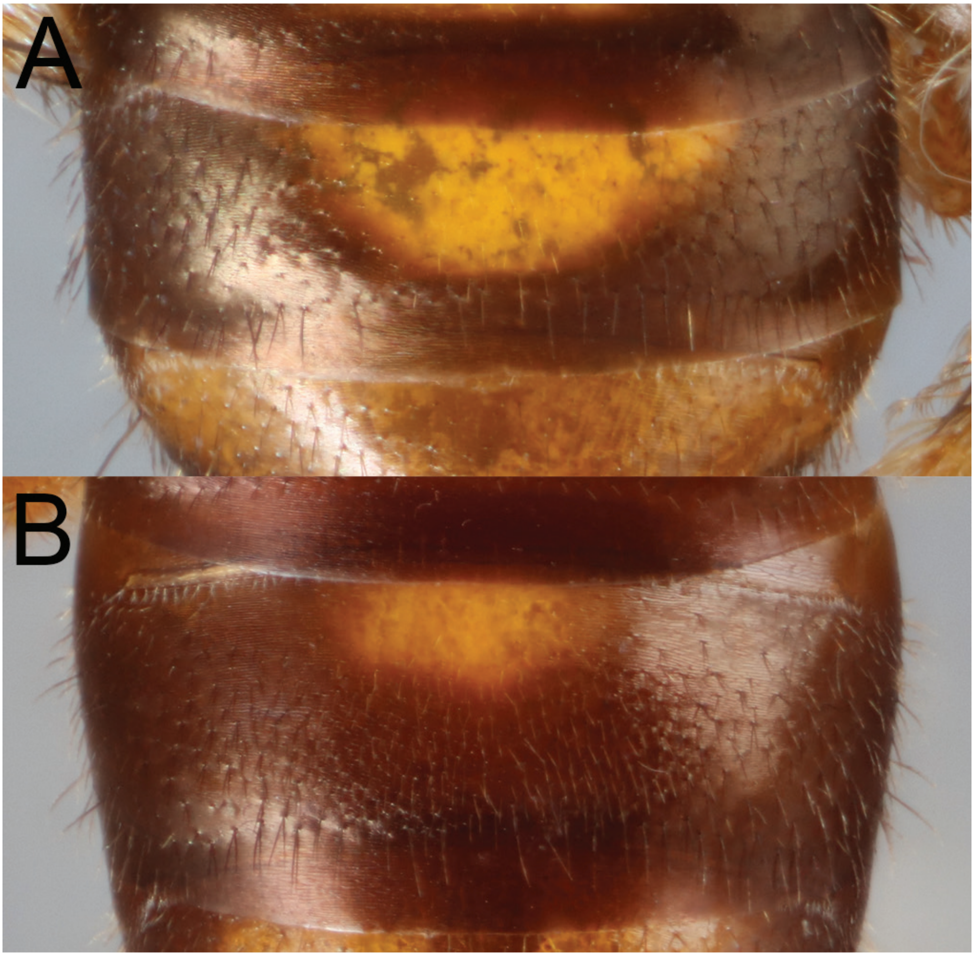

Figure 3. Metasomal tergum 3 of **A** *Habralictus reinae* sp. nov. **B** *Habralictus gonzalezi* Gibbs, 2012 to illustrate differences in setose puncture density.

Colouration. Head and mesosoma iridescent blue-green. Clypeus pale yellow on apical third. Labrum pale yellow. Mandible pale yellow, orange apically. Flagellum brown, F3-F11 yellowish brown ventrally. Pronotal lobe brown. Tegula translucent amber. Wing membrane faintly dusky, veins dark brown. Pro- and mesoleg yellow, except coxa dark with weak metallic reflections, femora ventrally and mesotibia infused with brown. Meta leg brown, except coxa metallic, and trochanter, apices and bases of femur and tibia, and tarsi yellowish brown. Metasoma brown, apical impressed areas reddish brown.

Pubescence. Body pilosity sparse, dull white to faintly yellowish. Gena with long setae (2–2.5 OD). Pronotal lobe with tomentum on posterior margin. Mesoscutal setae sparse, short (0.5 OD). Metasomal terga largely bare; sternal setae sparse (1–1.5 OD), moderately plumose, sparse, erect. Wing setae dark, short, sparse.

Surface sculpture. Clypeal punctures sparse (IS = 1–2 PD), interspaces shiny, weakly imbricate. Supraclypeal punctures sparse (IS = 1–3 PD), interspaces shiny, weakly imbricate. Lower paraocular punctures sparse (IS = 1–3 PD), interspaces shiny, weakly imbricate. Frons and upper paraocular area granular. Gena punctulate-polished; postgena shiny, weakly imbricate. Tegula mostly impunctate. Mesoscutal punctation indistinct, interspaces granular. Mesoscutellar punctation moderately sparse (IS = 1–1.5 PD), interspaces strongly imbricate. Metanotum punctate, interspaces imbricate. Metapostnotum finely reticulate-granular. Pre-episternum imbricate. Hypoepimeral area punctate (IS = 1–1.5 PD), interspaces shiny imbricate. mesepisternum finely punctate (IS = 1–4 PD), interspaces shiny imbricate. Metepisternum imbricate. Propodeum imbricate. Metasoma sparsely punctate (IS = 5–10 PD), apical impressed areas impunctate, interspaces coriarious.

Structure. Face length/width ratio 0.86 (± 0.05 SD). F1: pedicel length ratio 1.1. F2:F1 length ratio 2.5. Gena narrower than eye. Hypostomal carinae parallel. Pronotal angle obtuse. Mesoscutum length/width ratio 0.97 (± 0.03 SD); mesoscutum/mesoscutellum length ratio 2.96 (± 0.05 SD); mesoscutellum/metanotum length ratio 1.92 (± 0.14 SD); metanotum/metapostnotum length ratio 0.5 (± 0.03 SD). Lateral propodeal carina nearly reaching dorsal margin; oblique carina absent. Tegula ovoid. Forewing with 3 submarginal cells. Metatibial spurs ciliate. Metasoma slender, clavate, widest at T4.

Etymology. This brilliant, shining bee is appropriately named for Reina Rybuck, a curious and inquisitive girl who loved insects. Her light shone bright but too briefly. She is remembered with love and affection by those who knew her.

Notes. Of the five *Habralictus* species known from the Lesser Antilles, all seem to be limited to higher elevations (272–762 m) on the islands (Ashmead 1900; Smith-Pardo 2009; Gibbs 2012, 2016). *Habralictus reinae* was taken from protected canopy forests that are particularly wet. It is notable for future collection efforts that this species was predominantly collected from UV light traps, despite more frequent use of Malaise traps by collectors and daytime net collecting (M. Ivie, in litt.).

Habralictus claviventris (Ashmead 1900)

Fig. 4

Augochlora claviventris (1900: 217). Saint Vincent – windward side. 1500 feet. Holotype male by monotypy (NHMUK: BMNH 17.a.1037).

Augochlora claviventris: Ashmead (1900: 304) checklist; Friese (1909: 38) catalogue; Cockerell (1910: 489, 494) checklist, taxonomic notes).

Habralictus claviventris: Michener (1979: 181) new combination, checklist; Moure and Hurd (1987: 174) catalogue; Moure (2007: 837) catalogue; Smith-Pardo (2009: 53) taxonomic notes; Gibbs (2012: 3,9) taxonomic notes, key.

Notes. Currently only known from the holotype male.

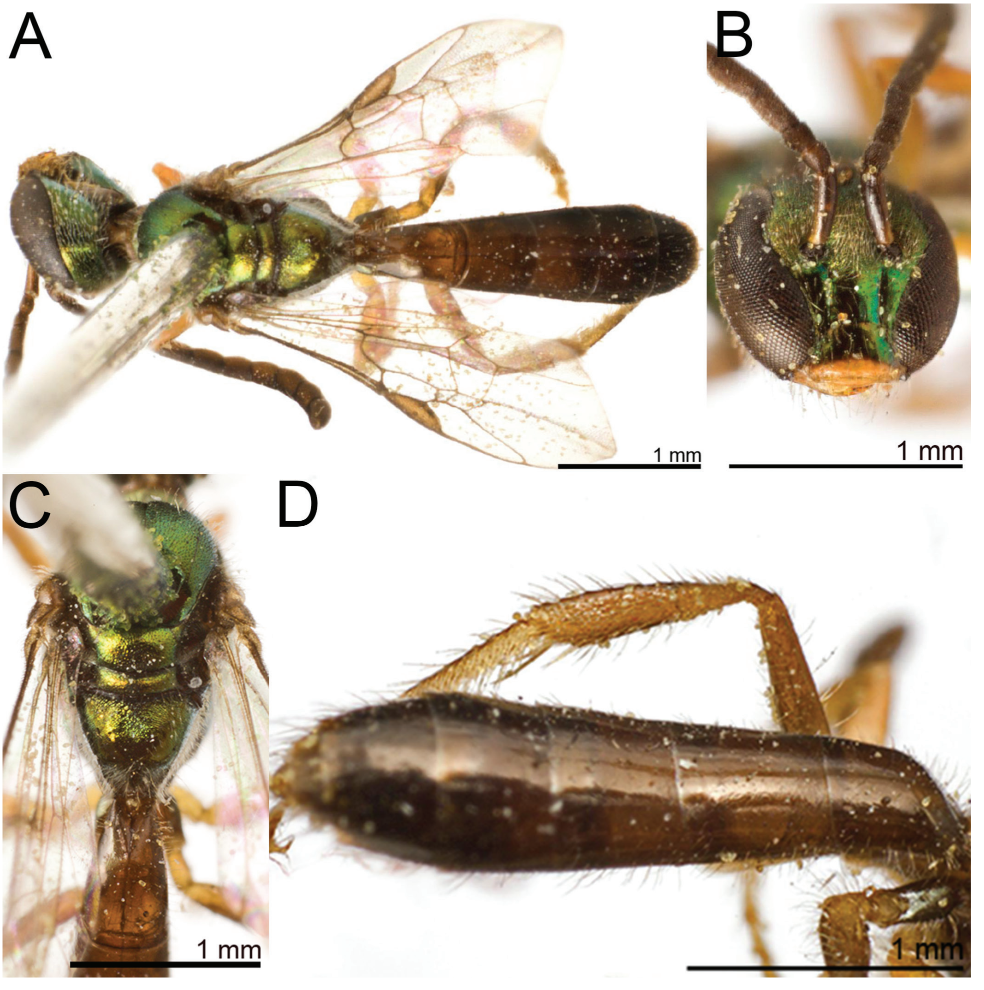

Figure 4. *Habralictus claviventris* Ashmead, 1900, holotype male **A** dorsal habitus **B** face, oblique frontal view **C** dorsal view of metasoma and tergum 1 **D** dorsolateral view of metasoma. Images courtesy of the Trustees of the Natural History Museum, London (https://creativecommons.org/licenses/by/4.0/).

Genus *Lasioglossum* Curtis, 1833

Subgenus *Dialictus* Robertson, 1902

Paralictus Robertson 1901: 229. Type species: *Halictus cephalicus* Robertson, 1892, by original designation

Dialictus Robertson, 1902a: 48. Type species: *Halictus anomalus* Robertson, 1892, by original designation and monotypy

Chloralictus Robertson, 1902c: 248. Type species: *Halictus cressonii* Robertson, 1890, by original designation

Halictus (*Gastrolictus*) Ducke, 1902: 102. Type species: *Halictus osmioides* Ducke, 1902, by monotypy

Halictomorpha Schrottky, 1911: 81. Type species: *Halictomorpha phaedra* Schrottky, 1911, by original designation

Rhynchalictus Moure, 1947: 5. Type species: *Rhynchalictus rostratus* Moure, 1947, by original designation

Halictus (*Smeathhalictus*) Warncke 1975: 88. Type species: *Melitta smeathmanella* Kirby, 1802, by original designation

Lasioglossum (*Afrodialictus*) Pauly 1984: 142. Type species: *Halictus bellulus* Vachal, 1909, by original designation

Gnathalictus Moure 2001: 493. Type species: *Gnathalictus capitatus* Moure, 2001, by original designation

Evylaeus (*Viridihalictus*) Pesenko 2007: 25. Type species: *Halictus viridis* Brullé, 1840, by original designation

Evylaeus (*Glauchalictus*) Pesenko, 2007: 26. Type species: *Halictus problematicus* Blüthgen, 1823, by original designation

Evylaeus (*Virenshalictus*) Pesenko, 2007: 26. Type species: *Hylaeus virens* Erichson, 1835, by original designation

Evylaeus (*Loethalictus*) Pesenko, 2007: 26. Type species: *Halictus loetus* Brullé, 1840, by original designation

Evylaeus (*Aerathalictus*) Pesenko, 2007: 27. Type species: *Melitta aerata* Kirby, 1802, by original designation

***Lasioglossum* (*Dialictus*) *luciae* sp. nov.**
http://zoobank.org/BF175658-2800-4F30-94FE-6B5743544478
Figs 5, 6

Holotype. Saint Lucia • Castries District • Piton Flore, Station no. 26, 10.I.1975, leg. J. Hance & G. Whitmyre (♂ FSCA).

Paratypes. Saint Lucia • Castries District • Castries, 0–210 m, VIII.1976, N.L.H. Krauss (2 ♀ AMNH); Castries, 10–22.IX.1919, leg. J.C. Bradley (2 ♂ USNM) **• Micoud District •** Escap Community, Fond Bay at beach, 13.8316, -60.893, 1 m, 8.V.2009, leg. C.M. Delphia and J.B. Runyon (1 ♀ MTEC).

Diagnosis. *Lasioglossum luciae* is one of only two *L.* (*Dialictus*) known from St. Lucia. It can be distinguished from *L.* (*D.*) *dominicense* by the larger size and longer head. It resembles *L. kilpatrickae* Gibbs, 2016 from Dominica and both *L. plumbeum* (Ashmead, 1900) and *L. sanctivincenti* (Ashmead, 1900) from Saint Vincent and the Grenadines.

Females of *L. luciae* and *L. kilpatrickae* are very similar and definitive characters for distinguishing them are not currently known. The gena of *L. luciae* may be more distinctly lineolate (Fig. 5D) and T1 more distinctly coriarious (Fig. 5E), but too few specimens are available of each species to be sure these characters are consistent. Both *L. luciae* and *L. kilpatrickae* are easily distinguished from *L. plumbeum* and *L. sanctivincenti* by absence of punctation on the apical impressed areas of T2, occurring only obscurely on

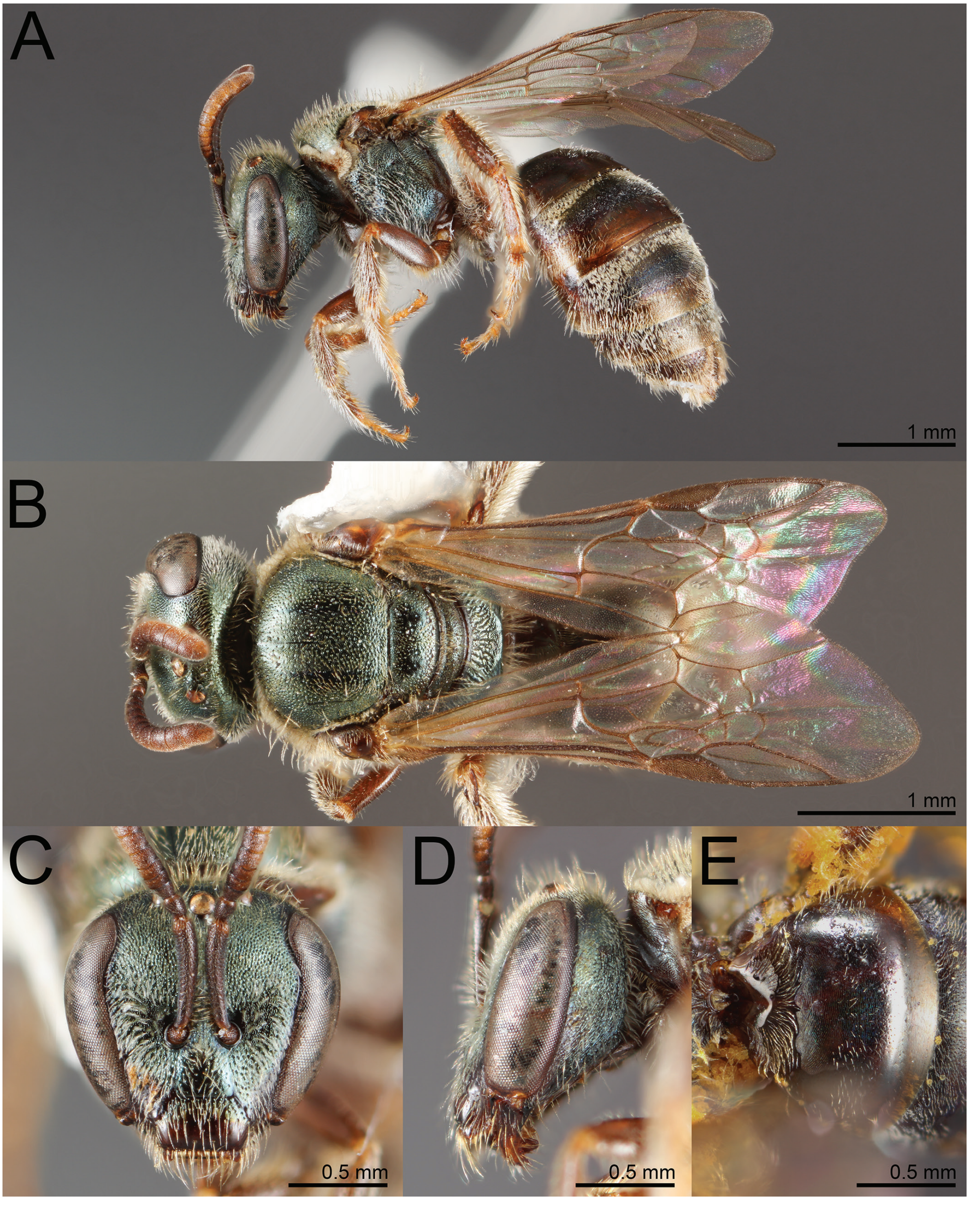

Figure 5. *Lasioglossum* (*Dialictus*) *luciae* sp. nov., paratype female **A** lateral habitus **B** dorsal habitus **C** head, frontal view **D** head, lateral view **E** tergum 1, dorsal view.

the lateral portions. In contrast, both *L. plumbeum* and *L. sanctivincenti* have distinct, albeit fine punctures across the apical impressed areas of T2.

The male of *L. luciae* differs from *L. kilpatrickae* by the less abundant tomentum of the face (Fig. 6C), which only weakly obscures the lower paraocular area, more evident microsculpture on the medial portion of the mesoscutum and anterior face of T1, and the relatively dense punctures on T1-T3, which end near the border of

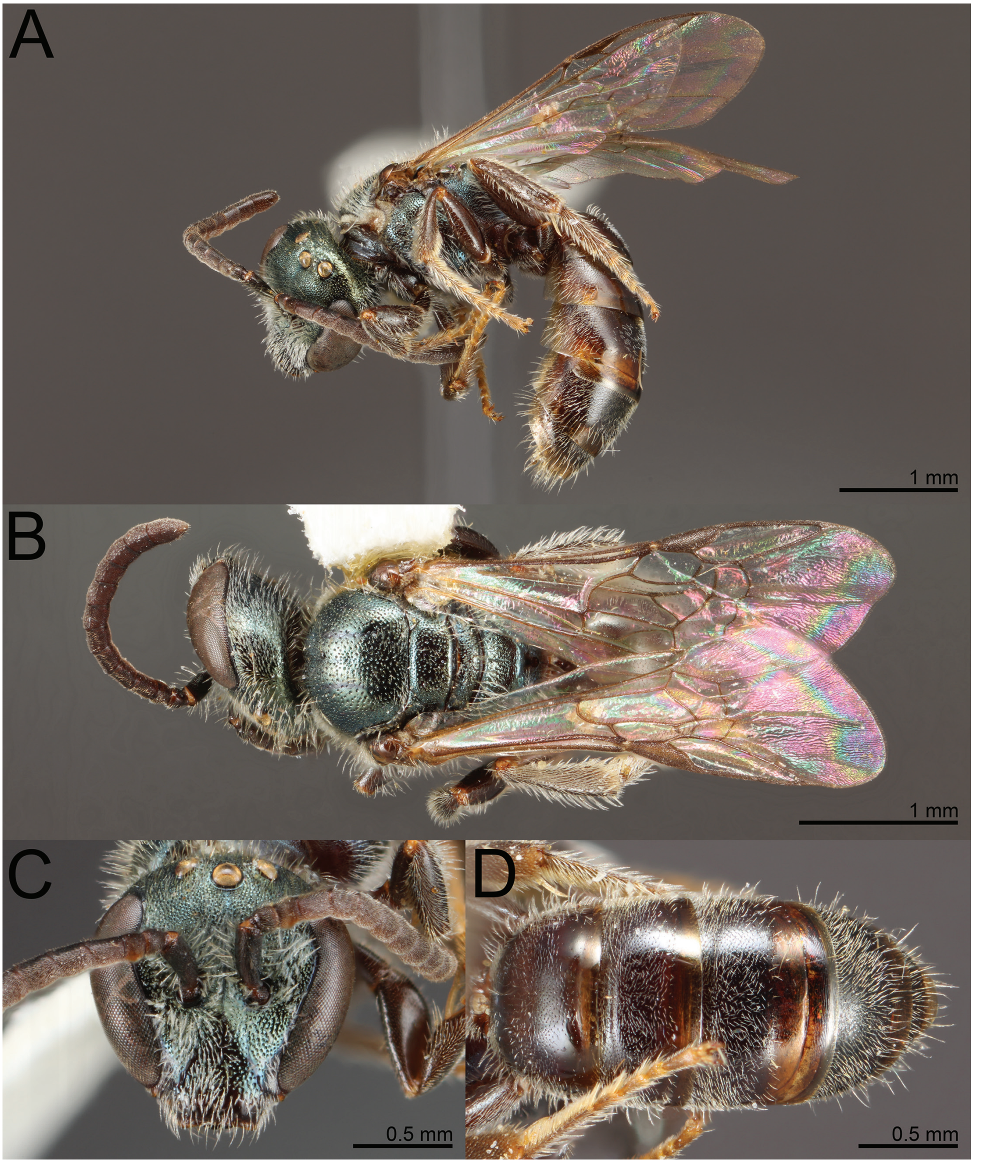

Figure 6. *Lasioglossum* (*Dialictus*) *luciae* sp. nov., holotype male **A** lateral habitus **B** dorsal habitus **C** head, frontal view **D** metasoma, dorsal view.

the apical impressed area, such that at least two thirds of the segments are densely punctate. *Lasioglossum kilpatrickae* has tomentum obscuring the lower paraocular area and proximal portion of the clypeus (Fig. 7B). The mesoscutum has microsculpture between punctures limited to the anterior portion and is largely polished on the anterior face of T1. Furthermore, the punctation of T1-T3 is weak distally such that nearly half the longitudinal length of the segment is sparsely punctate to impunctate. T1 has a nearly impunctate medial line.

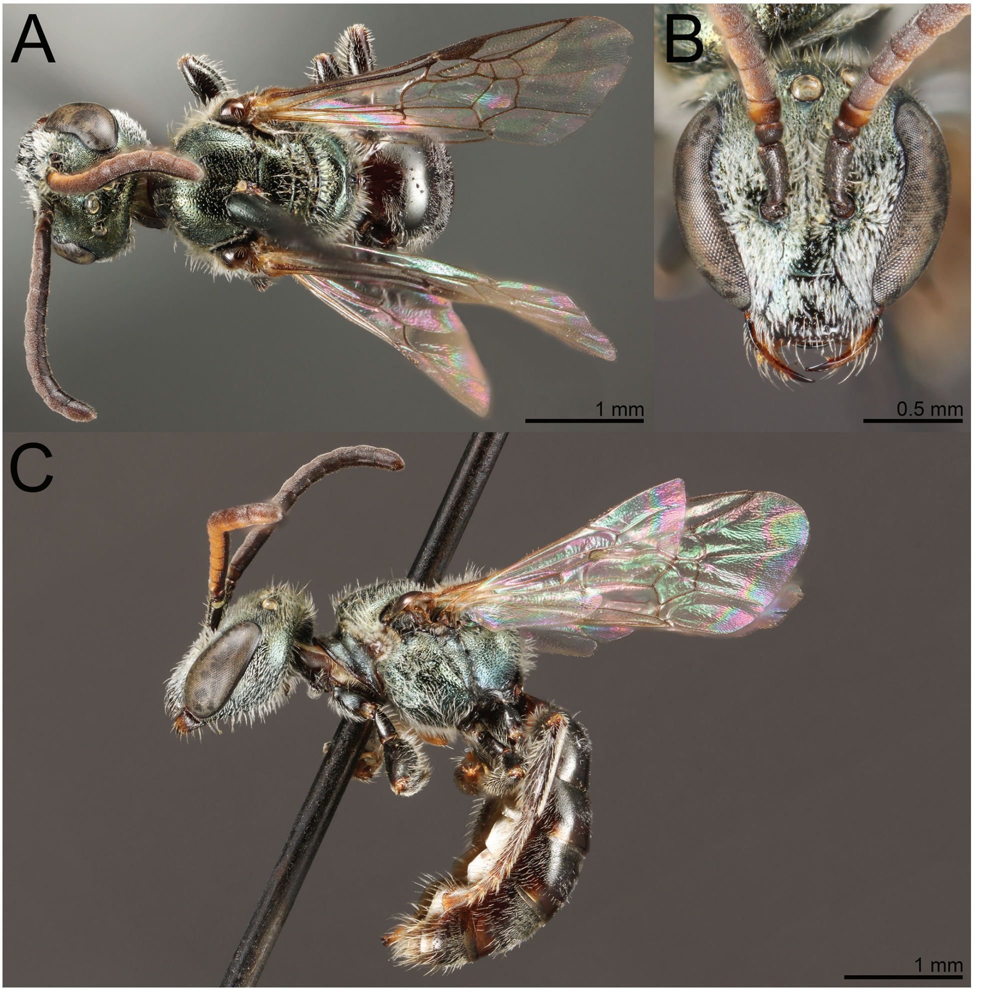

Figure 7. *Lasioglossum* (*Dialictus*) *kilpatrickae* Gibbs, 2016, male **A** dorsal habitus **B** head, frontal view **C** lateral habitus.

Description. Female (*n* = 2). Length 5 mm; head length 1.4 mm; head width 1.4 mm; intertegular distance 1.0 mm; wing length 1.7 mm.

Colouration. Head and mesosoma dull metallic blue-green. Clypeal apex dark brown, base yellow. Labrum reddish brown to orange. Mandible orange with black base and red apex. Flagellum dark brown, F2-F11 orange-brown ventrally. Pronotal lobe reddish brown. Tegula reddish brown. Wing membrane hyaline, veins with subcosta brown to dark brown, otherwise amber. Legs brown, except medio- and distitarsi and portions of metabasitarsus reddish brown. Metasoma blackish brown, apical impressed area reddish brown.

Pubescence. Body with sparse pilosity, dull white to faintly yellowish. Tomentum on gena near eye, pronotum dorsolateral angles and lobe, narrow basolateral patches of T2–T3 and sparsely on T4. Mesoscutal pilosity sparse, erect. Wing setae dark. Acarinarial fan complete, dense. T2 fringes absent, sparse laterally, T3 fringes absent, sparse laterally.

Surface sculpture. Clypeal punctures sparse (IS = 1–4 PD), becoming moderately dense in basal third (IS = 1–2 PD), interspaces polished. Supraclypeal area punctures sparse (IS = 1–3 PD), interspaces weakly imbricate. Paraocular area punctures dense (IS < 1 PD), except near antenna, interspaces imbricate. Frons punctures contiguous. Vertex punctures sparse, interspaces polished. Gena lineolate, postgena lineolate. Tegula punctures obscure. Mesoscutal punctures moderately dense (IS = 1 PD), becoming sparser submedially (IS = 1–1.5 PD) and denser laterad of parapsidal lines (IS ≤ 1 PD), interspaces imbricate, polished laterally; mesoscutellar punctures as in mesoscutum with submedial impunctate area, interspaces imbricate. Metapostnotal rugae strong, anastomosing or subparallel, reaching margin, sculpture imbricate. Pre-episternum rugulose-punctate. Hypoepimeral area densely punctate, interspaces polished. Mesepisternum distinctly punctate. Metepisternum lineolate dorsally, reticulate ventrally. Propodeal lateral face imbricate, sparsely punctate; posterior face imbricate, sparsely punctate. T1 anterior face coriarious; T1 dorsal surface punctures moderately dense (IS = 1–3 PD), absent or very sparse in large apicolateral oval patches, interspaces polished. T2 disc punctures moderately dense (IS = 1–3 PD), interspaces polished, rim impunctate, surface weakly coriarious.

Structure. Face length/width ratio 0.86 (± 0.01 SD). UOD/LOD ratio 1.21 (± 0 SD). Clypeus projecting ~75% below suborbital tangent; apicolateral denticles rounded knobs. Supraclypeal area length/width ratio 2.06 (± 0 SD). Hypostomal carinae parallel. Pronotal angle obtuse. Mesoscutum length/width ratio 0.83 (± 0.01 SD); mesoscutum/mesoscutellum length ratio 2.63 (± 0.1 SD); mesoscutellum/metanotum length ratio 1.66 (± 0.01 SD); metanotum/metapostnotum length ratio 0.75 (± 0.04 SD). Lateral propodeal carinae nearly reaching dorsal margin; oblique carina distinct. Tegula shape ovoid. Forewing with three submarginal cells. Distal hamuli arranged 2-1-2. Inner metatibial spur pectinate, with four branches not including apex of rachis, proximal branch much longer than width of rachis. Metasoma ovoid, apical impressed area medially ~ 1/2 longitudinal length of basal area.

Male (*n* = 3). Length 4.4–4.5 mm; head length 1.30–1.35 mm; head width 1.29–1.30 mm; intertegular distance 0.87–0.94 mm. Similar to female with usual sex-associated modifications.

Colouration. Head and mesosoma blue-green. Clypeal apex reddish brown. Labrum reddish brown. Mandible brown, orange apically. Flagellum brown, light brown ventrally. Pronotal lobe reddish brown. Tegula orange. Wing membrane hyaline, veins dark brown. Legs brown with reddish brown tarsi. Metasoma blackish brown, apical impressed areas reddish brown.

Pubescence. Body sparse pilosity, dull white to faintly yellowish. Tomentum moderately dense on lower paraocular area, sparse on clypeus, dense on pronotal lobe. Mesoscutal pilosity thin. Sternal pilosity short (1 OD), moderately plumose, sparse, erect. Wing setae dark, short, sparse.

Surface sculpture. Clypeal punctures dense (IS ≤ 1 PD), interspaces polished. Supraclypeal area punctures sparse (IS = 1–2 PD), interspaces polished. Paraocular area punctures dense (IS ≤ 1 PD), interspaces weakly imbricate around antenna socket, otherwise shiny. Frons punctate-reticulate. Gena punctulate-lineolate, postgena sculpture lineolate. Tegula mostly impunctate. Mesoscutal punctation moderately sparse medially (IS = 1–2 PD), denser laterad of parapsidal lines, interspaces weakly imbricate, polished laterally. Mesoscutellar punctation moderately sparse (IS = 1–2 PD), becoming denser on margins. Metanotum punctate. Metapostnotum incompletely rugulose, margin weakly tessellate. Pre-episternum sculpture punctate. Hypoepimeral area closely punctate (IS ≤ 1 PD), interspaces polished. Mesepisternum distinctly punctate (IS ≤ 1 PD), interspaces shiny. Metepisternum lineolate dorsally, punctate-reticulate ventrally. Propodeal lateral face tessellate-punctate, dorsolateral slope punctate. Propodeal posterior face sculpture tessellate-punctate. T1 anterior face weakly coriarious. T1 dorsal surface evenly punctate (IS = 1–2 PD), interspaces shiny. T2 disc punctures sparse (IS = 1–2.5 PD), interspaces shiny, apical impressed area impunctate, interspaces coriarious.

Structure. Face length/width ratio 0.87–0.88. F1: pedicel length ratio 1.27. F2:F1 length ratio 1.5. Gena narrower than eye. Hypostomal carinae parallel. Pronotal angle obtuse. Mesoscutum length/width ratio 0.82–0.85; mesoscutum/mesoscutellum length ratio 2.44; mesoscutellum/metanotum length ratio 1.78; metanotum/metapostnotum length ratio 0.77. Propodeum lateral carina nearly reaching dorsal margin; oblique carina absent. Tegula ovoid. Forewing with 3 submarginal cells. Metatibial spurs ciliate. Metasoma slender, parallel sided.

Etymology. The specific epithet is derived from the name of the island. Saint Lucia is the only sovereign nation named after a historical woman.

Notes. Males are associated with females in part by the shared head length consistent with patterns seen between *L. dominicense* and *L. kilpatrickae* in Dominica.

***Lasioglossum* (*Dialictus*) cf. *dominicense* Gibbs 2016**

Fig. 8

Lasioglossum (*Dialictus*) *dominicense* Gibbs 2016: 6–11, 42–43.

Material examined. Saint Lucia • Dauphin District • Louvette trap site, 13.9689, -60.8859, 25–29.VI.2009, leg. M.L. Gimmel and C.A. Maier, UV light trap (1 ♀ MTEC) • Grand Anse trap site, 14.0052, -60.8973, 38 m. 8–17.V.2009, leg. R.C. Winton and E.A. Ivie (1 ♀ MTEC) • **Micoud District** • Escap Community Trail to Fond Bay beach, 13.8324, -60.8986 to 13.8316, -60.893, 46 m to 1 m, 8.V.2009, leg. C.M. Delphia and J.B. Runyon, pan traps (1 ♀ MTEC) • Escap Community, 13.83242, -60.8859, 46 m, 22.V-6.VI.2009, leg. R.C. Winton, Malaise trap (1 ♀ WRME).

Notes. We ascribe the Saint Lucia material to *L. dominicense* without supporting evidence to the contrary. Although there seems to be some pattern of distinct species across islands in the Lesser Antilles, we are unable to confidently differentiate females of *L. dominicense* from Saint Lucia and Dominica at this time. As a lowland species occurring near the beach, it is most consistent with a multi-island distribution. Additional comparative study including males, specimens from Martinique, and molecular data would be useful.

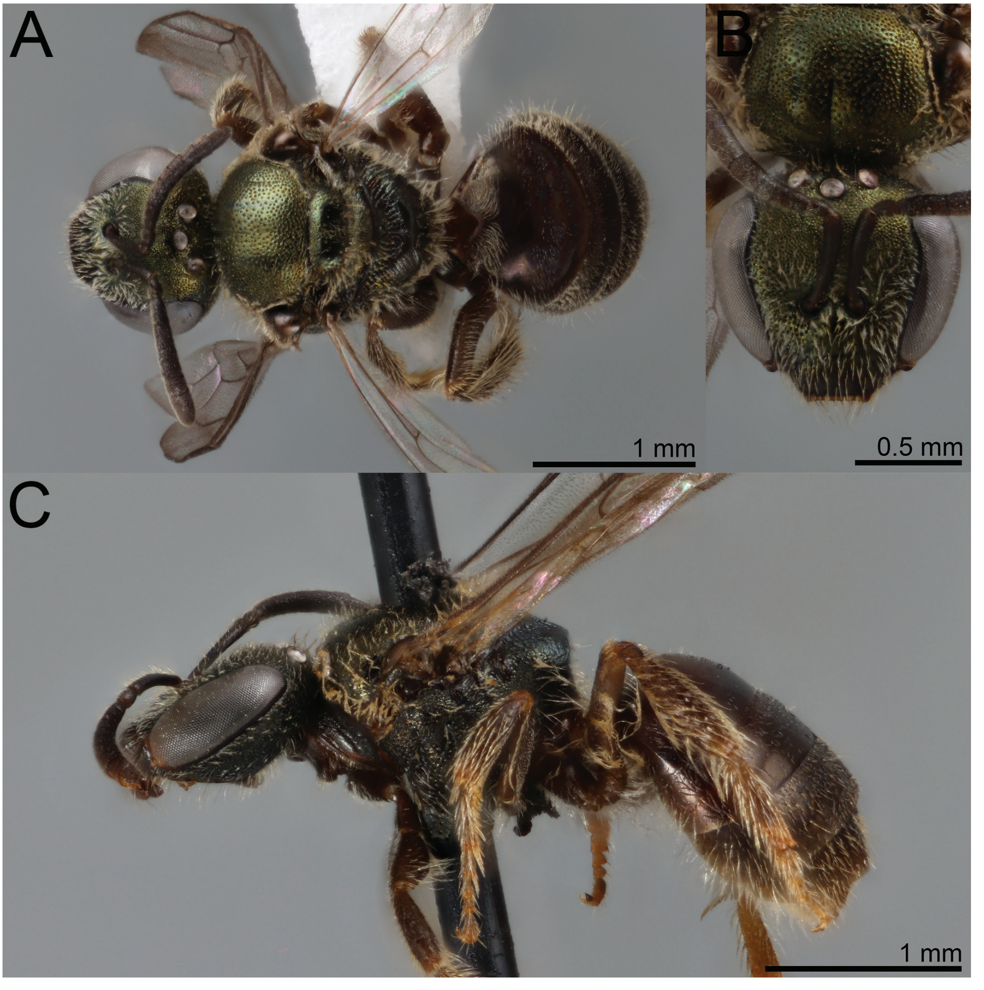

Figure 8. *Lasioglossum* (*Dialictus*) cf. *dominicense* Gibbs, 2016, female **A** dorsal habitus **B** head, frontal view **C** lateral habitus.

Subgenus *Habralictellus* Moure & Hurd, 1982

Habralictellus Moure & Hurd, 1982. Type species: *Halictus auratus* Ashmead 1900, by original designation

Lasioglossum (*Habralictellus*) *delphiae* sp. nov.

http://zoobank.org/D804A754-5BD9-4860-B4C5-793174EFE490
Fig. 9

Holotype. Saint Lucia. • Savannes [Bay] Mangrove Res., 13.766, -60.915 [13 45.97 60 54.88], 0–5 m, 3.V.2009, leg. C.M. Delphia (♀ MTEC, to be deposited in the USNM).

Paratypes. Saint Lucia • Micoud District • Escap Community Fond Bay at beach, [13 83.16 60 89.30], 1 m, 8.V.2009, leg. C.M. Delphia, J.B. Runyon (♀ MTEC).

Diagnosis. *Lasioglossum delphiae* is easily distinguishable as a member of the subgenus *Habralictellus*. It has two submarginal cells (1rs-m absent). It closely resembles *L. (H.) roseauense* from Dominica. *Lasioglossum delphiae* has the mesoscutellum very weakly sculptured, almost polished with distinct, sparse punctures (mesoscutellum dull, sculpturing stronger, similar to that of mesoscutum in *L. roseauense*) and the metasomal terga have orange bands basally (all dark in *L. roseauense*). There is more yellow on the foreleg of *L. delphiae* than *L. roseauense*, although such colour characters may not be reliable given the limited material available.

Description. Female (*n* = 2). Length 4.5 mm; head length 1.1–1.2 mm; head width 1.2–1.3 mm; intertegular distance 0.9–1.04 mm; wing length 1.7–1.8 mm.

Colouration. Head and mesosoma dull metallic golden-green, metapostnotum blue-green. Clypeal apex reddish brown. Labrum reddish brown to orange. Mandible orange with black base and red apex. Scape brown apically, orange basally. Flagellum brown, F3-F11 orange-brown ventrally. Pronotal lobe reddish brown. Tegula amber. Wing membrane hyaline, veins brown. Legs brown, except orange on pro- and mesotrochanters, protibia, protarsi, ventral surface of mesotibia, mesotarsi 2–5, and apices of metafemur and metatibia. Metasomal terga reddish brown with orange patches basally on terga.

Pubescence. Body with sparse pilosity, dull white to faintly yellowish. Tomentum on pronotal dorsolateral angles and lobe. Mesoscutal pilosity sparse erect. Wing setae dark. Acarinarial fan absent, only sparse erect setae on anterior face of T1. Terga with only sparse setae, without apical fringes or basal tomentum.

Surface sculpture. Clypeal punctures sparse (IS = 1–2.5 PD), interspaces weakly imbricate almost polished on apical half, basally tessellate-granular. Supraclypeal punctures sparse (IS = 1–3 PD), interspaces finely reticulate-granular. Paraocular area punctures sparse (IS = 1–2.5 PD), interspaces granular. Frons punctures indistinct, sparse (IS = 1–3 PD). Vertex granular. Gena lineolate, postgena lineolate. Tegula finely punctate on anterior half (IS = 1–2.5 PD), interspaces imbricate, posterior half glabrous. Mesoscutal punctures sparse (IS = 2–3.5 PD), interspaces tessellate; mesoscutellar punctures coarser, sparse (IS = 2–4 PD), interspaces shiny imbricate. Metanotum granular. Metapostnotum transversely lineolate at base, imbricate along apical margins. Preëpisternum tessellate-granular. Hypoepimeral area indistinctly punctate, interspaces tessellate-granular. Mesepisternum indistinct, sparsely punctate (IS = 1–3 PD), interspaces tessellate-granular. Metepisternum lineolate dorsally, imbricate ventrally. Propodeal lateral face tessellate-imbricate, sparsely punctate; posterior face imbricate, sparsely punctate. T1 anterior face polished, dorsally coriarious. T2-T5 sparsely punctate, interspaces coriarious.

Structure. Face length/width ratio 0.77 (0.01 SD). UOD/LOD ratio 1.18 (± 0 SD). Clypeus projecting ~70% below suborbital tangent; apicolateral denticles low rounded knobs. Supraclypeal area length/width ratio 0.7 (± 0.01 SD). Hypostomal carinae parallel. Pronotal angle obtuse. Mesoscutum length/width ratio 0.83 (± 0.04 SD); mesoscutum/mesoscutellum length ratio 2.7 (± 0.09 SD); mesoscutellum/

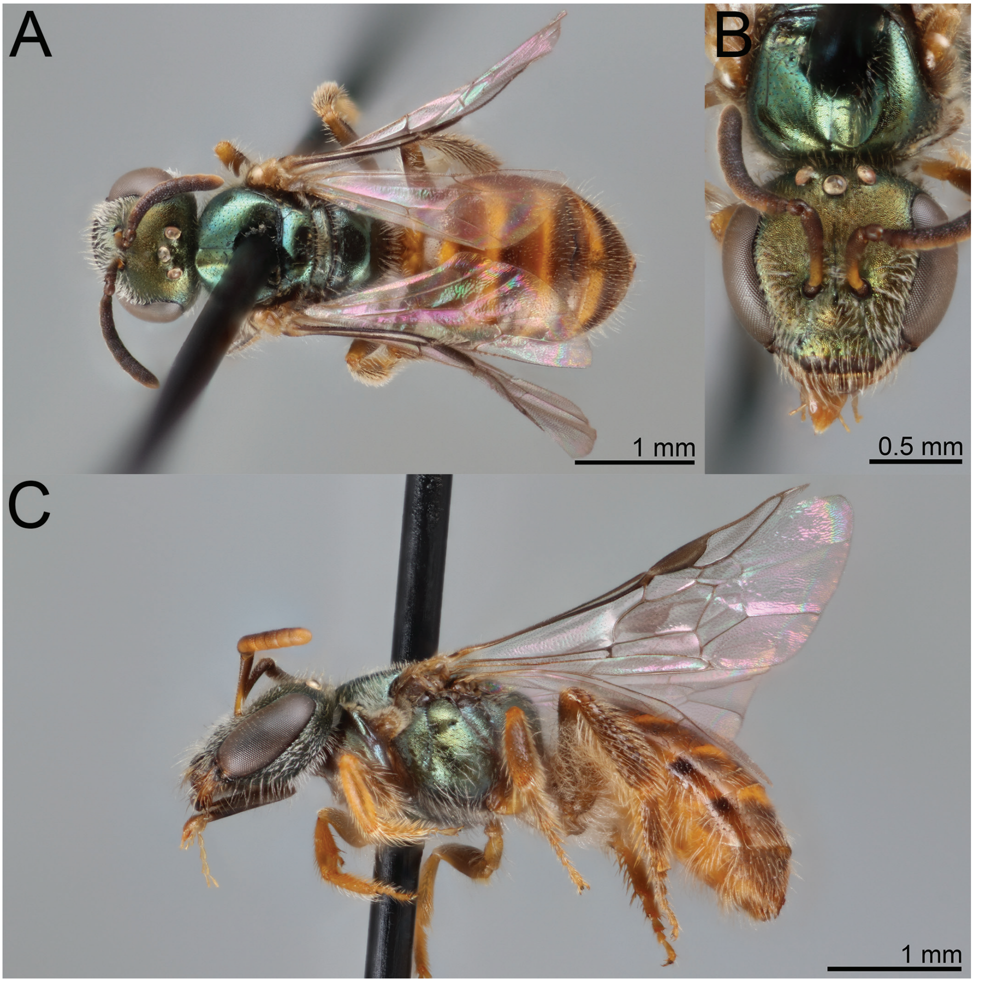

Figure 9. *Lasioglossum* (*Habralictellus*) *delphiae* sp. nov., paratype female **A** dorsal habitus **B** head, frontal view **C** lateral habitus.

metanotum length ratio 1.98 (± 0.1 SD); metanotum/metapostnotum length ratio 0.57 (± 0.06 SD). Propodeum lateral carinae reaching halfway to dorsal margin; oblique carina absent. Tegula shape ovoid. Forewing with two submarginal cells. Distal hamuli arranged 2-1-2. Inner metatibial spur pectinate, with four branches not including apex of rachis, proximal branch much longer than width of rachis. Metasoma ovoid, apical impressed area medially ~ 1/2 longitudinal length of basal area.

Etymology. The species is named for Casey Delphia for her kind support of JG's studies of Caribbean bees generally and in appreciation for collecting the specimens above and bringing them to his attention.

Notes. *Lasioglossum delphiae* was collected from dry forest/beach habitats near the coast (C. Delphia, in litt.).

***Lasioglossum* (*Dialictus*) *cyaneum* (Ashmead 1900)**
Figs 10–13

Halictus cyaneus Ashmead (1900: 218–220). Saint Vincent. Syntype males (2) and females (3) (NHMUK, USNM; Figs 10, 11).
Dufourea subcyanea Ashmead (1900: 215). Saint Vincent. Holotype male (NHMUK). Syn. nov.
Trigona nigrocyanea Ashmead (1900: 208). Saint Vincent – Leeward side. Holotype male (NHMUK; Fig. 12). Syn. nov.
Dufourea subcyanea: Ashmead (1900: 303) checklist; Friese (1909: 38) catalogue.
Halictus cyaneus: Ashmead (1900: 304) checklist; Friese (1909: 37) catalogue.
Dialictus cyaneus: Cockerell (1904: 235) taxonomic placement; Moure and Hurd (1987: 98) catalogue; Moure (2007: 848, 849) catalogue.
Dialictus nigrocyaneus: Moure (2007: 852) catalogue.
Dialictus subcyaneus; Cockerell (1922: 268) taxonomic notes; Sandhouse (1923: 194) checklist; Moure (2007: 855) catalogue; Moure and Hurd (1987: 132) catalogue.
Lasioglossum cyaneum: Gibbs (2016: 6) taxonomic characters.
Trigona nigrocyanea: Ashmead (1900: 299) checklist; Friese (1909: 39) catalogue; Lutz and Cockerell (1920: 499) checklist, type locality.

Material examined. SVG • Saint Vincent • Saint Vincent (*Halictus cyaneus* syntypes 1 ♀ 1 ♂ USNM); Saint Vincent (*Dufourea subcyanea* holotype ♂ NHMUK); Saint Vincent, leeward side (*Trigona nigrocyanea* holotype ♂ NHMUK; from photos) **• St. George Parish •** Majorca Mts., Riley Rd., 13.180694 -61.193556, 366 m, 13.V.2016, leg. Miklasevskaja and Ferrari (1 ♂ WRME) **• St. Patrick Parish •** Cumberland Valley, 17.VI.1977, leg., E.E. Grissell (6 ♂ FSCA).

Taxonomic notes. *Lasioglossum cyaneum* is structurally similar to *L. plumbeum* and *L. sanctivincenti* but is easily recognisable by the entirely blue body and dark wing venation. The male T1-T6 are blue on the disc and dark reddish brown on the lateral and apical margins. The head is distinctly shorter (female and male face length/head width = 0.82–0.85) than *L. plumbeum* (male face length/head width = 0.87–0.90). Both *Dufourea subcyanea* and *Trigona nigrocyanea* were described from single males in the same publication with *Halictus cyaneus.* The former differs from *L. cyaneum* only in the absence of vein 1rs-m, leading to two submarginal cells rather than three. Loss of this vein is relatively common in *L.* (*Dialictus*) (Gibbs 2010b; Scarpulla 2018; see also *L. gemmeum* below), which led to the synonymy of the genus-group names *Dialictus* and *Chloralictus* (Mitchell 1960). The holotype of *Trigona nigrocyanea* is glued to the side of a card and has most of the metasoma missing. It is very evidently a *Lasioglossum* (*Dialictus*). The first tergum is intact and shows distinct metallic reflections consistent with *L. cyaneum.* Ashmead (1900) describes the abdomen as 'rufous, black at base only', but cannot be verified with most of the metasoma missing. In other respects, the holotype matches well with *L. cyaneum*, including the relatively smooth metapostnotum between carinulae.

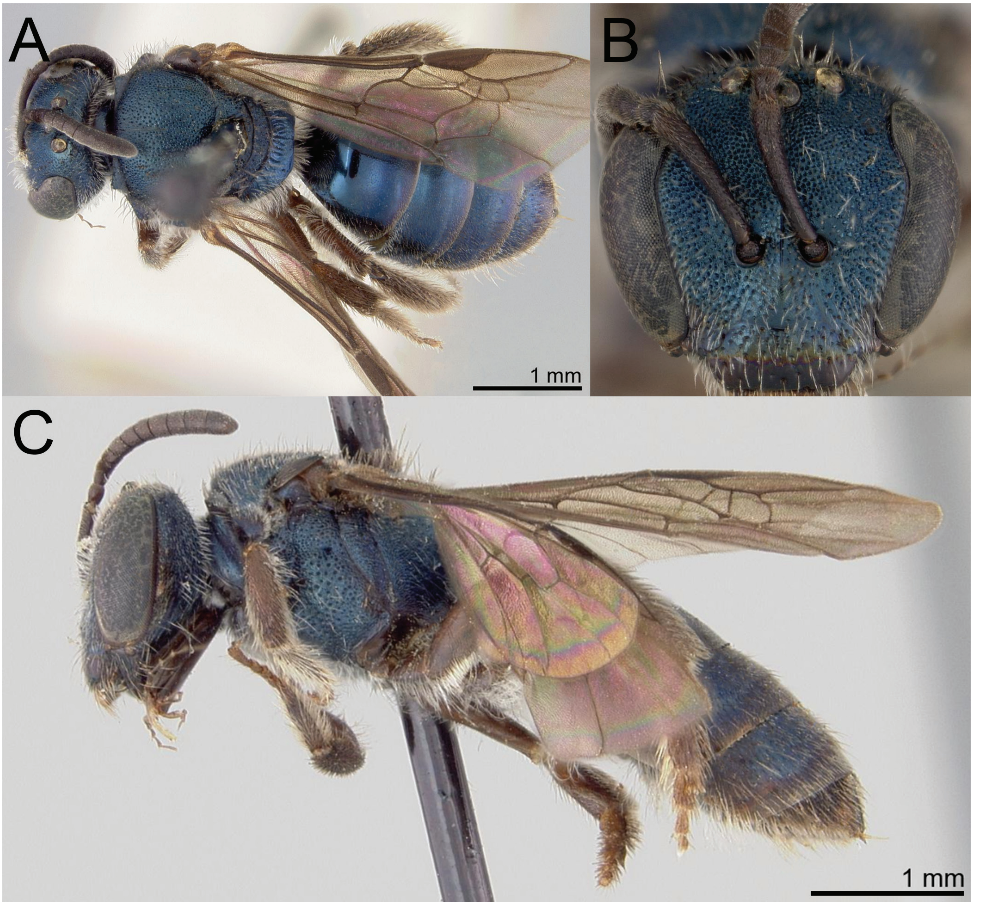

Figure 10. *Lasioglossum* (*Dialictus*) *cyaneum* (Ashmead), syntype female of *Halictus cyaneus* Ashmead **A** dorsal habitus **B** head, frontal view **C** lateral habitus. Images courtesy of the National Museum of Natural History, Smithsonian Institution. https://collections.nmnh.si.edu/search/ento/

***Lasioglossum* (*Dialictus*) *plumbeum* (Ashmead 1900)**
Figs 14–16

Halictus plumbeus Ashmead (1900: 218, 220). Saint Vincent. Syntype males and females (NHMUK, USNM; Fig. 14). Examined.

Halictus plumbeus: Ashmead (1900: 304) checklist; Friese (1909: 37) catalogue; Cockerell (1915: 9) taxonomic note; Cockerell (1938: 280, 281) taxonomic notes.

Halictus (*Chloralictus*) *plumbeus*: Sandhouse (1924: 4) identification key; Cockerell (1937: 113) taxonomic notes.

Dialictus plumbeus: Moure and Hurd (1987: 124) catalogue; Moure (2007: 853) catalogue.

Lasioglossum plumbeum: Gibbs (2016: 6, 15) taxonomic notes.

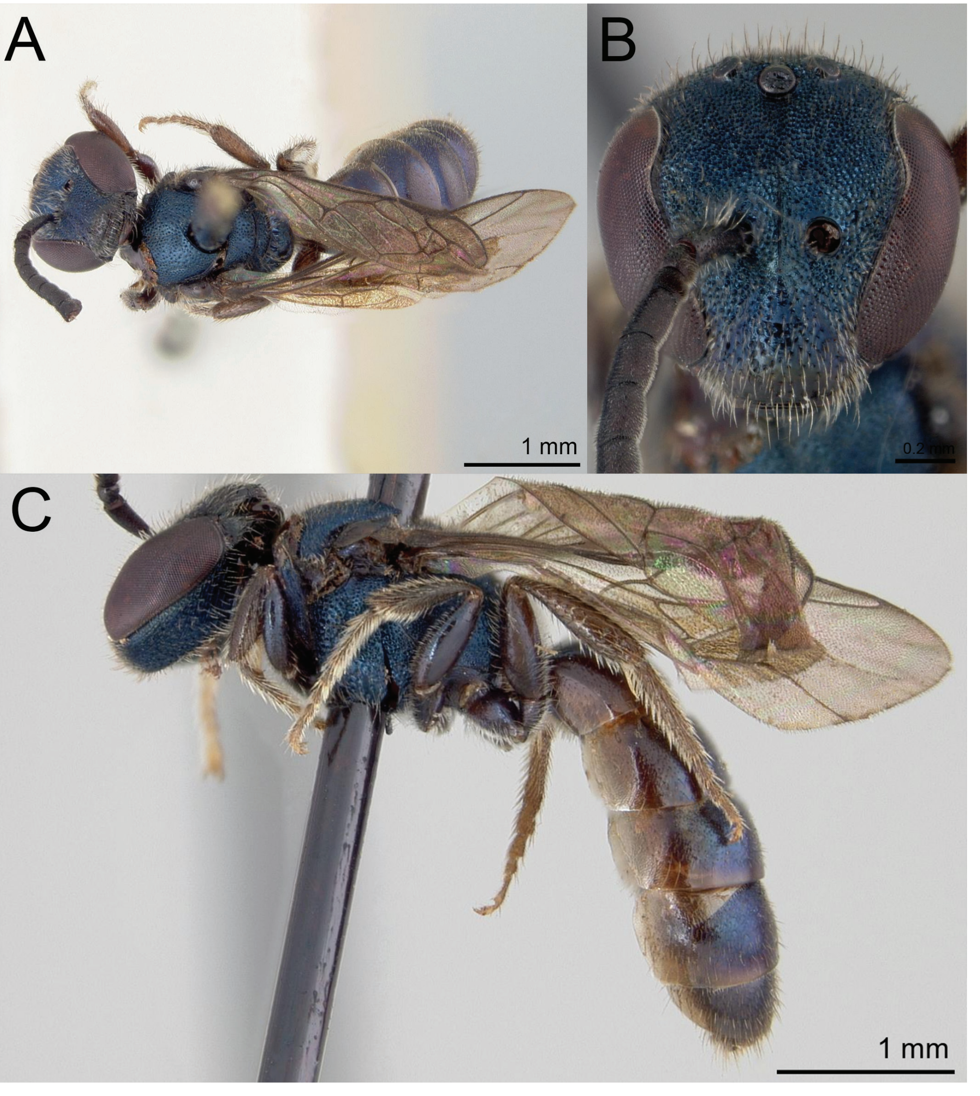

Figure 11. *Lasioglossum* (*Dialictus*) *cyaneum* (Ashmead), syntype male of *Halictus cyaneus* Ashmead **A** dorsal habitus **B** head, frontal view **C** lateral habitus. Images courtesy of the National Museum of Natural History, Smithsonian Institution. https://collections.nmnh.si.edu/search/ento/

Material examined. SVG • Saint Vincent • St. Vincent, leg. H.H. Smith (*Halictus plumbeus* syntypes 1 ♀ NHMUK, 1 ♀ USNM) • St. Vincent (Windward side), leg. H.H. Smith (2 ♀ USNM) • **Charlotte Parish •** Belair Mespo Peruvian Vale Rd., 13.173417 -61.151111, 71 m, 13.V.2016, leg. Miklasevskaja and Ferrari (1 ♂ WRME) • Fancy, 1 km S of Windward hwy. 13.380122 -61.170588, 55 m, 18.V.2016, leg. Miklasevskaja and Ferrari (1 ♂ WRME) • Greiggs, Charlotte Mtn.,13.222417

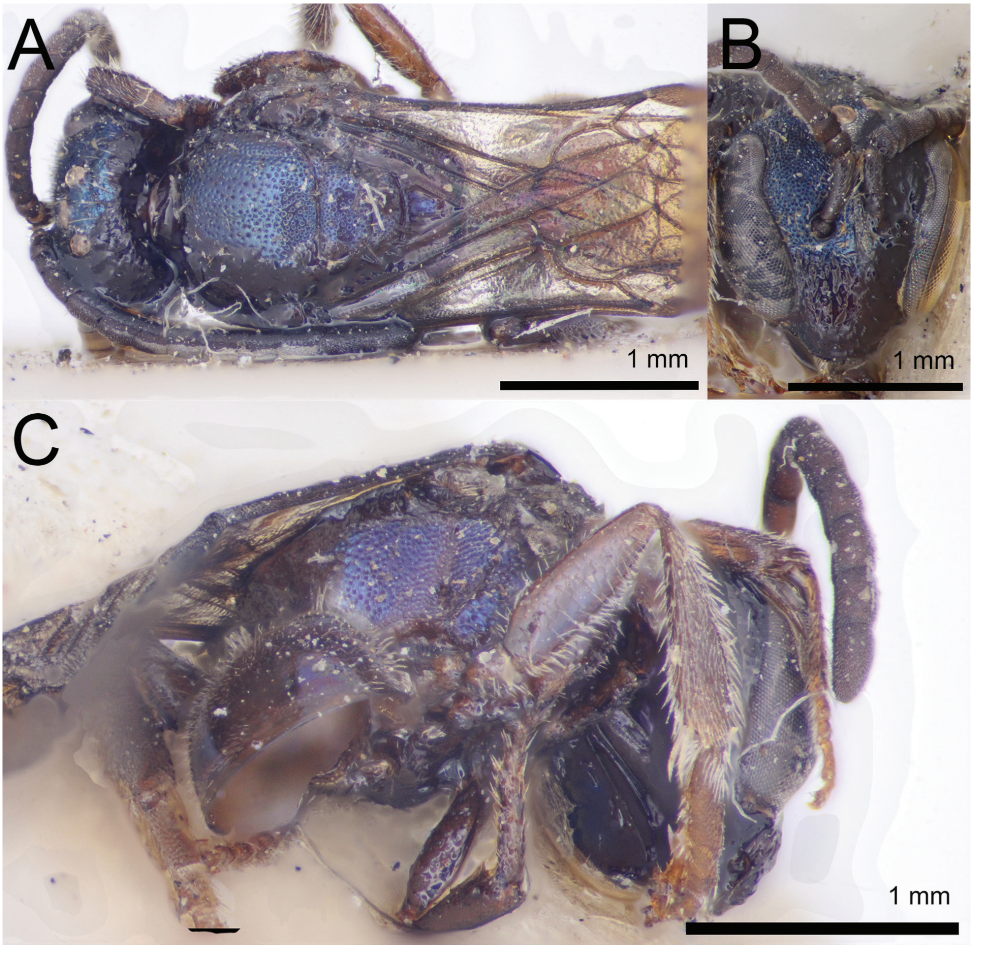

Figure 12. *Lasioglossum* (*Dialictus*) *cyaneum* (Ashmead), syntype male of *Trigona nigrocyanea* Ashmead **A** dorsal habitus **B** head, frontal view **C** lateral habitus. Images courtesy of the Trustees of the Natural History Museum, London (https://creativecommons.org/licenses/by/4.0/). Photographs by David Notton.

-61.173361, 478 m, 14.V.2016, leg. Miklasevskaja and Ferrari (1 ♂ WRME) • **St. Andrew Parish** • Vermont Trail Rd., 13.201639 -61.241333, 114 m, 15.V.2016, leg. Miklasevskaja and Ferrari (1 ♀ WRME) • **St. David Parish** • Cumberland Way, 19.IX.1991, leg. R.E. Woodruff, near beach (1 ♀ 1 ♂ FSCA) • Wallilabou, 14.X.1991, leg. R.E. Woodruff, day catch (10 ♀ 2 ♂) • **St. George Parish** • Cane Hall, 22.IX.1991, leg. R.E. Woodruff, sweeping (4 ♀ 9 ♂ FSCA) • Cane Hall, Rick's Apts., 17.IX.1991, leg. R.E. Woodruff, vacant lot (1 ♀ FSCA) • Rivulet Agr. Sta. 10–15.X.1991, leg. R.E. Woodruff, Malaise trap (3 ♀ FSCA); 27–30.IX.1991, leg. R.E. Woodruff, Malaise trap (1 ♀ 1 ♂ FSCA) • Majorca Mts., Riley Rd., 13.180694 -61.193556, 366 m, 13.V.2016, leg. Miklasevskaja and Ferrari (1 ♀ WRME) • **St.**

Figure 13. *Lasioglossum* (*Dialictus*) *cyaneum* (Ashmead), male **A** dorsal habitus **B** head, frontal view **C** lateral habitus.

Patrick Parish • Cumberland Valley, 17,VI.1977, leg. E.E. Grissell (11 ♀ 21 ♂ FSCA) • Hermitage Forestry Cottage, 11–13.X.1991, leg. R.E. Woodruff, day catch (2 ♀ 1 ♂ FSCA) • Rutland Vale, 1 km N on Leeward Hwy., 13.218727 -61.270954, 60 m, 19.V.2016, leg. Miklasevskaja and Ferrari (1 ♀ WRME) • **Grenadines** • Bequia, Industry, 24.IX.1991, leg. R.E. Woodruff (1 ♂ FSCA).

Notes. *Lasioglossum sanctivincenti* is quite similar to *L. plumbeum.* The most striking difference is the darker blue colour of the head and mesosoma of *L. plumbeum*. *Lasioglossum sanctivincenti* has a shorter head (face length/head width ratio = 0.82 SD 0.02) than *L. plumbeum* (0.86 SD 0.01). Mesoscutal puncture density is subtly different between the two species. In *L. sanctivincenti* punctures laterad of the parapsidal

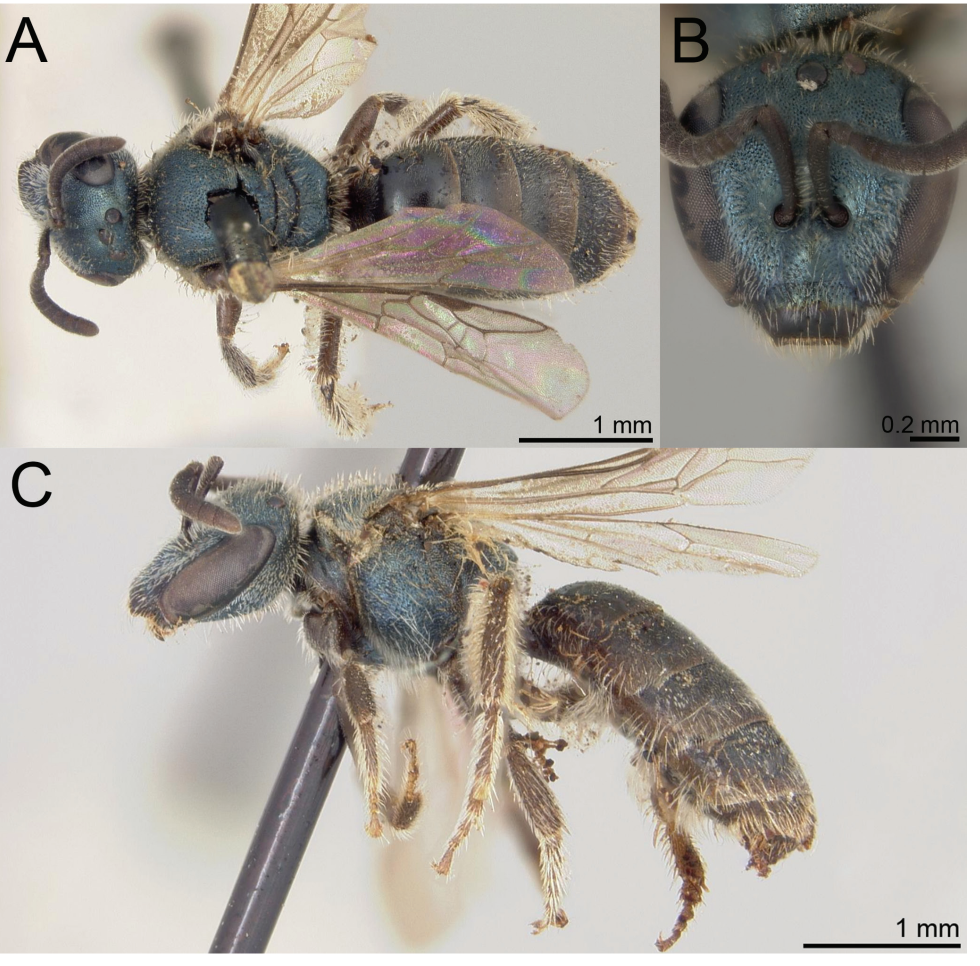

Figure 14. *Lasioglossum* (*Dialictus*) *plumbeum* (Ashmead), syntype female of *Halictus plumbeus* Ashmead **A** dorsal habitus **B** head, frontal view **C** lateral habitus. Images courtesy of the National Museum of Natural History, Smithsonian Institution. https://collections.nmnh.si.edu/search/ento/

line are dense, but distinctly separated. These are nearly reticulate in *L. plumbeum*, without clear interspaces. Immediately mesad of the parapsidal line, *L. sanctivincenti* has distinctly separated punctures (IS ≤ 1 PD), but these are denser in *L. plumbeum* (IS ≤ 0.5 PD). Ashmead's (1900) original measurements suggest that *L. santivincenti* is larger (4–5.5 mm) than *L. plumbeum* (3.5–4.5 mm). In Sandhouse's (1924) key, they separate at couplet 43 based on size and Cockerell (1938) also refers to the smaller size of *L. plumbeum*. However, this may be an artefact of H.H. Smith's original sample as more recently collected specimens of *L. plumbeum* include a large size range (> 5 mm) overlapping with that of *L. sanctivincenti*. The size variation in *L. plumbeum* may be an indication of weakly defined social castes in *L. plumbeum*, which is a common feature of eusocial halictines (Michener 1990).

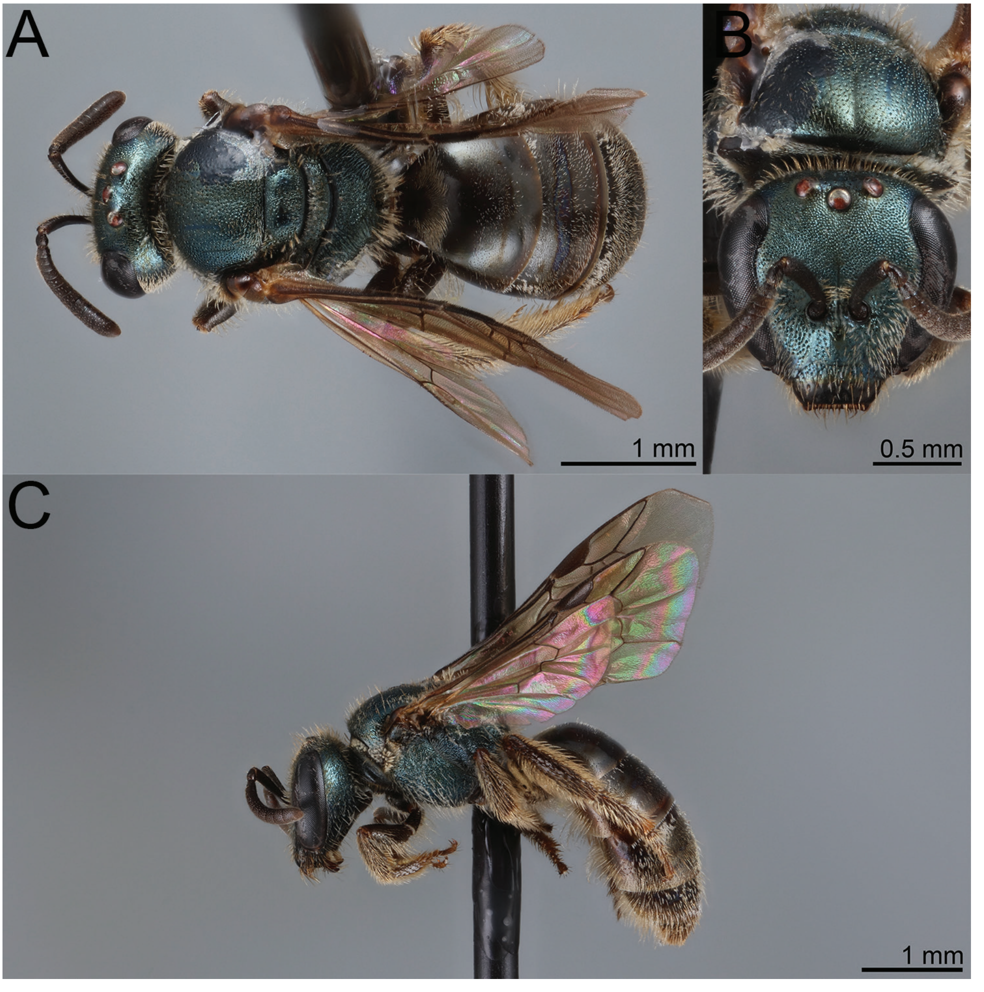

Figure 15. *Lasioglossum* (*Dialictus*) *plumbeum* (Ashmead), female **A** dorsal habitus **B** head, frontal view **C** lateral habitus.

***Lasioglossum* (*Dialictus*) *sanctivincenti* (Ashmead 1900)**
Figs 17–19

Halictus sancti-vincenti Ashmead (1900: 218–220). Grenada – St. George's; Mount Gay Estate (Leeward side), Saint Vincent. Syntype males and females (NHMUK, USNM; Fig. 17).

Halictus santivincent: Friese (1909: 37) catalogue [sic].

Halictus sancti-vincenti: Ashmead (1900: 304) checklist; Cockerell (1938: 280, 281) taxonomic notes.

Halictus (*Chloralictus*) *sanctivincenti*: Sandhouse (1924: 5) emendation, identification key; Cockerell (1937: 113) taxonomic notes.

Dialictus sanctivincenti: Moure and Hurd (1987: 128, 129) catalogue, possible synonymy; Moure (2007: 854) catalogue.
Lasioglossum sanctivincenti: Gibbs (2016: 6, 11) taxonomic notes.

Material examined. SVG • Grenadines • Canoun Island, 7.X.1991, leg. R.E. Woodruff (3 ♀ FSCA). Bequia Island, 1966–VI.1967, leg. Badger (1 ♀ UNSM). **Grenada •** Carricou Island, Hillsborough, the Sands Guest House, 1.III.1990, leg. R.E. Woodruff (1 ♀ FSCA) **• St. Andrew Parish •** Grand Etang, XI.1950, leg. N.L.H. Krauss (1 ♀ USNM) **• St. George Parish •** Mount Gay Est., leg. H.H. Smith (*Halictus sanctivincenti* syntype 1 ♂ USNM) • St. Georges (Leeward side), leg. H.H. Smith (2 ♀ USNM, *Halictus sanctivincenti* syntype 1 ♀ NHMUK) • St. Georges, XI.1950, leg. N.L.H. Krauss (11 ♀ USNM) **• St. John Parish •** Woodford, 5.VIII.1963, leg. O.S. Flint (1 ♀ USNM).

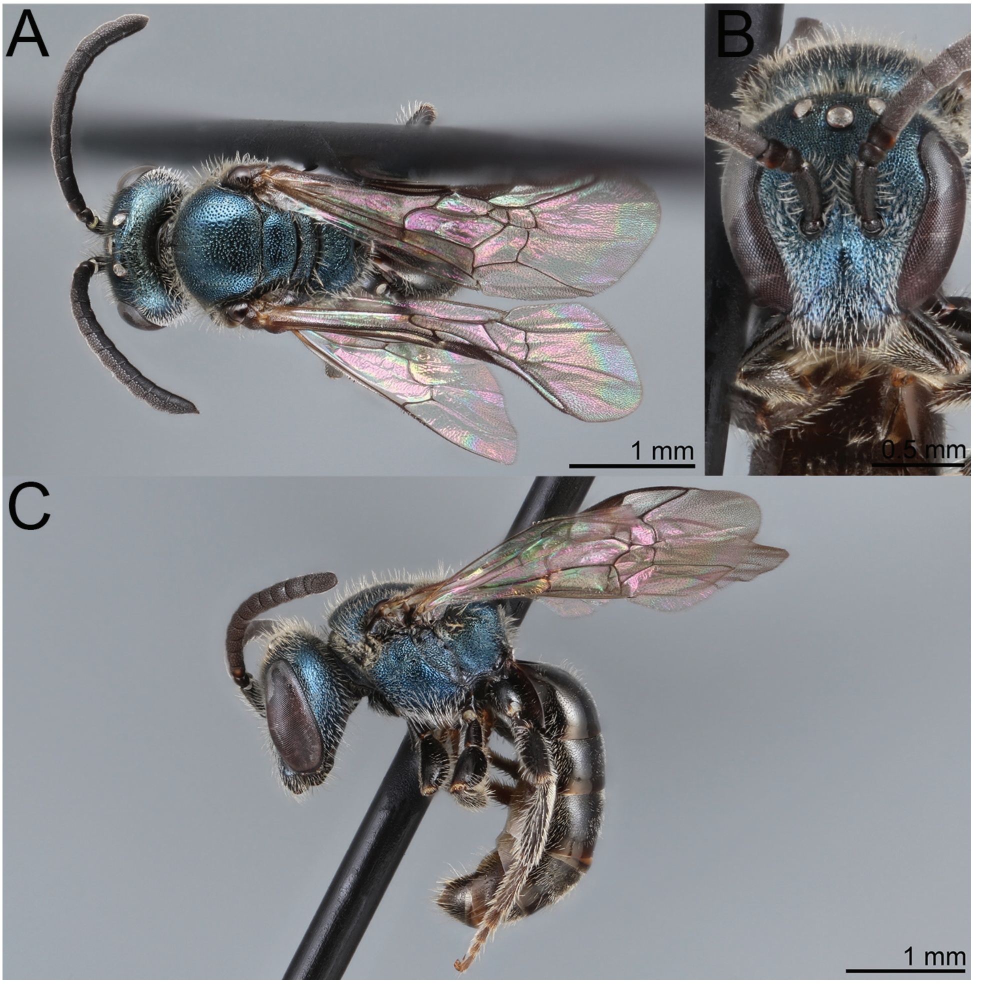

Figure 16. *Lasioglossum* (*Dialictus*) *plumbeum* (Ashmead), male **A** dorsal habitus **B** head, frontal view **C** lateral habitus.

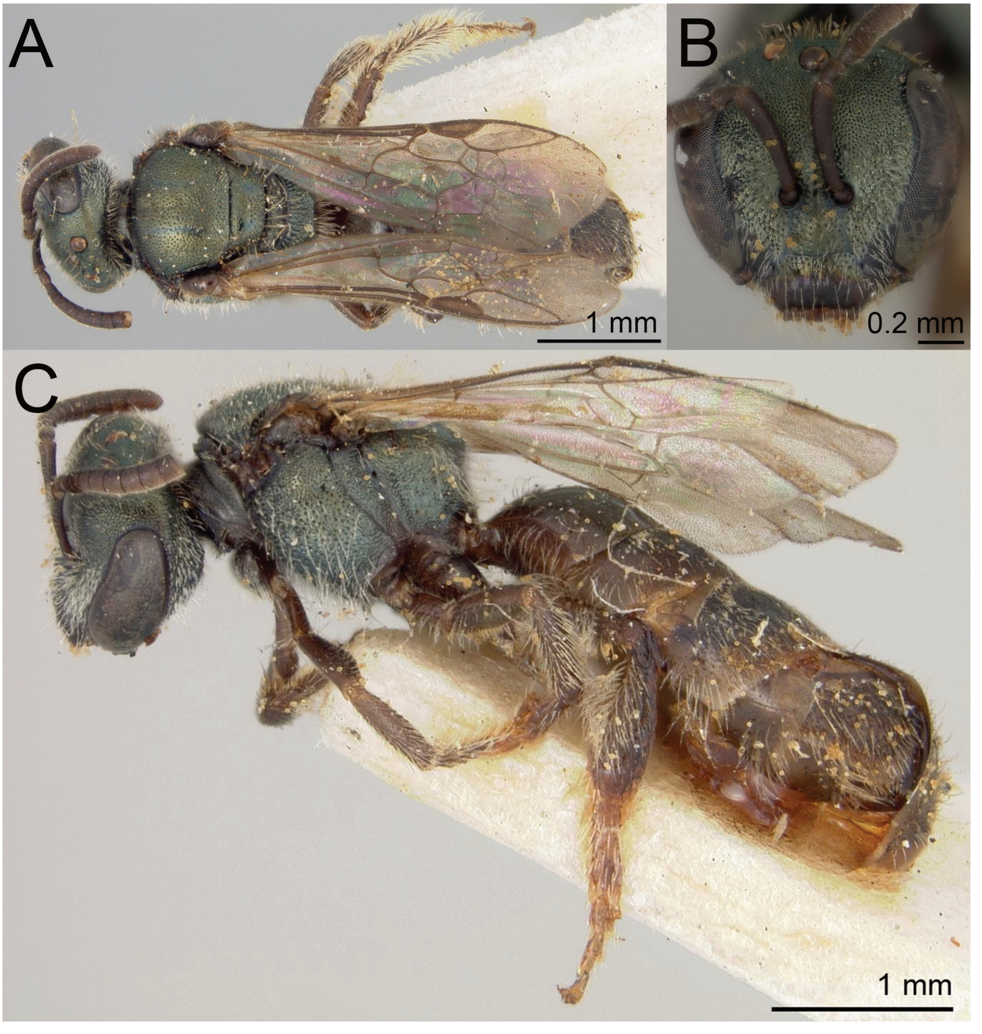

Figure 17. *Lasioglossum* (*Dialictus*) *sanctivincenti* (Ashmead), syntype female of *Halictus sanctivincenti* Ashmead **A** dorsal habitus **B** head, frontal view **C** lateral habitus. Images courtesy of the National Museum of Natural History, Smithsonian Institution. https://collections.nmnh.si.edu/search/ento/

Notes. The syntype series of *L. sanctivincenti* is divided between Grenada and St. Vincent (Ashmead 1900), which are islands separate by approximately 100 km. However, there are 22 intermediary islands in the Grenadine Island chain, so the maximum distance between landmasses is an order of magnitude less. Despite the name, *L. sanctivincenti* does not seem common on St. Vincent. In fact, all the specimens examined above belong are from islands to the south. To date, *L. sanctivincenti* and *Habralictus insularis* Smith-Pardo 2009 are the only halictid bees known from Grenada. Cockerell (1937) records *L. sanctivincenti* from Barbados, 160 km east of St. Vincent, however, his description of the darker colour and 'mesothorax highly polished' do not seem consistent with the syntype series of *L. sanctivincenti*.

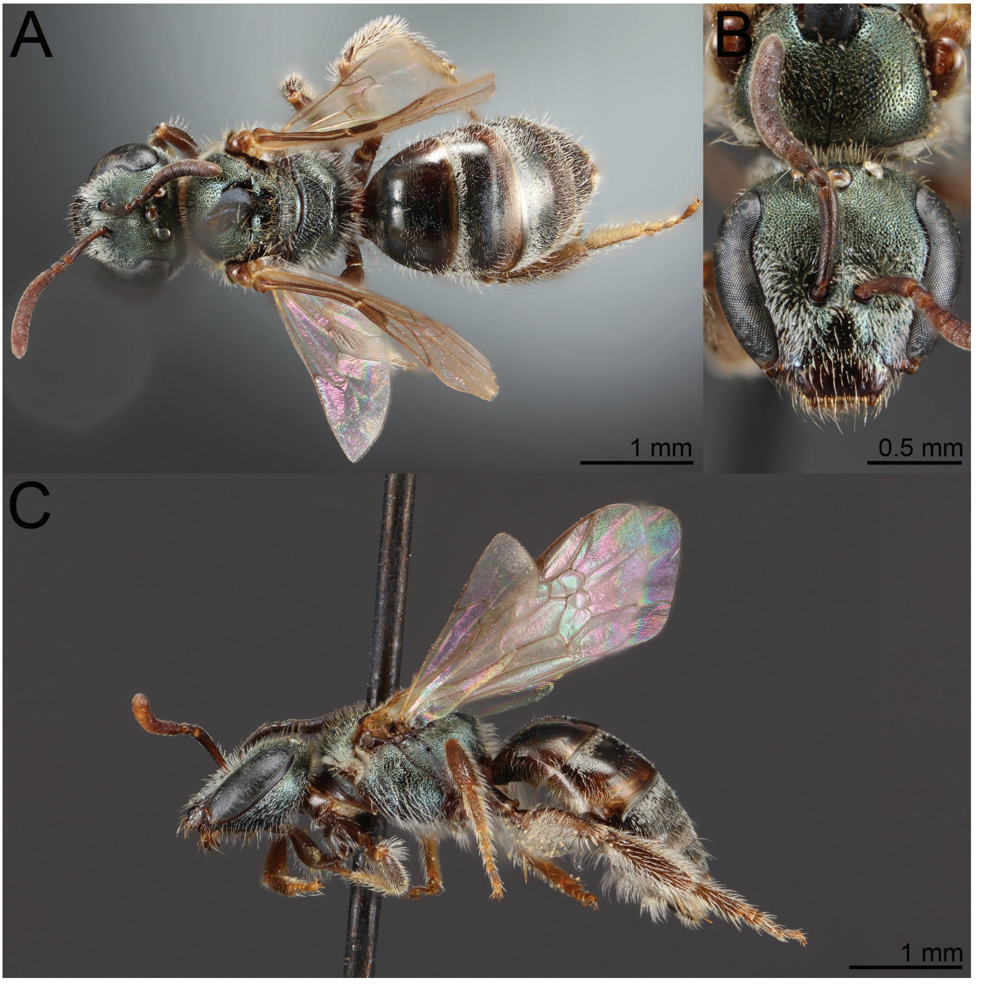

Figure 18. *Lasioglossum* (*Dialictus*) *sanctivincenti* (Ashmead), female **A** dorsal habitus **B** head, frontal view **C** lateral habitus.

***Lasioglossum* (*Dialictus*) *gemmeum* sp. nov.**
http://zoobank.org/61DF8422-3F04-4E4D-A201-4107060FE9B4
Figs 20, 21

Holotype. ♀. Saint Vincent, St. George Parish, 5–10.X.1991, leg. R.E. Woodruff, Malaise trap (FSCA).

Paratypes. SVG • Saint Vincent• St. George Parish • Rivulet Agr. Sta., 27–30-IX-1991, leg. R.E. Woodruff, Malaise trap (1 ♂); 5–10-X-1991, leg. R.E. Woodruff, Malaise trap (2 ♀ FSCA) • "24 // W. Indies / 99-331 // Dialictus not gemmatus det G.C. Eickwort" (1 ♀ NHMUK). One leg, both forewings and one hind wing missing.

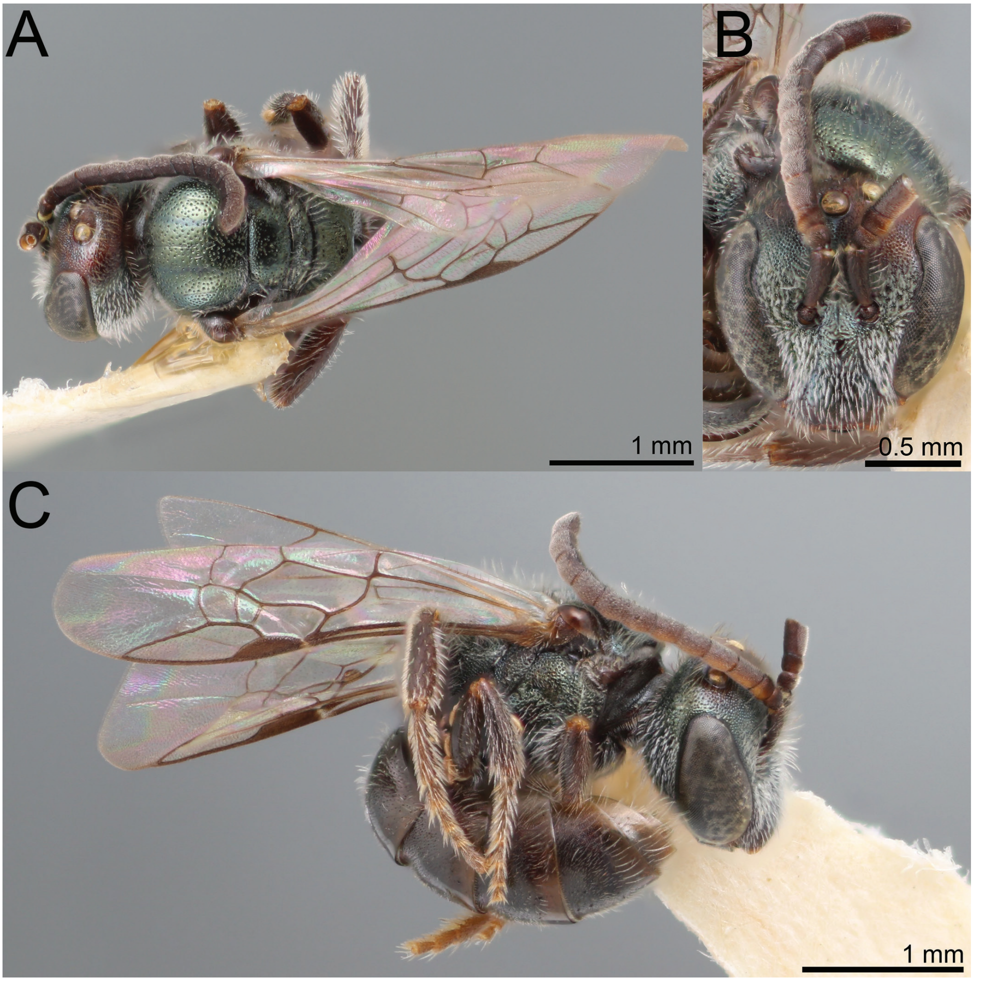

Figure 19. *Lasioglossum (Dialictus) sanctivincenti* (Ashmead), male **A** dorsal habitus **B** head, frontal view **C** lateral habitus.

"69 // W. Indies 99-331 // Halictus gemmatus Smith Ashm // Dialictus not gemmatus det G.C. Eickwort" (NHMUK). In good condition, two submarginal cells in both wings (1 ♀ NHMUK) • St Vincent, Majorea, VIII.1972 (2 ♂ SEMC).

Halictus gemmatus: Ashmead (1900: 218, 219, 303) key, distribution record (in part); Friese (1909: 37) catalogue. Non *gemmatus* Smith, 1853.

Dialictus gemmatus: Moure and Hurd (1987: 101) catalogue (in part); Moure (2007: 849) catalogue (in part). Non *gemmatus* Smith, 1853.

Diagnosis. Females of *L. gemmeum* are easily recognised by their orange-red metasoma and small size (~ 3.5 mm long). No other *L.* (*Dialictus*) in the Caribbean is known to have such a brightly coloured metasoma, although some *L.* (*Habralictellus*) do. Males can be distinguished from other SVG *L.* (*Dialictus*) by the elongate (1.5–2 MOD), pectinate setae on S5-S6. Other SVG *L.* (*Dialictus*) have short (1 MOD), simple setae on S5-S6, which contrast with plumose setae on preceding sternites.

Description. Female (*n* = 5). Length 3.3–3.6 mm; head length 1.03–1.11 mm; head width 1.08–1.19 mm; intertegular distance 0.71–0.84 mm; wing length 1.38–1.60 mm.

Colouration. Head and mesosoma dull metallic blue-green to golden-green, except as follows. Labrum reddish brown. Mandible yellow-orange with brown base and red apex. Clypeal apex dark brown. Antenna dark brown, flagellum with ventral surface reddish brown. Pronotal lobe yellow-orange. Tegula amber. Wing membrane hyaline with dark setae, venation pale brown. Legs amber-brown. Metasomal terga orange.

Pubescence. Dull white. Relatively sparse erect setae throughout, without tomentum, except on gena near eye, pronotal dorsolateral angle and lobe. Metasomal T1 with fan virtually absent, no erect setae medially. T2 without apical fimbriae, T3–T4 with only sparse fine setae on apical impressed areas. Scopa well developed on hind leg and metasomal sterna.

Surface sculpture. Face imbricate, punctation moderately fine. Clypeal punctation moderately sparse (IS = 1–s PD), denser proximally (IS = 1 PD), surface smooth distally. Supraclypeal area with punctures moderately sparse (IS = 1–2 PD), weakly imbricate in centre. Lower paraocular area punctation dense (IS ≤ PD). Upper paraocular area and frons reticulate-punctate (IS < PD). Ocellocular area punctate (IS ≤ PD). Gena and postgena punctate-imbricate, sculpturing weak on postgena. Mesoscutum weakly imbricate, polished submedially; punctation moderately coarse, dense laterad of parapsidal lines, posterior portion (IS < PD), sparsest submedially (IS = 1–2 PD), mesoscutellum similar with submedial impunctate area (IS = 1–3 PD). Metanotum finely punctate. Preëpisternum finely reticulate rugulose. Hypoepimeral area finely punctate. Mesepisternum below scrobe punctate (IS ≤ d), polished. Metepisternum dorsal 1/3 lineolate, ventral portion reticulate-imbricate. Metapostnotum medially with irregular carinulae reaching 2/3 distance to imbricate posterior margin, dorsolateral slope imbricate. Propodeum posterior and lateral surfaces weakly imbricate. Metasomal terga polished, finely coriarious basally, weakly coriarious on apical impressed margin of T3; punctation sparse (IS = 2–3 PD) on basal half, indistinct, sparser on apical impressed areas, T1-T2 apical impressed areas nearly impunctate. Metasomal sterna coriarious and finely, sparsely punctate (IS = 2–4 PD).

Structure. Face relatively short (length/width ratio = 0.82 ± 0.01 SD). Eyes weakly convergent below (UOD/LOD ratio = 1.29 ± 0.19 SD). Clypeus 2/3 below suborbital tangent, apicolateral denticles low rounded knobs. Gena narrower than eye. Hypostomal carinae subparallel. Pronotal dorsolateral angle obtuse. Pronotal ridge rounded, interrupted by sulcus. Mesoscutum length/width ratio 0.82 (± 0.02 SD); mesoscutum/mesoscutellum length ratio 2.72 (± 0.2 SD); mesoscutellum/metanotum length ratio 1.75 (± 0.06 SD); metanotum/metapostnotum length ratio 0.64 (± 0.03 SD). Tegula ovoid. Submarginal cells two or three, veins 1r-sm, 2rs-m and 2m-cu distinctly weak. Distal hamuli arranged 2-1-2. Inner metatibial spur pectinate,

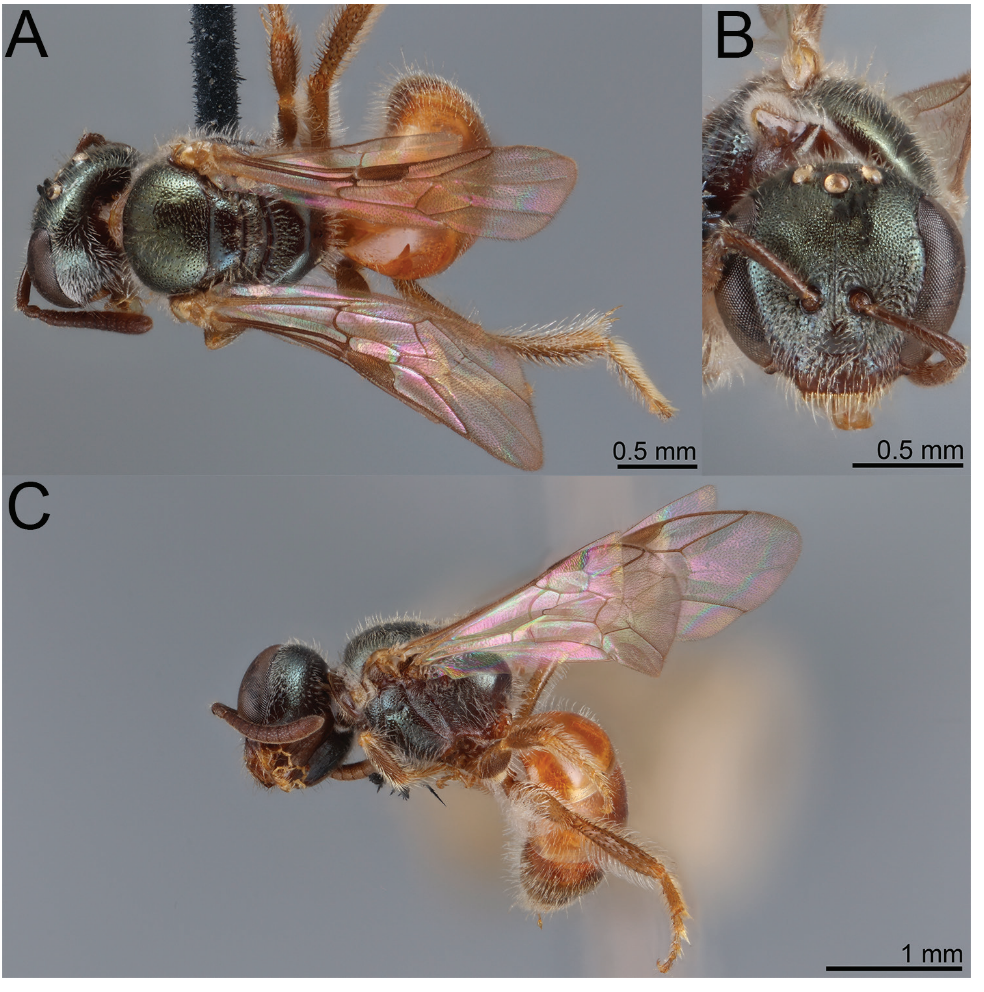

Figure 20. *Lasioglossum* (*Dialictus*) *gemmeum* sp. nov., holotype female **A** dorsal habitus **B** head, frontal view **C** lateral habitus.

with two or three branches not including apex of rachis, proximal branch much longer than width of rachis. Metapostnotum narrowly rounded onto posterior propodeal surface. Propodeum with lateral carina reaching 1/2 distance dorsal margin; oblique carina indistinct. Metasoma ovoid, T2–T4 impressed areas medially ~ 1/2 longitudinal length of basal area.

Male (*n* = 3). Length 3.3–3.5 mm; head length 1.00–1.08 mm; head width 1.00–1.11 mm; intertegular distance 0.67–0.79 mm. Similar to female with usual sex-associated modifications.

Colouration. Head and mesosoma green to golden green. Clypeal apex reddish brown. Labrum reddish brown. Mandible brown, orange apically. Flagellum reddish brown, sometimes orange ventrally. Pronotal lobe reddish brown to orange. Tegula

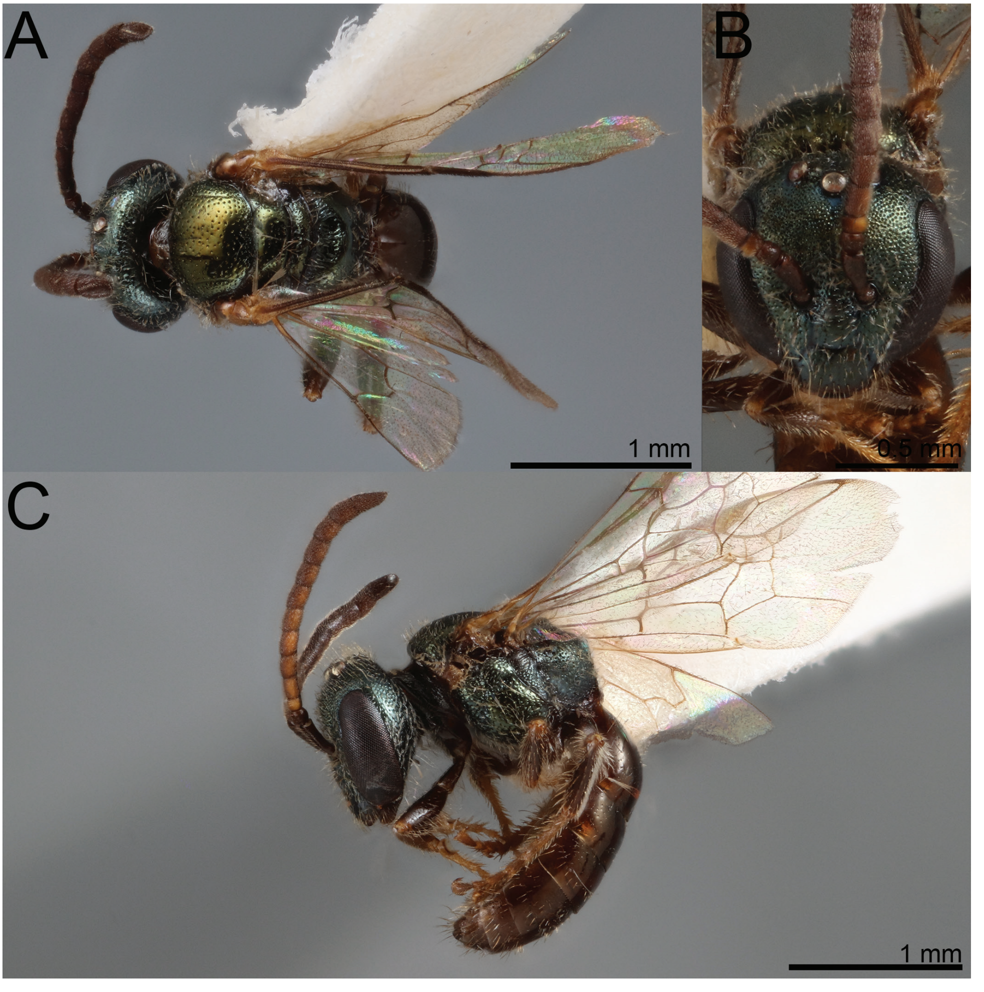

Figure 21. *Lasioglossum* (*Dialictus*) *gemmeum* sp. nov., paratype male **A** dorsal habitus **B** head, frontal view **C** lateral habitus.

orange. Wing membrane hyaline, veins brown to dark brown. Legs reddish brown with femur-tibia joints, base and apex of tibiae, and tarsi orange. Metasoma reddish brown.

Pubescence. Body sparse pilosity, dull white to faintly yellowish. Tomentum moderately dense on lower paraocular area, sparse on clypeus, dense on pronotal lobe. Mesoscutal pilosity thin. Sternal pilosity short (1.0–1.5 OD), densely plumose, dense, erect. Wing setae dark, short, sparse.

Surface sculpture. Clypeal punctures dense (IS ≤ 1 PD), interspaces polished. Supraclypeal punctures sparse (I = 1–2 PD), interspaces polished. Paraocular area punctures dense (IS ≤ 1 PD), interspaces shiny. Frons punctate-reticulate. Gena punctate-imbricate, postgena sculpture punctate-imbricate. Tegula mostly impunctate. Mesoscutal punctation sparse (IS = 1–3 PD), becoming dense marginally (IS = 1–1.5 PD), interspaces shiny. Mesoscutellar punctation sparse (IS = 1–2 PD). Metanotum punctate. Metapostnotum with incomplete carinulae, margin shiny to weakly imbricate. Pre-episternum sculpture punctate. Hypoepimeral area distinctly punctate IS ≤ 1 PD), interspaces polished. Mesepisternum distinctly punctate (IS ≤ 1 PD), interspaces shiny. Metepisternum lineate dorsally, weakly rugulose ventrally. Propodeal lateral face weakly imbricate-punctate, dorsolateral slope punctate. Propodeal posterior face sculpture polished-punctate. T1 anterior face polished. T1 dorsal surface sparse (IS = 2–6 PD), interspaces shiny. T2 disc punctures sparse (IS = 1–2.5 PD), failing well before premarginal line, interspaces shiny, apical impressed area impunctate, interspaces shiny.

Structure. Face length/width ratio 0.84 (± 0.03 SD). F1: pedicel length ratio 0.77–1.00. F2:F1 length ratio 1.76–1.89. Gena narrower than eye. Hypostomal carinae parallel. Pronotal angle obtuse. Mesoscutum length/width ratio 0.0.8 (± 0.02 SD); mesoscutum/mesoscutellum length ratio 2.51 (± 0.03 SD); mesoscutellum/metanotum length ratio 2.04 (± 0.25 SD); metanotum/metapostnotum length ratio 0.59 (± 0.07 SD). Propodeum lateral carina nearly halfway to dorsal margin; oblique carina absent. Tegula ovoid. Forewing with two or three submarginal cells. Metatibial spurs ciliate. Metasoma slender, parallel sided.

Etymology. The specific epithet is a Latin adjective in the nominal singular meaning glittering.

Taxonomic notes. Ashmead (1900) recorded three specimens of this species as *Halictus gemmatus* from the Leeward and Windward sides of St. Vincent. Comparison of two of his specimens to the type of *H. gemmatus* from Jamaica, indicated that they were quite distinct. Both specimens have labels attached from George Eickwort indicating it is not *gemmatus.* One of these is missing both forewings and the other has vein 1rs-m missing in both wings. The three other females have 1rs-m present, but the single male paratype has 1rs-m absent in the left wing and present in the right wing. *Lasioglossum gemmatum* is a member of the *gemmatum* species complex (also known as the *parvum* or *tegulare* species complex; Ellis 1914; Gibbs 2009, 2018), but *L. gemmeum* does not appear to be a member of this group.

***Lasioglossum* (*Habralictellus*) *auratum* (Ashmead 1900)**

Fig. 22

Halictus auratus Ashmead 1900: 220. Saint Vincent – windward side (1500 ft.), seven female and one male syntypes (NHMUK, USNM; Fig. 22).

Halictus auratus: Friese (1909: 37) catalogue; Cockerell (1913: 104) taxonomic notes; Crawford (1914: 133) comparative notes; Moure and Hurd (1987: 205) catalogue (unplaced taxon).

Habralictellus auratus: Moure and Hurd (1982: 46) taxonomy, genus description; Moure (2007: 858) catalogue.

Lasioglossum (*Dialictus*) *auratum*: Michener (2000: 361) genus-group synonymy.

Lasioglossum (*Habralictellus*) *auratum*: Gibbs (2016: 17, 2018: 43) taxonomic notes; Genaro (2021: 14) taxonomic notes, checklist.

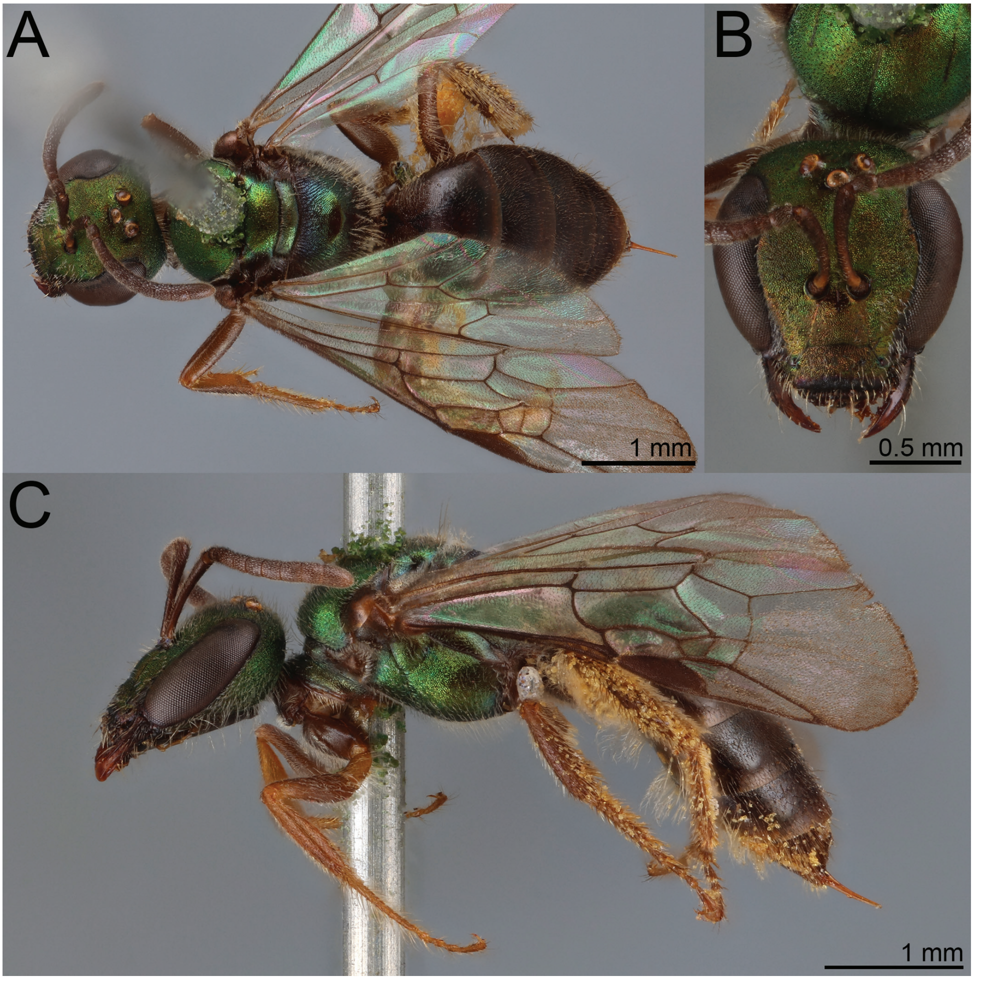

Figure 22. *Lasioglossum* (*Habralictellus*) *auratum* (Ashmead), syntype female of *Halictus auratus* Ashmead **A** dorsal habitus **B** head, frontal view **C** lateral habitus.

Material examined. SVG • Saint Vincent • Saint Vincent (windward side), 1500 ft. (*Halictus auratus* syntypes 1 ♀ NHMUK, 3 ♀ USNM).

Taxonomic notes. *Lasioglossum auratum* is the type species of *Habralictellus*, a genus group that has fluctuated between treatments as a genus (Moure and Hurd 1982; Engel 2001b), subgenus of *Lasioglossum* (Gibbs 2016, 2018; Genaro 2021), or a synonym of *L.* (*Dialictus*) (Michener 2000; Genaro 2001b, 2016). Preliminary molecular phylogenetic data suggests *L.* (*Habralictellus*) is distinct from *L.* (*Dialictus*) (Gibbs 2018). The differences in size, sculpturing, and male genitalia evident in described *L.* (*Habralictellus*) suggests that it may not be monophyletic (Gibbs 2018).

Key to *Lasioglossum* of Saint Vincent and the Grenadines

1 Head and mesosoma brilliant metallic golden-green (Fig. 22); mesoscutum granular with extremely fine and indistinct punctation; subgenus *Habralictellus* .... ***L. auratum***

– Head and mesosoma dull metallic golden-green to blue; mesoscutum imbricate to weakly polished with relatively coarse and distinct punctation; subgenus *Dialictus* **2**

2 Metasoma dark metallic blue (Figs 10–13); wings relatively dark .... ***L. cyaneum***

– Metasoma brown to orange; wings relatively pale........ **3**

3 Female **4**

– Male **6**

4 Metasoma orange-red (Fig. 20); tegula pale orange .... ***L. gemmeum***

– Metasoma brown; head longer; tegula reddish brown to dark brown **5**

5 Head and mesosoma blue (Figs 14, 15); face relatively long (length/width ratio = 0.86 SD 0.01); punctation near parapsidal line very dense (IS < 0.5 PD); mesepisternum with interspaces shiny due to weak microsculpture ......***L. plumbeum***

– Head and mesosoma golden green (Figs 17, 18); face relatively short (length/width ratio = 0.82 SD 0.02); punctation near parapsidal line sparser (IS ≤ 1 PD); mesepisternum with interspaces dull due to distinct microsculpture........ ***L. sanctivincenti***

6 Mesoscutum disc shiny, punctation sparse (Fig. 21); tegula pale orange; S5-S6 with long (1.5–2 MOD), pectinate setae .... ***L. gemmeum***

– Mesoscutum disc duller, punctation denser (Figs 16, 19); tegula reddish brown to dark brown; S5-S6 with short (1 MOD), simple setae **7**

7 Head and mesosoma blue; face relatively long (length/width ratio = 0.86) .... ***L. plumbeum***

– Head and mesosoma golden green; face relatively short (length/width ratio = 0.82)........ ***L. sanctivincenti***

***Lasioglossum* (*Dialictus*) *minutum* (Fabricius 1798)**

Fig. 23

Hylaeus minutus Fabricius 1798: 272. Americae insulus. Syntype ♂ (Natural History Museum of Denmark).

Prosopis minuta: Dalla Torre (1896: 27) catalogue; Fabricius (1804: 295) redescription.

Dialictus (*Chloralictus*) *minutus*: Moure (1960a: 101) redescription, taxonomic status, distribution; Moure (1960b: 76) redescription, taxonomic status.

Lasioglossum (*Evylaeus*) *minutum*: Ebmer (1974: 117, 122) taxonomic status, nomenclature, distribution.

Dialictus minutus: Moure and Hurd (1987: 114, 128, 129) taxonomic status, nomenclature, distribution; Moure (2007: 851) catalogue.

Taxonomic notes. The distribution and identity of *L. minutum* remains in doubt. Fabricius (1798) did not specify the number of specimens examined, but a single male type is known. Moure (1960a) examined this type of *Hylaeus minutus* Fabricius and transferred it to *Dialictus* (*Chloralictus*). The type locality is "*Americae insulus*", clarified subsequently to be "*Americae meridionalis insulus*" (Fabricius 1804). Moure (1960b) thought it was from St. Vincent. Moure and Hurd (1987) considered it a possible senior synonym of *L. sanctivincenti.* However, Ebmer (1974) suggests that the specimen may be from St. Thomas in the Virgin Islands, as the underside of

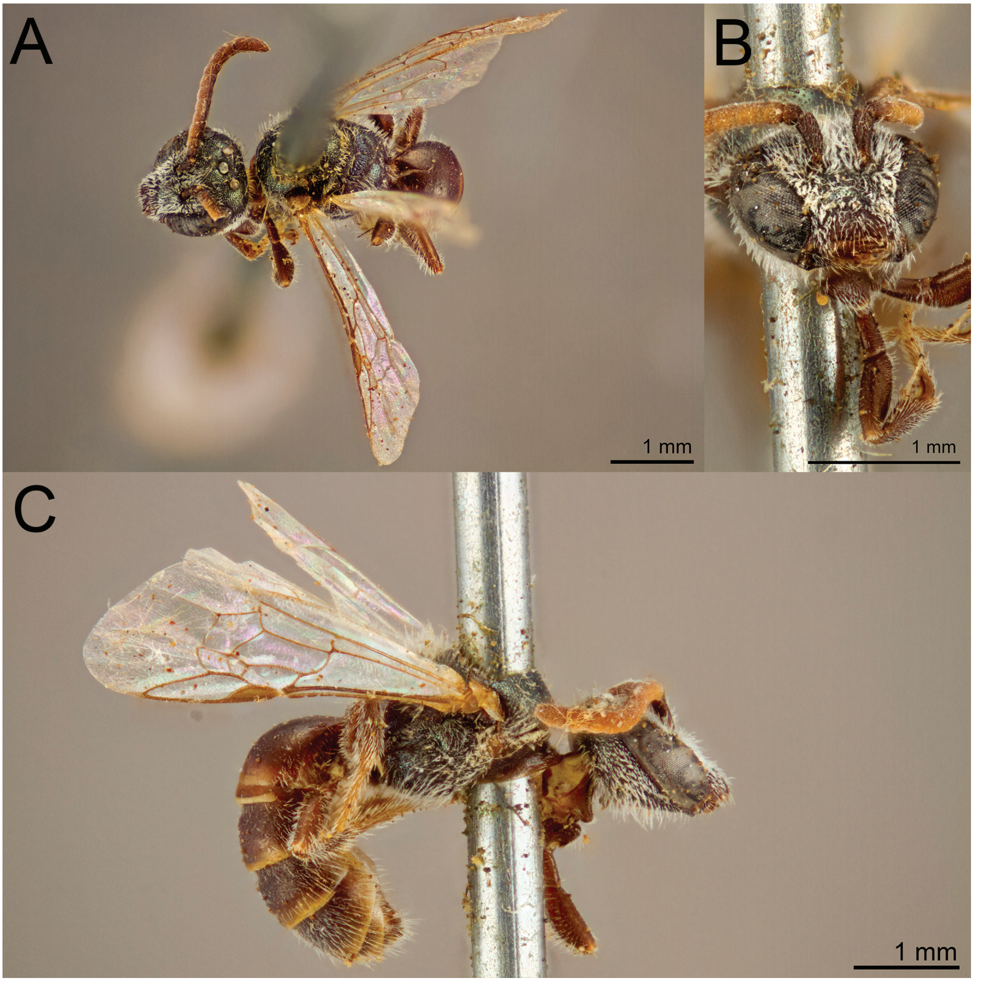

Figure 23. *Lasioglossum* (*Dialictus*) *minutum* (Fabricius), syntype male of *Hylaeus minutus* Fabricius **A** dorsal habitus **B** head, oblique frontal-ventral view **C** lateral habitus. Images courtesy of the Natural History Museum of Denmark. Photographs by Mikkel Høegh Post. http://www.daim.snm.ku.dk/search-in-types

the label read "S. Thomae". The latter locality information may not be a reliable indication of the specimen's original collection, but rather the shipping origin to Denmark (L. Vilhelmsen, *pers. comm.*). Photographs of the specimen were examined (Fig. 23), and it seems consistent with *L. sanctivincenti*. Without certainty of its island of origin or physical examination of the holotype of *L. minutum* a formal synonymy seems premature.

The nomenclature of *L. minutum* is somewhat confusing as discussed by earlier authors (Ebmer 1974). Moure and Hurd (1987) considered it preoccupied by Schrank (i.e., *Apis minuta* Schrank 1781). However, Ebmer (1974) considered Schrank's bee to be a *Hylaeus*, although Warncke (1976) disagreed. Unless Schrank's bee can be assigned to *Lasioglossum*, it cannot be considered a senior secondary homonym. Two definite cases of secondary homonymy exist, one of which has not been previously resolved. Kirby (1802: 61–62) described *Melitta minuta*, which he attributes to Schrank. However, Kirby is typically credited with authorship (Blüthgen 1921; Ebmer 1974) since he acknowledged key differences between his bee and Schrank's and doubted that they were the same. Kirby's bee is a secondary junior homonym of Fabricius's name. *Lasioglossum parvulum* (Schenck) is now the valid name for Kirby's bee. More recently, Pauly (1986) described *Homalictus minutus*, which is now transferred to *Lasioglossum* (Danforth and Ji 2001; Gibbs et al. 2012; Ascher and Pickering 2021), making it a secondary junior homonym of *L. minutum* (Fabricius). A new name is required for Pauly's species, so we propose the replacement name *Lasioglossum* (*Homalictus*) *minuens*. Some authors still maintain usage of *Homalictus* at the generic level (Campbell et al. 2007; Michener 2007; Groom et al. 2013; Niu et al. 2013; Dorey et al. 2019), which would make *L. minuens* a junior synonym of Pauly's name in that classification based on article 59.4 of the Code.

Discussion

Based on the species richness of the relatively well-studied islands of Dominica (26 spp.) to the north and Saint Vincent and the Grenadines (33 spp.) to the south (Ashmead 1900; Moure et al. 2007b; Gibbs 2016, 2020; Ascher and Pickering 2021), it can be expected that the number of bee species on Saint Lucia will eventually rise from ten to at least 25 given sufficient attention. The apid genera *Exomalopsis*, *Melissodes*, and *Xylocopa* and the megachilid genus *Coelioxys* are each known from Dominica, Martinique, and Saint Vincent and the Grenadines (Ashmead 1900; Crawford 1914; Meurgey and Dumbardon-Martial 2015; Meurgey 2016; Ascher and Pickering 2021), making their presence on St. Lucia probable. Furthermore, *Anthophora*, *Melipona*, and *Mesoplia* are known from nearby Dominica and Martinique (Meurgey and Dumbardon-Martial 2015; Meurgey 2016; Ascher and Pickering 2021). Four additional halictid genera, *Augochlora*, *Pseudaugochlora*, *Microsphecodes*, and *Sphecodes* (Ashmead 1900; Crawford 1914; Eickwort and Stage 1972; Gibbs 2016), are also known from the region, so the potential for additional halictid species on St. Lucia is high. Recent studies in the Greater and Lesser Antilles seem to suggest that halictid bee communities are largely distinct between islands (Engel 2001b, 2011; Genaro 2001b, 2021; Gibbs 2018). As such, representatives of these genera could constitute undocumented diversity. Many additional islands in the Lesser Antilles have few or no species of halictid bee known from them. Ongoing work in this area suggests that there are several additional species to describe from smaller islands in the Caribbean. Fourteen morphospecies of Halictidae were recorded from Montserrat, but none with species names (Ivie et al. 2008). In St. Kitts, the only known halictid bee is a brood parasite, but no potential hosts have been documented (Engel 2006b). Additional study of Monserrat, St. Kitts, and other islands in the Lesser and Greater Antilles is needed. This will allow future biogeographical and speciation studies of halictid bees through the Caribbean. Furthermore, baseline data are needed to assess any conservation concerns in the region. As noted previously, several species in the islands show limited distribution within islands and some have not been collected in more than a century (Gibbs 2016, 2018). Targeted surveys for these species would be prudent to determine their status.

Acknowledgements

Our sincere appreciation is given to the various collections managers and curators that have supported this research through the generous preparation of loans. Jerome Rozen (AMNH), Michael Ivie and Casey Delphia (MTEC), Michael Engel (SEMC), Laurence Packer (York University), Brian Harris and Seán Brady (USNM), and Kevin Williams (FSCA) provided specimens that were crucial to this study. David Notton (NHMUK) kindly photographed the holotype of *Trigona nigrocyanea* and provided loans of material. Mikkel Høegh Post and Lars Vilhelmsen (Natural History Museum of Denmark) provided images of the type of *Hylaeus minutus.* In particular, we thank Casey Delphia (MTEC) who alerted us to the material at MTEC and provided insightful comments on the manuscript. Michael Ivie also provided commentary on the manuscript and generously donated material to WRME. We also thank Alain Pauly and an anonymous reviewer for thoughts on an earlier draft, which improved the final paper. Our gratitude extends to Thorleif Dörfel for his editorial oversight and patience. The MTEC specimens were collected under the 2009 National Forest Demarcation and Bio-Physical Resource Inventory insect subproject, headed by Michael A. Ivie, funded by the European Union under the auspices of the Banana Industry Trust, and implemented by the Finnish Consulting Group (FCG) International Ltd in collaboration with the Saint Lucia Forestry Department. We acknowledge the support of the Natural Sciences and Engineering Research Council of Canada (NSERC), RGPIN-2018-05353. Cette recherche a été financée par le Conseil de recherches en sciences naturelles et en génie du Canada (CRSNG), RGPIN-2018-05353.

References

Alayo P (1973) Catálogo de los Himenopteros de Cuba. Editorial Pueblo y Educación, Havana, Cuba, v + 218 pp.

Alayo P (1976) Indroduccion al estudio de los Himenopteros de Cuba. Superfamilia Apoidea. Serie Biológica 68: 1–41.

Ascher JS, Pickering J (2021) Discover Life bee species guide and world checklist (Hymenoptera: Apoidea: Anthophila). Draft-55. http://www.discoverlife.org/mp/20q?guide=Apoidea_species

Ashmead WH (1900) Report upon the Aculeate Hymenoptera of the islands of St. Vincent and Grenada, with additions to the parasitic Hymenoptera and a list of the described Hymenoptera of the West Indies. Transactions of the Entomological Society of London 2: 207–367. https://doi.org/10.1111/j.1365-2311.1900.tb02379.x

Baker CF (1906) Halictinae de Cuba. In: Earle FS (Ed.), Primer Informe de la Estacion Central Agronomica. Ruiz y Hermano, Havana, Cuba, 253–274.

Blüthgen P (1823) Beiträge zur Kenntnis der Bienengattung *Halictus* Latr. Archiv für Naturgeschichte. Abteilung A 89: 232–332.

Blüthgen P (1921) Die deutschen Arten der Bienengattung *Halictus* Latr. (Hym.). Deutsche entomologische Zeitschrift 1: 267–302. https://doi.org/10.1002/mmnd.48019210103

Brullé GA (1840) Insectes. In: Barker-Webb MP, Berthelot S (Eds) Histoire Naturelle des Iles Canaries. T. 2, 2[e] partie. Béthune, Paris, France, 55–95.

Campbell JW, Hanula JL, Waldrop TA (2007) Effects of prescribed fire and fire surrogates on floral visiting insects of the blue ridge province in North Carolina. Biological Conservation 134: 393–404. https://doi.org/10.1016/j.biocon.2006.08.029

Cockerell TDA (1904) New records of bees. The Entomologist 37: 231–236. https://doi.org/10.5962/bhl.part.2883

Cockerell TDA (1910) Some bees of the genus *Augochlora* from the West Indies. Proceedings of the United States National Museum 37: 489–497. https://doi.org/10.5479/si.00963801.37-1717.489

Cockerell TDA (1913) Descriptions and records of bees.–LIII. Annals and Magazine of Natural History 12(8): 103–110. https://doi.org/10.1080/00222931308693377

Cockerell TDA (1915) Descriptions and records of bees.–LXVIII. The Annals and Magazine of Natural History 16(8): 1–9. https://doi.org/10.1080/00222931508693679

Cockerell TDA (1922) Descriptions and records of bees.–XCV. The Annals and Magazine of Natural History 10(9): 265–269. https://doi.org/10.1080/00222932208632777

Cockerell TDA (1937) The bees of Barbados. The Entomologist 70: 111–113. https://doi.org/10.4039/Ent69113-5

Cockerell TDA (1938) Bees from St. Vincent, British West Indies. The Entomologist 71: 280–283.

Crawford JC (1914) Hymenoptera, superfamilies Apoidea and Chalcidoidea, of the Yale Dominican expedition of 1913. Proceedings of the United States National Museum 47: 131–134. https://doi.org/10.5479/si.00963801.47-2048.131

Danforth BN, Ji S (2001) Australian *Lasioglossum* + *Homalictus* form a monophyletic group: resolving the "Australian enigma." Systematic Biology 50: 268–283. https://doi.org/10.1080/713849618

Dorey JB, Schwarz MP, Stevens MI (2019) Review of the bee genus *Homalictus* Cockerell (Hymenoptera: Halictidae) from Fiji with description of nine new species. Zootaxa 4674: 001–046. https://doi.org/10.11646/zootaxa.4674.1.1

Ducke A (1902) Ein neues Subgenus von *Halictus* Latr. Zeitschrift für Systematische Hymenopterologie und Dipterologie 2: 102–103.

Ebmer AW (1974) Von Linné bis Fabricius beschriebene westpaläarktische Arten der Genera *Halictus* und *Lasioglossum*. Nachrichtenblatt der Bayerischen Entomologen 23: 111–127.

Eickwort GC (1988) Distribution patterns and biology of West Indian sweat bees (Hymenoptera: Halictidae). In: Liebherr JK (Ed.) Zoogeography of Caribbean Insects. Cornell University Press, Ithaca, New York, 232–253.

Eickwort GC, Stage GI (1972) A new subgenus of Neotropical *Sphecodes* cleptoparasitic upon *Dialictus* (Hymenoptera: Halictidae, Halictinae). Journal of the Kansas Entomological Society 45: 500–515.

Ellis MD (1914) New American bees of the genus *Halictus* (Hym.). Entomological News 25: 151–155.

Engel MS (2001a) A monograph of the Baltic amber bees and evolution of the Apoidea (Hymenoptera). Bulletin of the American Museum of Natural History 259: 1–192. https://doi.org/10.1206/0003-0090(2001)259<0001:AMOTBA>2.0.CO;2

Engel MS (2001b) Three new *Habralictellus* bee species from the Caribbean (Hymenoptera: Halictidae). Solenodon 1: 33–37.

Engel MS (2006a) The *Sphecodes* of Cuba (Hymenoptera: Halictidae). Acta Zoologica Cracoviensia 49B: 73–78. https://doi.org/10.3409/000000006783995355

Engel MS (2006b) A new species of *Microsphecodes* from St. Kitts (West Indies) (Hymenoptera: Halictidae). Mitteilungen des Internationalen Entomologischen Vereins 31: 51–54.

Engel MS (2011) A new species of *Dialictus* from Sombrero Island, Anguilla (Hymenoptera, Halictidae). ZooKeys 86: 61–68. https://doi.org/10.3897/zookeys.86.909

Engel MS, Prado SG (2014) First record of the cleptoparasitic bee genus *Sphecodes* from Puerto Rico (Hymenoptera: Halictidae). Journal of Melittology 39: 1–6. https://doi.org/10.17161/jom.v0i39.4781

Erichson WF (1835) Beschreibung von 19 neuen Hymenopteren aus Andalusien. In: Waltl J (Ed.) Reise durch Tyrol, Oberitalien und Piemont nach dem südlichen Spanien, nebst einem Anhange zoologischen Inhalts (Über die Thiere Andalusiens). Verlag der Pustet´schen Buchhandlung (J.F. Winkler), Passau, 101–109.

Friese H (1909) Beitrag zur Bienenfauna der Kleinen Antillen und der Bermudas. Zoologische Jahrbücher supplement: 33–40.

Genaro JA (2001a) Especies nuevas de abejas de Cuba y La Española (Hymenoptera: Colletidae, Megachilidae, Apidae). Revista de Biología Tropical 49: 1027–1035.

Genaro JA (2001b) Tres especies nuevas del genero *Lasioglossum* (*Dialictus*), grupo *Habralictellus* para Cuba (Hymenoptera: Halictidae). Solenodon 1: 38–44.

Genaro JA (2006) A history of systematic studies of the bees of Cuba (Insecta: Hymenoptera, Anthophila). Zootaxa 60: 39–60.

Genaro JA (2007) Las abejas (Hymenoptera: Apoidea: Anthophila) de la Hispaniola, Antillas. Boletín Sociedad Entomológica Aragonesa 40: 247–254.

Genaro JA (2008) Origins, composition and distribution of the bees of Cuba (Hymenoptera: Apoidea: Anthophila). Insecta Mundi 52: 1–16.

Genaro JA (2016) Especies nuevas y nuevos registros de abejas para las Antillas (Hymenoptera: Anthophila; Colletidae, Halictidae). Novitates Caribaea 10: 38–51. https://doi.org/10.33800/nc.v0i10.28

Genaro JA (2021) Especies nuevas de *Lasioglossum* Curtis de las altas montañas de las Antillas Mayores y estado actual del conocimiento del taxon *Habralictellus* Moure y Hurd (Hymenoptera: Apoidea: Halictidae). Insecta Mundi 0853: 1–17.

Genaro JA, Franz NM (2008) The bees of greater Puerto Rico (Hymenoptera: Apoidea: Anthophila). Insecta Mundi 0040: 1–27.

Gibbs J (2009) Integrative taxonomy identifies new (and old) species in the *Lasioglossum* (*Dialictus*) *tegulare* (Robertson) species group (Hymenoptera, Halictidae). Zootaxa 2032: 1–38. https://doi.org/10.11646/zootaxa.2032.1.1

Gibbs J (2010a) Revision of the metallic species of *Lasioglossum* (*Dialictus*) in Canada (Hymenoptera, Halictidae, Halictini). Zootaxa 3073: 1–382. https://doi.org/10.11646/zootaxa.3073.1.1

Gibbs J (2010b) Atypical wing venation in *Dialictus* and *Hemihalictus* and its implications for subgeneric classification of *Lasioglossum*. Psyche 2010: 1–6. https://doi.org/10.1155/2010/605390

Gibbs J (2012) A new species of *Habralictus* Moure from Dominica, Lesser Antilles (Hymenoptera, Halictidae). ZooKeys 168: 1–12. https://doi.org/10.3897/zookeys.168.2524

Gibbs J (2016) Bees of the family Halictidae Thomson, 1869 from Dominica, Lesser Antilles (Hymenoptera: Apoidea). European Journal of Taxonomy 180: 1–50. https://doi.org/10.5852/ejt.2016.180

Gibbs J (2018) Bees of the genus *Lasioglossum* (Hymenoptera: Halictidae) from Greater Puerto Rico, West Indies. European Journal of Taxonomy 400: 1–57. https://doi.org/10.5852/ejt.2018.400

Gibbs J (2020) *Hylaeus* (*Hylaeana*) *dominicalis*, a new species and the first colletid bee recorded from Dominica, Lesser Antilles. Journal of Melittology, 1–6. https://doi.org/10.17161/jom.vi93.12054

Gibbs J, Brady SG, Kanda K, Danforth BN (2012) Phylogeny of halictine bees supports a shared origin of eusociality for *Halictus* and *Lasioglossum* (Apoidea: Anthophila: Halictidae). Molecular Phylogenetics and Evolution 65: 926–939. https://doi.org/10.1016/j.ympev.2012.08.013

Groom SVC, Stevens MI, Schwarz MP (2013) Diversification of Fijian halictine bees: Insights into a recent island radiation. Molecular Phylogenetics and Evolution 68: 582–594. https://doi.org/10.1016/j.ympev.2013.04.015

Harris RA (1979) A glossary of surface sculpturing. Occasional Papers in Entomology 28: 1–31.

Ivie MA, Markse KA, Foley IA, Guerrero KA, Ivie LL (2008) Species lists of the beetles, non-beetle hexapods and non-hexapod invertebrates of Montserrat. In: Young RP (Ed.) A biodiversity assessment of the Centre Hills, Monserrat. Durrell Wildlife Conservation Trust, Trinity, Channel Islands, 237–311.

Kirby W (1802) Monographia Apum Angliae. Privately published, Ipswich, 384 pp. [18 pls]

Lutz FE, Cockerell TDA (1920) Notes on the distribution and bibliography of North American bees of the families Apidae, Meliponidae, Bombidae, Euglossidae, and Anthophoridae. Bulletin of the American Museum of Natural History 42: 491–641. https://doi.org/10.5962/bhl.title.17909

Meurgey F (2014) Liste préliminaire des abeilles de Guadeloupe (Petites Antilles) et leurs relations avec la flore butinée (Hymenoptera: Apoidea, Megachilidae et Apidae). Annales de la Société entomologique de France (N.S.) 50: 89–110. https://doi.org/10.1080/00379271.2014.934039

Meurgey F (2016) Bee species and their associated flowers in the French West Indies (Guadeloupe, Les Saintes, La Désirade, Marie Galante, St Barthelemy and Martinique) (Hymenoptera: Anthophila: Apoidea). Annales de la Société entomologique de France (N.S.) 52: 209–232. https://doi.org/10.1080/00379271.2016.1244490

Meurgey F, Dumbardon-Martial E (2015) Les Abeilles de Martinique (Antilles françaises) et leurs relations avec la flore butinée (Hymenoptera: Apoidea: Megachilidae, Apidae). Annales de la Société entomologique de France (N.S.) 51: 346–360. https://doi.org/10.1080/00379271.2015.1131623

Michener CD (1979) New and little-known halictine bees from Colombia (Hymenoptera: Halictidae). Journal of the Kansas Entomological Society 52: 180–208.

Michener CD (1990) Reproduction and castes in social halictine bees. In: Engels W (Ed.) Social Insects: An Evolutionary Approach to Castes and Reproduction. Springer, New York, 77–121. https://doi.org/10.1007/978-3-642-74490-7_6

Michener CD (2000) The bees of the world. The Johns Hopkins University Press, Baltimore, 913 pp.

Michener CD (2007) The bees of the world. 2nd edn. The Johns Hopkins University Press, Baltimore, xvi + [i]+953 pp.

Mitchell TB (1960) Bees of the Eastern United States: volume I. N. C. Agricultural Experimental Station Technical Bulletin 141: 1–538.

Moure JS (1947) Novos agrupamentos genéricos e algumas espécies novas de abelhas sulamericanas. Museu Paranaense Publicações Avulsas 3: 1–37.

Moure JS (2001) Uma pequena abelha com cabeça e mandíbulas excepcionais (Hymenoptera, Halictidae). Revista Brasileira de Zoologia 18: 493–497. https://doi.org/10.1590/S0101-81752001000200020

Moure JS (2007) Halictini Thomson, 1869. In: Moure JS, Urban D, Melo GAR (Eds) Catalogue of bees (Hymenoptera, Apoidea) in the Neotropical region. Sociedade Brasileira de Entomologia, Curitiba, 823–870.

Moure JS, Hurd PD (1982) On two new groups of Neotropical halictine bees (Hymenoptera, Apoidea). Dusenia 23: e46.

Moure JS, Hurd PD (1987) An annotated catalog of the halictid bees of the Western Hemisphere (Hymenoptera: Halictidae). Smithsonian Institution Press, Washington DC, 405 pp.

Moure JS, Melo GAR, Vivallo F (2007a) Centridini Cockerell & Cockerell, 1901. In: Catalogue of bees (Hymenoptera, Apoidea) in the Neotropical region. Sociedade Brasileira de Entomologia, Curitiba, 83–142.

Moure JS, Urban D, Melo GAR (2007b) Catalogue of bees (Hymenoptera, Apoidea) in the Neotropical Region. Sociedade Brasileira de Entomologia, Curitiba, [xiv +] 1058 pp.

Niu Z-Q, Oremek P, Zhu C-D (2013) First record of the bee genus *Homalictus* Cockerell for China with description of a new species (Hymenoptera: Halictidae: Halictini). Zootaxa 3746: e393. https://doi.org/10.11646/zootaxa.3746.2.9

Pauly A (1984) Classification des Halictidae de Madagascar et des îles voisines I. Halictinae (Hymenoptera Apoidea). Verhandlungen der Naturforschenden Gesellschaft in Basel 94: 121–156.

Pauly A (1986) Les abeilles de la sous-famille des Halictinae en Nouvelle-Guinée et dans L'archipel Bismarck (Hymenoptera: Apoidea: Halictidae). Zoologische Verhandlingen 227: 1–58.

Pesenko YA (2007) Subgeneric classification of the Palaearctic bees of the genus *Evylaeus* Robertson (Hymenoptera: Halictidae). Zootaxa 1500: 1–54. https://doi.org/10.11646/zootaxa.1500.1.1

Raw A (2007) An annotated catalogue of the leafcutter and mason bees (genus *Megachile)* of the Neotropics. Zootaxa 1601: 1–127. https://doi.org/10.11646/zootaxa.1601.1.1

Robertson C (1890) New North American bees of the genera *Halictus* and *Prosopis*. Transactions of the American Entomological Society 17: 315–318.

Robertson C (1892) Description of new North American bees. American Naturalist 26: 267–274. https://doi.org/10.1086/275508

Robertson C (1901) Some new and little-known bees. The Canadian Entomologist 33: 229–231. https://doi.org/10.4039/Ent33229-8

Robertson C (1902a) Some new or little-known bees—II. The Canadian Entomologist 34: 48–49. https://doi.org/10.4039/Ent3448-2

Robertson C (1902b) Synopsis of Halictinae. The Canadian Entomologist 34: 243–250. https://doi.org/10.4039/Ent34243-9

Sandhouse GA (1923) The bee-genus *Dialictus*. The Canadian Entomologist 55: 193–195. https://doi.org/10.4039/Ent55193-8

Sandhouse GA (1924) New North American species belonging to the genus *Halictus* (*Chloralictus*). Proceedings of the United States National Museum 65: 1–43. https://doi.org/10.5479/si.00963801.2532

Scarpulla EJ (2018) Four submarginal cells on a forewing of *Melitoma taurea* (Say) (Hymenoptera: Apidae), and a summary of known records of atypical and variable numbers of submarginal cells. Insecta Mundi 0667: 1–28.

Schrottky C (1911) Descripção de abelhas novas do Brazil e de Regiões visinhas. Revista do Museo Paulista 8: 71–88.

Smith-Pardo AH (2009) A new species of *Habralictus* (Hymenoptera, Halictidae) from the Island of Grenada (Lesser Antilles) with comments on the insular species of the genus. ZooKeys 27: 51–58. https://doi.org/10.3897/zookeys.27.265

Vachal J (1909) Collections recueillies par M. le Baron Maurice de Rothschild dans l'Afrique orientale. Insectes hyménoptères: Mellifères. Bulletin du Muséum d'Histoire Naturelle (Paris) 15: 529–534.

Warncke K (1975) Beiträge zur systematik und Verbreitung der Furchenbienen in der Türkei (Hymenoptera, Apoidea, Halictus). Polskie Pismo Entomologiczne 45: 81–123.

ZooKeys 1089: 169–180 (2022)
doi: 10.3897/zookeys.1089.72485
https://zookeys.pensoft.net

RESEARCH ARTICLE

A peer-reviewed open-access journal
ZooKeys
Launched to accelerate biodiversity research

A new species of *Suwallia* Ricker, 1943 (Plecoptera, Chloroperlidae) from southwestern China, with an updated key to male *Suwallia* species

Abdur Rehman[1], Qing-Bo Huo[1], Yu-Zhou Du[1,2]

1 *School of Horticulture and Plant Protection & Institute of Applied Entomology, Yangzhou University, Yangzhou 225009, China* **2** *Joint International Research Laboratory of Agriculture and Agri-Product Safety, the Ministry of Education, Yangzhou University, Yangzhou 225009, China*

Corresponding author: Yu-Zhou Du (yzdu@yzu.edu.cn)

Academic editor: Sven Bradler | Received 2 August 2021 | Accepted 12 February 2022 | Published 18 March 2022

http://zoobank.org/95B980B1-7650-4823-8AEA-0E376B4A81D5

Citation: Rehman A, Huo Q-B, Du Y-Z (2022) A new species of *Suwallia* Ricker, 1943 (Plecoptera, Chloroperlidae) from southwestern China, with an updated key to male *Suwallia* species. ZooKeys 1089: 169–180. https://doi.org/10.3897/zookeys.1089.72485

Abstract
A new species of the genus *Suwallia* Ricker, 1943 (Plecoptera, Chloroperlidae), *Suwallia dengba* **sp. nov.**, is described from Tibet and Yunnan, southwestern China. A diagnosis and description of the adult habitus and aedeagal structure are illustrated with color images. Similarities in the terminalia with closely related species are discussed. In addition, an updated key to adult males of the *Suwallia* species of China is provided.

Keywords
Distribution, *Suwallia dengba* sp. nov., Tibet, Yunnan Province

Introduction

The family Chloroperlidae belongs to the superfamily Perloidea and is frequently referred to as "green stoneflies". It consists of two subfamilies: Chloroperlinae Okamoto, 1912 and Paraperlinae Ricker, 1943. Presently, more than 29 species of the family Chloroperlidae are reported from China, belonging to six genera, namely: *Alloperla* Banks, 1906, *Alaskaperla* Stewart & DeWalt, 1991, *Haploperla* Navás, 1934, *Suwallia* Ricker, 1943, *Sweltsa* Ricker, 1943 and *Utaperla* Ricker, 1952 (Wu 1938; Nelson and Hanson 1968; Du 1999;

Li and Wang 2011; Li et al. 2013, 2014, 2015a, b; Chen and Du 2015, 2016a, b, 2017; Dong et al. 2018; Yang and Li 2018; Chen 2019; Mo et al. 2020; Shi et al. 2022).

The genus *Suwallia* Ricker, 1943 belongs to tribe Suwalliini Surdick, 1985 of the subfamily Chloroperlinae. It is distributed in the East Palearctic and Nearctic regions (DeWalt et al. 2021). Most species of the genus *Suwallia* were revised and recorded by Alexander and Stewart (1999). *Suwallia* is mainly distributed in Russia, Mongolia, Japan, and North America (Alexander and Stewart 1999; Teslenko and Zhiltzova 2009; Judson and Nelson 2012). In China, the first species of *Suwallia* was reported by Li et al. (2015a), and until now seven species of this genus had been reported for the country: *Suwallia errata* Li & Li, 2021, *Suwallia decolorata* Zhiltzova & Levanidova, 1978, and *Suwallia talalajensis* Zhiltzova, 1976 were reported by Li et al. (2015a, b) and Li et al. (2021) from the Inner Mongolia Autonomous Region, northern China (Fig. 7), whereas *Suwallia wolongshana* Du & Chen, 2015 and *Suwallia jihuae* Chen, 2019 were reported by Chen and Du (2015) and Chen (2019) from the Sichuan Province of southwestern China. Recently, *Suwallia kuandian* Shi, Wang & Li, 2022 and *Suwallia asiatica* Zhiltzova & Levanidova, 1978 were reported by Shi et al. (2022) from Liaoning Province, northeastern China. In the current paper, a new species of *Suwallia* is described from Tibet and the Yunnan Province of southwestern China. This is the first record of the *Suwallia* genus from both regions. Tibet is also known as Xizang in Chinese and is positioned on the Tibetan plateau, known as the world's highest and largest plateau. The Yunnan Province lies adjacent to the Tibet, Sichuan, Guizhou, and Guangxi provinces of China and borders with Myanmar, Laos, and Vietnam. The taxonomy of the new species is discussed, a distributional map, and a key to the known species of *Suwallia* from China are provided.

Materials and methods

All specimens were collected by aerial net or hands and preserved in 75% ethanol. Terminalia were examined and illustrated by KEYENCE VHX-5000 and the final images were prepared using Adobe Photoshop CS6. The type specimens of the new species were placed in the insect collection of Yangzhou University **(ICYZU)**, Jiangsu Province, China. Data for the key and distribution map were extracted from the published literature (Chen and Du 2015; Li et al. 2015a, b; Chen 2019; Shi et al. 2022).

Results

Suwallia dengba **sp. nov.**
http://zoobank.org/51F6012D-7AB2-4F16-9095-2B1B9E7CE5BE
Figs 1–8

Type material. ***Holotype***, 1♂, China, Tibet Autonomous Region, Dengba village, Mangkam County, Qamdo city, 3437 m, 29°32.406'N, 98°13.425'E, 18.IX.2019, Leg. Huo Qing-Bo (ICYZU). ***Paratypes***, 6♂♂, 6♀♀, data same as holotype (Figs 7, 8);

5♂♂, 17♀♀, Yunnan Province, Diqing Tibetan Autonomous Prefecture, Shangri-la city, on the way from Diqing to Gezan Township, 3445 m, 27°45.656'N, 99°56.374'E, 7.IX.2019. Leg. Huo Qing-Bo (ICYZU); 2♂♂, 4♀♀, China, Yunnan Province, Diqing Tibetan Autonomous Prefecture, on national highway (G214) near Tongduishui and Deiyong Benglao, 3432 m, 28°18.282'N, 99°8.472'E, 9.IX.2019, Leg. Huo Qing-Bo (ICYZU); 1♂, 2♀, China, Yunnan Province, Diqing Tibetan Autonomous Prefecture, on national highway (G214) near Zhubagong, Deqin County (Fig. 7), 4027 m, 28°23.885'N, 98°59.143'E, 10.IX.2019, Leg. Huo Qing-Bo (ICYZU).

Diagnosis. The new species is characterized by the sclerotized median sclerite of tergum X and its aedeagus armature. The shape of the median sclerite of tergum X resembles a turtle or a hexagonal star. The aedeagus, with a large distinct sclerite divided into an eagle-shaped trifurcate structure, the large median sclerite, and one pair of wing-shaped lateral sclerites on both sides, is diagnostic (Figs 2–4).

Description. ***Adult habitus*** (Fig. 1A). Adult body length 8.5–9.5 mm (N = 10), forewing length 6.5–7.5 mm, hindwing length 5.5–6.5 mm. General color of body pale yellow in alcohol. Triocellate, head yellowish-white to yellowish-brown. Ocellar

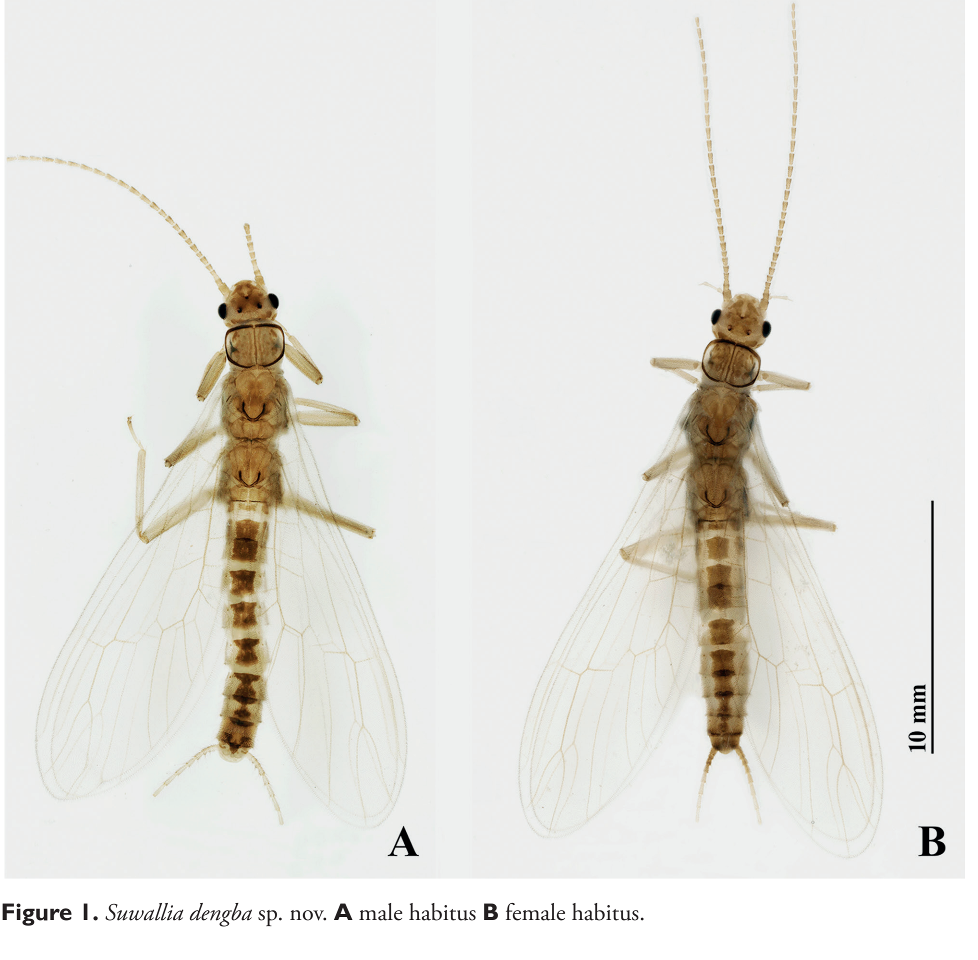

Figure 1. *Suwallia dengba* sp. nov. **A** male habitus **B** female habitus.

triangle and frontoclypeal area pale yellowish-brown, antenna pale brown, covered with small brown to dark brown setae. Pronotum disc margins covered with dark brown bands and with a thin dark medial stripe (Fig. 2A). Legs pale brown, mesonotum and metanotum with a distinct dark brown U-shaped marking, wings hyaline with yellow venation. Abdominal terga I–VIII with a wide medial trapezoidal dark brown stripe, slightly constricted medially on terga VII and VIII (Figs 1A, 2C–D).

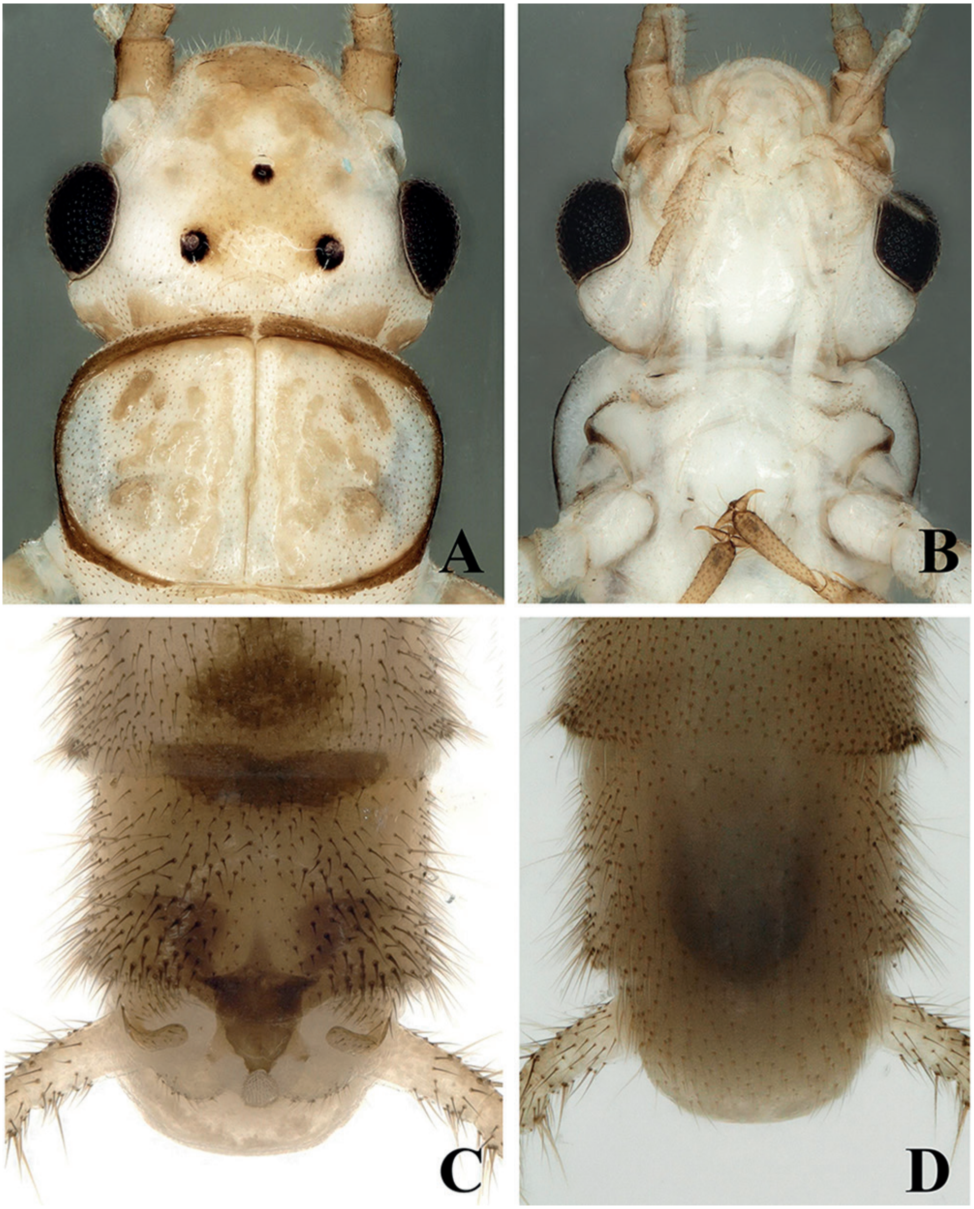

Figure 2. *Suwallia dengba* sp. nov. Holotype male **A** head and prothorax, dorsal view **B** head and prothorax, ventral view **C** terminalia, dorsal view **D** terminalia, ventral view.

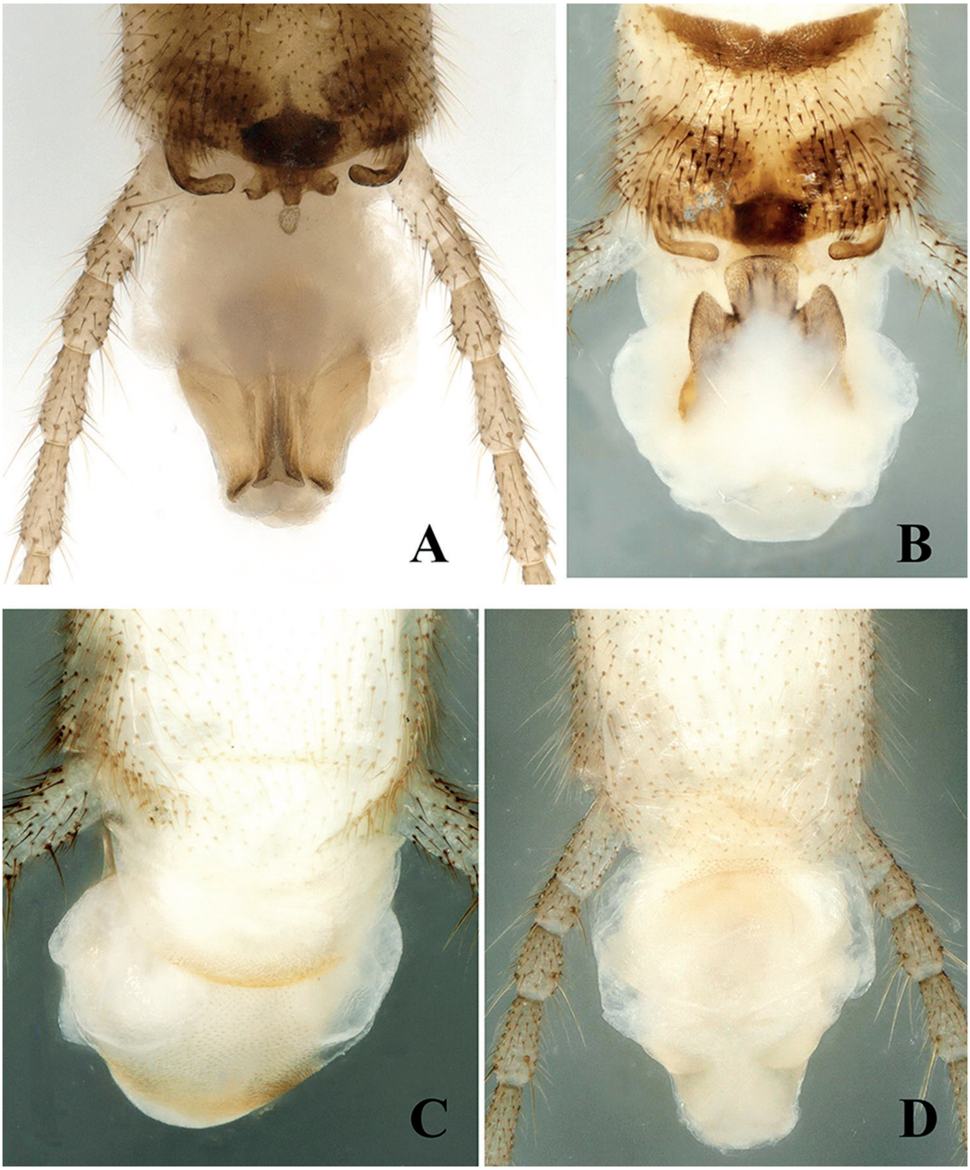

Figure 3. *Suwallia dengba* sp. nov. Male paratype. **A** terminalia with aedeagus, dorsal view **B** aedeagus everted, dorsal view **C** aedeagus, caudal ventral view **D** aedeagus, ventral view.

Male (Figs 2–4). Tergum IX concave medially with semicircular stripe anteriorly, posteriorly covered with dark brown, thick hairs. Tergum X divided, median portion with a distinct dark brown sclerite resembling a turtle or hexagonal star in dorsal view (Figs 2C, 6A). Hemitergal processes sclerotized, with tiny hairs, finger-shaped and curved forward. Epiproct membranous, circular, knob-like, covered with minute hairs. Sternum IX ventrally extended anteriorly (Fig. 2D). Aedeagus membranous with a distinct sclerotized sclerite after eversion. Aedeagal sclerite resembling an eagle, divided into a trifurcate structure, a large median sclerite, and one pair of lateral sclerites

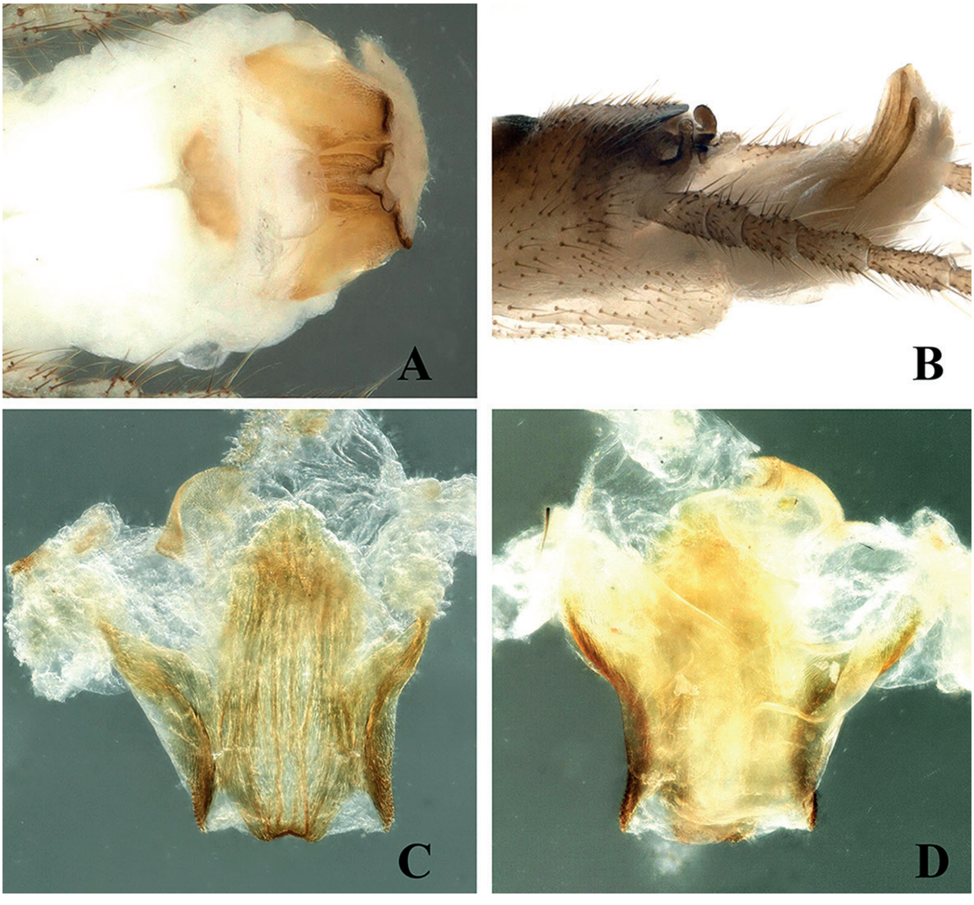

Figure 4. *Suwallia dengba* sp. nov. **A** aedeagus **B** terminalia, lateral view **C** aedeagal sclerite, dorsal view **D** aedeagal sclerite, ventral view.

(Figs 3A, 4A–D, 6B). Lateral sclerites armed with minute scales. Membranous part of aedeagus with fine cuticular asperities (Fig. 3A–D).

Female. ***Adult habitus*** (Fig. 1B). Body length 9.0–10 mm (N = 10), forewing length 7.5–8.5 mm, hindwing length 6.5–7.5 mm. General body color, shape and appearance similar to those of male. Head and pronotum similar. Dorsal segment of abdomen with trapezoidal dark brown stripe extended to sternum VIII, subgenital plate large, extending to posterior portion of sternum IX, constricted from base, expanded medially, then slightly tapering toward posterior margins. Subgenital plate covered with minute, fine hairs. Tergum X not produced posteriorly. Paraproct in the shape of a small triangle, bearing small hairs (Fig. 5A–C).

Egg and nymph. Unknown.

Distribution. Southwestern China (Tibet and Yunnan Province).

Etymology. The species is named after the type locality, Dengba village.

Remarks. The new species is closely related to *Suwallia talalajensis*, but can be distinguished by the sclerotized portion between the hemitergal processes, the

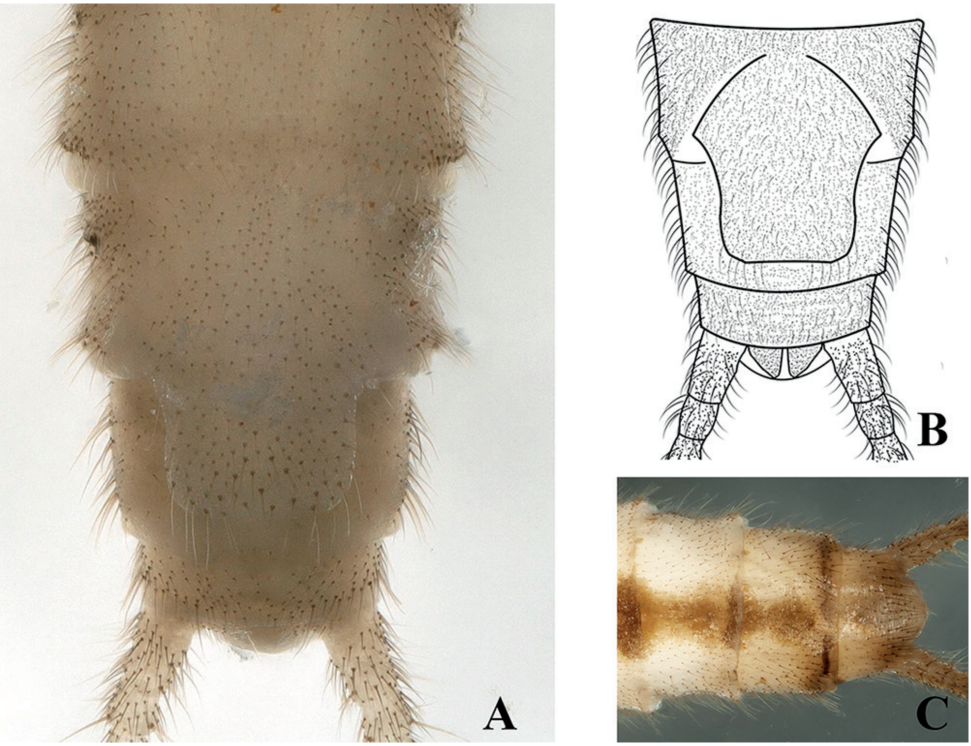

Figure 5. *Suwallia dengba* sp. nov. Female paratype. **A** terminalia, ventral view **B** terminalia, ventral view **C** terminalia, dorsal view.

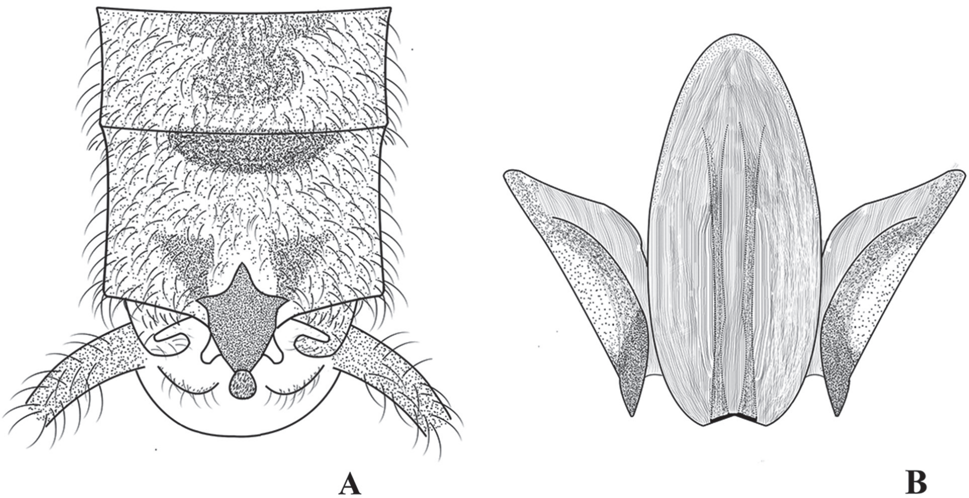

Figure 6. *Suwallia dengba* sp. nov. **A** male terminalia, dorsal view **B** aedeagal sclerite.

Figure 7. Revised map showing distribution of *Suwallia* species in China (modified from www.tianditu.gov.cn).

pigmentation of tergum IX, the armature of the aedeagus and the well-developed, membranous, knob-like epiproct. *Suwallia talalajensis* does not have a distinct aedeagal sclerite (Li et al. 2015b: fig. 5), whereas the new species has a distinct sclerite (Figs 4A–D, 6B). Tergum IX of the new species is covered with abundant, thick hairs, and its body pigmentation is different from that of *Suwallia talalajensis*. The new species also shows similar characteristics to *Suwallia errata* (Li et al. 2021), but it can be easily differentiated by the sclerotized portion between the hemitergal process and the shape of the aedeagus. *Suwallia errata* has a V-shaped aedeagal sclerite (Li et al. 2015a: figs 1–6), but the new species has the aedeagal sclerite of a different shape. The new species lives in fast-flowing rivers (width = 5 m), where a large gravel substrate is present. The adults occur on leaves of trees or shrubs near the river (Fig. 8).

Figure 8. Habitat at the type locality of *Suwallia dengba* sp. nov. Specimens were collected from the small trees and grasses near the stream (photograph Huo Qing-Bo).

Key to adult males of *Suwallia* species from China (modified from Chen 2019)

1	Epiproct reduced, tergum X with two median sclerites	**2**
–	Epiproct well developed, tergum X with undivided median sclerite	**3**
2	Tergum X with two longitudinal median sclerites (see Chen and Du 2015: figs 1–8)	***Suwallia wolongshana***
–	Tergum X with H-shaped median sclerite (see Chen 2019: fig. 3)	***Suwallia jihuae***
3	Tergum X with V-shaped median sclerite, aedeagus membranous, without spines or structures (see Shi et al. 2022: fig. 2)	***Suwallia asiatica***
–	Tergum X median sclerite triangular or subrectangular in shape, aedeagus with spines or structures	**4**
4	Tergum X median sclerite triangular in shape, epiproct small, aedeagus with triangular spines forming T-shaped structure (see Li et al. 2015b: fig. 2)	***Suwallia decolorata***
–	Tergum X median sclerite not as above, epiproct well developed and knob-like	**5**
5	Tergum X medial sclerite subrectangular, anterior margins with two separate sclerites	**6**
–	Tergum X median sclerite of turtle or hexagonal shape	**7**

6 Tergum X anterior margins divided into two sclerites, epiproct with long hairs and without posterolateral bifurcation, aedeagus with V-shaped sclerite (see Li et al. 2015a: figs 1–6)... ***Suwallia errata***

– Tergum X anterior margins with two separate paramedial sclerites, arch-shaped in lateral view, epiproct with stout posterolateral bifurcation, aedeagus with triangular sclerite, lateral margins darker (see Shi et al. 2022: fig. 1)...... ....***Suwallia kuandian***

7 Tergum X median sclerite turtle-like, aedeagus membranous, without distinct armature or sclerite (see Li et al. 2015b: fig. 2) ... ***Suwallia talalajensis***

– Tergum X median sclerite hexagonal star-shaped, pointed posteriorly, aedeagus with distinct trifurcate sclerite (Figs 2–4) ....***Suwallia dengba* sp. nov.**

Acknowledgements

This study was supported by the National Natural Science Foundation of China (No. 31872266, 31572295) and the Biodiversity Survey and Assessment Project of the Ministry of Ecology and Environment, China (No. 2019HJ2096001006). We express our deep gratitude to Xing-Min Wang, Wei-Dong Huang, Qing-Heng Tian (South China Agricultural University) and Yan-Dong Chen (Institute of Zoology, Chinese Academy of Sciences) for help collecting the specimens. Moreover, we express our heartfelt thanks to the reviewers for providing comments that significantly improved the manuscript.

References

Alexander K-D, Stewart K-W (1999) Revision of the genus *Suwallia* Ricker (Plecoptera: Chloroperlidae). Transactions of the American Entomological Society 125(3): 185–250. https://www.jstor.org/stable/25078681

Banks N (1906) On the perlid genus *Chloroperla.* Entomological News 17(5): 174–175.

Chen Z-T, Du Y-Z (2015) A new species of *Suwallia* (Plecoptera: Chloroperlidae) from China. Zootaxa 4018(2): 297–300. https://doi.org/10.11646/zootaxa.4018.2.9

Chen Z-T, Du Y-Z (2016a) A new species of *Haploperla* from China (Plecoptera, Chloroperlidae). ZooKeys 572: 1–6. https://doi.org/10.3897/zookeys.572.6270

Chen Z-T, Du Y-Z (2016b) Two new species of *Haploperla* (Plecoptera: Chloroperlidae) from China. Zootaxa 4196(3): 415–422. https://doi.org/10.11646/zootaxa.4196.3.5

Chen Z-T, Du Y-Z (2017) A new species of *Sweltsa* (Plecoptera: Chloroperlidae) from China, with a key to the *Sweltsa* males of China. Zootaxa 4337(2): 291–293. https://doi.org/10.11646/zootaxa.4337.2.8

Chen Z-T (2019) Review of the genus *Suwallia* (Plecoptera: Chloroperlidae) from China with description of *Suwallia jihuae* sp. nov. from Sichuan Province. Zootaxa 4603(3): 583–588. https://doi.org/10.11646/zootaxa.4603.3.11

DeWalt R-E, Maehr M-D, Hopkins H, Neu-Becker U, Stueber G (2021) Plecoptera Species File online. Version 5.0/5.0. http://plecoptera.speciesfile.org [Accessed on: 2021-7-28]

Dong W-B, Cui J-X, Li W-H (2018) A new species of *Sweltsa* (Plecoptera: Chloroperlidae) from Sichuan Province of southwestern China. Zootaxa 4418(4): 388–392. https://doi.org/10.11646/zootaxa.4418.4.5

Du Y-Z (1999) A taxonomic study on Plecoptera from China. Zhejiang University, Hangzhou, 324 pp.

Judson S-W, Nelson C-R (2012) A guide to Mongolian stoneflies (Insecta: Plecoptera). Zootaxa 3541(1): 1–118. https://doi.org/10.11646/zootaxa.3541.1.1

Li W-H, Wang R (2011) A new species of *Alloperla* (Plecoptera: Chloroperlidae) from China. Zootaxa 3040(1): 29–33. https://doi.org/10.11646/zootaxa.3040.1.4

Li W-H, Yao G, Qin X (2013) *Haploperla choui* sp. n. (Plecoptera: Chloroperlidae), a remarkable new stonefly from Qinling Mountains of China. Zootaxa 3640(4): 550–556. https://doi.org/10.11646/zootaxa.3640.4.3

Li W-H, Yang J, Yao G (2014) Review of the genus *Sweltsa* (Plecoptera: Chloroperlidae) in China. Journal of Insect Science 14(1): e286. https://doi.org/10.1093/jisesa/ieu148

Li W-H, Murányi D, Shi L (2015a) The first record of genus *Suwallia* Ricker, 1943 (Plecoptera: Chloroperlidae) from China. Illiesia 11(03): 23–28. http://illiesia.speciesfile.org/papers/Illiesia11-03.pdf

Li W-H, Murányi D, Shi L (2015b) New species records of *Suwallia* Ricker, 1943 (Plecoptera: Chloroperlidae) from China, with description of the nymph of *S. decolorata* Zhiltzova & Levanidova, 1978. Zootaxa 3994(4): 556–564. https://doi.org/10.11646/zootaxa.3994.4.4

Li W-L, Wang Y-Y, Wang Y, Li W (2021) A new species of *Suwallia* Ricker, 1943 from Japan, and the identity of *Alloperla teleckojensis* Šámal, 1939 (Plecoptera: Chloroperlidae). Zootaxa 5040(4): 575–581. https://doi.org/10.11646/zootaxa.5040.4.7

Mo R-R, Ye J-P, Wang G-Q, Li W-H (2020) The first record of the family Chloroperlidae (Plecoptera) from the Guangxi Zhuang Autonomous Region of southern China, with description of a new species of *Sweltsa* Ricker, 1943. Zootaxa 4853(2): 275–282. https://doi.org/10.11646/zootaxa.4853.2.8

Navás R-P-L (1934) Nevropteres et insects voisins (Chine et Pays environments). Notes d'Entomologie Chinoise. Museé Heude. Shanghai 2: 1–16.

Nelson C-H, Hanson J-F (1968) Two new species of *Alloperla* (Plecoptera: Chloroperlidae) from China. Journal of the Kansas Entomological Society 41: 425–428.

Okamoto H (1912) Erster Beitrag zur Kenntnis der Japanischen Plecopteren. Transactions of the Sapporo Natural History Society 4: 105–170.

Ricker W-E (1943) Stoneflies of southwest British Columbia. Indiana University Publications, Science Series 12: 1–145.

Ricker W-E (1952) Systematic studies on Plecoptera. Bloomington, Indiana University, 1–200.

Shi W-J, Wang H-L, Li W-H (2022) A new species and three new records of Chloroperlidae (Plecoptera) from northeastern China. Zootaxa 5093(5): 584–592. https://doi.org/10.11646/zootaxa.5000.5.7

Surdick R-F (1985) Nearctic genera of Chloroperlinae (Plecoptera: Chloroperlidae). Illinois Biological Monographs, 54. University of Illinois Press, Urbana and Chicago, Illinois, 146 pp.

Teslenko V-A, Zhiltzova L-A (2009) Key to the stoneflies (Insecta, Plecoptera) of Russia and adjacent countries. Imagines and nymphs. Dalnauka, Vladivostok, 382 pp.

Wu C-F (1938) Plecopterorum sinensium: A monograph of the stoneflies of China (Order Plecoptera). Yenching University, Beijing, 225 pp.

Yang D, Li W-H (2018) Species catalogue of China. Volume 2 Animals, Insecta (III), Plecoptera. Science Press, Beijing, 71 pp.

Zhiltzova L-A, Levanidova I-M (1978) Novie vidi vesnianok (Plecoptera) s Dalnego Vostoka. Novie Vidi Zivotnih, Aka-demia Nauk SSSR Trudy Zoologiceskogo Instituta 61: 3–29.

ZooKeys 1089: 181–186 (2022)
doi: 10.3897/zookeys.1089.80564
https://zookeys.pensoft.net

CORRIGENDA

A peer-reviewed open-access journal
ZooKeys
Launched to accelerate biodiversity research

Addenda and corrigenda: Gutiérrez N, Toledo-Hernández VH, Noguera FA (2020) Four new species of *Phrynidius* Lacordaire (Coleoptera, Cerambycidae, Lamiinae) from Mexico with an identification key for the genus. ZooKeys 1000: 45–57. https://doi.org/10.3897/zookeys.1000.56757

Nayeli Gutiérrez[1], Víctor H. Toledo-Hernández[2], Sergio Devesa[3], Eduardo Rafael Chamé-Vázquez[4], Felipe A. Noguera[5]

1 *Division of Invertebrate Zoology, Richard Gilder Graduate School, American Museum of Natural History. Central Park West & 79th St, New York, NY 10024, USA* **2** *Centro de Investigación en Biodiversidad y Conservación, Universidad Autónoma del Estado de Morelos, Av. Universidad 1001, Col. Chamilpa, Cuernavaca, Morelos 62209, Mexico* **3** *La Iglesia, 4, San Vicente do Grove, 36988 Pontevedra, Galicia, Spain* **4** *Ecología de Artrópodos y Manejo de Plagas, El Colegio de la Frontera Sur, Carretera Antiguo Aeropuerto Km. 2.5, CP 37000, Tapachula, Chiapas, Mexico* **5** *Estación de Biología Chamela, Instituto de Biología, Universidad Nacional Autónoma de México, Apartado Postal 21, San Patricio, Jalisco 48980, Mexico*

Corresponding author: Felipe A. Noguera (fnoguera@unam.mx)

Academic editor: Francesco Vitali | Received 14 January 2022 | Accepted 8 February 2022 | Published 18 March 2022

http://zoobank.org/6CE03FDF-0A8B-4161-9D76-97B1934BF5EB

Citation: Gutiérrez N, Toledo-Hernández VH, Devesa S, Chamé-Vázquez ER, Noguera FA (2022) Addenda and corrigenda: Gutiérrez N, Toledo-Hernández VH, Noguera FA (2020) Four new species of *Phrynidius* Lacordaire (Coleoptera, Cerambycidae, Lamiinae) from Mexico with an identification key for the genus. ZooKeys 1000: 45–57. https://doi.org/10.3897/zookeys.1000.56757. ZooKeys 1089: 181–186. https://doi.org/10.3897/zookeys.1089.80564

Abstract

After describing *Phrynidius jonesi* Gutiérrez, Toledo & Noguera, 2020 (Coleoptera, Cerambycidae, Lamiinae), the authors had the opportunity to study a conspecific individual of this species and recognize that the holotype had been erroneously determined as a male when in fact it was a female. Here, we rectify this error and provide morphological information for the identification of both sexes. Additionally, we record *Phrynidius armatus* Linsley, 1933 from Chiapas, Mexico. Finally, we document *P. cristinae* Gutiérrez et al. 2020 feeding on a fungus, which represents the first record for any species of the genus *Phrynidius* with this adult feeding habit.

Keywords
Biodiversity, Central America, longhorn beetles, taxonomy

Introduction

Knowledge of the genus *Phrynidius* Lacordaire, 1869 (Coleoptera, Cerambycidae, Lamiinae) is restricted to taxonomy and distribution, while host plant information is known for only one of its species. Fortunately, the collection of new specimens represents an opportunity to increase our knowledge about other aspects of the natural history of this group. This is the case for *P. jonesi* Gutiérrez, Toledo & Noguera, 2020 and *P. cristinae* Gutiérrez, Toledo & Noguera, 2020, both from Chiapas, Mexico, as well as for *P. armatus* Linsley, 1933 from Guatemala, of which we had the opportunity to study recently collected specimens. Following its description, an additional specimen of *P. jonesi* was collected at the type locality. This new specimen allowed for the reevaluation of our original description. In this note, we rectify the sexual identity of the holotype of *P. jonesi*, describe the sexually dimorphic characters of the species, and provide new information about its known hosts. In addition, we record for the first time *P. armatus* from Chiapas and adult feeding habits for *P. cristinae*.

Materials and methods

Photographs of *P. jonesi* were taken with a Canon EOS 5D Mark III DSLR equipped with a Canon MP-E 65 mm f/2.8 1–5× macro lens objective and automatically controlled with a Cognisys Stackshot. Photographs were focus stacked with the Zerene Stacker AutoMontage software and processed on Capture One 21. Photographs of the habitat were taken with an iPhone 8. The specimen is deposited in the Sergio Devesa Personal Collection (**SDPC**), Pontevedra, Spain. Photographs of *P. cristinae* were taken with a Canon 70D camera equipped with a Canon 60 mm, f /2.8 macro lens. Specimens of *P. cristinae* and *P. armatus* are deposited in Colección de Insectos de la Universidad de Morelos (**CIUM**), Morelos, Mexico and Colección de Insectos Asociados a Plantas Cultivadas en la Frontera Sur (**ECO-TAP-E**), Chiapas, Mexico.

Errata

Phrynidius jonesi Gutierrez et al., 2020

p. 51, ninth line: "Male holotype" should read "Female holotype".

Phrynidius armatus Linsley, 1933

p. 46, seventeenth line: "distributed in Guatemala and Nicaragua" should read "distributed in Guatemala, Mexico and Nicaragua".

p. 55, thirty-seventh line: "Guatemala and Nicaragua" should read "Guatemala, Mexico and Nicaragua".

Additions

Phrynidius jonesi **Gutiérrez, Toledo & Noguera, 2020**
Fig. 1A–D

Sex: Male. **Locality:** Mexico, Chiapas, Municipio de La Trinitaria, Lagunas de Montebello, 08-I-2019, 16°06'27.55N, 91°42'39.17W. S. Devesa leg.

The male differs from the female type in the following characters: smaller body size (10.2 vs. 11.7 mm); antennae longer relatively to body length (1.21 times longer than body, 1.15 times longer than body in female); antennal formula (ratio, based on length of the third antennomere) I = 0.88, II = 0.12, IV = 0.84, V = 0.36, VI = 0.32, VII = 0.32, VIII = 0.28, IX = 0.28, X = 0.28, XI = 0.28; abdomen more slender and elongated; last abdominal segment shorter, uniformly convex to the apical margin; apex almost glabrous and margin with a fringe of setae (in female, last abdominal segment more convex, with curvature not extending to apical margin, which is more flattened than in male).

The larva of *P. jonesi* was collected under bark of *Pinus oocarpa* Schiede ex Schltdl. (Pinaceae). This constitutes a new host record for the genus since the only host plant of *Phrynidius* species known to date was *Cupressus* sp. (Cupressaceae) (Becker 1955). The larva was collected on January 8th and the adult emerged on June 28th of the same year. This indicates that the development from larva to adult in this specimen lasted at least 6 months and 20 days. It is important to mention that the larva was kept in artificial conditions, therefore this developmental time could differ from development in the conditions of its habitat.

Phrynidius armatus **Linsley, 1933**

Sex: Male. **Locality**: México: Chiapas, Municipio Villacorzo, Ejido Sierra Morena, REBISE. 15-VI-2016, 1746 msnm, 16°08'16.88"N, 93°36'19.87"W (4 specimens). E.R. Chamé-V. col. **New state record**.

Male (9.7 mm) slightly longer than holotype (9.0 mm). Specimens of *P. armatus* were collected in a cloud forest with a high abundance of *Tillandsia usneoides* (L.) L. (Bromeliaceae). The specimens were collected using a beating sheet, which was placed under the vegetation (2 to 3 m high) and beaten with a pole. The type series was collected in Santa Ilena (probably Santa Elena), Guatemala, and the species was later recorded from Veracruz, México, and Selva Negra Mountain Resort, Nicaragua (Linsley 1933; Noguera and Chemsak 1996; Audureau and Roguet 2018). The specimens reported here were collected in Sierra Morena, Chiapas, which is part of the Sierra Madre of Chiapas, a mountain range connected with Chimaltenango, Guatemala. Both localities are in cloud forests.

Phrynidius cristinae **Gutiérrez, Toledo & Noguera, 2020**
Fig. 2A–D

Sex: Male. **Locality**: México: Chiapas, Municipio Villacorzo, Ejido Sierra Morena, REBISE. 03-VIII-2016, 1746 msnm, 16°08'16.88"N, 93°36'19.87"W. E.R. Chamé-V. col. (2 specimens).

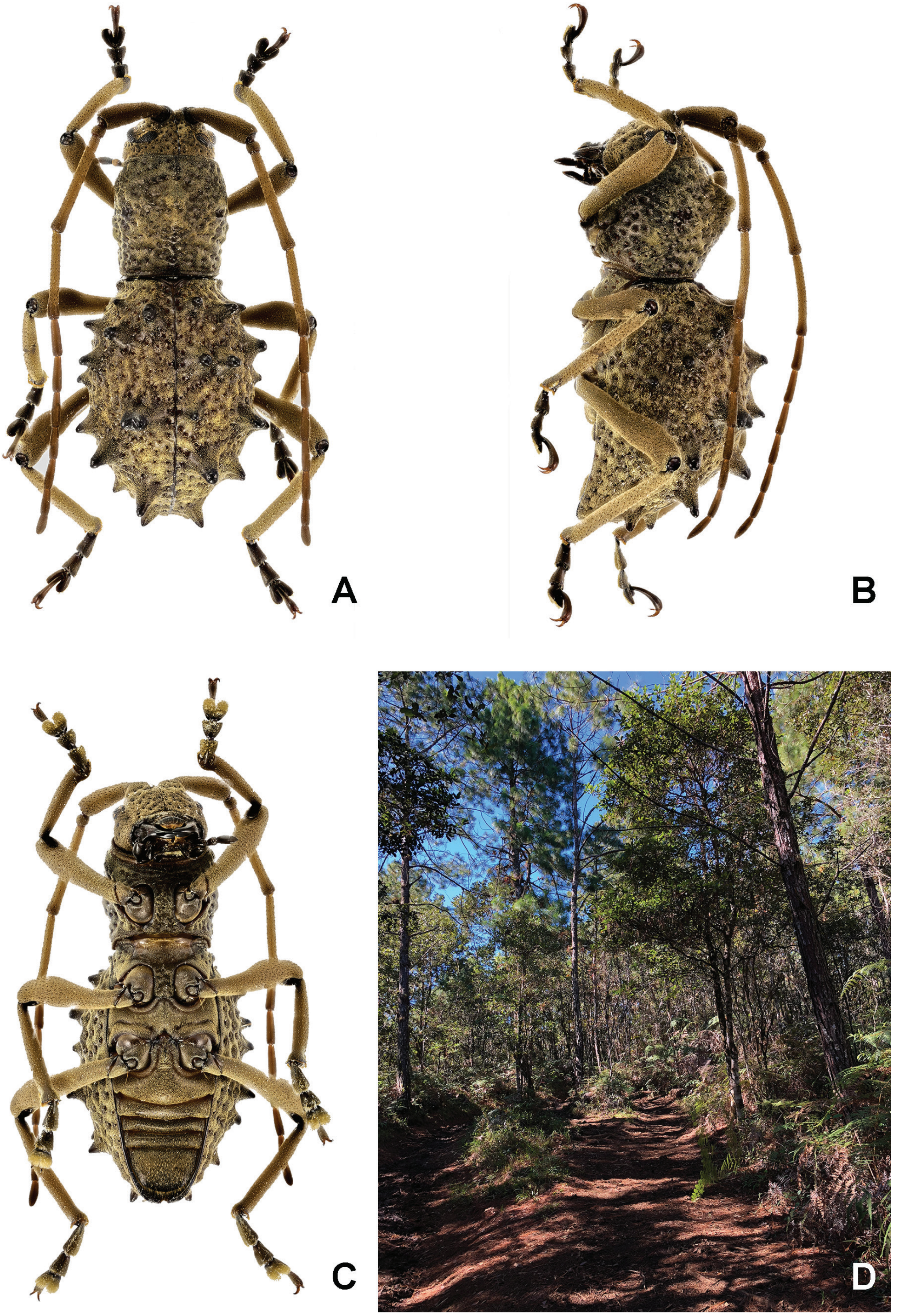

Figure 1. *Phrynidius jonesi* Gutiérrez, Toledo & Noguera, 2020: **A–C** male: Dorsal, ventral, and lateral views **D** habitat where the specimen was collected.

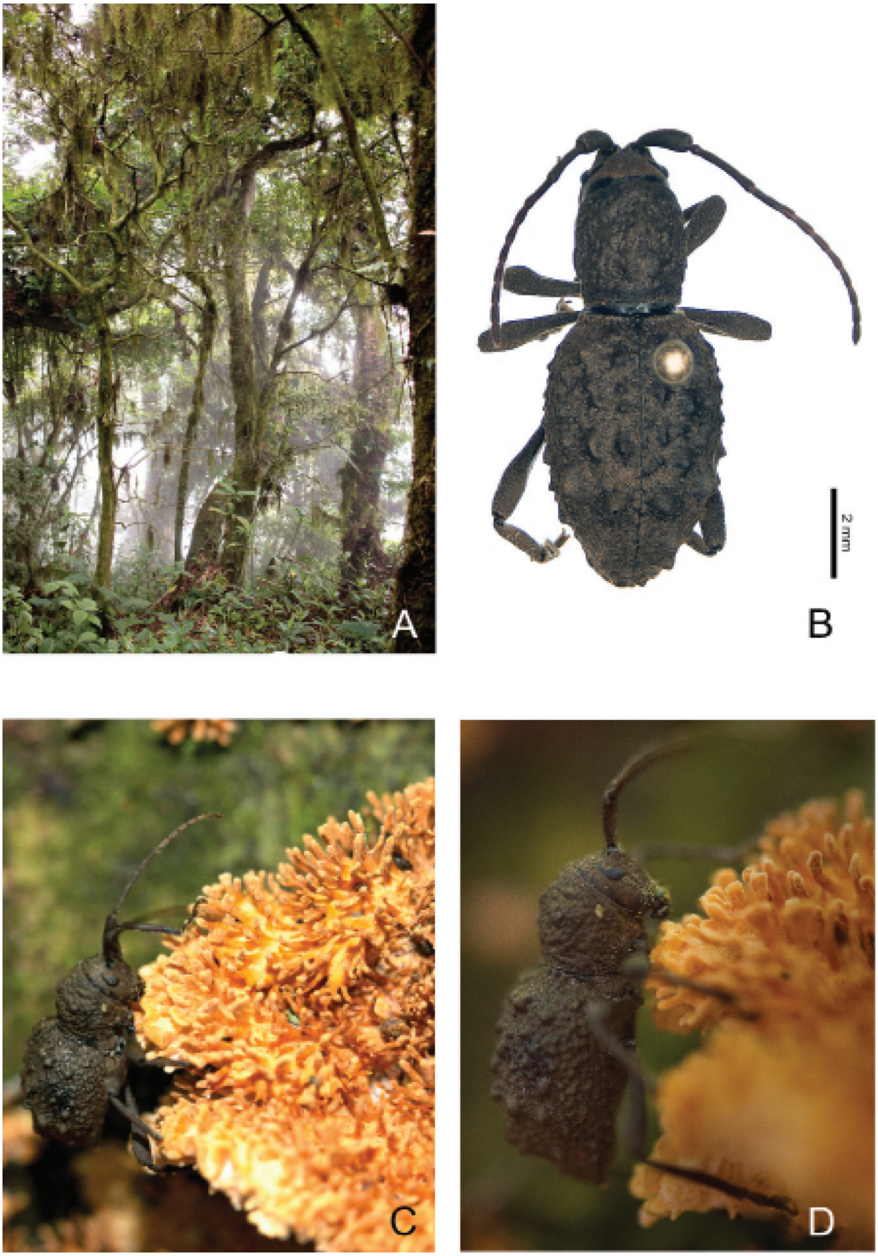

Figure 2. *Phrynidius cristinae* Gutiérrez, Toledo & Noguera, 2020: **A** habitat where the specimen was collected **B** dorsal view of male **C, D** specimen feeding on *Echinoporia aculeifera.*

On August 3, 2016 at 12:12 pm a specimen of *P. cristinae* with integument darker than that of the holotype was observed eating the pileus ornamentation of a specimen of *Echinoporia aculeifera* (Berk. & M.A. Curtis) Ryvarden, 1984 (Schizoporaceae). This fungus was found in a rotten log, which had a conglomerate of several individuals of this species.

Phrynidius species had only been associated with conifers (Cupressaceae and Pinaceae, recorded here), and no information was known about their feeding habits until now.

This is an interesting result, since only a few species of cerambycids have been recorded as fungal feeders as adults (Craighead 1923; Duffy 1953; Haack 2017; Michalcewicz 2002). Our findings emphasize the importance of observations in the field for a better understanding of the natural history of *Phrynidius*.

Acknowledgements

We are grateful to Benigno Gómez for helping us contact Neptalí Ramírez (ECOSUR), who identified the pine species, and Ricardo Valenzuela Garza (ENCB), who identified the fungus mentioned in the text. We thank Jeremy Frank for his comments on the manuscript and help improving the English language.

References

Audureau A, Roguet JP (2018) Contribution à la connaissance des Cerambycidae de la Région Nord du Nicaragua (Coleoptera, Cerambycidae). Les Cahiers Magellanes (NS) 30: 56–104.

Becker G (1955) Grundzüge der Insektensuccession in *Pinus*-Arten der Gebirge von Guatemala. Zeitschrift für angewandte Entomologie 37(1): 1–28. https://doi.org/10.1111/j.1439-0418.1955.tb00774.x

Craighead FC (1923) North American cerambycid-larvae. Bulletin of the Canada Department of Agriculture 27: 1–239.

Duffy EAJ (1953) A monograph of the immature stages of African timber beetles (Cerambycidae). British Museum (Natural History), London.

Gutiérrez N, Toledo-Hernández VH, Noguera FA (2020) Four new species of *Phrynidius* Lacordaire (Coleoptera, Cerambycidae, Lamiinae) from Mexico with an identification key for the genus. ZooKeys 1000: 45–56. https://doi.org/10.3897/zookeys.1000.56757

Haack RA (2017) Feeding biology of cerambycids. In: Wang Q (Ed.) Cerambycidae of the world; biology and pest management. Boca Raton, FLP CRC Press, 105–124.

Linsley EG (1933) A new longicorn beetle from Central America (Coleoptera, Cerambycidae). The Pan-Pacific Entomologist 9(3): 131–132.

Noguera FA, Chemsak JA (1996) Cerambycidae (Coleoptera). In: Llorente-Bousquets J, García-Aldrete AN, González-Soriano E (Eds) Biodiversidad, Taxonomía y Biogeografía de Artrópodos de México: Hacia una Síntesis de su conocimiento. Universidad Nacional Autonoma de México, México, 381–409.

Michalcewicz J (2002) Feeding of adults of *Leiopus nebulosus* (L.) (Coleoptera: Cerambycidae) on fruit-bodies of the fungus *Diatrype bullata* (Hoffm.: Fr.) Tul. (Ascomycotina: Sphaeriales). Wiadomosci Entomologiczne 21: 19–22.